Cape Peninsula
University of Technology

DESIGN AND IMPLEMENTATION OF IEC 61499 STANDARD-BASED NONLINEAR CONTROLLERS USING FUNCTIONAL BLOCK PROGRAMMING IN DISTRIBUTED CONTROL PLATFORM

By

JULIUS N'GON'GA MUGA

Thesis submitted in partial fulfilment of the requirements for the degree

Doctor of Technology: Electrical Engineering

In the Faculty of Engineering

at the Cape Peninsula University of Technology

Supervisor: Prof R. Tzoneva

Bellville campus
December 2015

DECLARATION

I, Julius N'gon'ga Muga, declare that the contents of this dissertation/thesis represent my own unaided work, and that the dissertation/thesis has not previously been submitted for academic examination towards any qualification. Furthermore, it represents my own opinions and not necessarily those of the Cape Peninsula University of Technology.

Signed **Date**

ABSTRACT

Majority of the industrial systems encountered are significantly non-linear in nature, so if they are synthesised and designed by linear methods, then some of salient features characterising of their performance may not be captured. Therefore designing a control system that captures the nonlinearities is important. This research focuses on the control design strategies for the Continuous Stirred Tank Reactor (CSTR) process. To control such a process a careful design strategy is required because of the nonlinearities, loop interaction and the potentially unstable dynamics characterizing the system. In these systems, linear control methods alone may not perform satisfactorily. Three different control design strategies (Dynamic decoupling, Decentralized and Input-output feedback linearization controller) are proposed and implemented .in the Matlab/Simulink platform and the developed strategies are then deployed to the design of distributed automation control system configuration using the IEC 61499 standard based functional block programming language. Twin CAT 3.1 system real-time and Matlab/Simulink (*www.mathworks.com)* environment are used to test the effectiveness of the models The simulation results from the investigation done between Simulink and TwinCAT 3 software (Beckhoff Automation) platforms in the case of the model transformation and closed loop simulation of the process for the considered cases have shown the suitability and the potentials of merging the Matlab/Simulink control function blocks into the TwinCAT 3.1 function blocks in real-time. The merits derived from such integration imply that the existing software and software components can be re-used. This is in line with one of the IEC 6144 standard requirements such as portability and interoperability. Similarly, the simplification of programming applications is greatly achieved. The investigation has also shown that the integration the of Matlab/Simulink models running in the TwinCAT 3.1 PLC do not need any modification, hence confirming that the TwinCAT 3.1 development platform can be used for the design and implementation of controllers from different platforms. Also, based on the steps required for model transformation the between the Matlab/Simulink to the TwinCAT 3 functional blocks, the algorithms of the control design methodologies developed, simulation results are used to verify the suitability of the controls to find whether the effective set-point tracking control and disturbance effect minimisation for the output variables can be achieved in real-time using the transformed Simulink blocks to the TwinCAT 3 functional blocks, then downloaded to the Beckhoff CX5020 PLC for real-time execution. Good set-point tracking control is achieved for the MIMO closed loop nonlinear CSTR process for the considered cases of the developed control methodologies. Similarly, the effects of disturbances are investigated. TwinCAT functional modules achieved good set-point tracking with these disturbances minimization under all the cases considered.

ACKNOWLEDGEMENTS

I wish to thank:

- My employer Technical University of Mombasa for granting me the study leave and scholarship for this noble undertaking. I will always remain grateful to the support I received during the course of study.
- My supervisor Professor Raynitchka Tzoneva for her supervision, guidance, advice and contribution throughout the thesis write up. To her, I say thank you very much.
- My wife Liz for the endurance, support, understanding and encouragement during the time of study.
- My sons Frank, Yves and Michael Muga for the endurance during my long period absence from home. I love you all.

The financial assistance of the National Research Foundation towards this research is acknowledged. Opinions expressed in this thesis and the conclusions arrived at, are those of the author, and are not necessarily to be attributed to the National Research Foundation.

DEDICATION

I dedicate this thesis to my little boy, Michael Muga

TABLE OF CONTENTS

CHAPTER THREE: ANALYSIS OF THE STEADY STATE AND DYNAMIC CHARACTERISTICS OF THE CSTR PLANT MODEL

CHAPTER FOUR: CONTROLLER DESIGN METHODS USING CONVENTIONAL TECHNIQUES

CHAPTER FIVE: DECENTRALIZED CONTROLLER DESIGN FOR THE CSTR PROCESS

CHAPTER EIGHT: CONCLUSION, DELIVERABLES, APPLICATIONS AND FUTURE WORK

LIST OF FIGURES

LIST OF TABLES

GLOSSARY

Terms/Acronyms/Abbreviations	Definition/Explanation
ADACOR	Adaptive holonic Control Architecture
ADS	Automation Device Specification
BLT	Biggest Log-modulus Transfer function
CAEX	Computer Aided Engineering Exchange
COM	Component Object Model
CORFU	Common Object-oriented Real-time Frame work For Unified development
CSTR	Continuous Stirred Tank Reactor
CX-5020 PLC	Programmable Logic Controller (Beckhoff Automation Inc.)
DCS	Distributed Control System
DLP	Dynamic Linear Part
DIAC	Framework for Distributed Industrial Automation and Control
EFA	Extended Finite Automata
ESS	Engineering Support System
FB	Function Block
FBench	An open source graphical software tool for automation
FBDK	Function Block Development Kit
FBRT	Function Block RunTime
FTC	Fault Tolerant Control
GLC	Globally linearizing Control
ICP	Instrumentation Control Points
ICS Triplex ISaGRAF	A software platform for development and monitoring of control applications
IEC	International Electro-Technical Commission
IDE	Integrated Development Environment
IMC	Internal Model Control
IO	Input/Output
IPMCS	Industrial Process Measurement and Control Systems
IQC	Integral Quadratic Constraint
ISA	International Standard of Automation
ISE	Integral Squared Error
LMI	Linearized Model Infinite-bus system
LPV	Linear Parameter Varying
LQC	Linear Quadratic Control
MIMO	Multi-Input Multi-Output
MLD	Mixed Logic Dynamic model
MPC	Model Predictive Control
MPP	Mini Pulp Process
MRAC	Model Reference Adaptive Control
MVC	Model-View-Controller
NCES	Net Condition/Event Systems
NDO	Nonlinear Disturbance Observer
NI	Niederlinski index
NIMC	Nonlinear Internal Model Control
NLPC	Nonlinear Predictive Control
NMPC	Nonlinear Model Predictive Control
NPAC	Nonlinear Predictive Adaptive Controller

nxtCONTROL	**The control logic of the nxtSTUDIO**
nxtSTUDIO	**Engineering software tool distributed control systems**
nxtRT	**The runtime platform of the nxtSTUDIO**
OOONEIDA	**Open Object Oriented knowledge Economy for Intelligent industrial Automation**
PI	**Proportional/Integral**
PID	**Proportional/Integral/Derivative**
PLC	**Programmable Logic Controller**
PSO	**Particle Swarm Optimisation**
PWA	**PieceWise Affine**
RGA	**Relative Gain Array**
SESA	**Signal net system analysis**
SIFB	**Service Interface Function Blocks**
SISO	**Single-Input Single-Output**
SNP	**Static Nonlinear Part**
SIPN	**Signal Interpreted Petri Nets**
SVD	**Single Value Decomposition**
TcCOM	**TwinCAT Component Object Model**
ThIThO	**Three-Input Three-Output**
TINI	**Tiny Inter-Net Interface**
TITO	**Two-Input Two-Output**
TSMC	**Terminal Sliding Mode Control**
TwinCAT	**The Windows Control Automation**
UML	**Unified Modelling Language**
XAE	**Extended Automation Engineering**
XAR	**Extended Automation Runtime**
XML	**Extensible Mark-up Language**
VEDA	**Verification Environment for Distributed Applications**
VIVE	**Visual Verifier**

MATHEMATICAL NOTATIONS

Symbols/Letters	**Definition/Explanation**
W	**Area for the heat exchange**
C_A	**Concentration of the component in the reactor**
C_{AO}	**Concentration of the component in the feed stream**
C_P	**Specific heat capacity of component in the reactor**
C_{PC}	**Specific heat capacity of the coolant**
q	**Process volumetric flow rate**
q_{in}	**Process feed input volumetric flow rate**
q_o	**Process output volumetric flow rate**
ρ_{in}	**Density of the incoming flow**
q_c	**Coolant volumetric flow rate**
k_o	**Pre-exponential factor**
R	**Ideal gas constant**
r	**Rate of reaction per unit volume**
T	**Reactor temperature**
T_O	**Feed temperature**

T_{CO}	Jacket temperature
hA	Overall heat transfer coefficient
V	Reactor constant volume
ΔE	Activation energy
$\left(-\Delta H\right)$	Heat of reaction
ρ	Density of component in the reactor
ρ_c	Density of the coolant
q_s	Steady state feed flow rate
$\mathrm{q_{cs}}$	Initial Coolant volumetric flow rate
$\mathrm{u_2}$	Control input for temperature
$\mathrm{y_1}$	Controlled output concentration
$\mathrm{C_{Ainit}}$	Initial value of concentration
$\mathrm{y_2}$	Controlled output temperature
$\mathrm{T_{init}}$	Initial value of temperature
u	Vector of control signals
$\mu\mathrm{C}$	Microcontroller
x	State vector variables of the CSTR variables
$\mathrm{x_1}$	Concentration state variable
$\mathrm{x_2}$	Temperature state variable
x_o	Initial state vector
$\mathrm{u_1}$	Control input for concentration
$f(x)$	n-dimensional vector of nonlinear functions
$g(x)$	nxm-dimensional matrix of nonlinear functions
$h(x)$	l-dimensional vector of nonlinear functions
A	Component in the reactor
f_1, f_2	Nonlinear functions of the CSTR
u_o	Initial control signal vector
G_P	CSTR plant transfer function matrix
$D(s)$	Decoupler matrix transfer function
$Q(s)$	Diagonal (apparent) transfer function matrix of CSTR
z	The power of the IMC filter
$V(s)$	Control input vector from linear controllers
$C(s)$	Linear controller vectors
Λ	Relative Gain Array matrix
F	Detuning factor
ζ	Damping factor
M_P	Maximum (Peak) overshoot
T_s	Settling time
ω_n	Undamped natural frequency
ω_d	Damped natural frequency
λ	Element by element in the RGA
β	Time constant of the non-invertible element
γ	Adjustable fitter factor

$f(s)$ **The IMC filter transfer function**

CHAPTER ONE
INTRODUCTION
PROBLEM STATEMENT, OBJECTIVES, HYPOTHESIS AND ASSUMPTIONS

1.1 Introduction

Majority of the industrial systems encountered are significantly non-linear in nature, so if they are synthesised and designed by linear methods, then some of salient features characterising of their performance may not be captured. Therefore designing a control system that captures the nonlinearities is important. Nevertheless, linear controller design methods have proved adequate in many applications (Schweickhardt and Allgöwer, 2007; O'brien and Carruthers, 2013; Andrade, et al., 2015). The important nonlinear diversity in practical systems makes it impossible for a systematic and general theory for the design of nonlinear control systems (Hunt et al., 1992). Linear systems obey the principles of homogeneity and superposition. When these two properties are fulfilled for any linear system then the performance of such system is, guaranteed under any operating condition. In contrast to the linear case, a nonlinear system having its best performance for certain input signal may show highly unsatisfactory performance when the signal amplitude experiences sudden change. Also, the analysis and synthesis of the control properties for nonlinear systems can be extremely difficult and time consuming (Hunt et al., 1992). However, the design and implementation of robust nonlinear controllers that captures the process nonlinearities, is of great interest. Plenty of research papers for the control of nonlinear industrial systems are available and different approaches are available. Approaches such are feedback linearization, back stepping control, sliding mode control, Linearization based on Lyapunov theory, Differential Geometry concepts, as well as those based on artificial intelligence etc., have been proposed. A few examples are (Hunt et al., 1992; Wang and Li., 2005; Schweickhardt and Allgower, 2007; Marinescu, B., 2010; Vlad et al 2012; Hammer, 2014). Another challenging aspect is if the system is Multi-Input Multi-Output (MIMO). In MIMO processes, the coupling between different inputs and outputs makes the design of the controller difficult. Generally, each input will have an effect on every output of the process. Because of this coupling, signals can interact in unexpected ways. One solution is to design additional controllers to compensate for the interactions (Jevtovic and Matausek, 2010; Sujatha, and Panda, 2013; Leena and Ray, 2014). This research focuses on the control design strategies for the Continuous Stirred Tank Reactor (CSTR) process. To control such a process a careful design strategy is required because of the nonlinearities, loop interaction and the

potentially unstable dynamics. In these systems, linear control methods alone may not perform satisfactorily. The proposed research work is aimed at the design and implementation of nonlinear controllers and the deployment of the developed controllers to the design of distributed automation control system configuration using the IEC 61499 standard based functional block programming language. Twin CAT 3.1 system real-time (Beckhoff Automation) and Matlab/Simulink (*www.mathworks.com)* environment are used to test the effectiveness of the developed models and methods in realizing the thesis objectives. The IEC 61499 standard was developed by the International Electro technical commission and the objective of the standard is to address the limitations of the popular programmable logic controller (IEC 61131-PLC) programming languages in implementing real-time control. The standard also offers benefits such as the ease of configurability, interoperability, portability and event driven approach to the implementation of control strategy. Comparative performance analyses using the two platforms (Matlab/Simulink and TwinCAT 3.1) such as configurability and decentralization assessment are carried out. Simulation will be used to show the suitability of the Distributed control system in line with the functional block programming concepts. It is envisaged that the thesis out contributions will provide a platform for understanding the concepts of the TwinCAT 3.1 software environment, its application to practical distributed control systems, as well as a guide for model transformation between the two environments (Matlab/Simulink and TwinCAT 3.1) for modelling, data analysis and real-time simulation.

This chapter is further subdivided as follows: Section 1.2 shows the awareness of the research problem, while section 1.3 gives the problem statement. Section 1.4 lists the aims and objectives of the research. Then sections 1.5, 1.6, 1.7 respectively provide the hypothesis, the delimitations of the research work and the motivation followed by the assumptions in section 1.8. Section 1.9 gives the thesis contribution and deliverables. Section 1.10 is the outline of the proceeding chapters and lastly the conclusion is provided in section 1.11.

1.2 Awareness of the problem

Research in nonlinear control is motivated by the inherently nonlinear characteristics of the dynamic systems to be controlled. In reality, virtually most practical systems encountered are significantly nonlinear in nature so that the salient features characterising of their performance may be completely compromised if they are modelled, analysed and designed by linear control

methods (Guay at al., 2005). The important nonlinear diversity in practical systems makes it impossible for a systematic and general theory for the design of nonlinear control systems (Hahn and Marquardt, 2003). However, the design and implementation of robust nonlinear controllers that captures the process nonlinearities, is of great interest. Linear systems obey the principles of homogeneity and superposition. When these two properties are fulfilled for any linear system then the performance of such system is guaranteed under any operating condition. In contrast to the linear case, a nonlinear system having its best performance for certain input signal may show highly unsatisfactory performance when the signal amplitude experiences sudden change. Also, the analysis and synthesis of the control properties for nonlinear systems can be extremely difficult and time consuming. The increasing tough requirements imposed on product quality and energy utilization, and also, the safety and environmental impacts require that industrial processes operate such that their inherent nonlinearities are emphasized. Thus developing and implementing controllers which are suitable when process nonlinearities must be accounted for, is of great interest .It is on this context that the nonlinear theory is suggested for the design and implementation of nonlinear distributed controllers for the nonlinear plants. The prototyping environment that is proposed for the construction, implementation and simulation is the new IEC 61499 function blocks standard platform (Vyatkin, V.,2011) The IEC 61499 was developed to support distributed control. The structure developed is integrated with the TwinCAT 3.1. IEC 61499 based real-time environment and the Matlab/Simulink (www.mathworks.com) environment to test the suitability of the proposed methods. Based on the factors mentioned the main research questions of the thesis can be formulated as follows:

- Linear or nonlinear methods for design of controllers for MIMO nonlinear processes contribute to better performance of the closed loop system for various process conditions, as changing set point and disturbances.
- Is the software TwinCAT 3.1 capable for programming of the developed decentralized distributed closed loop control systems and to perform real-time simulation.
- Can the real-time Twin CAT 3.1 environment be capable to assure the same performance characteristics of the closed loop systems through real-time simulation in comparison with the obtained through the simulation in Matlab/Simulink environment.

1.3 Problem Statement

The need for decentralized control in complex manufacturing setup is tremendously growing because of reasons, such as flexibility and reliability. In contrast to a centralized controlled system, any failure in any part of the system results in a breakdown in the system. The IEC 61131-3 standard function block diagram programming of the PLCs are not suitable for implementation of distributed control. Also, the increased complexity of present day industrial set-ups implies that the control design methods like nonlinear controller design which can overcome limitations on the conventional feedback control design methods are needed. The IEC 61499 standard-based PLC environment is the solution in order to achieve distributed control of complex nonlinear industrial systems. The thesis focuses on nonlinear control design and its real-time implementation in a distributed set-up that utilizes some of the features of the IEC 61499 standard using functional block programming in a distributed control platform. Multi-input Muliti-output (MIMO) Continuous Stirred Tank Reactor (CSTR) model is used as case study to show the suitability of the algorithms developed. The problem can be split into: Nonlinear controller design, and real-time implementation of the developed control system.

The thesis focuses on the development of nonlinear MIMO control system methodology based on the platforms complaint with the IEC 61499 standard, thereby exploiting the potentials of this platform for distributed control applications. MIMO (CSTR) bench mark model is selected as the nonlinear plant to be controlled.

1.3.1 Sub-problem1 (design).

This problem can be addressed through the following steps:

- To formulate the mathematical model for the MIMO nonlinear plant
- To develop methods for the linearization and stability analysis relevant to MIMO nonlinear plant model.
- To develop methods for the design of linear controllers based on the conventional decoupling (Jacobian) linearization techniques, relevant to the MIMO nonlinear plant model
- To develop methods for the design of nonlinear controllers based on dynamic decoupling techniques relevant to the MIMO nonlinear plant model.
- To develop methods for the design of nonlinear decentralized controllers techniques relevant to the MIMO nonlinear plant model.

- To develop methods for the design of nonlinear controllers based on input/output feedback linearization techniques relevant to the MIMO nonlinear plant model.
- To design linear controllers, additional to the dynamic decoupling, decentralized and input/output linearization controllers to improve the closed loop system performance.
- To develop Matlab/Simulink software and simulate the MIMO closed loop systems.

1.3.2 Sub-problem2 (implementation).

- To perform simulations for the developed closed loop decoupled control system in Matlab/Simulink environment
- To perform simulations for the developed closed loop decoupled control system in Matlab/Simulink environment
- To perform simulations for the developed closed loop decentralized control system in Matlab/Simulink environment
- To perform simulations for the developed closed loop input/output feedback linearization control system in Matlab/Simulink environment
- To transform the developed control software from Matlab/Simulink environment to the IEC 61499 standard-based TwinCAT 3 simulation environment (Function blocks).
- To perform real-time simulation of the closed loop systems in the TwinCAT PLC platform to demonstrate the effectiveness of the transformations.
- To perform real-time distributed control simulations of the closed loop systems in in the TwinCAT PLC platform

1.4 Research Aim and Objectives

The research investigations are looking at the following aim and objectives.

1.4.1 Aim

The aim of the investigation is to design nonlinear controllers and implement them in the functional block based PLC environment in order to achieve real-time simulation of the distributed closed control of complex industrial systems.

1.4.2 Objectives

1. To model, linearize and simulate the nonlinear MIMO CSTR in Matlab/Simulink environment.

2. To design decoupling control and develop Matlab/Simulink software and simulate the closed loop system in Matlab/Simulink environment for set-point tracking control and disturbance rejection.
3. To design decentralized control and develop Matlab/Simulink software and simulate the closed loop system in Matlab/Simulink environment for set-point tracking control and disturbance rejection.
4. To design input/output linearized feedback control and develop Matlab/Simulink software and simulate the closed loop system in Matlab/Simulink environment for set-point tracking control and disturbance rejection.
5. To perform comparative analysis of the Dynamic decoupling controller design, Decentralized control strategy and Input-output state feedback linearization in terms of set-point tracking capabilities and disturbance rejection.
6. To transform the developed software from Matlab/Simulink environment to IEC 61499 standard-based TwinCAT 3 simulation environment (Function blocks).
7. To perform real-time simulation of the closed loop system in order to demonstrate the effectiveness of the transformation.

1.5 Hypothesis

The developing and implementing of controllers which are suitable when process nonlinearities must be accounted for are of great interest. Hence the designs of such controllers are preferable. Also the increased degree of distribution and the type of real-time automation implies that the software tools that would make it possible to design the control application in a distributed way is needed. On the bases of the above, the hypotheses are:

1. Design of controllers using the principles of decoupling, decentralization and input-output linearization can be successfully provided for nonlinear multivariable systems.
2. The mathematical expression of the designed controllers can be programmed in the software environment of the TwinCAT 3 software for real-time simulation and implementation of nonlinear distributed control systems.

Thus, developing a control system methodology based on the new TwinCAT 3 functional block programming complaint with the requirements of the IEC 61499 standard offers great potentials in all those control applications that require real-time solutions for multivariable nonlinear dynamic processes.

1.6 Delimitation of the research

The proposed research is focused into the design and implementation of nonlinear controllers using Matlab functional block programming environment. It considers a prototype MIMO Continuous Stirred Tank Reactor (CSTR) plant model with two control loops. The control structures developed are limited to the methodology adopted by the linear theory (dynamic decoupling control and decentralized control) and the nonlinear theory (input/output feedback linearization within the control loops). These structures are implemented both in the Matlab/Simulink platform and in the TwinCAT 3.1 (Beckhoff Automation) supporting the IEC 61499 standard as case studies. Simulations are used to show the suitability of the control systems. A comparative performance analyses are carried out. Real-time control simulation is carried out by transformation of the developed Matlab/Simulink closed loop systems into the TwinCAT 3.1 Beckhoff Automation software and Beckhoff CX-5020 PLC.

1.7 Motivation of the Research

Strongly nonlinear systems cannot be controlled optimally by linear feedback controllers. The increased complexity of present day industrial set-ups implies that the control design methods like nonlinear controller design which can overcome limitations on the conventional feedback control design methods are needed. The IEC 61499 standard based TwinCAT 3.1 environment is the next generation control design software for the automation industry. It was developed to support distributed control. The standard is currently evolving and has not been used in actual factory applications. Thus, the research is motivated by developing control system design methods based on this new standard requirement that offer great potentials in all those distributed control applications that require real-time solutions for MIMO nonlinear dynamic processes.

1.8 Assumptions

In order to achieve the objectives of the research, the following assumptions are made on different parts of the work.

- The process dynamics are highly nonlinear and the operating points are explicitly stated.
- The nature of the equations describing the process to be controlled allows the controller to be designed by both linear and feedback linearization techniques.
- The IEC 61499 standard-based function block complaint platform TwinCAT 3.1 should be able to describe both nonlinear control and data relationship for

the distributed closed loop control system design for both hardware and software implementation and real-time simulation.

1.9 Contributions of the Research and Deliverables.

1. Development of the methods for the design of the linear controllers based on decoupling control philosophy
2. Development of the methods for Design of the linear decentralized controllers for the nonlinear MIMO system
3. Design of nonlinear controllers based on input/output feedback linearization of the nonlinear MIMO system
4. Simulations of the control algorithms in Matlab/Simulink for comparative analysis.
5. Development of a guide or algorithm for transformation of the developed software from Matlab/Simulink environment to IEC 61499 standard-based TwinCAT 3.1 simulation environment (Function blocks).
6. Real-time simulation comparison of the various closed loop systems by the Beckhoff CX-5020 PLC and TwinCAT 3.1 software environment.
7. Publication.

1.10 Outline of the thesis

The thesis is made up of eight chapters with a breakdown as follows:

Chapter 1 serves as a foundation for understanding and interpreting the contents of the thesis. It provides problem awareness, problem statement, aim and objectives of this research, hypothesis and assumptions, the motivation for the research as well as the research contribution and deliverables.

Chapter 2 is concerned with the review on the relevant aspects of the areas which concern this thesis and subdivided into sections as follows: General nonlinear systems and nonlinear controller design techniques, the nonlinear MIMO Continuous stirred tank reactor (CSTR) bench mark model, CSTR modelling and the control design methodologies and tools that have been used, review of the Distributed control methods, review of the IEC 61499 standard in process industry, and a review of implementation of the nonlinear control with IEC 61499 functional block programming.

Chapter 3 This chapter discusses the nonlinear MIMO Continuous Stirred Tank Reactor. This has been chosen as a case study example for this research. The

nonlinear CSTR process model's steady state and dynamic responses are analysed. The simulations on the developed nonlinear model of the CSTR plant with a first order exothermic reaction are performed to show the behaviour of the plant model for step changes in the inputs. This allows for the choosing of optimal working points for the various controller designs and implementations.

Chapter 4 This chapter presents the multivariable control of the ideal nonlinear CSTR process model using decoupling controller design strategies to control the reactor concentration and temperature. First, the nonlinear CSTR plant model is linearized at one of the operating point and then decoupling control is designed. Decoupling control ensures that the MIMO closed loop control system is decoupled so that each output is controlled independent of the other outputs. The preliminary theory of the method is presented, then the details of the design of the control schemes are provided, and lastly the developed closed loop system is tested by simulation in the Matlab/Simulink environment and is evaluated in terms of the performance specifications for various initial conditions, disturbances and set points.

Chapter 5 This chapter presents the multivariable control of the linearized ideal nonlinear CSTR process model using decentralized controller design strategies to control the reactor temperature and the concentration. For the design of the decentralized controllers, input output pairing is performed based on the Relative Gin Array (RGA)-the ratio of the open loop gain to the closed loop gain of the considered control system. The preliminary theory of the method is presented, then the details of the design of the control scheme are presented, and lastly the developed closed loop system is tested by simulation in Matlab/Simulink environment and is evaluated in terms of the performance specifications for different system conditions.

Chapter 6 This chapter develops an input/output feedback linearization controller design method for the nonlinear multi input multi output process of the reactor temperature and concentration in a CSTR. Input/output feedback linearization is a type of control design technique that uses feedback signal to cancel the inherent nonlinearities in a system, and creates linear differential relationship between the outputs and the newly defined virtual inputs. The preliminary theory of the method is presented, then the details of the design of the control methodologies are provided, and lastly the proposed closed loop system is tested by simulation in

the Matlab/Simulink environment in terms of the performance specifications for various system conditions. A comparison with the other conventional methods developed in chapters four and five is made.

Chapter 7 The concept of real-time control for the MIMO CSTR is introduced. The chapter introduces the TwinCAT 3.1 software as a tool used for integration with Matlab/Simulink software in order to implement real time control of the developed control algorithms. The chapter presents a methodology of transforming the developed continuous time controller blocks in Chapters 4, 5 and 6 as well as the complete closed loop systems application from Matlab/Simulink environment to the Beckhoff Embedded PCs using the capabilities of TwinCAT 3.1 simulation environment. Then the Beckhoff CX-5020 Programmable Logic Controller is used for real-time simulation of the closed loop systems. It presents the development of the algorithm (guide) for the transformation therein.

Chapter 8 presents the conclusion of the thesis. It outlines the deliverables achieved and suggestions for future works in relation to the nonlinear control based on IEC 61499 standard. In addition the publication derived from the results of the study is also listed.

1.11 Conclusion

This chapter presents the background of the project, the problem statement, the aims and objectives of the project. The assumptions, the delimitation of the research and the motivation is also given. It also outlines the contribution and deliverables expected.

In order to achieve the stated aims and objectives, a comprehensive literature review on nonlinear systems and nonlinear controller design techniques, and control of MIMO systems with emphasis on the CSTR plant is essential. Also a review on Design of distributed control, the IEC 61499 Standard for distributed control application, and the implementation of the control using the IEC 61499 functional block programming techniques is important.

Chapter 2 presents review on the existing literature on nonlinear systems and nonlinear controller design techniques, control of MIMO CSTR systems, distributed control and the IEC61499 standard.

CHAPTER TWO
LITERATURE REVIEW

2.1 Introduction

For enhanced functionality, flexibility and reliability, the tendency of the present day industrial set-up is to embed the disciplines of computing, communication and control together to form different levels of information processes and plant operation. The IEC 61499 standard gives a methodology that embeds computing, communication and control to model, design and implement the distributed process measurement and control systems applications. The standard is still new and evolving. The thesis focuses on the development of nonlinear Multi-input Multi-output (MIMO) control system philosophies based on the platforms complaint with this standard thereby exploiting the potentials for distributed control applications that require real-time solutions. Multi-input Multi-Output Continuous Stirred Tank Reactor (CSTR) bench mark model has been chosen as the nonlinear plant to be controlled. This chapter therefore is concerned with the review on the relevant aspects of the areas which concern this research investigation subdivided into sections as follows:

Section 2.2 presents an introduction to the General nonlinear systems and nonlinear controller design techniques. In section 2.3, a review of the existing literature for the CSTR modelling and the control design is presented. In section 2.4 a review on Distributed control and the IEC 61499 standard in process industry is presented. In section 2.5 discussion of the comparative review is presented, and lastly, the conclusion of the chapter is presented in section 2.6.

2.2 Nonlinear systems and nonlinear controller design techniques

Research in the field of nonlinear control is motivated by the inherently nonlinear characteristics of the dynamic systems to be controlled. Strongly nonlinear systems cannot be controlled in an optimum way by a linear feedback controller. The increased complexity of present day industrial set-ups implies that the control design methods like nonlinear controller design which can overcome limitations on the conventional feedback control design methods are needed. While the theory of modelling for linear systems is well understood, as well as there is availability of the mathematical tools for the analysis, there is still a wide gap in the control theory to analyse and design the nonlinear systems. The distinction between linear and nonlinear systems is that any system that satisfies the properties of homogeneity and superposition is a linear system. If the system fails to satisfy these two properties then it is nonlinear. Thirdly, nonlinear systems may have many equilibrium points unlike the linear systems which have only one

equilibrium point. This therefore means that for nonlinear systems, their stability needs must be explicitly specified. Majority of the industrial systems encountered are significantly non-linear in nature, so if they are synthesised and designed by linear methods, then some of salient features characterising their performance may not be captured. Therefore designing a feedback control system to capture these nonlinearities is important and significant. Nevertheless, linear controller design methods have proved to be adequate in many applications (Schweickhardt and Allgöwer, 2007). The important nonlinear diversity in practical systems makes it impossible for a systematic and general theory for the design of nonlinear control systems (Hunt et al., 1992). As it was mentioned above, linear systems obey the principles of homogeneity and superposition. When these two properties are fulfilled for any linear system then the performance of such system is guaranteed under any operating condition. In contrast to the linear case, a nonlinear system having its best performance for certain input signal may show highly unsatisfactory performance when the signal amplitude experiences sudden change. There is no equivalent mathematical theory, on which base a full theory of the non-linear control systems can be built. Also, the analysis and synthesis of the control properties for nonlinear systems can be extremely difficult and time consuming (Hunt et al., 1992). The increasing tough requirements imposed on product quality and energy utilization, and also, the safety and environmental impacts require that industrial processes operate such that their inherent nonlinearities are emphasized. Thus developing and implementing controllers which are suitable when process nonlinearities must be accounted for, is of great interest both academically and for industry. Plenty of research papers on the analysis and control of nonlinear systems are available and many different methods have been proposed. Such approaches are feedback linearization, back stepping control, sliding mode control, trajectory linearization based on Lyapunov theory, those based on Differential Geometry concepts, as well as those based on artificial computing approaches etc. A few examples are from (Desoer and Wang, 1980; Hunt et al., 1992; Enqvist and Ljung, 2004; Schweickhardt and Allgower, 2007; Marinescu, B., 2010; Zhai and Qian, 2012; Hammer, Jacob, 2014).

Another challenging aspect is if the system to be controlled is Multi-Input Multi-Output (MIMO). In MIMO systems the coupling between different inputs and outputs makes the controller design to be difficult. Generally, each input will affect every output of the system. Because of this coupling, signals can interact in

unexpected ways. One solution is to design additional controllers to compensate for the process and control loop interactions (Meng, Zhao-Jun et al., 2010; Lee, II Hwan, 2011; Sujatha, and Panda, 2013; Ghosh, A., and Das, S. K., 2012; Leena, G., and Ray, G., 2014).

2.3 Review of the existing literature for the CSTR modelling and control design

The Continuous Stirred Tank Reactor (CSTR) has been selected as a case study in this thesis. Reactors are the primary focus of many chemical plants. Many variables must be regulated in a reactor for good process operation. This section of the chapter presents a review of the control design methods for the nonlinear MIMO exothermic CSTR process. The control of such a process demands proper design because of the nonlinearities, the loop interactions and the potentially unstable dynamics. In these systems, control based on the linear methods for design alone such as the conventional linear PID controllers may not always yield satisfactory results. The linear controllers have been the sole selection over the years even though many other advanced control methods have been developed, is mainly because of their ability to produce satisfactory results for most control problems, if these controllers are properly tuned and installed. They are simple, transparent and feasible. It must also be emphasized that the literature on robust control, monitoring, and optimization methods is available in plenty, with each method presenting a solution to a particular problem.

According to (Wayne Bequette, 1991) the following common process characteristics cause difficulty in the control of both linear and nonlinear systems: the interactions between the control variables and the controlled variables, the unmonitored state variables, unmonitored and frequent load disturbances, higher order and distributed processes, uncertain and time varying variables, constraints on the control and state variables, and dead time on the inputs and the outputs. Such features of the multivariable nonlinear systems illustrate the need for and difficulty of feedback control system design. Research efforts have focused on presenting control design methodologies that can handle many of these features. However, it may be accepted that presently there is not one methodology that will solve all the control problems that can prevail in the modern plants. This is because; different plants have different problems to be solved.

In general, the nonlinear control algorithms can be classified as:

- Model-Based Control
- Intelligent Control

The thesis is focussed on the former method for the design of controllers for nonlinear systems. These are then reviewed in the following.

2.3.1 Model based controller design method

The objective of this section is to review the existing literature on the control design strategies on model based control based that have been used over the years for the solution to nonlinear problems, specifically for the CSTR. Table 2.1 provides the number of publications considered and Figure 2.1 illustrates the graph of the reviewed papers year wise on model based control from 1966 to 2015. For this review a total of 120 papers are considered.

Table 2.1: Number of the reviewed publications for model-based control verses the year

NUMBER OF PUBLICATIONS IN THE YEAR		
REFERENCE	**YEAR OF PUBLICATION**	**NUMBER OF PUBLICATIONS**
(Bristol, 1966)	1966	1
(Uppal and Ray, 1974)	1974	1
(Desoer and Wang, 1980).	1980	1
(Economou and Morari, 1986); (Li and Luyben, 1986)	1986	2
(Grosdidier and Morari, 1987); (Luyben, W and. Luyben, M., 1997)	1987	2
(Kravaris and Polanski, 1988)	1988	1
(Skogestad and Morari, 1989); (Daoutidis and Kravaris, 1989)	1989	2
(Kravaris and Kantor, 1990a); (Kravaris and Kantor, 1990b); (Chien and Fruehauf, 1990); (Henson and Seborg., 1990)	1990	4
Bequette., 1991)	1991	1
(Astorga, 1992); (Pottmann and Seborg.,1992)	1992	2
(Seborg, 1994); (Hovd and Skogestad, 1994)	1994	2
(Isidori, 1995)	1995	1
(Viel, et al, 1997)	1997	1
(Marchand and Alamir, 1998); (Marchand et al., 1998); (Gagnon et al., 1998)	1998	3
(Aris and Amundson, 2000)	2000	1
(Antonelli and Astolfi, 2001)	2001	1
(Chen and Seborg, 2002); (Panda et al., 2002); (Rangaiah and Toh, 2002)	2002	3
(Antonelli and Astolfi, 2003); (Chisci, et al, 2003)	2003	2
(Bequette, 2004); (Enqvist and Ljung, 2004);.(Hahn and Marquardt, 2004)	2004	3
(Wang and Li, 2005); (Guay, et al., 2005); (Hedrick and Girard, 2005); (Vojtesek and Dostal, 2005); (Ye Xudong, 2005)	2005	5
(Cai and Xiong, 2006); (Garelli, et al.,2006); (Nordfeldt and Hagglund, 2006); (Selvakumar et al., 2006); (Tavakoli et al., 2006); (Yang, et al.,2006)	2006	6
(Jingjing et al, 2007); (B. Wayne Bequette, 2007)	2007	2
(Rehan, et al, 2008); (Cai, et al., 2008); (Jouili et al., 2008); (Wu, et al.,2008)	2008	4
(López, et, al, 2009); (Bartolini, et al.,2009); (Bakosova and Vasickaninova, 2009)	2009	3
(Rahul and Singla, 2010); (Kamala and Renganathan,	2010	10

2010), (Jevtovic and Matausek, 2010); (Vojtesek and Dostal, 2010); (Cai, et al., 2010); (Ganesh and Chiambaram, 2010); (Hadisujoto et al., 2010); (Marinescu, 2010); (Vinodha and Prakash, 2010); (Fikar, 2000)		
(Allgower et al, 2011); (Dostal, et al, 2011); (Hong, et al., 2011) (Anitha and Subbulekshmi, 2011); (Ge, et al., 2011); (Hirama et al., 2011); (Lee, et al., 2011); (Li, et al., 2011)	2011	8
(Bachir et al, 2012), (Saleh and Mohamed, 2012); (Bachir et al, 2012); (Gholami et al, 2012); (Gao et al., 2012); (Mohamed, et al, 2012); (Hong and Cheng, 2012); (Lopez et al, 2012); (Kamala and Renganathan, 2012); (Ghosh, and Das., 2012,); (Lengare, et al., 2012); (Chen et al., 2012); (Chidambaram and Rajapandiyan, 2012); (Fu et al., 2012); (Mehta and Mahji, 2012); (Kumar and Khanduja, 2012.); (Liu, et al., 2012); (Maghade and Patre, 2012); (Ramzi et al., 2012); (Rosinova, and Kozakova, 2012); (Zhai, et al., 2012)	2012	21
(Hoang et al, 2013); (Yasabie and Sahu, 2013); (Rao and Chimmiri, 2013); (Sujatha, and Panda, 2013); (Chen, et al., 2013); (Dong-Juan et al., 2013); (Kurniawan, et al., 2013)	2013	7
(Wang, et al., 2014); (Ding Li et al., 2014); (Leena, and Ray., 2014); (Jacob, 2014); (Chen and Yun, 2014); (Garrido and Morilla, 2014); (Kwon and Choi, 2014); (Nunes, et al., 2014); (Ulrich and Jurek, 2014); (Yu and Liu, 2014); (Zhu et al. 2014)	2014	11
(Kaldmae and Moog, 2015); (Zhang et al., 2015); (Rehman, and Peterson, 2015); (Vivekananathan and Ponnusamy, 2015); (Yang and, Liu, 2015); (Yang and Wang ,2015); (Dana Copot et al.,2015); (Prashant and Sharad, 2015); (XU Jiao, et al., 2015); (Dongya Zhao et al., 2015)	2015	10

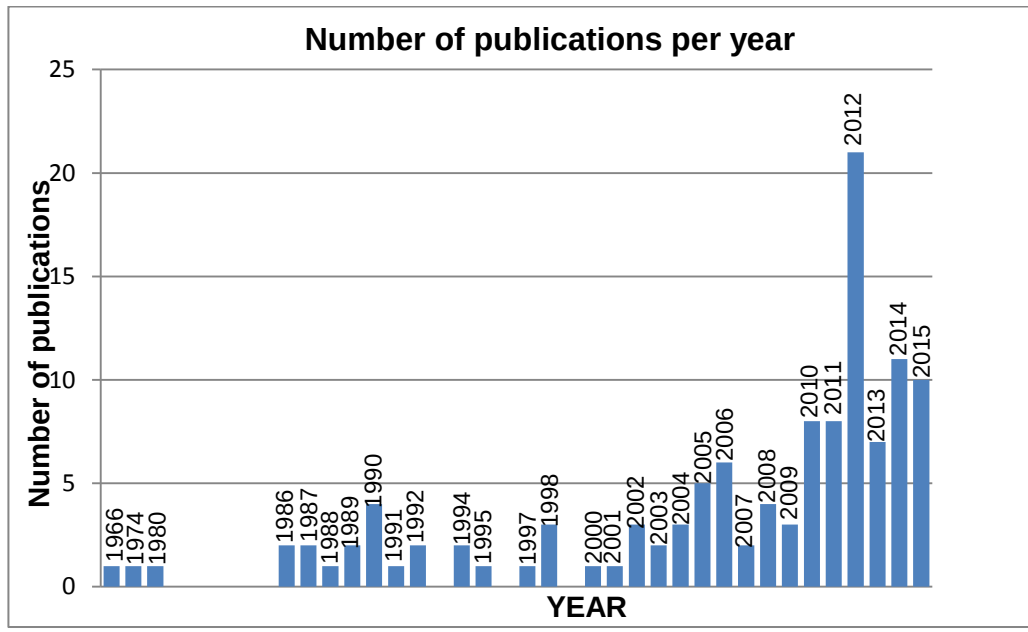

Figure 2.1: Number of publications year by year

Model-based control can be defined as a mathematical and visual technique of solving the problems associated with complex control systems design. In these control systems design methods involves four steps: namely: modelling of the plant, analysing and synthesizing of the controller, simulation of the plant and controller, and finally, merging all the phases by implementing the closed loop control. The model-based nonlinear control design techniques are presently the topic of much interest because of the possibility of employing the process nonlinearities directly in the control methodology. For example, (Seborg, 1994) presented an article *"perspective on advanced control strategies for process control"* where the controllers are classified according to the degree to which they have been used in industry and concluded by the remarking that most advanced control strategies continue to be model based but intelligent control techniques are receiving widespread attention and that the key research issue is how to integrate the intelligent control based strategies with the model based approaches in a practical and cost effective manner Model-Based Control techniques contain algorithms in which an explicitly separately identifiable dynamic model of the plant is used. Nonlinear Internal model control (Economou, et al., 1986; Henson and Seborg, 1991), nonlinear model predictive control (Silva and Kwong, 1999) Lyapunov based control and those based on Differential geometric concepts (Kravaris and Kantor, 1990), and Multivariable control (Jones and Tham, 1987; Tham et al, 1991) are typical examples. These methods share common characteristics, namely (Seborg, 1994);

- They are all designed on a mathematical model of the plant and hence their robustness and stability can thus be evaluated analytically.
- All these methods use the inverse of the process model either explicitly or implicitly to calculate the necessary control action.

A brief introduction of the principle of operation and a review of the model-based controller design methods are given in the following sections together with a summary of the applications. The objectives and results of the controller design methods are presented in Table 2.2. The review is categorized under five different control schemes: those based on differential geometric concepts, nonlinear model predictive control, nonlinear internal model control, those based on Lyapunov stability and those based on multivariable control respectively.

2.3.1.1 Differential geometric concepts:

Over the years, differential geometry has been used as an effective tool for the analysis and design of nonlinear control systems. In these methods, linearity of

the closed loop system is sought in some sense. Differential geometric concepts allow a certain class of systems to be linearized using the state feedback and coordinate transformations. The primary issue is the design of nonlinear change of coordinates and nonlinear feedback that make the system behave in a linear manner. An overview of this approach is given by (Isidori, 1995, Nijmeijer and Van der Schaft, 1996, Kantor, 1987, Henson and Seborg, 1990, Kravaris and Kantor, 1990; Yu, Ding Li et al., 2014). Similarly there is a good overview of general nonlinear approaches to chemical process control system design by (Bequette, 1991). One of the main contributions of differential geometric approach is input/output linearization which seeks to reduce the original nonlinear system to a linear system in an input/output sense via state feedback. There is a wide range of possible control laws using output and state feedback for output tracking, input-state and input-output linearization, and decoupling control. These methods have been applied to the CSTR problem to obtain exact state linearization, exact input/output linearization and state linearization with disturbance rejection (Ye Xudong, 2005; Zhang and Chen, 2014; Yu, and Liu, 2014; Zhu et al., 2014; Yang et al., 2006). As an example, the work of (Hong, et al., 2011) is based on stabilization and tracking control for a class of nonlinear systems. A nonlinear state feedback stabilization control is proposed which guarantees global asymptotic output and state tracking with zero tracking error in the steady state. The proposed methodologies are illustrated using simulation examples of chaotic and unstable dynamics. The work of (Yang and Liu, 2015) is based on adaptive output feedback controller design for a MIMO nonlinear system with unknown nonlinear parameters, uncertain nonlinearities, bounded disturbance, unmodeled dynamics and uncertain control parameters. Through the design and the simulation results the effectiveness of the proposed controller is proved. In (Chen, Z., et al., 2012) robust output tracking control design is proposed for a general class of uncertain non-affine nonlinear systems. The design employs feedback linearization, coupled with a high gain filter which is built to estimate the feedback linearization error. The simulation results show the effectiveness of the approach. Input-output feedback linearization technique is used in this study and therefore is covered in detail in Chapter 6. This is a control design methodology that uses a feedback signal to cancel the inherent nonlinear dynamics and to create a linear differential relation between the output and a newly defined synthetic input.

2.3.1.2 Nonlinear model predictive control

The common way of controlling process systems with strong nonlinearities is to apply model based predictive controllers where a detailed dynamic process model is used in an optimization framework. The model predictive control (MPC) has been used widely in the process industries because of its many appealing features such as handling multivariable systems with time delays. In addition, the constraints on manipulated inputs, states and output variables are explicitly handled in the formulation of the optimization problem (Panjapornpon, 2005). Model predictive control is a class of computer control algorithms that control the future behavior of a plant through the explicit use of a dynamic model of the plant. At each control interval, the model predictive algorithm computes an open loop sequence of the manipulated variables, for a time termed a control horizon in order to optimize the process behavior in the time ahead known as the prediction horizon. Process constraints and any changes in the process objectives or operating conditions can be implemented on line. A new process measurement is injected in the control loop and the entire optimization is repeated at subsequent control intervals. At the heart of the model predictive controller is the model, which is used not only to forecast the effects of future inputs, but also to estimate the current state of the plant from the given history of the past measurements and controls (Khalid, 2006).

MPC technology was originally developed for power plant and petroleum refinery control applications, but can now be found in a wide variety of manufacturing environments including chemical, food processing, automotive, aerospace, metallurgy, and pulp and paper (Thomas Badgwell and Joe Qin, 2001). Further introductory literature on model predictive control can be found in several text books such as (Maciejowski, J.M., 2002; Byrd, Richard H. et al, 2006) although most processes are inherently nonlinear, the vast majority of MPC applications to date are based on linear dynamic models. Nevertheless, there are cases where nonlinear effects are significant enough to justify the use of the nonlinear model predictive control technology. These include regulator control problems where the process is highly nonlinear and subject to large frequent disturbances like the continuous stirred reactor or servo control problems where the operating points change frequently.

Nonlinear Model Predictive Control (NMPC) is an effective strategy for controlling nonlinear chemical processes with constraints and time delays (Sistu and

Bequette, 2004). 2005). NMPC offers great potential in those areas where process nonlinearities are strong and it is required to improve performance or even to achieve stable operation. However, (Bequette, 2007) presented a paper where he provided a concise overview of some of the challenges of developing and implementing the non-linear predictive control algorithms, with regards to his experience and the published results. He singled out the optimization problem which leads to solution with multiple minima, plant mismatch with additive inputs which result into poor performance when actual disturbances occur in the inputs. Therefore designers of the NMPC techniques should give more attention to the problem of disturbance estimation, prediction and compensation. Also, model development remains an ongoing challenge and it is usually not clear whether the additional effort of developing a non-linear model, instead of a linear model, will result in an economic benefit. He noted that while many investigators have developed non-linearity measures, these are not easy to apply in practice and usually require the *apriori* development of a non-linear model. For a more detailed discussion of the theoretical issues pertaining to the NMPC design methods, there are review articles by Mayne et al, 2000 and Allgower et al, 1999.This control strategy is not used in this research project and therefore is not exhaustively reviewed.

2.3.1.3 Nonlinear Internal model control:

The scheme is one of the most popular methodologies in the process industry because of its simplicity, capability to reject disturbances and robustness. It can be used both for linear and nonlinear systems. A first step toward a practically applicable nonlinear controller design technique was proposed (Economou and Morari, 1986) where it was shown that the nonlinear Internal Model Control (IMC) works well even in the case where no linear controller can yield stable behavior. Since then, the IMC has been applied in several areas as chemical processes such as CSTR (Varshney et al., 2009; Zhang and Li, 2009), batch reactors (Azwar et al., 2006; Liu et al., 2010), pH control (Jalili-Kharajoo et al., 2003; Wang and Shi, 2005), and distillation (Han and Clough, 2006; Li et al., 2009). A unifying review of the internal model control type schemes was first presented by (Garcia and Morari, 1982) who defined the IMC structure for single-input single-output, discrete-time systems and further as a nonlinear controller by (Economou et al, 1986) who developed a nonlinear IMC by employing an approximate inverse of the model, using local linear approximation. As the name suggests, the scheme utilizes the inverse of the model of the plant to design the controller. In

order for the IMC structure to be stable, certain conditions must be fulfilled namely; the plant model must be an exact match of the plant and the inverse of the model must exist. When the model is an exact match of the plant then stability of both controller and plant is sufficient to guarantee overall system stability. Similarly, when the model is exact match of the plant, and the controller is the inverse of the model, then the controller is perfect and the plant output is equal to the reference signal, hence there will be no offset in the plant output if the reference signal is asymptotically constant.

IMC is very popular and continues to enjoy widespread popularity in industrial control applications due to its fine disturbance rejection capabilities and robustness. More information on the IMC can be found in (Alexander et al, 2002; Datta and Ochoa, 1996; Henson and Seborg, 1991; Morari. and Zafiriou, 1989; Patwardhan and Madhavan, 1998; Wang, et al 2001; Xie. and Rad., 2000; Chien and Fruehauf, 1990; B, Wayne Bequette, 2004). This principle is used in the design of decentralized controllers for the CSTR model under this study.

2.3.1.4 Lyapunov based controller design:

This section gives an overview on some of the approaches of the Lyapunov design methods that have been used for the CSTR. Lyapunov theory allows in particular determination of the region of attraction of the stable equilibrium points. Lyapunov based design has been a primary tool for nonlinear control system design, stability and performance analysis since its introduction in 1982 by the Russian mathematician Alexandr Mikkailovich Lyapunov. Lyapunov's work, titled: *The General Problem of Motion Stability* includes two methods for stability analysis: the linearization method and the direct method The linearization draws its conclusions about a nonlinear system's local stability around an equilibrium point from the stability properties of its linear approximation (Jianying Gao, 2004). The direct method determines the stability properties of a nonlinear system by constructing a scalar energy-like function for the system and examining the functions time variations. The details of these two methods are summarized in many control engineering books, for example (Slotine and LI, 1991). The Lyapunov direct method is the most important tool for the analysis and design of nonlinear systems. The use of Lyapunov-based methods for robust controller design in conjunction with differential geometric methods was first introduced by Ha and Gilbert (1987). They addressed the case where the nominal state feedback provides linearity of both the state equations and the output. For example, (Antonelli and Astolfi, 2003) made use of methodologies and tools from

the Lyapunov theory in the design of bounded output feedback control laws for the temperature stabilization of a class of CSTRs with exothermic or endothermic reactions. It is shown that these controllers yield global asymptotic stability and do not require precise knowledge of the system parameters. In (Ge, S.S. et al., 2011), adaptive tracking control for a class of uncertain MIMO nonlinear systems with input constraints is proposed and closed loop bounded stability is achieved via the Lyapunov synthesis through simulation studies.

2.3.1.5 Multivariable Control:

Because of the presence of interactions, the multivariable processes are difficult to control simply due to several output variables being monitored simultaneously by manipulating several input channels. There are several multivariable control techniques available such as those based on the Nyquist arrays which are based on frequency domain techniques for interaction analysis and for design of pre-compensators and post compensators (Maciejowski, 1989; Chen and Seborg, 2002), and sequential closing design methods where each controller is designed sequentially (Hovd and Skogestad, 1994; Rangaiah and Toh, 2002; Rehan, M., et al, 2008), In this method, the controller of the quickest loop is first tuned. This is done by considering the case of the selected input-output pair. The loop is the closed, then tuned after which the other loops are then tuned sequentially and so on. In the Independent design method, each controller is tuned on the basis of paired transfer functions while satisfying some specified constraints as a result of process interactions (Skogestad and Morari, 1989). Then there is the more popular method known as the Biggest Log-Modulus Tuning (BLT) method of (Luyben, 1986; Jevtovic and Matausek, 2010; Ghosh, A., and Das, S. K., 2012, Lengare, et al., 2012; Wang, et al., 2014) where every controller for the multi-loop system is first designed using the general classical techniques by ignoring the process coupling from the other loops. After which the couplings are factored in by detuning each set of controller parameters until some performance index is reached. The Relay auto-tuning of (Shen and Yu, 1994) applies the relay feedback methodology to design each corresponding SISO controller. A review of the three different MIMO controller design strategies is carried out, below:

Decoupling control ensures that the MIMO control system is decoupled by incorporating a pre-compensator to compensate for the process and loop interactions, so that each output is controlled independently (Luyben, W. and, Luyben, M., 1997). This control strategy has been used by several other authors

over the years with success, among them (Luyben W. and. Luyben, M., 1997; Jevtovic and Matausek, 2010; Ghosh and Das, 2012; Lengare, et al., 2012; Wang, et al., 2014). For example, the work of (Jevtovic and Matausek, 2010) is focused on an ideal decoupler plus PID controller for optimization in the case of constraints on robustness and sensitivity to the measurement noise. The validity of the proposed tuning is confirmed on a TITO test bench process. The study by (Ghosh and Das, 2012) is based the continuous-time, linear time-invariant, non-minimum-phase, unstable, MIMO plant. The control strategy is to first perform input-output decoupling in the open-loop and then effecting zero placements of the decoupled loops using SISO periodic feedback. The study achieves superior multi-channel output gain margin compensation and arbitrarily large multi-channel output gain margin is also found out. An example is provided to demonstrate the design procedure and the controller capability.

Decentralized control on the other hand tries to control the MIMO process by a suitable decoupling into SISO control loops. However, the decentralized controllers cannot eliminate the interactions of the plant. Thus, in order to design decentralized controllers, input output pairing is performed based on the Relative Gain Array (RGA) method proposed by (Bristol, E. H., 1966), in which the decentralized control design is made possible by finding the best control structure pairing between the controlled and manipulated parameters that tries to reduce the couplings. This implies that two independent diagonal controllers can be designed while disregarding the coupling between the input pairs. After that an interaction measure is designed to account for the effect of the coupling on the stability and performance of the whole system (Wuhuau et al., 2010; Rosinova and Kozakova, 2012; Kurniawan, E., et al., 2013).

For example, (Wuhuau et al., 2010) proposed an approach of decentralized PID controller design for MIMO processes by first finding the input/output pairing by using the RGA-Niederlinski index criteria; the equivalent-transfer functions of the individual loops are then derived. Based on the equivalent transfer functions decentralized PID controllers are tuned to stabilize the MIMO processes independently. To demonstrate the efficiency of the proposed approach, three industrial MIMO processes with different dimensions and interaction modes are employed.

(Seborg, D. E, 1994) presented *"a perspective on advanced control strategies for process control"* where the controllers are classified according to the degree to which they have been used in industry and concluded by remarking that the most

advanced control strategies continue to be the model based but the intelligent control techniques are receiving widespread attention and that the key research issue is how to integrate the intelligent control based strategies with model based approaches in a practical and cost effective manner.

Wang and Li, (2005) proposed nonlinear PI controllers for a class of nonlinear singularly perturbed systems. The original MIMO system is decoupled into two reduced order systems and the nonlinear PI controllers are applied to each decoupled subsystem. The results are combined to construct a composite controller of the full-order system. Excellent performance results of the presented scheme are achieved.

(Wu, Y.-X., et al., 2008) proposed a robust adaptive controller for a class of MIMO uncertain nonlinear systems which combines the adaptive Backstepping with sliding mode control. The results of numerical simulation for output tracking control are presented to show the suitability of the proposed approach.

On the basis of the review done above, Table 2.2 is a brief summary of the review papers carried out on the model based methods for the design of the controllers for the CSTR process highlighting the objectives of the design together with the findings, shortcomings and recommendations.

Table 2.2: Review papers on model based control design for CSTR.

Reference Paper	Controlled variables	constraints	Controller Description (methodologies)	Theoretical development	Deliverables: Achievements and drawbacks
(Hoang et al, 2013)	Reactor temperature control	steady state multiplicity and the exhibition of minimum phase behavior	Lyapunov Control law	Thermodynamics stability analysis and its use for nonlinear stabilization of the CSTR	A description of the thermodynamic availability concept. Its use for open loop dynamic analysis of the non-isothermal CSTR. Its use for Lyapunov based control laws. Derivation of the non-isothermal CSTR. Illustration of the performances of the controller by simulations. Comparison of the controller with a proportional control strategy.
(Yasabie and Sahu, 2013)	Temperature control and Concentration control	Noise in the form of random inputs	1. Model Reference Adaptive Controller(MRAC) 2.Conventional Controller	Provides an understanding of how to implement an adaptive controller and to compare an adaptive controller with conventionally designed controller in various situations.	Demonstrated that while the adaptive controller exhibits superior performance in the presence of noise the convergence time is typically large (greater than 10 seconds) and there is large overshoot.
(Rao and Chimmiri, 2013)	Temperature and concentration control	Deterministic disturbance and stochastic load disturbance generated through random Gaussian noise	PID and a nonlinear internal model control (NIMC) strategy	Nonlinear Model Based Control of Complex Dynamic Chemical Systems which is supported by a nonlinear model based estimator	A nonlinear internal model control (NIMC) with an estimator is designed NIMC strategy is evaluated by applying it for the control of a non-isothermal CSTR and a homo-polymerization reactor. The results show the superior performance of the estimator based NIMC strategy over the conventional PID controllers.
(Bachir Daaou et al, 2012)	Concentration and Reactor temperature	Noise and model uncertainties	Linearizing Feedback Controller and Lyapunov stability theorem based controller	Development of an observer-based nonlinear control scheme for a CSTR.	The closed-loop dynamic simulations are developed to illustrate the effectiveness of the proposed approach

(Saleh and Mohamed, 2012)	Tank level and mass concentration control	External disturbances as well as parametric uncertainties are introduced into the model	PI Controller Back stepping controller and Lyapunov function-based controller	Nonlinear control of a three-state CSTR using the back stepping technique. The back stepping controller is first designed. Then an augmented back stepping control law is designed, based on the sliding mode control theory to add robustness to the proposed controller.	The proposed controllers are shown to drive the output trajectories to their respective desired values, hence, ensuring the stability of the closed-loop system. Finally, several simulation studies are presented to illustrate the effectiveness of the proposed control laws.
(Bachir et al, 2012)	Temperature control	Modeling uncertainties and noisy measurements.	Observer-based control scheme using feedback linearization technique and Lyapunov stability technique**.**	Development of Linearizing Feedback Control with a Variable Structure Observer.	Observer-based control scheme using feedback linearization is addressed. The Lyapunov stability is used to establish the stability of the system. Performance is illustrated *via* simulations which show that the controller is able to regulate the reactor temperature in the presence of modeling uncertainties and noisy measurements.
(Gholami et al., 2012)	Temperature, and Concentration control	Nonlinear processes imposed by input constraints as: the rate of heat input and the temperature	A Fault-Tolerant Control (FTC) methodology has been presented. The proposed methodology uses a combination of Feedback Linearization and Model Predictive Control (FLMPC) schemes	Fault-Tolerant Control of a Nonlinear Process with Input Constraints	FTC is a challenging issue when the process inputs face constraints. Two sets of fault scenarios were organized to address the two critical input constraints. The obtained results demonstrate the successful activation of the proposed method by replacing the candidate control configurations via the dedicated supervisor.
D. X. Gao et al., 2012	Temperature and density are the state and output variables to be controlled while control variable is	NIL	1.State Feedback Linearization 2.Optimal control	Feedback Linearization and Optimal Control Approach for Bilinear Systems.	State feedback exact linearization approach of optimal control for bilinear systems is designed by solving the Riccati equation and introducing state feedback with state prediction. Simulation results show

	the flow rate of the cooling.				that the proposed approach is valid and easy to implement
(B. Mohamed, et al., 2012)	Concentration and temperature reactor control with feed low rate and jacket temperature as the manipulated variables.	Noisy measurements and dynamics uncertainty	1.Nonlinear observer design 2.Input-output feedback linearization controller design 3.Lyapunov stability technique	Observer-based input-output linearization control of a multivariable continuous chemical reactor	The observer proposed offers the advantage of only one tuning parameter. The observer is coupled with a nonlinear controller. The controller is constructed through feedback linearization for concentration and temperature control. Lyapunov stability is used to establish the stability of the closed loop system. The proposed control exhibits a satisfactory performance.
(Hong and Cheng, 2012)	The inlet coolant temperature is the input-regulated variable used as the manipulated variable to maintain proper reactor temperature control as the system output.	Parameter uncertainty	Nonlinear Predictive Adaptive Controller and Nonlinear Disturbance Observer (NDO) for CSTR process and a Lyapunov function to analyze the stability	NPAC is presented to solve the presence of parameter uncertainty in strong nonlinear systems. The controller is composed of an optimal NPAC and a NDO. NDO is used to estimate the steady-state response error, and the optimal NPAC improves the system stability.	CSTR tracking with uncertain-parameter problem has been investigated. The NPAC scheme based on NDO was implemented. The presented control laws can guarantee that the steady-state response error asymptotically converges to zero. The proposed compensation method can greatly reduce the effect of disturbances and improve the system tracking accuracy and robustness.
(Ricardo Aguilar Lopez et al., 2012)	The reactor temperature is regulated by means of water flowing through a cooling jacket.	The temperature measurements are corrupted by noise with a ± 5% around the current temperature value.	1.I/O Linearizing Controller; 2. High-order Sliding-mode Controller; 3.Sliding-mode controller. 4. Lyapunov-type analysis	Temperature Control of Continuous Chemical Reactors under noisy measurements and model uncertainties. The design is based on a sliding-mode uncertainty estimator The estimation of convergence is done by the Lyapunov-type analysis	A sliding-mode observer based I/O Linearizing control law is designed. It is considered that the reaction heat is unknown and noisy measurements exist such that an uncertainty estimation methodology is based on algebraic-differential concepts and a sliding-mode frame work. Numerical simulations in which a class of oscillatory chemical system is used as application example to show the

					effectiveness.
(Allgower et al, 2011)	Concentration and Temperature and coolant temperature as the only manipulated variable	multiple hard output constraints imposed on a CSTR	A blending or sliding mode controller is utilized	The objective is to design a control system that can satisfy the three different constraints using only one control input, namely: the coolant temperature.	It is shown analytically and with simulations, that there are critical combinations of constraints, where robust constraint satisfaction cannot be guaranteed. As a consequence violation of at least one constraint has to be allowed.
(P. Dostal, et al., 2011)	The reactant temperature control	Changes of the input signals in strongly nonlinear regions.	Static Nonlinear and Dynamic linear Controller	Nonlinear Control of a Chemical Reactor. The developed control strategy is also suitable for other similar technological processes such as tubular chemical reactors.	The strategy is based on a factorization of the controller into linear and nonlinear part. The nonlinear part is approximated through recursive parameter estimation. Tuning is via pole placement. Simulation demonstrates its usefulness for greater changes of input signals in the strongly nonlinear regions.
(Dostál, et al., 2011)	The coolant flow rate is taken as the control input and the controlled output is the reactant temperature.	Changes of the reactants volumetric flow rate.	Static Nonlinear Part (SNP)and Dynamic Linear Part (DLP) of the controller	Simulation of nonlinear adaptive control of a continuous stirred tank reactor	The control strategy is based on factorization of a controller into the adaptive Dynamic Linear Part (DLP) and the Static Nonlinear Part (SNP). DLP design employs simulated Steady-state characteristics of the process. Then, the DLP and a nonlinear model of the CSTR are approximated by a continuous time external linear model. Simulation results demonstrate the applicability of the control strategy and its usefulness for other similar nonlinear technological processes.
(Rahul and Singla, 2010)	Temperature and Concentration control	Nil	Adaptive nonlinear controller and PID controller	Adaptive and PID controllers are tested by using Matlab/Simulink program and their performance is compared	The results prove that adaptive controllers are appropriate to be used under non-linear difficulties.

				for different temperature and concentration. Adaptive controller exhibits superior control in the presence of a nonlinearities. This is illustrated on the control of non-linear system (CSTR).	
(Pablo A. López Pérez, et, al., 2009)	Temperature control	Chattering phenomenon caused by the discontinuity of the input injection	Sliding-mode controllers under the frame of the differential algebra	Dynamic nonlinear feedback for temperature control of continuous stirred tank reactor with complex behavior	Sliding-mode controllers under the frame of differential algebra are designed. An estimator is coupled to the proposed controller to infer the measured and uncertain terms. The reactor temperature trajectories are controlled successfully in comparison with other nonlinear controllers.in dismissing the chattering of the standard sliding-mode controllers.
Jingjing et al., 2007)	Concentration is the output, and the temperature of the coolant is the input of the CSTR system	High nonlinearity, multiple operating points, and a wide operating range.	Model predictive control (MPC). MPC based on Mixed Logical Dynamical (MLD) model	Modeling and Control of a Continuous Stirred Tank Reactor based on a Mixed Logical Dynamical Model (MLD)	A mixed logical dynamical (MLD) model based-Model Predictive Control (MPC) is proposed for CSTR with high nonlinearity, multiple operating points, and a wide operating range. The control law is synthesized by a moving horizon technique for an optimal transition. Drawbacks: Computation complexity which increases with the number of logic variables. More efforts are required to solve these problems.
(B. Wayne Bequette, 2007)	Temperature regulation	Plant mismatch and disturbances in the inputs	Nonlinear model predictive control	An overview of Non-linear Model Predictive Control (NMPC) is presented, with an extreme bias towards the author's experiences and published results.	Overview of some of the challenges of developing and implementing NMPC algorithms. Optimization problem which leads to multiple minima solution, plant mismatch with additive inputs which resulting in

					poor performance when disturbances occur in inputs. Therefore designers to give more attention to disturbance estimation, prediction and compensation
(Antonelli and Astolfi, 2003)	Ttemperature stabilization	Input constraints and uncertainty on the kinetic parameters	Output feedback control laws and Lyapunov theory	Lyapunov theory is used in the design of bounded control laws for the temperature stabilization of a class CSTR's with exothermic and endothermic reactions	The proposed approach offers some important advantages including constraint handling capability and computational simplicity: Some numerical simulations, illustrating the theoretical results, are presented.
(L. Chisci, et al., 2003)	Reactor temperature (controlled output) and the temperature of the coolant stream (manipulated input).	Stringent input and state constraints	Linear Parameter Varying (LPV) embedding techniques in the design of a gain-scheduling controller.	Set-point tracking for a class of constrained nonlinear systems with application to a CSTR	A case-study of constrained nonlinear control relative to the temperature control of a Continuous Stirred Tank Reactor (CSTR). The use of Linear Parameter Varying (LPV) embedding techniques along with an admissible set theory allow fast and safe tracking in presence of stringent input and state constraints
(Antonelli and Astolfi, 2001)	Temperature stabilization	Uncertainty in inputs and kinetic parameters	Lyapunov adaptive Linearizing technique and Global stabilization by state feedback	Stability analysis	It is shown that these controllers yield Global Asymptotic Stability and do not require precise knowledge of the system parameters
(Marchand and Alamir, 1998)	Concentration and Temperature control	Nil	The design of the feedback is based on the knowledge of a control Lyapunov function**.**	State feedback is presented for the stabilization of a nonlinear system based on the generation of open-loop trajectories. Lyapunov theory is given applicable to a CSTR case study.	The paper gives conditions on Open-loop trajectory generators in order to use them for the design of a nonlinear feedback. The construction of such a feedback is proposed on a CSTR case study.
(Nicolas Marchand and Mazen Alamir, 1998)	Reactor temperature is the controlled output and the jacketed fluid temperature is	Time lag in the control input.	The state feedback control and Lyapunov theory	The application of the feedback to a Continuous Stirred Tank Reactor, known to exhibit unstable steady states, is provided.	A new state feedback is presented for the stabilization of nonlinear systems. It is based on the generation of open-loop trajectories to design a stabilizing feedback. A

	the manipulated variable and				general theoretical background based on Lyapunov theory is given. The application of the feedback to a CSTR known to exhibit unstable steady states is provided.
(Kravaris, and Palanki, 1988)	Concentration control	Structured model uncertainty	Robust Nonlinear State Feedback Under Structured Uncertainty and Lyapunov-based approach is to guarantee uniform ultimate Boundedness.	Given upper bounds on the modeling error of the nonlinear process, design a nonlinear state feedback law that guarantees stability and performance for all perturbations within the given bounds**.**	A robust nonlinear state feedback is proposed for uncertainties considered as a class of bounded perturbations to the state model. A Lyapunov-based approach is used to guarantee uniform ultimate boundedness. The control of the process was simulated using the "true" process, and the robust controller. It is observed that the output of the true process is ultimately bounded, as predicted.
(Viel, et al., 1997)	Temperature and concentration control	Input constraints with strong uncertainties on the dependence of the kinetic function with respect to the temperature.	I/O state feedback linearization and robust state observer	For a general class of CSTR's, a set of controllers that guarantee the global temperature stabilization in spite of strong uncertainties and the dependence of the kinetic functions with respect to the temperature is proposed. The main feature of these controllers lies in their capability of handling input constraints in some instances	A set of controllers that can guarantee the global temperature stabilization of CSTR in spite of strong uncertainties and the dependence of the kinetic function with respect to the temperature have been proposed. The uniform Boundedness of the concentrations with respect to the temperature was the key point in the proofs. A practical consequence of these results lies in the opportunity of operating chemical reactors at unstable open-loop steady states that correspond to optimal operating conditions.
(Dale Seborg,	General perspective of	Nil	1.Conventional strategies. 2. Classical techniques.	The paper provides a personal perspective on the current status of Advanced process	Most prominent methods are discussed critically with emphasis placed on key design issues and

1994)	process control variables		3. Advanced control (widely used techniques). 4. Advanced control (new techniques with some industrial applications). 5. Advanced control: proposed strategies with few industrial applications.	control strategies by classifying them according to the degree which they have been used in industry.	unresolved research problems.
(Kravaris and Kantor, 1990)	Concentration and temperature control	Nil	Mathematics and systems theory background, including linear tools from differential geometry, nonlinear inversion, and zero dynamics.	Review for geometric methods in nonlinear process control. The concept of feedback linearization of nonlinear systems is introduced. Gives background theory	Reviews theoretical results that are relevant to control applications and provides representative chemical engineering examples on the geometric methods for nonlinear process control
(Kravaris and Kantor, 1990)	Nonlinear pH Control in a CSTR.	Nil	The Internal Model Control (IMC) and Globally Linearizing Control (GLC) structures	Review of The Internal Model Control (IMC) and Globally Linearizing Control (GLC) structures for nonlinear processes	The main mission is to solve the feedback linearization problems and to show their application in controlling nonlinear processes (controller synthesis).
(Daoutidis and Kravaris, 1989)	Case 1. The concentration and temperature are the outputs and the manipulated input is the heat input in the third vessel. Case 2. The inlet temperature is controlled and the manipulated input is the heat input in the first vessel. Case 3. The major inlet concentration	Presence of disturbances to inlet concentration and temperature	Feed forward/State feedback control law	The general feedforward/feedback control problem for nonlinear SISO systems is addressed and control laws that lead to elimination of the effect of the measurable disturbances, on the process output and at the same time provides input-output linearity linearity with respect to set point changes are solved for 3 CSTR in series.	The proposed methodology was proven to be a very powerful technique in completely eliminating the effect of the measured disturbances and providing satisfactory servo behavior.

	is controlled and the manipulated input is the heat input in the first vessel.				
(Economou and Morari, 1986)	The inlet stream feed temperature and the desired product output concentrations are selected as manipulated and controlled variables, respectively.	Disturbances and/or unmodeled system dynamics.	Internal Model Control (IMC)	1. An extension of the IMC design for MIMO nonlinear systems. 2. Attractive features of linear IMC are carried over naturally to the nonlinear case. 3. This is a first step toward a practically applicable nonlinear feedback controller design technique.	Operator formalism is used to extend the IMC design approach to nonlinear systems. Simulation examples demonstrate the simplicity of the design procedure and the good performance characteristics, and show that the nonlinear IMC works well even in the case where *no* linear controller can yield stable behavior.
(Kamala Thyagarajan and Renganathan, 2010)	Effluent concentration and reactor temperature are process outputs and feed flow rate and the coolant flow rates are the manipulated variables	Set-point tracking and Load Disturbance rejection	1. Decentralized controllers design using IMC method and detuning factor 2. Design of decoupling controllers using IMC method and detuning factor	Comparative analysis between decentralized control and decoupling control strategies	It is shown that decoupling controllers provide better set point tracking and load disturbance rejection than the decentralized controllers
(Kamala Thyagarajan and Renganathan, 2012)	Effluent concentration and reactor temperature	Set-point tracking and Load Disturbance rejection	IMC based conventional control scheme Particle Swarm Optimization decentralized PID controller	Comparative analysis between PSO and IMC control strategies PSO is utilized to optimize the coefficients of the decentralized PID controller tuned to cover the nonlinear range of the process. The effectiveness of the control scheme is demonstrated by simulation studies on the CSTR process.	The proposed controller provides better set-point tracking and load disturbance rejection than the IMC based conventional control scheme.
(Wang and	Temperature	Set-point	Two nonlinear PI control	Stabilisation of a class of	The simplicity and performance of

Li, 2005)	control	tracking and Load Disturbance rejection	laws to form the composite controller	singularly perturbed systems using nonlinear PI control techniques is addressed by decomposition of the system to overcome the unknown nonlinear uncertainties due to unmodeled dynamics and external disturbances of each subsystem	the proposed methodology is demonstrated through a mathematical example
(Chen and Seborg, 2002)	Level control of distillation column	Disturbance rejection and set-point tracking	IMC with PID controllers based on the direct synthesis approach	Although the PI/ PID controllers are designed for disturbance rejection, the set-point responses are usually satisfactory and can be independently tuned via a standard set-point weighting factor or a set-point filter constant without affecting the disturbance response	Nine simulation examples to demonstrates that very good control for a wide variety of processes including those with integrating and/or non-minimum phase characteristics is possible
(Hovd and Skogestad, 1994)	Methanol, concentration, reflux flow rate and the steam flow rates	Set-point tracking and disturbance rejection	PI controller tuning using Biggest Log Modulus (BLT)-approaches and sequential design approaches	A new sequential design procedure that involves minimizing the performance criterion at each design step is proposed. The key basis for design is the factorization of the overall system in terms of the estimates for the complementary sensitivity functions of the loops that are to be designed	A procedure for sequential design of decentralized controllers for linear systems is presented. It is shown how to include a simple estimate of the effect of closing subsequent loops into the design problem for the loop which is to be closed.
(Rehan, M., et al., 2008)	Flow and temperature control of a Coupled Three Tank System	Set-point tracking and Load Disturbance rejection	Use of Integral Quadratic Constraint (IQC), and minimum maximum Linear Quadratic Gain(LQG) control approaches	The scheme uses a copy of the plant nonlinearity along with its inverse function in the controller.	Robust nonlinear output feedback controller design, including copies of the inverses of the nonlinearities in the controller. Compressor surge system is used to show the effectiveness of the proposed

					scheme
(Skogestad and Morari, 1989)	Methanol, concentration, reflux flow rate and the steam flow rates	satisfy robust performance in terms of set-point tracking and reduction of model uncertainties	Diagonal PID controllers	Two design methods are addressed: sequential loop-closing design and the independent design of each loop.	The decentralized control problem is formulated as a series of independent designs. Simple bounds on these individual designs are derived, which, guarantee robust performance of the overall system. The results provide a generalization of the interaction measure.
(Jevtovic and Matausek, 2010)	Composition and temperature control	Fast set-point responses and fast disturbance rejection, under constraints on robustness and control effort.	Ideal decouplers and PID control	The validity of the system is confirmed using a test batch consisting of Two-Input Two-Output (TITO) stable, integrating and unstable processes, and one Three-Input Three-Output (ThIThO) stable process	Designing multivariable controller based on ideal decoupler and controller optimization under constraints on the robustness and sensitivity to measurement noise is done
(Ghosh, A., and Das, S. K., 2012)	Frequency response analysis of the transfer function	robustness measures of multi-channel output gain margins for SISO plants	Ideal decouplers and PID control	It is shown that decoupled compensation may be employed to provide good multi-channel output gain margin compensation for MIMO plants even when they are unstable as well as contain non-minimum-phase zeros.	Achieves superior multi-channel output gain margin compensation of continuous-time, non-minimum-phase, unstable, MIMO plants by first input–output decoupling these in open-loop and then effecting zero placements of the decoupled loops using SISO feedback.
(Lengare, et al., 2012)	General	Set-point tracking and Load Disturbance rejection	Decentralized PID controller design using IMC theory.	The method has no limitations regarding systems weak or strong interactions, and multiple delays	Direct controller synthesis approach is used. A detuning factor for each loop is specified based on the closed-loop time constant. Then appropriate controller settings are determined using the Maclaurin series expansion. Simulation examples demonstrate the usefulness of the proposed method.
(Wang, et al., 2014)	Product composition control	The improvement of	Smith delay compensator is employed, where PI	PI controllers with two unitary matrices are derived from	Decoupling control based on singular value decomposition. Moreover, the

	of the Wood berry distillation column	dynamic quality and resistance to model error	controllers are designed via internal model control (IMC	SVD, and then decoupling is obtained. Noteworthy improvements of the method include wide adaptability, i.e., square system and non-square system, but also its convenience of quantitatively regulating response performance	method overcomes the effect of model error caused by parameter perturbation. Two illustrative examples are provided to demonstrate the effectiveness of the proposed method. The integral of squared error (ISE) performance criterion is applied for evaluation.
(Chen, Z., et al., 2012)	The temperature of ceramic kiln	Set-point tracking and Load Disturbance rejection	Feedback linearization, coupled with two high-gain observers	The approach handles the difficulty in controlling non-affine nonlinear systems and also simplifies the stability analysis due to its linear control structure	Control design for a general class of uncertain non-affine nonlinear systems. Simulation results show the effectiveness of the approach.
(Hong, et al., 2011)	Chaos control and state variables control of unstable dynamical systems	Stabilization, tracking control, optimal disturbance rejection	Nonlinear state feedback by means of quadratic Lyapunov function	Guarantees global asymptotic output and state tracking with zero tracking error in the steady state.	Provide, for MIMO nonlinear systems, a tracking control based on nonlinear state feedback. The methodologies are illustrated using two simulations of chaotic and unstable dynamical systems.
(Ding Li et al., 2014)	Effluent concentration is controlled	Set-point tracking and Load Disturbance rejection	Input-output feedback linearization using the theories of differential geometry and linear PID control.	Linearization is realized by input variable-substitution and then, mature linear control theory for the sub linear system is used	Designed a controller for the CSTR system. Simulation results show that the proposed control scheme is efficient and the system contains good static and dynamic performance.
(Vojtesek and Dostal, 2010)	Changes of the heat removal as manipulated variable and the temperature of the reactant as the controlled output	Set-point tracking and Load Disturbance rejection	Proportional Controller	Control based on polynomial synthesis and the pole-placement provides good control results in spite of negative control properties such as non-minimum phase behaviour and changes in the sign of the controller gain	A methodology for simulation of a nonlinear CSTR reactor with adaptive control is presented. The results demonstrate the usability of the control method, in terms of stability of the output response
(Ray, G.,	Torque and voltage	Set-point	Decentralized PID	A linearized model of multi-	An LMI optimization problem is

2014)	control	tracking and Load Disturbance rejection	controller based on Hermite Biehler theorem	machine infinite-bus system is considered for simulation to show the effectiveness of the design procedure	formulated to ensure the stability of the composite system while the designed decentralized controllers are employed. A genetic algorithm based search technique is adopted to select an optimal PID controller gains from a designed search space of the stabilizing controllers in order to have an optimum value of the performance index
(Sujatha, and Panda, 2013)	Product composition control, at the top and bottom of the distillation column	Set-point tracking and Load Disturbance rejection	Controller tuning using IMC PI Laurent tuning rule	The proposed method of control configuration selection and closed loop identification can be used to retune the decentralized multi-loop controller for linear MIMO systems.	Uses input/output data from interactive loop to formulate a model using relay feedback and to quantify interaction measures for selection of control configuration. Simulation results have demonstrated the effectiveness of the proposed control configuration.
(Jacob, 2014)	control of a tight neighbourhood of the bounded outputs	Robust asymptotic stabilisation	Static state feedback controllers	A simple methodology for the design of state feedback controllers for nonlinear continuous-time systems is introduced	It is shown that controllers can be derived by solving a set of inequalities obtained directly from system's equation. The results are applied to the design of controllers that achieve robust asymptotic stabilisation for the general class of nonlinear systems
(Zhang et al., 2015)	desired trajectory of the composition measurements	Stability analysis and trajectory control	an adaptive fuzzy control developed by using backstepping design technique	adaptive fuzzy backstepping control problem of the two-stage chemical reactor with recycle streams	It is shown that all the signals of the resulting closed-loop system are bounded and the tracking error remains at an adjustable neighbourhood of the origin with the prescribed performance bounds.
(Rehman and Peterson, 2015)	output feed control for the compressor surge system	uncertainties and nonlinearities elimination	A robust dynamic state feedback controller based on the use of integral quadratic constraint (IQC)	The scheme uses a copy of the plant nonlinearity along with its inverse function in the controller by. using an integral	A compressor surge system is used to show the effectiveness of the proposed scheme

			and Linear quadratic regulation (LQR) control.	quadratic constraint (IQC) approach which gives a smaller bound on the closed loop cost function	
(Vivekanana than and Ponnusamy, 2015)	Reactor temperature	Servo and regulatory controls	Decentralized PI controllers	The scheme uses auto tuning algorithm for two different cases: the servo and regulatory problems. MATLAB and SIMULINK tools are used for system modelling and control design.	The performance indices for the Multiple Input Multiple Output-based decentralized PI controller for the CSTR system is evaluated and presented
(Yang and Wang ,2015)	Reactor concentration	steady state stability in the presence of disturbances	Explicit Model Predictive Control of CSTR System Based on piecewise affine (PWA) system	The paper provides a practical method to control the CSTR system	The simulation results show that the CSTR system is capable of running in accordance with the desired index and demonstrate the effectiveness of the presented approach to control the CSTR system.
(Dana Copot et al.,2015)	Reactor temperature control	Constraints such as the propeller speed, preheating of the inlet gases and catalyst basket are analysed	Proportional controller and Internal model control (IMC)-based controller	Development of a control strategy for efficient operation of a CSTR reactor	Two control strategies were designed and tested on the real system
(Prashant and Sharad, 2015)	effluent concentration and temperature of the reaction	stability under circumstances of partial pole-zero cancellation	Decoupling Based model Predictive Control	Loop interactions are compensated for by directly modifying the plant model without changing its response characteristics provided plant and model mismatch is at minimum	The proposed strategy is compared for its simplicity with multi-variable decoupling control strategies Simulations show that proposed technique efficiently reduces loop interactions in CSTR process.
(XU Jiao, et al., 2015)	effluent concentration and temperature of the	Nil	State feedback linearization control method based on	A nonlinear control method for a (MIMO) nonlinear non-minimum phase system is	the method is applied to isothermal continuous stirred tank reactor (CSTR) non-minimum phase system,

	reaction		differential geometry	provided that can guarantee the stability of the zero dynamics while meeting the performance requirements of external dynamics.	and the simulation results verify the effectiveness of the proposed method
(Dongya Zhao et al., 2015)	Reactor temperature	Set point tracking and external disturbance rejection	Output feedback terminal sliding mode control (TSMC) framework. Lyapunov stability analysis	The paper focuses on the finite time stability of the temperature loop in the presence of an external disturbance in the concentration loop. Compared with the existing sliding mode control approaches, the proposed approach has a much stronger robustness and faster converging speed without requiring high control gain.	Proposes a control mode which can estimate the system states and stabilize the system output tracking error to zero in a finite time. Illustrative examples are demonstrated by using Matlab simulations to validate the effectiveness of the proposed approach.

2.3.2 Concluding remarks

Several control strategies that are proposed in the existing literature for the stabilization, set point tacking, regulatory control and disturbance rejection problems for the CSTR process are reviewed based on the model-based control concepts such as the differential geometric concepts, the model predictive control, the internal model control, the multivariable control and the Lyapunov stability analysis concepts. These strategies are also demonstrated by several simulations and practical applications to various types of the CSTR process. Successful application of these control strategies has been reported with almost every author posting good results However, it must be noted that the review is by no means exhaustive. Model predictive control can be viewed as the most successful practical technique because of the capability of handling multi variable systems subject to constraints. However, the main intention of the review is to grasp a general knowledge of the various techniques available for the design of nonlinear controllers for the MIMO CSTR process. The following conclusions are drawn:

- Control strategies based on the differential geometric methodology which allow a certain class of systems to be linearized using state feedback and coordinate transformation such as I/O linearization, state feedback linearization, sliding mode control, and back stepping technique for state transformation, sliding mode control has been considered quite often for the nonlinear control design of the CSTR process subject to constraints. Lyapunov based approach has been utilized to guarantee or establish robust stability. These schemes offer some important advantages including constraint handling capabilities and computational simplicity. Strategies based on factorization of the controller into linear and nonlinear parts are also considered. Tuning is by pole placement techniques. Adaptive control (e.g. model reference adaptive control) and PID control are also considered in the presence of constraints. It has been suggested that the strategy eliminate disturbances.
- Nonlinear model predictive control strategies as well as a combination of model predictive control and feedback linearization have been also considered for high nonlinearity, multiple operating points over wide ranges. It has been noted that there are challenges to be addressed in developing and implementing nonlinear model predictive control algorithms optimization leading to multiple minima solution and plant mismatch. Therefore designers

are encouraged to give more attention to disturbance estimation, prediction, and compensation.

- Nonlinear internal model control (NIMC) strategies are also considered for the control of the CSTR to provide increased process stability when the presence of constrained inputs and measured disturbances. It has been found through simulation that NIMC provides superior performance over conventional PID controllers.
- Another challenging aspect is if the system to be controlled is a MIMO system. In MIMO systems the coupling between different inputs and outputs makes the design of the controller difficult. Generally, every input will affect every output of the system. Because of this coupling, signals can interact in unexpected ways. One of the solutions is to design additional controllers to compensate for the process and control loop interactions. This strategy is known as decoupling control and can be designed in a number of ways (static, dynamic, and diagonal, block diagonal, triangular or inverted). The other solution is to design decentralized control for the MIMO system. Different design methods have been investigated such as; the sequential loop tuning method, the method of detuning, the method of independent loop tuning, and the method of Relay auto-tuning. Each method has its merits and demerits.
- It is noted that getting a desired performance is the major concern, especially when the system under control (CSTR) inherits nonlinear dynamic characteristics. Important aspects from these reviews reveal the performance indices that are important to be evaluated as: the accuracy in changes in set point tracking (predicting model output response faithfully) in terms of the rise time, the settling time and the peak overshoot, the regulation control cases, the model disturbance rejection, the plant model mismatch, wide operating range conditions and the stability proof of the closed loop system which is being controlled. This is shown in whichever method that is adopted to ensure robustness of the system under closed loop.
- It has also been noted that the coolant temperature or the feed flow rate is usually employed as the control input variables, while either the reactor temperature and/or concentration are selected as the controlled variables. Then the purpose is to find the missing state variables that are used in the control strategy. In the majority of the papers reviewed, Lyapunov based approaches are used to guarantee or establish robust stability of the CSTR

closed loop control system behavior, subject to constraints including measurement error and/or unmeasured disturbances.

The objective of this thesis is to provide a comparative analysis between three different control design strategies which are applicable to the control of the nonlinear MIMO exothermic Continuous Stirred Tank Reactor (CSTR) process. Dynamic decoupling controller design, Decentralized control strategy and Input-output state feedback linearization controller design strategies are analysed and implemented for set-point tracking control of the MIMO CSTR, and a comparison of their performance is made. These concepts are discussed in detail in Chapters four five and six

The section that follows is a review on distributed control approach and the IEC 61499 standard application in process industry which are used for real-time control implementation.

2.4 Overview of the distributed control approach and the IEC 61499 standard application in process industry

As the major objective of this work is to design and implement nonlinear controllers in a distributed control environment by using functional block programming language satisfying the IEC 61499 standard, this section of literature review presents related materials on the design and implementation of distributed control approaches in industrial process and their corresponding applications based on functional block programming complaint with the IEC 61499 standard that has been successfully implemented in some studies and thereby exploiting the salient features such as, the interoperability, portability and configurability of the control system. Present PLCs are conventionally designed specifically for centralized control systems. However, with the increasing demands for distributed control in industry, the present PLCs are limited in their application by the IEC 61131-3 standard. It must also be noted that the current industrial practice is to have distributed control paradigm to solve complex control problems by breaking them into smaller modular controls placed throughout the process set up to control a variety of devices within their jurisdiction while the main controller oversees the entire operation of the complex process. Distributed control paradigm is being extensively used for monitoring, regulation, sequential control, optimization, alarms, and various other tasks. In this way the control/regulation tasks are being more flexible, manageable and more responsive to changes. However, (A. Zoitl et al., 2007) notes that although IEC 61499 has been around for some time, the most published articles on it up to now

have been more of academic or of prototype case studies. Their paper presents an overview of the past and present works and the implementation related to the IEC 61499 standard and explores the potential of the standard for eventual application scenarios. They argue that the implementation of this new concept to the distributed control concept is rather too slow. They give the main reasons as semantic issues which are still unresolved, lack of development guidelines, lack of clear application arrears and lack of industrial grade platforms for testing the standard. Similarly, (Vyatkin V, 2011) presented a comprehensive review of the standard in which he discussed the various industrial and research works in relation to the IEC 61499 standard architecture for distributed automation systems. The review concluded that the applicability of the IEC 61499 based control systems in industry is increasing. With the promising application areas including flexible material handling, flexible reconfigurable industrial automatic systems, intelligent power distributed networks and smart Grid, and also different aspects of embedded networked systems.

(Thramboulidis et al., 2005) presented a paper titled, “IEC 61499 in Factory Automation”, where he noted that though many research works on the standard have been on for some time to exploit the new standard in factory automation, its adoptability in industry has still lacking. The paper surveyed research results reported on IEC 61499 models and attempted to pinpoint the drawbacks of the standard in implementing the whole development procedure for distributed control in industrial applications with regard to software engineering. Then in the following year, (Thramboulidis et al., 2006) noted that even though the IEC 61499 provides the basic forum towards open market in the control and automation area, this new standard still possess many open questions that must be answered before a reasonable design procedure for distributed control systems is guaranteed. In their article, the inefficiencies of the IEC 61499 with regard to the design phase are outlined and how these efficiencies could be overcome is addressed. A laboratory system, “the FESTO, Modular Production System” is used as a running example to show the alternatives of possible design. Lastly, (Thramboulidis, K. 2013) presented a comparative analysis between the two standards (IEC 61499 vs. IEC 61131). His argument was that the claims of the main features of the IEC 61499 standard, such as the reusability, the portability, the interoperability, and the event driven execution has been promoted by academic world based on unsubstantiated findings. A number of misconceptions are discussed in the paper to demonstrate that the comparison, which appears between IEC 61499 and 61131 are not always provided with proof. (Wang Chi-

Ming, 2003) investigated the use of IEC 61499 function block standard as an implementation strategy for the solution of system fault-findings and fault recovery works in distributed systems. In particular, the focus was on how efficient the IEC 61499 standard is as a modelling tool in comparison to other modelling approaches like the real-time object oriented modelling approach in assisting this process. (Strasser et al, 2004) investigated the IEC 61499 standard concept as a tool for the application in the field of closed loop control. Based on this investigation, new function blocks types were identified and developed for the important functionalities that are needed for the design of the closed loop control systems. The applications and drawbacks of the IEC 61499 for distributed closed control were effected on a real-time experiment (seesaw problem). (Yang and Vyatkin, 2012) presented a new approach called model-based engineering which bridges MATLAB/Simulink block models with IEC 61499 function block models. To achieve this, a transformation between the two block diagram languages was proposed. The transformation that supported by these models provided the fundamentals for the verification and validation frame work for the IEC 61499 function blocks in closed loop with the MATLAB/Simulink block models of the plant. The frame work also provided the means of running distributed simulations for complex highbred closed loop control systems. It also paved the way of building complex models using the satisfactory object installation methodologies of the IEC 61499. (Reinhardt et al, 2012) proposed an outline on how the closed loop control systems can be implemented for the industrial automation applications with regards to IEC 61499 function blocks. In order to find out the right execution procedure for the closed loop control using the IEC 61499 events, three different processing methodologies are designed and implemented. Because of its event based execution concept, the IEC 61499 has some advantages with regards to the closed loop control. (Thramboulidis et al 2007) were the first researchers to examine how the IEC 61499 function block model concepts can be applied for batch process control. They proposed a hybrid approach that integrates the IEC 61499 function block model with the Unified Modelling Language (UML) to exploit the current approaches in software engineering such as object oriented technology, model driven technology, and component based technology. The FESTO Mini Pulp Process (MPP), which is a laboratory prototype, was used to implement a transitional methodology that resulted in a reduction of the switching cost from the ISA SP88 industrially accepted family of standards for batch process control. (Strasser et al., 2011), discussed the design and execution matters in the IEC 61499 standard for

distributed control and automation systems. They noted that the implementation of the standard with regards to published work, there are certain ambiguities with regards to different execution behaviour of the IEC 61499 elements on different control devices. These are the execution, the resource, and the function blocks. The article discussed different design strategies and execution matters in relation to these problems and presented a profile of compliance for the interpretation of the standard that result on the desired objectives.

The research in the concept of Distributed control system (DCS) encompasses almost every field as shown by the following examples: (Tsang and Wang, 1994; Alonso et al., 2000) for development of a distributed control scheme for lighting control, (Stewart et al., 2003) for the design of feedback controller for a spatially distributed system with application to paper machine problem, (Vyatkin, 2008) for the distributed IEC 61499 Intelligent control of a reconfigurable manufacturing system with application to airport baggage handling systems, (Qiang Yang et al, 2011) on communication structure for distributed control of power distributed networks with distributed generators, etc. Without loss of the intention of this review the following sections are based on those practical applications implementing the IEC 61499 standard concept in a distributed control platform.

2.4.1 Basic ideas of the IEC 61499 standard application in the industrial automation control systems

Most of the industrial automation systems are designed using Programmable Logic Controllers (PLC). Operations of these controllers are based on the International standard, the IEC 61131-3. However there are challenges of applying PLCs for large distributed systems based on this standard since these PLCs are mainly structured for the centralized scan-based architecture control and the most important factors such as the flexibility, the re-configurability and the portability of distributed control systems are lacking on the IEC 61131-3 standard. The IEC 61499 standard is an approach that can handle increased complexity of the present day automation control systems and which is an improvement of the IEC 61131 PLC system engineering. The IEC 61499 standard finally got published in the year 2005 (Christensen et al, 2012). It was initiated by the IEC to complement the 61131-3 standard and it presents guidelines for the application of function blocks in the design and implementation of the distributed control in the industrial process, measurement and control systems. The standard addresses needs for modular software that is vendor-independent that can be applied for the distributed industrial process control by defining basic concepts of the design of

modular, reusable distributed components The standard also specifies the software tool requirements. In using the IEC 61499 standard, it is possible to design and implement distributed control that cover multiple resources and distributed over multiple devices. The IEC 61499 defines three categories of function blocks: - Basic function blocks, composite function blocks, and service interface function blocks-for capturing and saving platform-dependent functions of devices. Each function block has a set of input and output variable nodes. The input variables are read by the internal algorithm when it is executed, while the results from the algorithm are written to the outputs and read at the output variable nodes.

2.4.2 The IEC 61499 standard executing tools

In terms of the software tools, the runtime environments and the libraries of the software components, that supports IEC 61499 standard, (Christensen et al, 2012) notes that number of software tool vendors that are providing software tools and runtime environments for the IEC 61499 architecture, which are either commercially supported or operates as open source and meets the standard objectives such as portability, configurability and interoperability have increased. They are: the Function Block Development Kit (FBDK) available as an open source and widely used in research trial implementation (http://www.holobloc.com), ICS Triplex ISaGRAF, development tool, which is a Rockwell Automation Company software tool (http://www.isagraf.com), which is available as a commercial tool, Distributed Industrial Automation and Control – Integrated Engineering Environment known as the 4DIAC-IDE (http://www.eclipse.org) developed at the Vienna University of Technology is an open source software tool project for research and development, and finally, nxtSTUDIO is developed by the Australian company nxtControl (http://www.nxtcontrol.com), as a commercial tool. The other tools developed but not currently active are such as CORFU ESS, TORERO IDE, OOONEIDA Workbench or FBench. (http://www.isa.org), and the software platforms supporting IEC 61499 and available either as open source or commercially supported are FBRT, ISaGRAF Runtime, FORTE, and nxtRT61499 platforms. The efforts of making these tools available can make significant contribution to the on-going development and improvement of the IEC 61499 standard. However, as noted in (Vyatkin, 2011) state of the art review, these tools have been successfully applied in many automation projects but mostly in academic and research labs and not for industrial purposes.

Since its inception, there have been several published case studies with various applications for implementation of distributed control in industry, which are subsequently reviewed here giving the objectives of the design, supporting tools, semantic execution, and application together with findings, shortcomings and recommendations, followed with summary and conclusive remarks on the way forward.

2.4.3 The IEC 61499 standard and distributed control review

A brief overview and analysis of published materials related to the IEC 61499 with respect to the design and every aspect of implementation of the distributed control paradigm is thus given in Table 2.2 and a graph of Figure 2.2 showing how the field has developed over the years. The Table 2.2 provides the number of publications considered the reviewed papers year wise from 1966 to 2015. For this review a total of 116 papers are considered. Table 2.3 show the review done under the headings: references, control application, supporting tools and platforms, benefits/usability of their implementations, and finally, the overall remarks.

Table 2.3: Number of publications on the distributed control and the IEC 61499 Standard

NUMBER OF PUBLICATIONS IN THE YEAR		
REFERENCE	YEAR OF PUBLICATION	NUMBER OF PUBLICATIONS
(Vyatkin and Hanisch, 2001)	2001	1
(Thramboulidis, 2002)	2002	1
(Feng Xia, et al 2004), (Brennan et al, 2004), (Strasser et al 2004), and (Thramboulidis, 2004)	2004	4
(Stromman et al, 2005), (Jose Lastra et al, 2005), (Arndt Luider et al, 2005), (Thramboulidis, 2005), (Olsen et al, 2005), (Dubinin et al, 2005), (Vyatkin and Hanisch, 2005), and (Lastra et al, 2005)	2005	8
(Doukas et al, 2006),and (Thramboulidis, 2006)	2006	2
(Thramboulidis et al, 2007), (Hussain and Frey, 2007), (Sünder, et al, 2007), and (Hamid et al, 2007)	2007	4
(Dimitrova et al, 2008), (Dimitrova et al, 2008), (Goran and Akesson, 2008), (Vyatkin, et al, 2008), (Yang and Vyatkin, 2008), (Vlad and Turcu, 2008), (Vyatkin and Chouinard, 2008), (Black and Vyatkin, 2008), and (Sünder and Vyatkin, 2008)	2008	9
(Hegny et al, 2009), (Sünder and Vyatkin, 2009), and (M. Minhat et al, 2009)	2009	3
(Higgins, et al, 2010), (Preuße et al, 2010), (Strasser et al 2010), (Maryam, 2010), (Li Yoong, 2010), (Dai and Vyatkin, 2010), (Cheng and Vyatkin, 2010), and (Vyatkin and Dubinin, 2010)	2010	8
(D. Hästbacka et al. 2011), (Antonova and Batchkova, 2011), (Yan and Vyatkin, 2011), (Cheng et al, 2011), and (Winkler et al, 2011)	2011	5
(Hegny et al, 2012), (Campanelli et al, 2012), (Yang and	2012	5

Vyatkin, 2012), (Sandeep Patil et al, 2012), and (Hametner et all., 2012)		
(Oana and, Popescu, 2013). (Kleanthis Thramboulidis, 2013), (Mulubika and Basson, 2013), (Robert Feldmann, 2013), (Kruger and Basson, 2013)	2013	5
(Saey et al., 2014)	2014	1
(Stefano Campanelli et al.,2015), (Dimitrova and Dimitrov, 2015), (Volker Renken, 2015)	2015	3

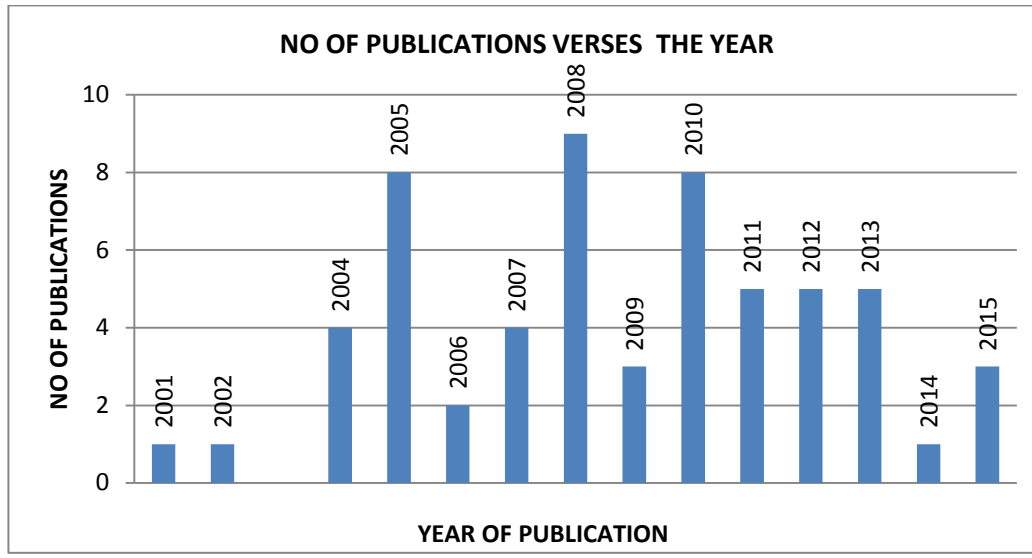

Figure 2.2: Number of publications year by year

Table 2.4.: Review papers on the distributed control and the IEC 61499 standard.

References	Control Application (Case study)	Software tools and run-time platforms	Benefits/usability of their implementations	Remarks (Short description of the aim and applications)
(Higgins, et al., 2010)	Smart Grids distributed power system automation	Involves the use of the IEC 61499 as an integration, extension, and verification mechanism for the IEC61850-based systems.	IEC 61850 lacks the specification of functions, and IEC 61499 lacks "standard" communication services. The best features of each standard can satisfy the needs of the other, creating an architecture for truly flexible and adaptable power system automation.	Presents a new approach to power system automation, based on distributed intelligence control. The paper investigates the interplay between IEC 61850 and IEC 61499 standards, and proposes a way of combining the application functions of IEC 61850-compliant devices with IEC 61499-compliant logics using the communication services of IEC 61850-7-2. The results greatly enhance the flexibility and adaptability of automation systems, toward the realization of the smart grid concept.
(Hegny et al., 2012)	Industrial Robotics and smart Energy Systems	Instrumentation-and Control-Points (ICP) as Process Interface in Hierarchical IEC 61499 control application	The analysis and evaluation provided shows that the ICP concept together with the adapter concept greatly improves the control application design and implementation leading to better structured and more reusable control software.	A concept based on a logical grouping of input/output devices (I/O) to so called Instrumentation- and Control-Points and decoupling them from the control application by applying IEC 61499 function blocks based adapter concept is investigated. Two industrial motivated application examples show that this concept fulfills the requirements for increasing the reusability of control code by separating control logic from hardware specific code. Moreover, it leads to a better application software structure which is easier to maintain and to understand.
(Hegny et al., 2009)	Design of control and diagnostic applications for the palette transfer system (PTS) of ACIN's Odo Struger Lab transport system.	Function Block Development Kit (FBDK)	The hierarchical composition of IEC 61499 applications proved to be useful, if the system consists of many components of the same type. The SIFBs were identified as the central connection element for simulation and implementation	The work analyses existing approaches for designing distributed control applications using plant models. A hierarchical extension of the layered model-view-control design pattern is presented. Furthermore generic Service Interface Function Blocks are presented that allow seamless transition from simulation to implementation.
(Campanelli et al., 2012)	Simple test case consisting of three different personal computers to test the functionalities of the architecture.	Integration of IEC 61131-3 and IEC 61499 runtime environments by using 4DIAC platform	Demonstrated that the system correctly realizes the distributed control	Presents a method for the integration of the two standards (IEC 61131 and 61499), that allows the exploitation of the benefits of both. The proposed architecture is based on the parallel execution of both environments that interact with each other through some specific interfaces. A test implementation of the architecture is presented to demonstrate the feasibility

				of the proposed solution.
(D. Hästbacka et al.. 2011)	AUKOTON development process	IEC 61499 and UML automation profile	Supports industrial practices and are able to utilize existing control system platforms. Successfully applied to small-scale process control applications. The practical applicability and benefits for engineering industrial process control applications are also addressed	Presents model-driven development and domain-specific modeling approach concepts to the development of industrial process control applications. The approach is based on established practices of the industrial automation and control domain, a compatible UML profile, and an integrated and standards-based tool environment for modeling and transformation execution thereby increasing productivity and enhancing platform independent solution reuse.
(Thrambouli dis, 2002)	RTLinux as the Industrial Process Control Protocol	Virtual Field Bus (VFB), which is an IEC 61499 compliant field bus as a case study performed by the IPCP Protocol.	The architecture is very helpful in the development process of function block oriented Engineering Support System. It helps to easily identify services for application management, such as function block creation, deletion, inter connection and activation.	Presents Common Object-oriented Real-time Framework for the Unified development (CORFU), an object oriented (OO) framework to improve the engineering process of IPMCSs in terms of reliability, development time and degree of automation. The defined framework embodies an abstract design that is capable to provide solutions for the family of distributed IPMCSs.
Doukas et al., 2006)	Machine automation (robotic arm)	CORFU Engineering Support System and Archimedes system platform software tools	The system was demonstrated successfully, proving the effectiveness of the FB model as well as the usability of the proposed execution environment.	The applicability of the IEC 61499 model in a well-known PID-based control application for robotic arms is examined. A specific code generator was developed to automatically produce the executable model of the application for a prototype Linux-based FB execution environment.
(Oana and, Popescu, 2013)	Process Control Plants	FBDK and Matlab platforms	Allows portability on equipment from different vendors and on different development environments that conform to the IEC 61499 standard by creating sub-applications and using them either locally or in distributed system configurations.	Designed a process control library of advanced control and optimization algorithms for large – scale industrial plants, written in a standardized format based on IEC 61499. Presents the structure, design and functions of this library including communication mechanisms allowing the integration of its components in a local or distributed application
(Dimitrova et al., 2008)	The approach is illustrated using the Festo Mini Pulp Process (MPP) Laboratory	ISA SP88 and Function Block Development Kit (FBDK) as tool for IEC 61499 implementations	This concept allows re-configuration of the control without altering the function block diagram. Hence the proposed approach offers analyzable formal	A new way to combine the concepts of SP88 for design with the models of IEC 61499 for implementation is proposed. To describe the control sequences Signal Interpreted Petri Nets (SIPN) are used to get a more formal model of the control. Based

	automation		models, re-usable basic components, and easy re-configurability	on these description basic functions based on IEC 61499 for the control as well as the corresponding activation sequences are determined. The interconnection to the required sequences is implemented using a scheduler concept.
(Goran and Akesson, 2008)	The ball sorting process	IEC 61499 runtime environment called Fuber	The control code and the process model are expressed using the IEC 61499 language thus making it easier to use the formal verification in the control software development.	A new control software development method is presented. It uses IEC 61499 function blocks for control software and provides tools for simulation, execution, automatic model generation and formal verification during the development. Simulation and execution are supported by the same tool, the Fuber runtime environment. Formal modeling is done using extended finite automata (EFA) and an automatic model generation tool.
(Stromman et al., 2005)	Control application for a lifter unit of a manufacturing line	FBDK repository	The research analyzes alternative solutions developed by automation designers using IEC 61499 and notes that it is very difficult to rate their reuse potential absolutely and also not possible to present detailed guidelines applicable to the entire industry.	Research goal was to increase the understanding of the use of IEC 61499 by industrial practitioners. Need for guidelines were demonstrated by identifying many specific design decisions that must be addressed before the commercial development of reusable software can begin.
(Jose Lastra et al., 2005)	Control of inverted pendulum	CORFU, FBDK and TUT-IPE Visio TM Template	Shows possibility of achieving control of real-time closed loop applications using a Java based industrial controller as runtime platform for IEC 61499 applications.	A software application that enables the deployment of IEC 61499 applications into a chosen scan-based controller to demonstrate how an event-based system implemented with IEC 61499 can be adopted for a scan-based embedded controller.
(Arndt Luider et al., 2005)	A pusher example which can be extended and retracted by valves	Conversion of Function Block Systems to Net-Condition/Event-Systems. and the Integration of model design within the FBSD tool.	Based on the modeling steps provided an automatic Function Block Systems design is possible.	A methodology for automatic modeling of IEC 61499 compliant function block systems by Net-Condition/Event-Systems. Using these models it is possible to formally validate and/or verify the behavior of function block systems to ensure correctness within control systems.
(Feng Xia, et al., 2004)	DC Servo control system	FB control applications modeled as task graphs (TGs) that describe the	The quality of control can be improved by the method, which is illustrated by an example of a DC	The problem of how to allocate Function Blocks onto Real time Distributed Control Systems holding periodicity, time, and precedence and resource

		logical structure, the communication and precedence constraints among FBs.	Servo control system.	systems constraints is investigated. By fully utilizing the pipelined parallelism, a heuristic FB allocation algorithm is proposed to minimize the control period.
(Brennan et al., 2004)	A Dallas Semiconductors Tiny Inter-Net Interface (TINI) board including a microcontroller for prototyping	Function Block Development Kit (FBDK) developed by Rockwell Automation	A simple example of a distributed control application is implemented on a Java-based embedded control platform employed to test this approach	Focuses on the use of software design patterns to assist in the design and development of distributed control software. The Model-View-Controller (MVC) framework is used to develop IEC 61499 function block applications.
(Preuße et al., 2010)	EnAS Project Demonstrator.	Review of various tools like FBDK, 4DIAC-ITE, ISaGRAF, and nxtControl	Development of formal techniques for the IEC 61499 standard	Summarizes the development of formal modeling and verification of Function Blocks following the IEC 61499, provides a critical review on what has been done, and opens the view for further challenges in the development of formal techniques for IEC 61499 standard.
(Vyatkin, et al., 2008)	Manufacturing automation and mechatronic industry	Function blocks (FB), Unified Modelling Language (UML), Simulink, and Net Condition/Event Systems (NCES)	The paper appeals to developers of automation systems and automation software tools via showing the pathway to improve the system development practices by combining several design and validation methodologies and technologies.	A new framework for design and validation for the design of automated manufacturing systems from intelligent mechatronic components complying to the IEC 61499 architecture and the automation object concepts. It is illustrated how to use these with UML, Simulink, and NCES, form a framework that enables pick-and-place design, simulation, formal verification, and deployment with the support of a suite of software tools.
(Yang and Vyatkin, 2012)	An example of a motor Simulink model	Matlab Simulink and Function Blocks of IEC 61499 standard	Main benefits of the approach are: – Automated model transformation reduces time and effort on model development and greatly helps in validating the designs based on IEC61499 Function Blocks – Embedded models extend the capabilities in implementation of model-predictive controls in the IEC 61499 environment;	A mathematically rigorous transformation method from MATLAB Simulink for IEC61499 Function Blocks has been described. The method aims to help in design of complex distributed systems by taking advantage of the simulation and analysis capability of MATLAB Simulink. The proposed approach has been validated on a number of industrial use-cases. Adopting this methodology can make the use of IEC 61499 for commercial development environments advantageous
(Yang and Vyatkin,	Batch Process Reactor and its	A hybrid approach of integration of IEC 61499	An overview of the implementation and challenges of	An overview of the works on design and validation of distributed control in process industry. It is shown that

2008)	hybrid lab-scale model FESTO MMP (Mini Pulp Process),	with UML and IEC61804 Standard	the new distributed control approaches in the process industry are surveyed	a distributed control can bring benefits such as flexibility, re-configurability and software reusability by implementation of the new approaches based on International standards such as IEC61499 and IEC 61804 newly introduced Function Block (FB) concepts.
(Hametner et al., 2012)	An incinerator for energy production	4DIAC function block library	Through the evaluation of the proposed concepts after implementation, several fields of application could be identified.	The implementation of the closed loop control algorithm is done in IEC 61499 concepts using the open source project called 4DIAC. Two controller instances to control the MIMO plant behavior are done. The requirements applicable for industrial controller algorithm implemented on embedded devices like Programmable Logic Controllers are shown.
(Strasser et al., 2004)	The control of the challenging seesaw balancing problem	FBDK (Function Block Development Kit) and FBRT (Function Black Run Time) from Rockwell Automation were used	From different experiments it turned out that the arrangement of closed loop control experiments is limited: The execution of the whole real-time control is too slow to keep track of the correct position of the cart on the seesaw which can cause instability of the system	Investigated the possibilities for applying the concept of the IEC 61499 standard to the field of closed *loop* control. New FB types are identified and developed and added to the library to cover the core functionality that is necessary for the implementation in closed loop control systems. The usage and limitations of the IEC 61499 for distributed *closed* loop control is demonstrated on a real experiment - the control of the challenging seesaw Problem.
(Thrambouli dis, 2006)	FESTO Modular Production System	CORFU FBDK	It was shown that the use of Function Block Interaction Diagrams (FIDs) with a modified Execution Control Chart can produce more expressive design diagrams that are better understood by the control engineers.	The inefficiencies of IEC 61499, at least as far as the design phase is considered, are highlighted and the way that these inefficiencies can be addressed is discussed. A laboratory system, the FESTO Modular Production System, was used as a running example to demonstrate possible design alternatives.
(Thrambouli dis et al., 2007)	Batch control of FESTO Mini Pulp Process (MPP), a laboratory system	The Java-based IEC61499- compliant run-time. The CORFU framework and the Archimedes System Platform	The new approach exploits the best practices of software engineering in the form of UML and IEC 61499, and the goal has been to make this accessible to professional automation designers with minimal retraining.	A hybrid approach that integrates the IEC61499 Function Block Model (FB) with the Unified Modeling Language is exploited and customized to the batch control domain. A toolset was customized and presented to demonstrate the applicability of this approach. Research experience with industrial engineers in the context of IEC 61499 and SP88 is used to motivate the development of the methodology.

				The Java-based IEC 61499-compliant run-time environment is used for the execution of the control application.
(Hussain and Frey, 2007)	FESTO MPS didactic model of a typical industrial application and a lift control application	FBDK	An analytic approach for deployment conforming to the standard and execution semantics realized in certain implementations of the IEC 61499 standard	This work addresses the issue of finding a feasible as well as optimal deployment of IEC 61499 compliant distributed control applications. The proposed work also addresses the context of differing execution semantics and acknowledges that there are still certain points which need to be resolved regarding the execution semantics. Therefore, certain assumptions are made to make the matters simple and intuitive
(Strasser et al., 2010)	Function Blocks (FBs) and Function Block Networks (FBN)	FBDK	The investigations are contributions in order to find a compliance profile for an interpretation of the standard that achieves the goals of: portability, (re)configurability, interoperability, and distribution.	This paper discusses different design and execution issues related to IEC 61499 distributed automation and control systems. Different models for the execution of FBs in IEC 61499 devices and resources as well as the execution of CFBs and sub applications are discussed. It is found that stricter and more precise provisions are required in order to achieve the main goals of the IEC 61499 standard as: portability, (re)configurability, interoperability, and distribution. The paper is a contribution in order to find a compliance profile for an interpretation of the standard that achieves these goals.
(Thrambouli dis, 2005)	Review study	CORFU FBDK	Open problems and future challenges are discussed.	This paper surveys research results reported so far about the IEC 61499 model and attempts to highlight the inefficiencies of this paradigm to support the whole development process of distributed control applications as far as the software engineering point of view is considered.
(Vyatkin and Hanisch, 2001)	A Simple plant – Boring station consisting of a boring machine (drill) and a transfer stage that delivers work pieces to the home position of the drill.	Software tool called VEDA	Verification helps to contribute to the improvement of testing of function blocks	In this paper a software tool called VEDA (Verification Environment for Distributed Applications) for modeling and verification of distributed control systems is presented. The tool provides an integrated environment for formal, model-based verification of the execution control of function blocks following the new IEC 61499 standard. The modeling is performed in closed loop way using manually developed models of plants and automatically generated models of the controllers.

(Thrambouli dis, 2004)	The Teabag Boxing System	CORFU FBDK	UML brings in the development process the best software engineering practices	The use of UML in control and automation is examined and a description of the use of a hybrid approach in the development process of distributed control systems is given. The proposed approach integrates UML with the already well accepted by control engineers FB construct, to cover the analysis and design phases of the development process. A model driven approach is adapted from analysis through design, to implementation. The applicability of the UML profile for scheduling, performance and time, to the proposed development process, is examined**.**
(Maryam, 2010)	Automatic Iron Cutting Device	IEC 61499, Function Block, FBDK, FBRT, Net master software environment, JVM, SIFB	One special feature in this research is the device independent control application design followed by the code distribution among available devices and the communication code integration	IEC61499 Function Blocks concept, Function Block Development Kit (FBDK), Function Block Run Time Environment (FBRT), Net master, and a design pattern for developing the Automatic Iron Cutting Device distributed in two devices using IEC61499 FBs Editor are discussed and benefits are fully described. It is shown that IEC 61499 provides easy communication via network. The Communications between two devices provided by publish and subscribe FBs with an exclusive IP address and a port so that data can be written to and read from a specific address.
(Antonova and Batchkova, 2011)	Distribution Station that is part of didactic test bench, manufactured by FESTO Corp.	Use of UML/SysML, FIPA reference model and IEC-61499 standard	The most essential features of this approach is that control engineers are able to model the closed loop control system and to apply the different type of analysis techniques for performance requirements, without knowledge of the inner techniques.	Suggested a methodology for the development of multi-agent control systems based on the combined use of UML/SysML, FIPA and IEC-61499 standards for development of open, interoperable, re-configurable, and distributed control system. This methodology allows describing the whole life-cycle of the control system and achieving software encapsulation and re-use of the defined entities (agents).
(Vlad and Turcu, 2008)	Manufacturing process of products composed by two components that are first machined and then assembled in an	FBDK licensed by Rockwell Automation MVC - an architectural pattern used in software engineering	Some benefits of this IEC 61499 approach are, Intuitive programming, reutilizing of function blocks and easy debugging.	Describes a modeling application based on the IEC 61499 standard and the modified MVC pattern, for a manufacturing system consisting of two machining lines, one assembly line and the transport system The application represents a first step in a more complex project dealing with the reconfiguration problem of the manufacturing systems.

	end product			
(Olsen et al., 2005)	A conveyor belt system for transporting parts to a manufacturing process	Rockwell Automation function blocks development kit (FBDK) for software implementation and Dallas semiconductor Tiny Inter-Net Interface (TINI) for the hardware implementation.	The anticipated advantages of this method is that it should overcome application loading issues and open the door for more intelligent approaches to reconfigurations	A dynamic approach to programmable logic controller (PLC) reconfiguration that is based on IEC 61499 standards for real-time distributed control systems are proposed. With this proposal, contingencies are made for all possible changes that may occur. To illustrate this approach, a simple configuration that uses Rockwell Automation function block development kit (FBDK) for software implementation and Dallas semiconductor Tiny Inter-Net Interface (TINI) for the hardware implementation are used.
(Li Yoong, 2010)	Modeling a baggage handling system	4DIAC-IDE (version 0.3) and FBDK (version 20081003) as well as MHVIS (Material Handling Visualize) tools	The semantics for synchronous execution is proved correct for any arbitrary composition of function blocks and run-time scheduling overhead is eliminated. These semantics further enable formal verification of function blocks using the concept of synchronous observers.	Proposed a formal model for distributed IEC 61499 systems based on the globally asynchronous locally synchronous (GALS) paradigm. For a centralized implementation, function block networks are executed synchronously, while distributed implementations are executed as a collection of synchronous islands that communicate with each other.
(Dai and Vyatkin, 2010)	A Conveyor System of a Simple Airport Baggage Handling System	nxtSTUDIO IEC 61499 Editor	This approach can be also beneficial in terms of performance, as the event flow can be directed only to those FBs which are necessary to be involved in the reaction to a certain input event in the environment.	The paper discusses the problem of migration from the PLC control to the event-driven and component based architecture of IEC 61499 function blocks and illustrate three different migration methods: object-oriented in basic function block, object-oriented in composite function block and class-oriented in basic function block. The advantages and limitations are summarized and guideline for migration is provided.
(Dubinin et al., 2005)	The test bed is a model of modular production system	The tool sets are FBRT that is a Java based run-time platform and Function Block Development Kit (FBDK) – the engineering software tool from Rockwell Automation	The paper presented an approach supporting the automation systems' engineering that is based on UML and IEC61499. Application of several UML diagrams has been studied that provide a comprehensive support of the engineering process.	Suggests a comprehensive engineering framework for software design for component-based distributed industrial automation based on the combination of UML with the function block concept of the newly emerging international standard IEC61499. Four UML diagram types have been used, namely: class, sequence, cooperation and state-chart diagrams. The UML design is transformed then to the executable function block specification following the IEC61499.
(Cheng and	The demonstrative	Object-oriented data	The demonstrative example	Presents the first step to seamlessly incorporate IEC

Vyatkin, 2010)	FESTO Distributing Station	format called Computer Aided Engineering Exchange (CAEX) of IEC 62424 and IEC 61499 FBs	illustrates the design flexibility using IMCs. Further research focuses on applying the CAEX templates to more practical engineering tools and standards.	61499 standard with other tools and standards to support the development lifecycle of control program for automation system following a systematic design methodology by addressing two issues: a systematic approach of developing and organizing IMC elements and a seamless and scalable way supporting IMC composition and reconfiguration.
(Sünder and Vyatkin, 2009)	A linear drive system	4DIAC FB networks and runtime environment (FORTE) and Petri Nets modeling language (NCES)	The proposed methodology does not only enhance the expressiveness of model checking for proving the properties of a given system, but may be used also for better analysis during the system design	Focuses on the IEC 61499 control applications for automation objects, the building blocks for intelligent mechatronic systems. A comprehensive approach for their formal description of control behavior incorporating also the operating system policy and physical time as parameter for real-time behavior is given on the basis of Net Condition/Event Systems for a typical control device configuration.
(Vyatkin and Chouinard, 2008)	The 'LED Chaser' reference example	FBDK and ISaGRAF structures	The approach has benefits, both for the developer, who did not have to change much the tool and run-time from the IEC61331-3 version, and for the end-user, who, arguably, will easier migrate from IEC 61131- 3 to IEC 61499.	This paper presents first results of comparison of ISaGRAF implementation of IEC 61499 with that of FBDK – the tool traditionally used for experiments with this standard in the research community. The relation of ISaGRAF standard's compliance for current and future IEC61499 implementations are addressed in terms of migration from cyclic scanned programmable logic controllers (PLC) of IEC61131-3 to the event driven controllers conforming to IEC61499. It is shown how some structures of the ISaGRAF implementation can be mapped to FBDK implementation and vice versa.
(Yan and Vyatkin, 2011)	Modular Baggage Handling System design	The solution was prototyped using ISaGRAF for implementation of IEC 61499 and tested on a network of 50 networked control nodes. The Ethernet communications framework was utilized.	This design approach can be regarded as cyber-physical since it naturally combines simulation models into the design life-cycle, providing ready to use simulation within the design framework	The proposed design methodology leverages IEC 61499 Function Blocks as a supporting architecture feasibility of a fully distributed automation design of Baggage Handling Systems automation. Each physical element of the BHS is represented by a Function Block that encapsulates functionality into a single re-usable module. The proposed solution demonstrates such benefits as flexibility, fault resilience and design re-use. A graph based representation of the system layout was used for rendering of the visualisation.
(Cheng et	material handling	NxtSTUDIO IEC 61499	The proposed method can be	Proposes a method of time-driven control with high-

al., 2011)	system	IDE standard with support of the IEEE 1588 protocol.	applied in any domain that requires distributed precision time control despite unpredictable asynchronous nature of IEC 61499 run-time platforms and communication networks like Ethernet.	precision synchronous clocks in distributed control systems built following the IEC 61499 standard on the performance of material handling systems. A time-driven control system is developed using IEC 61499 Function Blocks architecture with support of the IEEE 1588 Precision Time Protocol. Analytic performance is developed and comparisons between the time-driven and two other possible control designs have been conducted and elaborated in terms of costs, logic design, and system throughput.
(M. Minhat et al., 2009)	CNC milling machine	FB Development Kit (FBDK) by Rockwell Automation	Showcased a methodology to facilitate the transition from a centralized system to a distributed system and from a simulated system to a physical system. The STEP-NC controller making use of the IEC 61499 takes maximum advantage of its highly visual nature.	This paper discusses the two new standards, ISO 14649 and IEC 61499, with a focus on the development of a STEP-NC enabled controller. The controller architecture is presented and a prototype system based on this architecture has been developed. The development tools used in this research are also discussed.
(Sandeep Patil et al., 2012)	A re-configurable pick and place robot	NxtSTUDIO (IEC 61499 function blocks) and ViVe and SESA tools.	A new reusable and scalable model for formal verification that is not time consuming, has been proposed, developed and tried on different reconfigurable systems.	Introduces an approach to automatic verification of mechatronic systems designed as plug-and-play of Intelligent Mechatronic Components (IMC) using model-checking by the Vive/SESA model checker. Net Condition Event Systems formalism is used to model the decentralized control logic and discrete-state dynamics of the plant. A multi closed loop model of Plant and Controller is used and controller is extensively verified for safety, liveliness and functional properties of the robot. Computational Tree Logic (CTL) is used to specify these properties.
(Sünder, et al., 2007)	Infineon C167CS microcontroller (µC), mounted on a development board.	IEC 61499 runtime environment C++FBRT. by use of NCES,	We have evaluated our results within a test example with real-world measurements, and we have found very small deviations	This paper investigates on the introduction of the runtime behavior and real-time constraints into the verification process of IEC 61499 based automation systems. It is shown that, the event propagation policies as well as the necessary execution time for all actions within the automation system need to be described for a complete model of the automation system. The basis of the formal description provides an analytic methodology for the event propagation

				policy of an IEC 61499 runtime implementation.
(Vyatkin and Dubinin, 2010)	Pneumatic cylinder-based control system	*AGG* is a rule-based visual programming environment and nxtControl for the IEC 61499 function block editing tool	The refactoring can help in implementing equivalent transformation of control programs without introducing errors.	This paper deals with refactoring of execution control charts of IEC 61499 basic function blocks as a means to improve the engineering support potential of the standard. The main purpose of the refactoring is removal of arcs without event inputs as well as getting rid of potential deadlock states. The ECC refactoring is implemented as a set of graph transformation rules using the AGG software tool.
(Vyatkin and Hanisch, 2005)	A manufacturing system in laboratory scale.	Execution is by means of FBRT – Function Block Run-Time platform of Function Block Development Kit FBDK of Rockwell Automation and modeling formalism is by Net Condition/Event Systems (NCES).	This closed-loop approach to the modeling enables expression of the specifications directly in terms of the machine behavior (not only input and output signals of the controller).	Describes formal modeling and verification of automation systems from the system engineering point of view by applying the concept of reuse of model components. The reuse is achieved by the combination of modular modeling of automation systems with object-oriented description of models in UML style. This allows benefiting from advantages of both worlds: efficiently manage highly hierarchical complex models with UML tools and end up with efficiently executable models with distributed states that are compatible also with IEC61499 function block specifications.
(Lastra et al., 2005)	FlexLink lifter a pallet-based conveyor system.	IEC 61499-compliant editors (e.g. CORFU, FBDK and TUT-IPE Visio Template	The paper shows that despite the contrasting approaches in the two execution models it is possible to implement the IEC 61499 execution on scan-based controllers of the present industrial systems.	Developed a software tool (IEC 61499 Application Generator) that enables the deployment of IEC 61499 applications to scan-based embedded controllers to demonstrate how an event-based system implemented with IEC 61499 can be adopted for a scan-based embedded controller
(Black and Vyatkin, 2008)	intelligent BHS automation	FBDK from Rockwell automation	Simulation is used to demonstrate the effectiveness of the agent-based control system and a utility is presented for real-time viewing of the system	Presents a multi agent control approach for a baggage handling system using IEC 61499 Function Blocks. It focuses on demonstrating a decentralized control system that is scalable, reconfigurable and fault tolerant.
(Winkler et al., 2011)	Processing station with rotary table, drilling module and testing module	Net Condition/Event Systems (NCES) and their subclass safe NCES (sNCES) as modular modeling language.	Allows system behavior analysis and improves the application of the supposed synthesis method.	A methodology to enhance the synthesis of discrete process control by generating a controller model automatically by the application of new structural analysis methods for the used formal modeling language safe Net Condition/Event Systems, derived from Petri net

(Sünder and Vyatkin, 2008)	IEC 61131-3 and IEC 61499 libraries	IEC 61131-3 and IEC 61499	Analyses the capabilities of the both standards IEC 61131-3 and IEC 61499 to be treated as component framework. A Component system architecture is envisaged that is based on an enhanced IEC 61499 runtime environment.	Proposed the mapping approach of software components to the elements of the two standards IEC 61131-3 and IEC 61499 by addressing the following different aspects: (i) enhancement of the possibilities of existing IEC 61131-3 implementations, (ii) tight coupling of IEC 61499 control logic to existing IEC 61131 applications, and (iii) the ability to distribute also IEC 61131-3 FB networks within the same platform.
(Hamid et al., 2007)	Siemens S7 PLC PID function block	Siemens S7 PLC and Matlab Neural network toolbox	The accuracy of the implemented block is investigated regarding to the calculation and programming limits of the PLCs	The aim of this project is to introduce and implement a new function block of a neural network to the function library of PLC. The block can be used in manual or automatic mode. Finally the application of the new block is compared with a classic simulated block and the results are presented.
Stefano Campanelli et al., 2015	IEC 61131-3 and IEC 61499 libraries with LowEffort INTegration architecture	LowEffort INTegration architecture (LE-INT) to realize the coexistence of code modules written in the two standards	The proposed architecture is based on the coexistence of control software of the two standards. Modules written in one standard interact with some particular interfaces that encapsulate functionalities and information to be exchanged with the other standard.	An architecture to integrate IEC 61131-3 systems in an IEC 61499 distributed solution In particular, the architecture permits to utilize available run-times without modification, it allows the reuse of software modules, and it utilizes existing features of the standards. It is described via a case study to prove feasibility and benefits. Experimental results demonstrate that the proposed solution does not add substantial load or delays to the system when compared to an IEC 61131-3 based solution
Kruger and Basson, 2013	Lab-scale Reconfigurable Assembly System (	Java-based FBDK (Function Block Development Kit) and ADACOR (ADAptive holonic COntrol aRchitecture)	The research proposes multi-agent systems and IEC 61499 function blocks (FBs) as possible control strategies for implementation in reconfigurable systems.	Software agents and IEC 61499 function blocks are evaluated as alternative strategies for implementing holonic control for a modular feeder subsystem of an experimental Reconfigurable Assembly System. The strategies are evaluated through four reconfiguration experiments. The results show that agent-based control is more suitable in the specific case study.
Robert Feldmann, 2013	PLC unit in a paper machine model developed in Simulink environment	TwinCAT 2.11 as the platform for compiling to the soft PLC	The research compares the implementations of the different code generation for the PLC unit in terms of complexity The codes are C-Code, Structure Text-Code and the CFC block diagram	An approach for the quality assessment of three different automatically generated controller implementations on a PLC in terms of complexity and performance
Volker	Local heat-flow in a	Matlab/Simulink platform	Investigations of two meta-models	An approach for implementation of real-time control

Renken, 2015	bridge model	and TwinCAT environment	for the purposes of implementing real-time control of a real-simple forming process	systems for manufacturing error-free goods at first time
Mulubika and Basson, 2013	Lab-scale Reconfigurable Assembly System	Java-based FBDK (Function Block Development Kit) and Java Agent Development platform (JADE)	Comparison of IEC 61499 function block control and Agent-based control	Approaches for comparison of the IEC 61499 function blocks and the JADE platforms to implement control of a modular robot are proposed.
Saey et al., 2014	Motion control demonstrator	Matlab/Simulink platform and Simulink coder Target for the PLC	Use of a Matlab generated real-time code to control a torsion drive system	The article proposes a design method that combines a controller, high speed remote input/output Ethernet-based network to control a torsion drive system
Kleanthis Thramboulidis, 2013	Up-counter function block, IEC 61499 Tank function block application and a network of time-triggered function blocks	ISaGRAF model based on IEC 61131 and IEC 61499 standards	The article presents some misperceptions regarding a comparative analysis based on the two standards IEC 61131 and IEC 61499	It is shown that the IEC 61499 standard cannot be considered as an effective successor of the IEC 61131 with regard to the development of industrial automation systems.
Dimitrova and Dimitrov, 2015	SCADA laboratory imitation models	Digital Simulator (DISIM-V) for operational dispatching of the train traffic and Digital Simulator (DISIM)-E for monitoring and control of the electrical equipment	Proposed a simulation model of SCADA system for monitoring and control of train traffic and power supply in Sofia metropolitan	The simulation model is used for training students and personnel in the metropolitan.

2.5 Discussion on the application of the IEC 61499 standard for Distributed Control

In the foregoing section, the applicability of the IEC 61499 standard's function blocks for embedded distributed control system design approaches was investigated. About 60 related works are cited in this investigation. The discussion in regard to this review can be drawn as follows:

- In the area of closed loop control, there is a natural link between block diagram description of closed loop control elements and the function block concepts of the IEC 61499 standard architecture as investigated by the different researchers, where closed loop control applications using the popular controller algorithm (PID) have been implemented with success. However it is found that the IEC 61499 standard function block library for closed loop control applications is not populated enough with mathematical formalisms for solving different and complex control problems. In this regard special library block diagram elements for different control problems and corresponding approaches are needed. For example, the neural network function block has not been developed in the IEC 61499 PLC systems. It is therefore envisioned that tools will be developed that will model, validate and simulate the behaviour of such complex networks of function blocks specifically in the field of process control.
- Analyses of different software tools that aid in the transformation of closed loop block diagrams directly to IEC 61499 function blocks have also been researched. For example very popular tools for modelling and implementation of closed loop control problems such as Matlab/Simulink from MathWorks and LabView from National Instruments have been used to help in the design of complex distributed systems. The proposed approach has been validated on a number of industrial use-case studies and it is concluded that adopting this transformation methodology can make the use of the IEC 61499 standard for commercial development environments advantageous as that automated model transformation reduces time and effort on model development and greatly helps in validating the designs based on the IEC61499 Function Blocks environment.
- Another aspect that emanates from this review is the concept of migration from the legacy IEC 61131 to IEC 61499 where design patterns, migration approaches and execution semantic rules are discussed. In addition, different aspects: such as tight coupling of IEC 61499 control logic to existing IEC 61131 applications, and the ability to distribute also the IEC 61131-3 FB networks within the same platform that allows the exploitation of the benefits of both standards are discussed. Other researchers developed a software tool (IEC 61499 Application Generator) that enables the deployment of IEC 61499 applications to scan-based

embedded controllers based on the IEC 61131 to demonstrate how an event-based system implemented with the IEC 61499 standard can be adopted for a scan-based embedded controller. Test implementations of the architectures are presented to demonstrate the feasibility of the proposed solutions. However, from the literature reviewed it may be noted that different approaches have been proposed and there is no clear guide on the procedure to effect the migration since different code representations are used.

- Implementation software tools, run-time platforms and modelling languages and execution semantics are another factor that emanates from the review. In order to implement the IEC 61499 standard fully, a compliant tool set that consists of a work bench for editing function block designs and translating them into executable form and some kind of run-time environment that supports the execution must be available. There are open source and commercial Integrated Development Environments (IDE) that are IEC 61499 complaints which have been developed to implement distributed control projects and tested them with success. These environments are such as: the ISaGRAF of ICS Triplex and the nxtControl, for commercial application environments, the open source projects 4DIAC and the FBDK from Rockwell Automation tool for research and demonstration, and CORFU engineering support system software that can be used for the deployment and execution of the created IEC 61499 standard FB design models. In addition, to the work bench editors, researchers have proposed other tools and modeling and verification languages to run parallel to the development environments using IEC 61499 standard as a vehicle to enhance the synthesis of control paradigms, thereby demonstrating such benefits of flexibility, fault resilience and easier implementation methods. However, these proposals are suitable to specific scheduling policy to execute function blocks and for specific applications. Such modeling tools and languages proposed in the literature are : Net Condition/Event Systems (NCES) as a formal graphical language that fits well for modelling and verification of distributed embedded and control systems, ViVe/SESA-ViVe is an interactive graphical model-building and analysis tool for building models of large and complex distributed systems and SESA-a command line software tool for the analysis of Signal-Net Systems, AGG-a rule based visual language supporting an algebraic approach to graph transformation, and Unified Modelling Language (UML) for modelling objects to support the development life-cycle of control program, are suggested.
- Industrial applicability of projects under the IEC 61499 standard is another factor to be discussed. From the review it shows that most of the projects undertaken are on the laboratory equipment’s mostly, from university laboratories, mainly,

because the impact of the standard is still minimal due to the limited experience of trained personnel with the standard, limited knowledge available, very high cost of implementation, no methodology that guides the definition of the Function Block network that models the control applications, and no guidance on how to identify the Function Block types that are required to compose a control application, among others. However the field of control application is wide ranging from motion control, material handling, lab scale process control, smart grid distributed power systems, motor control, building management systems, assembly, machine tools, monitoring, mechatronic, and agriculture, and food processing, with almost all the research work trying to demonstrate the potential of the IEC 61499 as compared to IEC 61131 when used in industrial automation application. ISaGRAF was the first vendor to implement a commercial project which is IEC 61499 complaint and have demonstrated the usability of the concepts in highly distributed applications with high speed performance. The company have put on the market over 10,000 controllers which are IEC 61499 standards complaint.

In conclusion it can be said that experience with IEC 61499 concepts is still lacking for most control engineers and the challenges of applying the standard in distributed systems are still on-going. However, it is also worth noting that there is increasing number of commercially supported tools that are IEC 61499 complaint. There is also need to formulate application guidelines for use, as well as standardized libraries. Similarly, the success of the features the standard possess such as component based, open architecture with event driven functional modules, portability, interoperability and configurability, can only be measured upon by developing software tools from multiple vendors which are to be adopted by industry on real practical and complex plants. For example, portability and interoperability of library elements features test can only be measured when different vendor library tools can exchange information in different engineering environments and hardware like transformation between function block models created under 4DIAC.to Simulink model of MathWorks environments etc. The proposed research work is aimed at the deployment of the developed controllers to the design of distributed automation control system configuration using the IEC 61499 standard based complaint platforms. Twin CAT 3.1 (Beckhoff automation) system's real-time and Matlab/Simulink (*www.mathworks.com)* environment are used to test the effectiveness of the models Comparative performance analyses using the two platforms (Matlab/Simulink and Twin CAT 3.1) such as configurability, decentralization assessment are presented in chapter 7.

2.6 Overall Conclusion regarding this chapter and the way forward

Overall, the review considered different aspects of design and implementation of control systems with specific bias to a nonlinear CSTR plant. In the beginning the nonlinear plant was introduced and the significance of the plant as the case study as well as the motivation towards the review of the research objectives was highlighted. The methodologies adopted over the years to the control of nonlinear plants were reviewed. As stated earlier, the motivation of this research is to use a combination of linear and nonlinear based process models of the nonlinear plant with different control strategies such as decentralized, decoupling control, and feedback linearization techniques to provide a methodology for design and implementation of the control of the nonlinear CSTR plant. Table 2.2 provided summary of the review of the general mode-based design methods employed for the nonlinear control with their advantages and disadvantages, followed with a discussion on how the conventional concepts are intended to be applied as part of the thesis objectives.

The control paradigm employing input-output feedback linearization techniques with emphasis to CSTR model is adopted as method to be developed for the case of the CSTR process. The reason for feedback realization technique as opposed to the other control methods .is the simplicity of the technique and also that feedback linearization technique is suitable and efficient method for controlling a broader class of nonlinear systems. The nonlinear plant also being a MIMO system requires control strategies that aim to eliminate interaction between control loops, decentralized control and decoupling control strategies are proposed based on the linear system model.

Tables 2.4 presents a summary of the review papers on the new IEC 61499 standard developed to be adopted for the design and implementation of distributed control, and automation where several issues regarding the design and implementation rules, semantic, workbench platforms, software tools, runtime environments, as well as real time applicability are reviewed and discussed. The approach proposed in this thesis is to integrate the concepts of the Matlab/Simulink transformation to the Functional block programming environment of TwinCAT 3.1, and utilize them to design and implement nonlinear controllers for the CSTR nonlinear plant. This can be achieved by introducing and implementing a new function blocks of the plant as well as for the controllers to the function library of PLC system in order to achieve the envisaged objectives. The approach of the transformation is described in chapter seven.

Chapter three discusses the nonlinear MIMO CSTR process model, its static and dynamic characteristics and its significance in this research

CHAPTER THREE
ANALYSIS OF THE STEADY STATE AND DYNAMIC CHARACTERISTICS OF THE CSTR PLANT MODEL

3.1 Introduction

This chapter discusses the Continuous Stirred Tank Reactor (CSTR) which has been selected as a case study in the thesis. The nonlinear CSTR process model's steady state and dynamic characteristics are analysed in order to help in developing a clear understanding of the steady state and dynamic behaviour of the system for various changes on the input conditions. The Simulations are performed on the nonlinear model of the CSTR with a first order exothermic reaction to show the behaviour of the plant model for step changes in the inputs. This allows for the choosing of optimal working points for the controller design.

The chapter is structured as follows: In section 3.2, a general problem formulation of nonlinear systems is presented. In section 3.3 the ideal CSTR process as the case study is presented. In section 3.3 the modelling equations describing the dynamics of the CSTR process are derived. In section 3.4 the state space form of the CSTR dynamic equations is presented. In section 3.5 the steady state performance analysis is given. In section 3.6 the dynamic analysis and simulation of the CSTR process is derived. Section 3.7 presents the discussions and conclusion arising from the analyses and the significance of the obtained results for the next chapter.

3.2 The mathematical description of nonlinear systems

Nonlinear control covers a wider class of systems that do not obey the superposition principle and homogeneity property. It applies to many real-world systems, because virtually all real systems are nonlinear. While the theory of dynamic modelling for the linear systems is well understood as well as the mathematical tools for their analysis, there is still a wide gap in control theory for the analysis of nonlinear systems. Design methods for designing controllers for the nonlinear systems are not fully developed and are often difficult to use. The distinction between the linear and nonlinear systems is that any system that satisfies the properties of homogeneity and superposition is a linear system. If the system does not satisfy these two properties then it is nonlinear. Thirdly, nonlinear systems may have many equilibrium points unlike the linear system which has only one equilibrium point. This therefore means that for the nonlinear systems, their stability needs must be explicitly specified. Many physical quantities such as a vehicle's velocity, thermal, fluidic, chemical, biological or electrical signals, have upper bound. When that upper bound is reached, the linearity is lost. The differential equations governing such systems are nonlinear in nature. It is

therefore advantageous to consider their nonlinearities directly when analysing and designing controllers.

Nonlinear continuous time-invariant systems can be generally described by the set of state-space nonlinear equations of the form:

$$\dot{x} = f[x,u]$$
$$y = h[x,u] \tag{3.1}$$

Where, $x = [x_1, x_2, ...x_n]^T$ represents state vector, $u = [u_1, u_2, ...u_m]^T$ is the input vector, $f = [f_1, f_2, ... f_n]^T$ and $h = [h_1, h_2, ...h_l]^T$ are the nonlinear vector functions while $y = [y_1, y_2, ...y_l]^T$ represents the output vector. The mathematical model of Equation (3.1) is then defined with initial conditions. Each state variable needs as many initial conditions as is the number of the components of the vector of the state. Equation (3.2) is the initial conditions for the nonlinear system, i.e.

$$x(0) = x_o \tag{3.2}$$

Where x_o is obtained from the steady state analysis.

In the following section, the nonlinear Continuous Stirred Tank Reactor (CSTR) bench mark model is presented.

3.3 The Ideal CSTR process

The CSTR process has been selected as a case study for the design and implementation of the various control laws, due to the simplicity of the mathematical representation and because of the inherent nonlinearity property of the model. A CSTR is a common phenomenon in chemical and petrochemical reaction plants in which an impeller continuously stirs the content of a tank or reactor, thereby ensuring proper mixing of the reagents in order to achieve a specific output (product). The CSTR process is normally run at steady state with continuous flow of reactants and products. Chemical reactions are either exothermic (release energy) or endothermic (require energy input) and therefore it is necessary that energy be either removed or added to a reactor for a constant temperature to be maintained. Exothermic reactions are the most interesting systems to study because of the potential safety problems (rapid increase in temperature behaviour) and possibility of the exotic behaviour such as multiple steady states. This means that for the same value of the input variable there may be several possible values of the output variable (Uppal and Ray, 1974; Russo and Bequette, 1998; Aris and. Amundson, 2000; Bequette, 2004; Vojtesek and Dostal, 2005; Bakosova and Vasickaninova, 2009; Vojtesek and Dostal, 2010; Kumar and Khanduja, 2012). These features therefore make the CSTR an important model

for research. Many practical examples of the CSTR exist in industry including various types of polymerization reactors which produce polymers that are used for plastic products such as plastic bottles or polystyrene coolers. Although industrial reactors typically have more complicated kinetics than an ideal CSTR, the characteristic behaviour is similar, hence the interesting features can still be realised using the ideal one. It is also worth noting that most of the reactors, dealt with in the literature for control purposes, have been modelled as ideal CSTRs. In addition, the CSTR is an example of a MIMO system in which the formation of the product is dependent upon the reactor temperature and the feed flow rate. The process has to be controlled by two loops, a concentration control loop and a temperature control loop. Changes to the feed flow rate are used to control the product concentration and the changes to the reactor temperature are made by increasing or decreasing the temperature of the jacket (varying the coolant flow rate). However, changes made to the feed would change the reaction mass, and hence temperature, and changes made to temperature would change the reaction rate, and hence influence the concentration. This is an example of loop interactions. For control design, loop interactions should be avoided because changes in one loop might cause destabilizing effects on the other loop.

3.3.1 Derivation of the modelling equations

To describe the dynamic behaviour of the considered CSTR process model from Figure.3.1, mass, component and energy balance equations are developed. In the process, an irreversible, exothermic reaction A occurs in a constant volume reactor that is cooled by a single coolant stream. Proper knowledge of how to manipulate these equations for control will results in the successful operation and production of the desired products. For this analysis, the system is assumed to have two state variables; the reactor temperature and the reactor concentration and these are also the output variables to be controlled. The manipulated variables are the feed flow rate and the coolant flow rate.

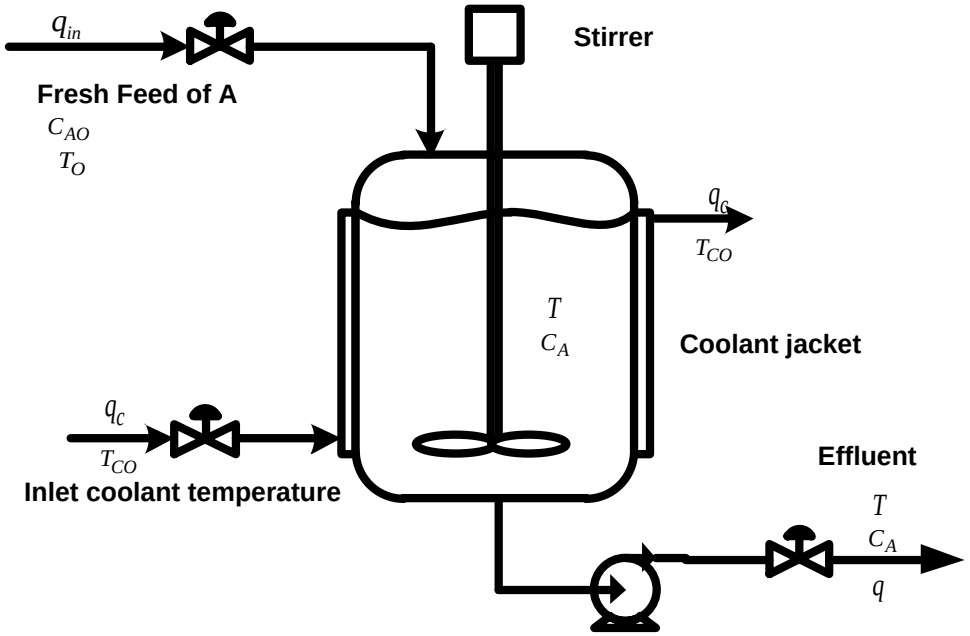

Figure 3.1: A basic scheme of the CSTR Process

A jacket surrounding the reactor also has feed and exit streams. The jacket water is assumed to be perfectly mixed and at a lower temperature than the temperature of the reactor. Energy then passes through the reactor walls into the jacket, removing the heat generated by the reaction.

For simplicity, the following assumptions are made in the development of the CSTR model:

- Cooling jacket temperature can be directly manipulated, so that an energy balance around the jacket is not required
- Heat losses from the process (well-insulated) to the atmosphere are negligible.
- Perfect mixing- the mixture density and heat capacity are assumed constant.
- The coolant is perfectly mixed and therefore the temperature everywhere in the jacket is the same.
- The mass of the material walls is negligible so that the thermal inertia of the metal need not to be considered.
- Constant volume assumed.
- The exit stream has the same concentration and temperature as the entire reactor liquid
- Constant parameter values. There are no spatial variations in the concentration and temperature or reaction rate throughout the reactor.

The parameters and variables that appear in the modelling equations are as listed:

W Area for the heat exchange

C_A Concentration of the component A in the reactor

C_{AO} Concentration of the component A in the feed stream

C_P, C_{PC} Specific heat capacities (Calories/mass*temperature) where C_P is the specific heat capacity of A in the reactor and C_{PC} is the Specific heat capacities of the coolant

q Process volumetric flow rate (volume/time)

q_{in} Process feed input volumetric flow rate (volume/time)

q_o Process output volumetric flow rate (volume/time)

ρ_{in} Density of the incoming flow (mass/volume)

q_c Coolant volumetric flow rate (volume/time)

k_o Pre-exponential factor (time^{-1})

R Ideal gas constant (Calories/mole*temperature)

r Rate of reaction per unit volume (mole/volume*time)

t Time

T Reactor temperature

T_O Feed temperature

T_{CO} Jacket temperature

hA Overall heat transfer coefficient (Calories/(time*area*temperature))

V Reactor constant volume

ΔE Activation energy (Calories/mole)

$(-\Delta H)$ Heat of reaction (Calories/mole)

ρ, ρ_c Densities (mass/volume), where ρ is the density of A in the reactor and $, \rho_c$ is the density of the coolant

Model development basis is a set of fundamental balance equations which are mathematical statements of physical laws that require conversion of mass, energy, momentum and quantities by particular chemical species while introducing appropriate variables. Chemical processes have important thermal effects hence it is necessary to develop material and energy balance models for these systems. The two basic mathematical equations required to describe the CSTR performance are the mass (material) balance and the energy balance which are explained and derived as follows:

3.3.2 Mass and Energy balances for the CSTR process:

The two laws of physics (the law of mass and the law of energy conservation provide the basic tools which are used in the study of the chemical reaction processes. The law of mass states that the mass can neither be produced nor destroyed, i.e. mass is conserved. Similarly, the law of conservation of energy states that energy cannot be created nor destroyed, although energy can be changed from one form to another form.

3.3.2.1 Overall and component A material balances for the CSTR process (continuity equation)

The material (mass) balance for a reactant can be described in a general first principles-based derivation of the form applicable to any type of a reactor as follows (Bequette,1998):

$$\begin{bmatrix}\text{Rate of}\\ \text{accumulation}\\ \text{within the system}\end{bmatrix}=\begin{bmatrix}\text{Rate of inflow}\\ \text{into the system}\end{bmatrix}-\begin{bmatrix}\text{Rate of outflow}\\ \text{from the system}\end{bmatrix}\pm\begin{bmatrix}\text{Rate of generation}\\ \text{by chemical reaction}\\ \text{within the system}\end{bmatrix} \quad (3.3)$$

Equation (3.3) implies that given a constant volume, the rate of accumulation of mass in the reactor is equal to the sum of mass inflow into the system minus the sum of mass outflow minus (plus) the mass flow of the consumed or generated mass.

For the CSTR process under investigation, the following are assumed.

- Mass flow rate into the reactor $= q_{in}.\rho_{in}$
- Mass flow rate out of the reactor $= q_o.\rho$
- Rate of production or consumption of mass within the reactor $= 0,$ and,
- Rate of accumulation of mass within the reactor is $\frac{dV}{dt}.\rho$

Substituting these terms in the continuity Equation (3.3))

Where for the whole reactor it is obtained:

$$\frac{dV}{dt}.\rho = q_{in}\rho_{in} - q_o\rho \quad (3.4)$$

Assuming that the density of the mass in the reactor remains constant throughout the reaction then, Equation (3.4) simplifies to:

$$\frac{dV}{dt} = q_{in} - q_o \quad (3.5)$$

The mass balance equation for the component A in the reactor has the same structure as in Equation (3.3) with the following components.

- Rate of the component A into reactor is $q_{in}.C_{AO}$
- Rate of the component A out of reactor is $q_o.C_A$

- Rate of generation of the component A by a chemical reaction is $-rV$
- Rate of accumulation of the component A within the reactor is $V\frac{dC_A}{dt}$

Here r is the rate of disappearance of the component A. Substituting all these terms in the mass balance Equation (3.3), the following is obtained.

$$V\frac{C_A}{dt} = q_{in}C_{AO} - q_oC_A - rV \tag{3.6}$$

Assuming that a constant amount of the material is in the reactor (Denn, 1986), then: $q = q_{in} = q_o$ and equation (3.6) can be written as:

$$V\frac{dC_A}{dt} = qC_{AO} - qC_A - rV \tag{3.7}$$

Where, r is the rate of the reaction per unit volume and is given by the Arrhenius equation $r = k_o \exp\left(\frac{-\Delta E}{R.T}\right)C_A$ (3.8)

From Equations (3.7) and (3.8) it is noted that the time rate of change of the component A is a function of both the reactant concentration of the component A and the reactant temperature of component A within the CSTR.

Similarly, the Energy Balance equation of the component A is derived in the following subsection.

3.3.2.2 Energy Balance of the component A for the CSTR process

The forms of energy in a given substance can be divided into two: internal and external. Internal energy is part of a molecular structure of a substance while external energy results from motion of a substance. Chemical internal energy is the energy in the chemical bonds of a substance and is composed of the strengths of the atomic bonds in the substance and the energy in the bonds between the molecules. For chemical processes where there are thermal effects, the external energy may be neglected because their contribution is generally at least two orders of magnitude less than that of the internal energy (Bequette, 1998).

The energy balance Equation is described in the following way (Bequette, 1998):

$$\begin{bmatrix}\text{Rate of energy}\\ \text{accumulation}\end{bmatrix} = \begin{bmatrix}\text{Net rate of}\\ \text{energy input}\end{bmatrix} + \begin{bmatrix}\text{Rate of energy added by}\\ \text{exothermic chemical reaction}\end{bmatrix} \tag{3.9}$$

Where,

$$\begin{bmatrix}\text{Net rate of}\\ \text{input energy}\end{bmatrix} = \begin{bmatrix}\text{Rate of heat input from the}\\ \text{heating jacket to the reactor}\end{bmatrix} - \begin{bmatrix}\text{Rate of heat output from}\\ \text{reactor to the cooling coil}\end{bmatrix} \tag{3.10}$$

For the considered CSTR reactor,

- Rate of the energy going into the reactor is $q\rho C_P T_O$

- Rate of the energy going out of the reactor is:

$$q\rho C_P(T_O - T) + \rho_c C_{pc} q_c \left(1 - \exp\frac{-hA}{\rho C_P q_c}\right)(T_{CO} - T)$$

- Rate of the energy added by the exothermic reaction is:
- $(-\Delta H)Vr = (-\Delta H)Vk_o \exp\left(\frac{-\Delta E}{RT}\right)C_A$,and the
- Rate of accumulation of energy added by the exothermic reaction is $V\rho C_P \frac{dT}{dt}$

Here $(-\Delta H)Vr$ is the rate of energy contributed by the exothermic reaction.

Thus using the energy Equations (3.9) and (3.10) the final energy balance equation for the component A derived with the assumption of a constant volume, heat capacity and density is given as:

$$V\rho C_P \frac{dT}{dt} = q\rho C_P(T_o - T) + (-\Delta H)Vr + \rho_c C_{PC} q_c \left(1 - \exp\frac{-hA}{\rho C_P q_c}\right)(T_{CO} - T) \qquad (3.11)$$

The energy balance reaction described by the Equation (3.11) is assumed to be of the first order.

3.3.2.3 Conclusion regarding the Balance Equations for the CSTR process

A methodology for developing dynamic models of the CSTR has been presented. Two first order nonlinear differential equations are derived from the first principles based on mass balance and energy balance. Equation (3.7) is the first order equation describing the mass (material) balance of the component A to analyse its concentration, while Equation (3.11) is the second first order equation describing the dynamics of the energy balance of the component A the reactor temperature for the CSTR process. In the process of the derivation, the assumptions of the perfectly stirred constant volume tank reactor are used. With regards to the two Equations derived, it is noted that there is mutual coupling between the material and energy balance equations as well as nonlinearities with respect to time. The nonlinearities can be seen to be due to the exponential relations in the two Equations. These couplings may lead to complex behaviour of the process and difficulties in its control.

3.4 State space Form of the Dynamic Equations of the CSTR process

The mathematical model of the CSTR is composed of the mass and energy balance equations, plus necessary equations for the calculation of the rate reactior and the heat transfer. For this analysis, the systems is assumed to have two state variables, namely the reactor temperature and the reactor concentration and from Equations

(3.7) and (3.11) the following two first order differential equations modelled in state space variable form are obtained:

$$f_1(C_A,T)=\frac{dC_A}{dt}=\frac{q}{V}(C_{AO}-C_A)-r \tag{3.12}$$

$$f_2(C_A,T)=\frac{dT}{dt}=\frac{q}{V}(T_o-T)+\frac{(-\Delta H)r}{\rho C_P}+\frac{\rho_c C_{PC} q_c}{\rho C_P V}\left(1-\exp\frac{-hA}{\rho C_P q_c}\right)(T_{CO}-T) \tag{3.13}$$

where each term in the two Equations have already been defined. The nonlinearity of the model is hidden mainly in the computation of the reaction rate r which is a nonlinear function of the temperature, T and it is computed from Arrhenius law given in Equation (3.8). The system is modelled and analysed using the parameters specified in Tables 3.1 and 3.2. These parameters represent both the steady state and the dynamic operating conditions (Vinodha et al, 2010; Vojtesek and Dostal, 2012; Prakash and Srinivasan, 2008).

Table 3.1: Steady state operating data

Process variable	Nominal operation condition	Process variable	Nominal operation condition
Reactor Concentration (C_A)	$0.0989 mol/l$	CSTR volume (V)	$100l$
Temperature (T)	$438.7763K$	Heat transfer term (hA)	$7*10^5 cal/(\min.k)$
Coolant flow rate (q_c)	$103l/\min$	Reaction rate constant (k_o)	$7.2*10^{10}\ \min^{-1}$
Process flow rate (q)	$100.0l/\min$	Activation energy (E/R)	$1*10^4 K$
Feed concentration (C_{AO})	$1mol/l$	Heat of reaction $(-\Delta H)$	$-2*10^5 cal/mol$
Feed temperature (T_O)	$350.0K$	Liquid densities (ρ,ρ_c)	$1*10^3 gal/l$
Coolant temperature (T_{CO})	$350.0K$	Specific heats (C_P,C_{PC})	$1cal/(g.k)$

Table 3.2: Steady state operating points.

Operating points	$q(lpm)$	$q_C(lpm)$	$C_A(mol/l)$	$T(K)$
Operating points 1	102	97	0.0762	444..7
Operating points 2	100	103	0.0989	438.77
Operating points 3	98	109	0.01275	433

The analysis of this system can be performed for both steady state and dynamic behaviour in order to understand, how the system works in different states and various changes of the inputs. The steady state values help in fixing of the initial conditions for the controller design. The steady state analysis shows behaviour of the system in the steady-state, i.e. as time tends toward infinity and results in an optimal working point in the sense of maximal effectiveness and concentration yield. Dynamic analysis means that the state and output variables are observed in time after a step

change of some input variable. Before analysing the dynamics of the system, it is important to understand its steady state behaviour.

3.5 Steady state and dynamic analyses

The steady state solution is obtained when $\frac{dC_A}{dt} = 0$, and $\frac{\mathrm{dT}}{dt} = 0$ in Equations (3.14) and (3.15), i.e.:

$$f_1(C_A, T) = \frac{dC_A}{dt} = 0 = \frac{q}{V}(C_{AO} - C_A) - r \tag{3.14}$$

$$f_2(C_A, T) = \frac{dT}{dt} = 0 = \frac{q}{V}(T_o - T) + \frac{(-\Delta H)r}{\rho C_P} + \frac{\rho_c C_{PC} q_c}{\rho C_P V}\left(1 - \exp\frac{-hA}{\rho C_P q_c}\right)(T_{CO} - T) \tag{3.15}$$

Solution to Equations (3.15) and (3.14) for C_A and T is possible if all the numerical values of the parameters and variables are as given in Table 3.1. Previous studies for the steady state response (Russo and Bequette, 1995, 1997, 1998; Bequette, 1998; Bequette, 2007) have shown interesting steady-state behaviours of this reactor. It is shown that the solution of these equations, whatever the initial guesses for the concentration and temperature, leads to different steady state values. It is important also to use physical insight about the possible range of the solutions. For example, since the feed concentration of A is 1 mole/litre and the reaction only consumes A, the possible range for the concentration of A is $0 < C_A < 1$. Also, it is easy to show that a lower bound for the temperature is $350K\ (77^{\circ}C)$ which would occur if there was no reaction at all, since the feed and jacket temperatures are both $350K\ (77^{\circ}C)$. There is a correlation between concentration and temperature meaning that if the concentration A is high, then not much reaction has taken place and hence little energy is released by reaction. Therefore the temperature will not be much different than the feed temperature and jacket temperatures and vice versa. It has been shown that different initial conditions causes the system to converge to three different steady state operating points which are as illustrated in Table 3.2 above.

3.5.1 Simulation of the controlled variables at the steady state operating conditions.

The model of the CSTR process, whose dynamics are defined by the Equations (3.12) and (3.13) can represented in a black box form as shown in Figure 3.2.

Figure 3.2: Black box model of the nonlinear CSTR process

where the inputs are the steady state values of the feed flow rate q_s and the coolant flow rate q_{cs} respectively. This model is subsequently built in the Matlab/Simulink environment is shown in Figure 3.3 using parameters of Table 3.1. The simulated open loop curves of the controlled variables steady at one of the operating points as indicated in Table 3.2 where the control inputs of the coolant flow rate the feed flow rate and the initial points of the concentration and the temperature respectively are selected to have the steady state values for this operating point as:

$q_s = 102mol/l,\ q_{cs} = 97mol/l, C_{As} = 0.0762mol/l,$ and $T_s = 444.77K$,

are re illustrated in Figures 3.4 and 3.5.

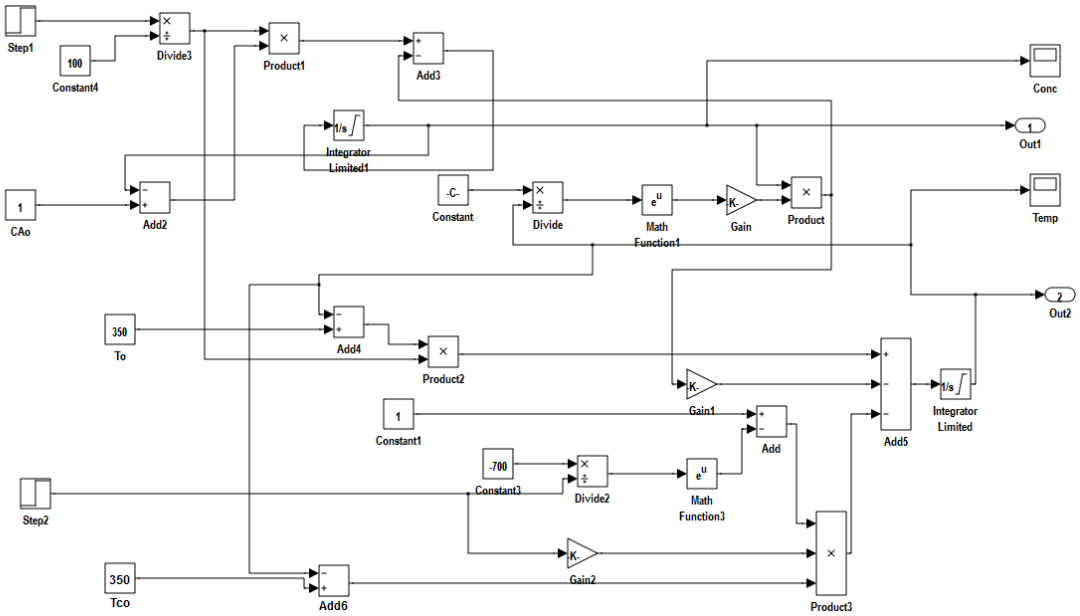

Figure 3.3: Simulink block diagram of the nonlinear CSTR model

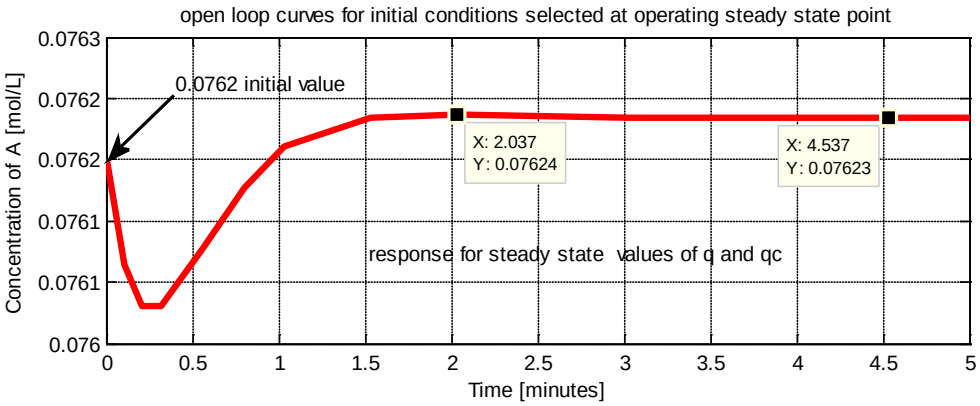

Figure 3.4: Time response of the Concentration values of input at steady state operating point

Reference to Figure 3.4, the initial condition is at steady state operating point of 0.0762 mole/litre and settles at some value of 0.07623 mole/litre with steady state error of 0.04%

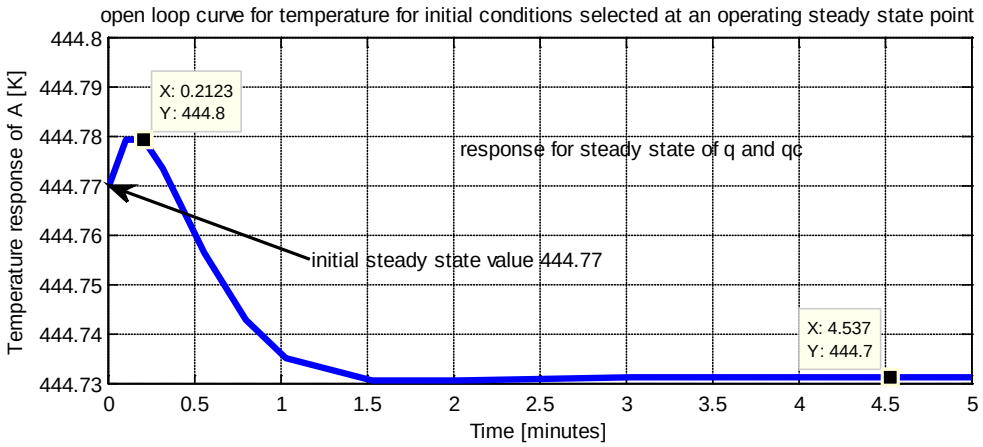

Figure 3.5: Time response of the Temperature for values of input at the steady state operating point

Reference to Figure 3.4, the initial condition is at the steady state operating point of $444.77K$ and settles at some value of $444.7K$ with steady state error of 0.16% From the simulated time responses of the concentration and the temperature as illustrated in Figures 3.4 and 3.5, it is noted that in both the outputs, there is a steady state error implying that if the process is disturbed from the steady state point, it cannot go back to the steady state without closed loop control. This means that it needs to be controlled.

3.5.2 Dynamic analysis and Simulation.

In order to investigate the dynamic behaviour of the process, simulation has to be undertaken regarding the modelling equations. The transient response of the state variables can then be found by numerically solving the differential algebraic equations. Several numerical optimization algorithms are available for different classes of ordinary differential equations solutions such as the Runge-Kuttas fourth and fifth order method, and the Euler Langrage method of integration. The transient response implies that an observation of the trajectories of the state variables in time after step change in some input variables can be calculated. In this study, the state x and the input u are vectors given by $x = [C_A \ T]^T$ where, C_A is the effluent concentration and T is the temperature of the effluent to be controlled. The input vector is $u = [q \ q_c]^T$, where, q and q_c are the volumetric step changes in the flow rates of the inlet feed concentration and coolant respectively. In the analysis, the steady state values of Table 3.2 at the operating point 1 where,

($q_s = u_1$=102.0l/m; $q_{cs} = u_2 = 97.0$l/m; $y_1 = C_{Ainit} = 0.0762$mol/l; $y_2 = T_{init} = 444.7$K) are taken as the initial conditions for the Equations (3.12) and (3.13). Several step changes in each input variable while maintaining the other variable constant and vice versa by $(\pm 10\%)$ of its value in the operating point 1 were simulated and the results are shown in the following figures. Figures 3.6 to Figure 3.10 respectively are the concentration time responses.

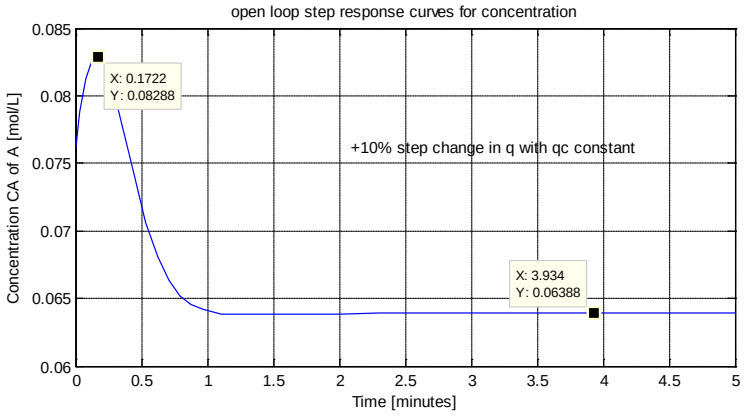

Figure 3.6: Response of the concentration for $+10\%$ step change in q with q_c constant

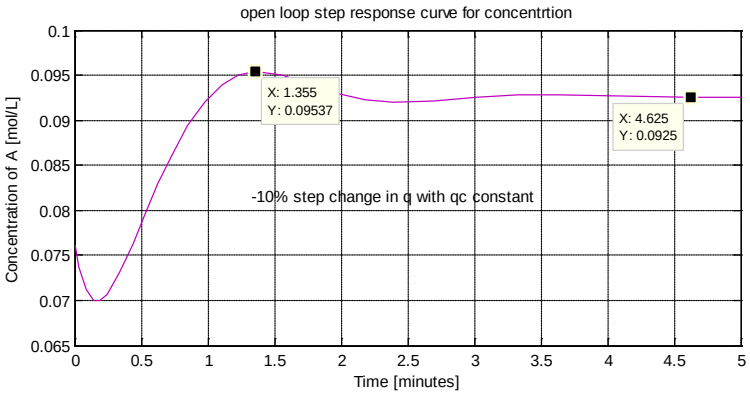

Figure 3.7: Response of the concentration for -10% step change in q with q_c constant

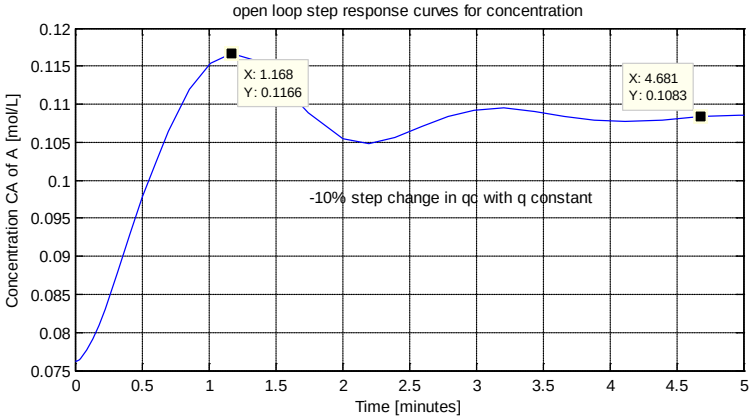

Figure 3.8: Response of the concentration for -10% step change in q_c with q constant

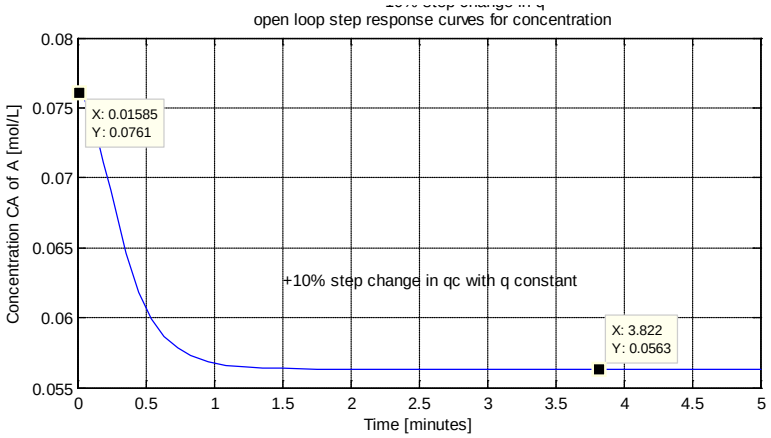

Figure 3.9: Response of the concentration for $+10\%$ step change in q_c with q constant

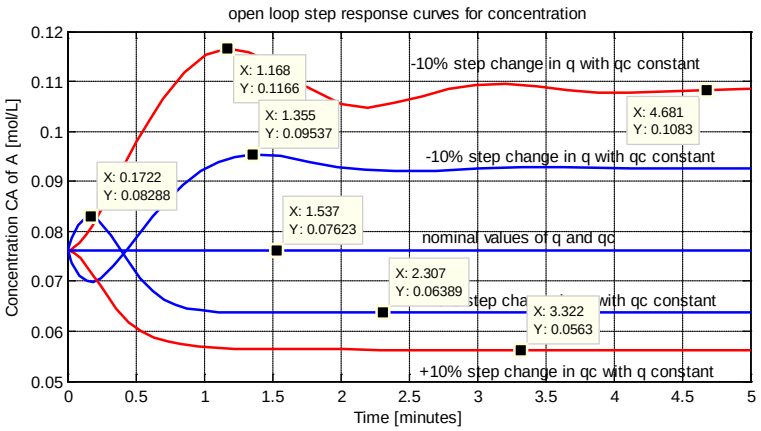

Figure 3.10: Time response of the Concentration for $(\pm 10\%)$ step changes in the inputs volumetric flow rates q and q_c

Figures 3.11 to 3.15 respectively are the various time responses for the temperature.

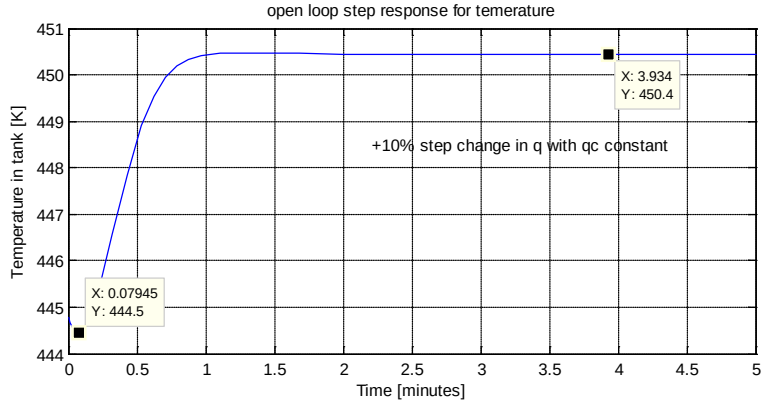

Figure 3.11: Response of the Temperature for $+10\%$ step change in q with $\mathrm{q_c}$ constant

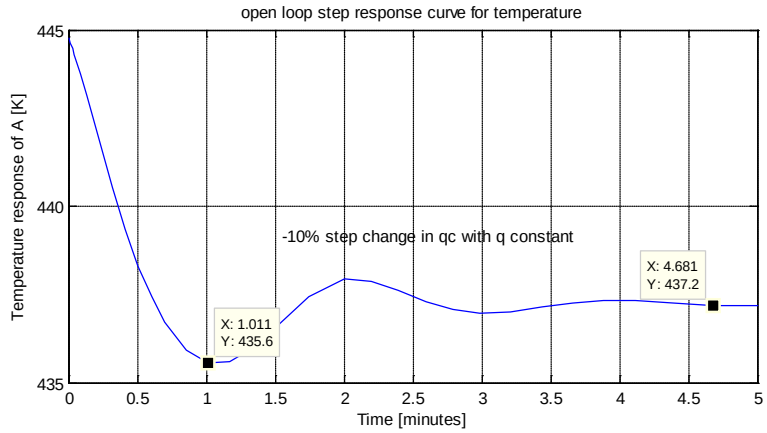

Figure 3.12: Response of the Temperature for -10% step change in $\mathrm{q_c}$ with q constant

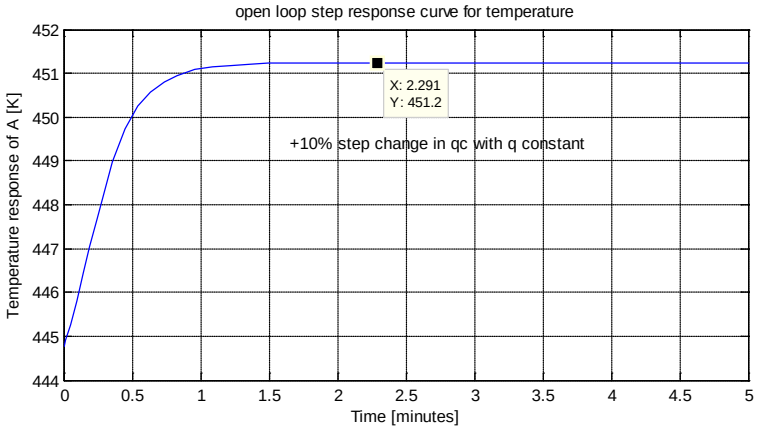

Figure 3.13: Response of the Temperature for $+10\%$ step change in q_c with q constant

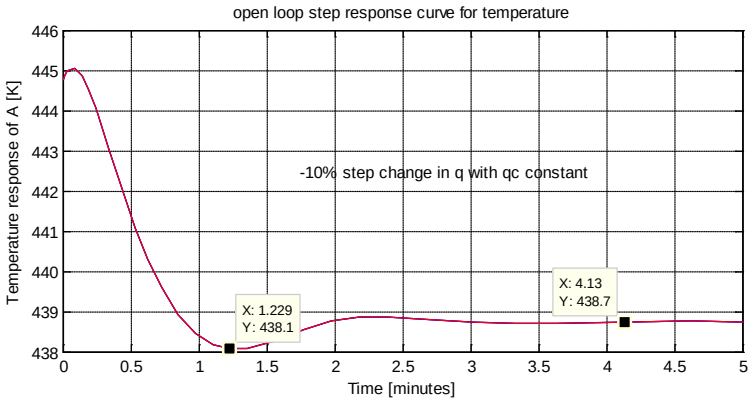

Figure 3.14: Response of the Temperature for -10% step change in q with q_c constant

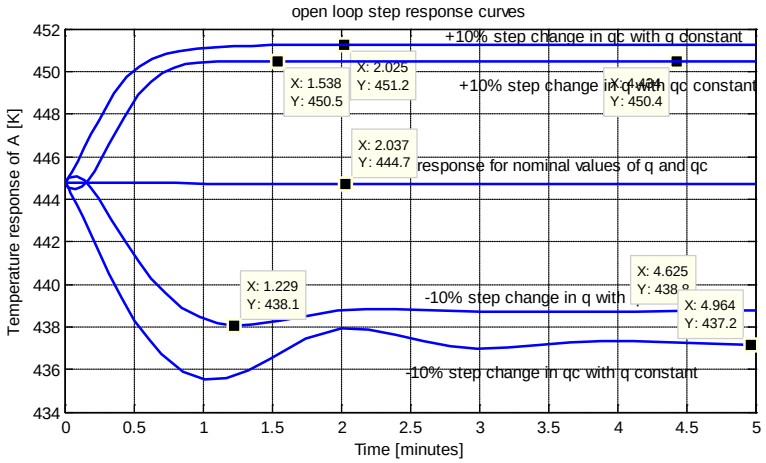

Figure 3.15: Time response of the Temperature for $\pm 10\%$ step changes in q and q_c

Table 3.3 gives the comparative analyses of the various steady state magnitudes as illustrated in the figures above with initial values $C_{Ainit} = 0.0762 mol/l$; $T_{init} = 444.7K$

Table 3.3: $\pm 10\%$ step changes in input volumetric flow rates q and q_c

Magnitude of input variable	Magnitude of steady state concentration	Magnitude of steady state temperature
-10% Step change in feed flow rate q.	$0.1083\mathrm{mol/l}$	$438.7\mathrm{K}$.
$+10\%$ Step change in feed flow rate q	$0.06388\mathrm{mol/l}$.	$450.4\mathrm{K}$
-10% Step change in coolant flow rate $\mathrm{q_c}$	$0.0563\mathrm{mol/l}$	$437.2\mathrm{K}$
$+10\%$ Step change in coolant flow rate $\mathrm{q_c}$	$0.1166\mathrm{mol/l}$	$451.2\mathrm{K}$
Nominal value of coolant flow rate $\mathrm{q_c}$	$0.0762\mathrm{mol/l}$	$444.77\mathrm{K}$
Nominal value of feed flow rate q	$0.0762\mathrm{mol/l}$	$444.77\mathrm{K}$

Appendix A1 presents the function file for the MIMO CSTR process with the parameter values that are used for the development of different models in Simulink **while t**he main file for the CSTR process model for simulating the function file for various magnitudes of perturbations over the initial steady state conditions is in appendix A2.

Appendix B presents the script file for the linearization of the CSTR process model by finding the Jacobian matrices, the state space matrices and the transfer functions of the state space model

3.6 Discussion and Conclusion

In this chapter, the first principles-based model of the CSTR process is derived and simulation studies are performed. The mathematical model of the CTR dynamics is formulated with the assumption of the ideal case, where the inputs considered are the feed flow and the coolant flow rates respectively and the outputs to be monitored are the product concentration and the temperature respectively.

The graphs of Figures 3.4 and 3.5 where the steady state values of q and q_c are used for one of the operating points of the process show that $\mathrm{C_A}$ settles at the steady state value of $0.0762\mathrm{mol/L}$ while T settles at $444.77\mathrm{K}$ which are for the operating point 1 of Table 2. However when the system is perturbed by a $\pm 10\%$ of the control signal q while maintaining $\mathrm{q_c}$, at its steady state value as illustrated in Figures 3.11 and 3.15, the reactor temperature changes nonlinearly from the initial steady state value of $444.7\mathrm{K}$ to about $450.5\mathrm{K}$ with time for a positive change and to a value of $439\mathrm{K}$ for a negative change as illustrated in Figures 3.14 and 3.15 respectively. Similarly, by maintaining $\mathrm{q_c}$ at its steady state value while perturbing the control q by a $\pm 10\%$ step change from its steady state value, $\mathrm{C_A}$ changes nonlinearly from its initial steady

state value to a value of about $0.06388 mol/l$ for a positive change as illustrated in Figures 3.6 and 3.11 then to about $0.0922\ mol/L$ for a negative change as illustrated in Figures 3.7 and 3.10 respectively. Maintaining q constant and perturbing q_c by a $\pm 10\%$ step change from its steady state value also yields nonlinear responses as depicted in Figures 3.7, 3.8 and 3.9 respectively. In conclusion, the simulation results demonstrate that the CSTR exhibits highly nonlinear dynamic behaviour. This is because of the coupling and the inter-relationships of the states and in particular, the exponential dependence of each state on the reactor temperature as well as the reaction rate being an exponential function of the temperature. This type of nonlinearity is generally considered significant (Vojtesek and Dostal, 2009). Hence, there rises a need to develop control schemes that are able to achieve tighter control of the process dynamics. A more detailed discussion on the reactor design and operability can be found in (Russo and Bequette, 1995, 1997, 1998; Bequette, 2007).

To address these problems, three different control design strategies are proposed, implemented and compared in chapters 4, 5 and 6. These are; Decoupling controller design method, Input-Output state feedback controller design methodology and the Decentralized controller design methodology utilizing the concept of Relative Gain array. Decoupling control strategy is first developed in Chapter 4. It requires that the nonlinear system be linearized at the given operating point and the resulting state space equations can then be directly used in the design of standard linear controllers. Second is the Decentralized controller design methodology developed in Chapter 5, also requiring the linearized model of the CSTR process model. Chapter 6 deals with the Input-output state feedback controller design methodology and a comparison of the performance analysis of the three methods in terms of the suitability to control the MIMO CSTR process under study is discussed.

CHAPTER FOUR
MULTIVARIABLE DECOUPLING CONTROLLER DESIGN

4.1 Introduction

This chapter presents a method for design of a multivariable decoupling controller of the temperature and concentration in the ideal nonlinear MIMO CSTR process. Decoupling control ensures that the MIMO control system is decoupled so that each output is controlled independently on the other outputs. The preliminary theory of the method is presented, then the details of the design of the MIMO control schemes dynamically decoupled PI controllers are provided, and lastly the closed loop system is tested and investigated by simulation in the Matlab/Simulink environment in terms of the performance specifications to demonstrate the effectiveness of the control strategy.

The chapter is structured as follows: In section 4.2 the philosophy of the multivariable control design is presented. Section 4.3 presents the linearization procedure adopted and the stability analysis for the nonlinear MIMO CSTR process. Section 4.4 presents the general dynamic decoupling control design strategy. In section 4.5, PI controller design by pole placement is described. Section 4.6 presents the simulation of the closed loop system under various process conditions. Section 4.7 is the discussion emanating from the simulated results, and finally section 4.8 is the conclusion of the chapter.

4.2 Multivariable Control design

Processes where only one output is controlled by a single manipulated variable are called Single Input Single Output (SISO) systems. However systems with more than one control loop, perhaps interacting are known as multi-input multi-output or multivariable systems. The control objective for the multivariable systems is to obtain desirable behaviour of several output variables by simultaneously manipulating several input variables. Some MIMO processes may be nonlinear as well. Control of such processes is very challenging because the nonlinear processes do not share many properties of the linear systems and therefore no systematic procedure is available due to different forms of nonlinearities.

One of the most challenging aspects of the control of MIMO systems is the interaction between different inputs and outputs. In general, each input will have an effect on every output of the system. Because of the coupling, signals can interact in unexpected ways and thereby result in a destabilizing effect on the other loops.

Another challenging aspect is when the system to be controlled has nonlinear dynamics and some elements of dead time.

A PID controller algorithm is the most popular feedback controller used for industrial processes because of its robustness and excellent control capabilities However, when the controlled process is nonlinear, and multivariable, a fixed gain PID controller cannot produce satisfactory control performance. If a fixed gain controller is utilized, the closed loop performance may be degraded to the point of instability. To avoid loop interactions multivariable systems can be decoupled into separate single input single output systems. Decoupling may be done using several different techniques, including restructuring the pairing of variables, minimizing interactions by detuning conflicting control loops, opening loops and putting them in manual control or using linear combinations of manipulated and/or controlled variables.

The proposed control technique is to design additional controllers to supplement the conventional PID controllers in order to compensate for the process and control loop interactions in one strategy and to restructure the pairing of variables in the other strategy. To be able to design the controllers the dynamic model equation is linearized about the given steady state operating point in order to obtain the standard linear state space form and its corresponding matrix transfer function. Decoupling controller designs are then based on the linearized model of the CSTR process. These controller design methods are proposed in order to transfer the control problem to a series of single loop controller design problems. The following subsection gives the linearization procedure of the nonlinear CSTR model.

4.3 The CSTR model linearization and stability analysis

The modelling equations of the CSTR process contain nonlinear functions of T and C_A therefore the equations are in general nonlinear ones. The variables T and C_A are also coupled and it is not possible to solve one variable independent of the other. For designing controllers for such a nonlinear system, one of the approaches is to approximate the dynamics with a family of linear differential equations to explore the model dynamic response and stability and then to apply the linear control theory design techniques. It suffices to represent the nonlinear system as a family of local linear models by approximating the nonlinearities (Isidori, 1989). One basic approach is to truncate a Taylor series approximation of the original system about some operating points. The general procedure is briefly outlined below.

Assume the general nonlinear dynamic plant of the form of Equation. (3.1); the problem is to find an approximate linear model about some operating point (x_o, u_o). This requires the construction of matrices of the partial derivatives of the model equation with respect to the states and the inputs. A first order Taylor series expansion of Equation (3.1) around the steady state (x_o, u_o) truncated to include only the linear terms is:

$$\dot{x} \approx f(x_o, u_o) + \left.\frac{\partial f}{\partial x}\right|_{\substack{x=x_o \\ u=u_o}} (x - x_o) + \left.\frac{\partial f}{\partial u}\right|_{\substack{x=x_o \\ u=u_o}} (u - u_o) \tag{4.1}$$

$$y \approx h(x_o, u_o) + \left.\frac{\partial h}{\partial x}\right|_{\substack{x=x_o \\ u=u_o}} (x - x_o) + \left.\frac{\partial h}{\partial u}\right|_{\substack{x=x_o \\ u=u_o}} (u - u_o) \tag{4.2}$$

Where the ij th element of the Jacobian matrix $\partial f / \partial x$ is $\partial f_i / \partial x_i$. The linearized system of Equations (4.1) and (4.2) can then be written in the state space form as:

$$\dot{\bar{x}} = A\bar{x} + B\bar{u} \tag{4.3}$$

$$\bar{y} = C\bar{x} + D\bar{u} \tag{4.4}$$

Where $\bar{x} = x - x_o; \bar{u} = u - u_o \text{and } \bar{y} = y - h(x_o, u_o)$.The constant matrices A, B, C and D are values of the Jacobian matrices representing the state variables, input variables and output variables and defined as:

$$A = \left.\frac{\partial f}{\partial x}\right|_{\substack{x=x_o \\ u=u_o}}, \qquad \mathrm{B} = \left.\frac{\partial f}{\partial u}\right|_{\substack{x=x_o \\ u=u_o}} \tag{4.5}$$

$$C = \left.\frac{\partial h}{\partial x}\right|_{\substack{x=x_o \\ u=u_o}}, \qquad \mathrm{D} = \left.\frac{\partial h}{\partial u}\right|_{\substack{x=x_o \\ u=u_o}} \tag{4.6}$$

Equations (4.3) and (4.5) are in state space form in terms of deviation variables $\bar{\mathrm{x}}$ and $\bar{\mathrm{u}}$ which can then be directly used in the design of standard linear controllers.

In the following, this linearization method is applied to the nonlinear CSTR model to give the state space representation where, the state, input and output vectors are in the deviation variable form and are defined by the following:

$$x = \begin{bmatrix} C_A - C_{AS} \\ T - T_S \end{bmatrix} = \begin{bmatrix} x_1 \\ x_2 \end{bmatrix} = \text{ State variables}$$

$$u = \begin{bmatrix} q - q_s \\ q_c - q_{cs} \end{bmatrix} = \begin{bmatrix} u_1 \\ u_2 \end{bmatrix} = \text{ Input variables}$$

$$y = \begin{bmatrix} C_A - C_{AS} \\ T - T_S \end{bmatrix} = \begin{bmatrix} x_1 \\ x_2 \end{bmatrix} = \text{ Output variables}$$

Where $C_{AS}, T_S, \mathrm{q_s}$ and q_{cs} are the steady state values of the effluent concentration, reactor temperature, the feed flow rate, and the coolant flow rate respectively.

Using the values of the parameters provided in Tables 3.1 and 3.2, and letting,

$$a_1 = E/R = 1*10^4,\ a_2 = \frac{(-\Delta H)k_o}{\rho C_p} = 1.44*10^{13},$$

$$a_3 = \frac{\rho_c C_{pc}}{\rho C_p V} = 0.01, \text{ and } a_4 = \frac{-hA}{\rho c_p} = 700,$$

then Equations (3.11) and(3.12) may be written as:

$$f_1(x_1, x_2) = -k_o x_1 e^{-a_1/x_2} + \frac{(C_{AO} - x_1)u_1}{V} \tag{4.7}$$

$$f_2(x_1, x_2) = a_2 x_1 e^{-a_1/x_2} + \frac{(T_O - x_2)u_1}{V} + a_3(T_{CO} - x_2)u_2 * (1 - e^{-a_4/u_2}) \tag{4.8}$$

Then state space equations for the Jacobian matrices of the CSTR model (4.7) and (4.8) are derived in terms of x and u as follows:

$$A = \begin{bmatrix} \frac{\partial f_1}{\partial x_1} & \frac{\partial f_1}{\partial x_2} \\ \frac{\partial f_2}{\partial x_1} & \frac{\partial f_2}{\partial x_2} \end{bmatrix}.$$

Where the elements of the state-space A matrix are found as:

$$A_{11} = \frac{\partial f_1}{\partial x_1} = \frac{\partial f_1}{\partial (C_A - C_{AS})} = \frac{\partial f_1}{\partial C_A} = \frac{-u_1}{V} - \frac{k_o}{\mathrm{e}^{(a_1/x_2)}}$$

$$A_{12} = \frac{\partial f_1}{\partial x_2} = \frac{\partial f_1}{\partial (T - T_S)} = \frac{\partial f_1}{\partial T} = \frac{-(a_1 k_o x_1)}{(x_2{}^2\, \mathrm{e}^{(a_1/x_2)})}$$

$$A_{21} = \frac{\partial f_2}{\partial x_1} = \frac{\partial f_2}{\partial (C_A - C_{AS})} = \frac{\partial f_2}{\partial C_A} = \frac{a_2}{\mathrm{e}^{(a_1/a_2)}}$$

$$A_{22} = \frac{\partial f_2}{\partial x_2} = \frac{\partial f_2}{\partial (T - T_S)} = \frac{\partial f_2}{\partial T} = a_3 u_2 \left(\frac{1}{\mathrm{e}^{(a_4/u_2)}} - 1\right) - \frac{u_1}{V} + \frac{(a_1 a_2 x_1)}{(x_2{}^2\, \mathrm{e}^{(a_1/x_2)})}$$

From which the A matrix is,

$$A = \begin{bmatrix} \frac{-u_1}{V} - \frac{k_o}{\mathrm{e}^{(a_1/x_2)}} & \frac{-(a_1 k_o x_1)}{(x_2{}^2\, \mathrm{e}^{(a_1/x_2)})} \\ \frac{a_2}{\mathrm{e}^{(a_1/a_2)}} & a_3 u_2 \left(\frac{1}{\mathrm{e}^{(a_4/u_2)}} - 1\right) - \frac{u_1}{V} + \frac{(a_1 a_2 x_1)}{(x_2{}^2\, \mathrm{e}^{(a_1/x_2)})} \end{bmatrix} \tag{4.9}$$

Similarly, the Jacobian for the B matrix is

$$B = \begin{bmatrix} \frac{\partial f_1}{\partial u_1} & \frac{\partial f_1}{\partial u_2} \\ \frac{\partial f_2}{\partial u_1} & \frac{\partial f_2}{\partial u_2} \end{bmatrix}$$

Where the elements of the state-space B matrix are found as:

$$B_{11} = \frac{\partial f_1}{\partial u_1} = \frac{\partial f_1}{\partial (q - q_s)} = \frac{\partial f_1}{\partial q} = \frac{(C_{Ao} - x_1)}{V}$$

$$B_{12} = \frac{\partial f_1}{\partial u_2} = \frac{\partial f_1}{\partial (q_c - q_{cs})} = \frac{\partial f_1}{\partial q_c}$$

$$B_{21} = \frac{\partial f_2}{\partial u_1} = \frac{\partial f_2}{\partial (q - q_s)} = \frac{\partial f_2}{\partial q_s} = \frac{(T_o - x_2)}{V}$$

$$B_{22} = \frac{\partial f_2}{\partial u_2} = \frac{\partial f_2}{\partial (q_c - q_{cs})} = \frac{\partial f_2}{\partial q_c} = -a_3\left(\frac{1}{\mathrm{e}^{(a_4/u_2)}} - 1\right)(T_{CO} - x_2) - \frac{(a_3 a_4 (T_{CO} - x_2))}{(u_2 \exp(a_4 / u_2))}$$

From which the B matrix is,

$$B = \begin{bmatrix} \dfrac{(C_{Ao} - x_1)}{V} & 0 \\ \dfrac{(T_o - x_2)}{V} & -a_3\left(\dfrac{1}{\mathrm{e}^{(a_4/u_2)}} - 1\right)(T_{CO} - x_2) - \dfrac{(a_3 a_4 (T_{CO} - x_2))}{(u_2 \exp(a_4 / u_2))} \end{bmatrix} \tag{4.10}$$

The values of the matrices A, B, C and D for the steady state variable values at the given operating point 1

($q_s = 102$ lpm, $q_{cs} = 97$ lpm, $C_{As} = 0.0762$ mol/l, and $T_s = 444.7$K), are:

$$A = \begin{bmatrix} -13.9 & -0.046 \\ 2518.6 & 7.9 \end{bmatrix} \quad B = \begin{bmatrix} 0.0092 & 0 \\ -0.947 & -0.9413 \end{bmatrix} \quad C = \begin{bmatrix} 1 & 0 \\ 0 & 1 \end{bmatrix} \quad D = \begin{bmatrix} 0 & 0 \\ 0 & 0 \end{bmatrix} \tag{4.11}$$

C is an identity matrix since both states are measured. From these matrices, the matrix transfer function of the linearized CSTR model at the given operating point 1 is found to be:

$$\frac{Y(s)}{U(s)} = G_P(s) = \begin{bmatrix} G_{11}(s) & G_{12}(s) \\ G_{21}(s) & G_{22}(s) \end{bmatrix} = \begin{bmatrix} \dfrac{0.009238s - 0.02633}{s^2 + 5.99s + 17.58} & \dfrac{0.04672}{s^2 + 5.99s + 17.58} \\ \dfrac{-0.947s + 10.66}{s^2 + 5.99s + 17.58} & \dfrac{-0.9413s - 13.11}{s^2 + 5.99s + 17.58} \end{bmatrix} \tag{4.12}$$

Where, $U(s) = \begin{bmatrix} U_1(s) \\ U_2(s) \end{bmatrix}; Y(s) = \begin{bmatrix} Y_1(s) \\ Y_2(s) \end{bmatrix}$

Analysis of the Eigen values of this system shows complex conjugate poles of $-2.995 \pm j2.9345$ located on the left hand side of s-plane. The real part being negative indicates a stable closed loop operating conditions and therefore controllers can be designed for this system. A system is stable to changes in state at an operating point if the eigenvalues of A are negative. Equation (4.12) in block diagram representation is as shown in Figure. 4.1.

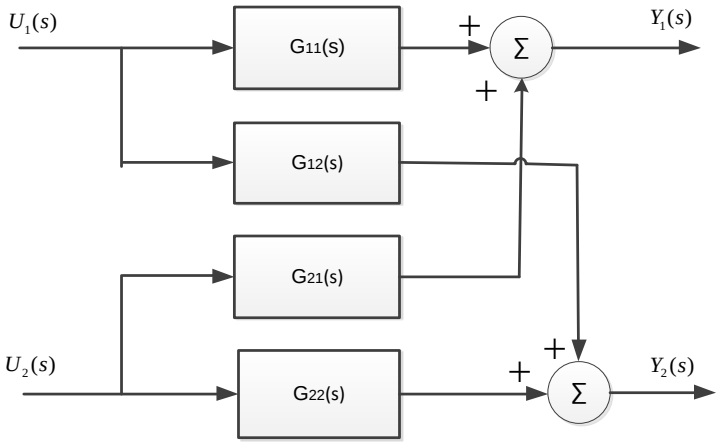

Figure 4.1: The block diagram of the linearized $2x2$ MIMO CSTR system.

The system has two inputs and two outputs, i.e. it is a $2x2$ system. This means that it is a MIMO system or to be specific, it is a two inputs and two outputs (TITO) system. As can be seen, the inputs and outputs are interacting. Thus, a disturbance at any of the inputs causes a response in all the two outputs. Such interactions make the control and stability analysis very complicated. Consequently, it is not immediately clear which input to use to control the individual outputs. It is therefore necessary to reduce or eliminate the interactions by designing control system that compensates for such interactions so that each output can be controlled independently of the other output.

Attempts are made to make use of the concept of decoupling problem first and secondly, to make use of the concept of Relative Gain Array (RGA) in conjunction with the Niederlinski index (NI) for the design of Decentralized controllers. Decoupling is possible by introducing appropriate cross-controllers (decouplers) in the system. The decentralized control design is made possible by finding the best control structure pairing between the controlled and manipulated variables and then applying a detuning factor (interaction measure) to compensate for the coupling. This type of design is described in Chapter 5.

4.4 Decoupling Controller design

The term decoupling control generally implies diagonal decoupling such that the resulting input/output relationships are independent. That is to eliminate complicated loop interactions so that a change in one process variable will not cause corresponding changes in other process variables. Decoupling is possible by introducing appropriate cross-controllers in the system (Luyben, 1997; Jevtovic and Matausek, 2010; Ghosh and Das, 2012; Lengare, et al., 2012; Wang, et al., 2014). These are placed before the process. Figure 4.2 shows the general decoupling

control system for the two-input, two-output (TITO) scheme, where $G_p(s), D(s)$ and $C(s)$ are the process model gain matrix, the decoupler matrix and the diagonal controller gain matrix respectively.

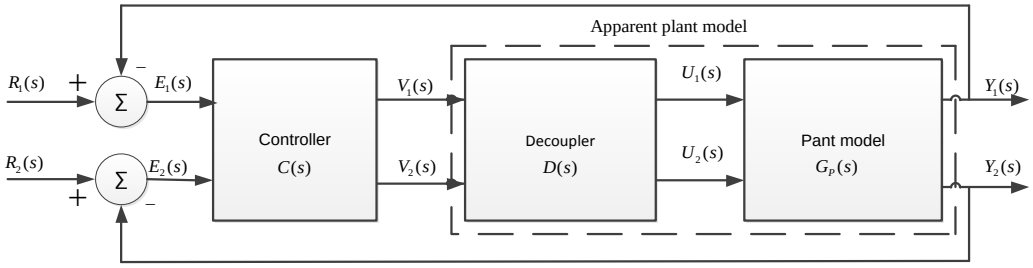

Figure 4.2: The decoupled closed loop control system.

The procedure is to design $D(s)$ in such a way that the process interactions are minimized and that the controller $C(s)$ sees the modified or apparent process gain matrix $G_p(s)D(s)$ as a set of two completely independent loops thereby enabling the independent control of the individual loops by their respective designed controllers. Decoupling strategies can be broadly divided into two main sub-categories: dynamic and static decoupling (Fikar, M., 2000). Dynamic decoupling guarantees that under any operating conditions, the manipulated variables influence independently the respective controlled outputs. Static decoupling on the other hand is concerned only on the problems of steady state conditions, hence decoupling is guaranteed only on specific choice of input values. Another disadvantage is that the control loop interactions still exist during the transient conditions.

In the following, a systematic design procedure is presented for the case of the dynamic decoupling strategy for the TITO system under study. The control objective is to control $Y_1(s)$ and $Y_2(s)$ independently, in spite of the changes in $U_1(s)$ and $U_2(s)$ Therefore, to meet these objectives, the first step is to design the decouplers and secondly, to design the controllers for the decoupled systems.

There are three different types of decoupling methods available for the design of stable systems each with merits and demerits. These are the ideal decoupling technique, the simplified and the inverted (adjoint-based decoupling). For example the ideal decoupler is designed as the inverse of the transfer function matrix of the process. However this kind of the decoupler results in more complicated calculations and hence implementation, especially for processes with higher orders, is often difficult. In addition the method suffers from stability problems, is more sensitive to errors and also is difficult to be realized. Therefore the method is rarely used in

practice. The simplified decoupling method is more popular, because of the simplicity of its elements however, the controller tuning can be often difficult and therefore in practice, an approximation of element transfer functions is often suggested in order to facilitate the controller tuning. The inverted or adjoint based decoupling control utilizes the adjoint of the transfer function matrix of the process for the controller realization resulting in a less complicated system. The method presents the main advantages of both the simplified and the ideal decoupling (Gagnon et al., 1988).

The simplified decoupling method is adopted in the design of the CSTR controller below (Luyben, 1986 and 1997; Gagnon et al, 1988; Tavakoli et al., 2006; Cai et al., 2008; Maghade and Patre, 2012)

In Figure 4.3 (simplified decoupling), decoupling at the input of a $2x2$ process transfer function $G_p(s)$ requires the design of a transfer function matrix $D(s)$, such that $G_p(s)D(s)$ is a diagonal transfer function matrix $Q(s),$

Where,

$$Q(s) = G_P(s)D(s)$$

$$D(s) = \begin{bmatrix} D_{11}(s) & D_{12}(s) \\ D_{21}(s) & D_{22}(s) \end{bmatrix}, G_P(s) = \begin{bmatrix} G_{11}(s) & G_{12}(s) \\ G_{21}(s) & G_{22}(s) \end{bmatrix}$$

$$Q(s) = \begin{bmatrix} Q_{11}(s) & 0 \\ 0 & Q_{22}(s) \end{bmatrix} and \begin{bmatrix} Y_1(s) \\ Y_2(s) \end{bmatrix} = Q(s) \begin{bmatrix} V_1(s) \\ V_2(s) \end{bmatrix} \quad (4.13)$$

$V_1(s)$ and $V_2(s)$ are the control inputs produced by an additional linear controller $C(s)$. For complete decoupling, it is assumed that $Y_1(s)$ is only affected by the control signal $V_1(s)$ and $Y_2(s)$ is only affected by the control signal $V_2(s)$. This requires that the decouplers should be designed according to the equation:

$$D(s) = G_P^{-1}(s).Q(s) \quad (4.14)$$

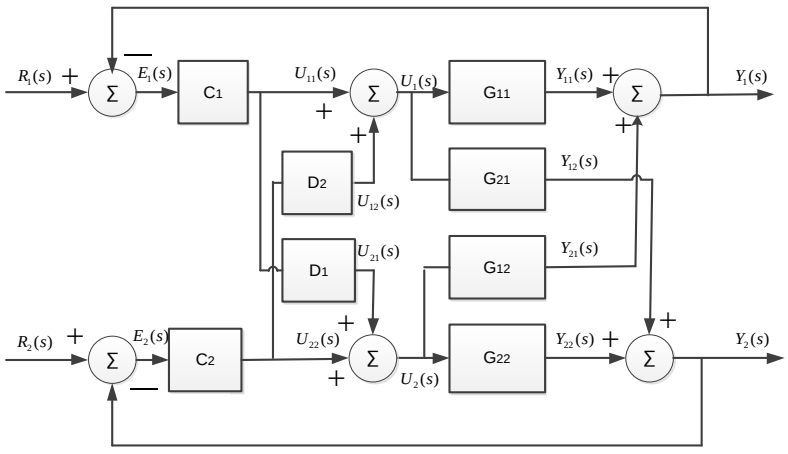

Figure 4.3: The closed loop system with the decouplers.

The strategy consists of setting the diagonal elements of the decoupler to be 1 as shown in Figure 4.3 and then selecting the off-diagonal elements as follows:

$$D(s)=\begin{bmatrix} 1 & D_1(s) \\ D_2(s) & 1 \end{bmatrix} \tag{4.15}$$

Then, the matrix of $Q(s)$ can be expressed as:

$$\begin{aligned} Q &= \begin{bmatrix} G_{11} & G_{12} \\ G_{21} & G_{22} \end{bmatrix}\begin{bmatrix} 1 & D_1 \\ D_2 & 1 \end{bmatrix} \\ &= \begin{bmatrix} G_{11}(s)+G_{12}(s)D_2(s) & G_{11}(s)D_1(s)+G_{12}(s) \\ G_{21}(s)+G_{22}(s)D_2(s) & G_{21}(s)D_1(s)+G_{22}(s) \end{bmatrix} = \begin{bmatrix} Q_{11} & 0 \\ 0 & Q_{22} \end{bmatrix} \end{aligned} \tag{4.16}$$

From Equation (4.15) in order that the matrix $Q(s)$ to be diagonal, it can be written such that:

$$\begin{aligned} &\rightarrow G_{11}(s)D_1 s)+G_{12}(s)=0 \\ &\rightarrow G_{21}(s)+G_{22}(s)D_2(s)=0 \end{aligned} \tag{4.17}$$

The solution of equation (4.17) is:

$$\begin{aligned} D_1(s) &= -\frac{G_{12}(s)}{G_{11}(s)} \\ D_2(s) &= -\frac{G_{21}(s)}{G_{22}(s)} \end{aligned} \tag{4.18}$$

The diagonal parts of the matrix transfer function $Q(s)$ after substitution of Equation (4.17) in Equation (4.15) are:

$$\begin{aligned} Q_{11}(s) &= G_{11}(s)+G_{12}(s)D_2(s) = G_{11}(s)-\frac{G_{12}(s)G_{21}(s)}{G_{22}(s)} \\ Q_{22}(s) &= G_{22}(s)+G_{21}(s)D_1(s) = G_{22}(s)-\frac{G_{21}(s)G_{12}(s)}{G_{11}(s)} \end{aligned} \tag{4.19}$$

The resulting apparent process transfer function matrix obtained is:

$$Q(s)=\begin{bmatrix} G_{11}(s)-\dfrac{G_{12}(s)G_{21}(s)}{G_{22}(s)} & 0 \\ 0 & G_{22}(s)-\dfrac{G_{21}(s)G_{12}(s)}{G_{11}(s)} \end{bmatrix} \tag{4.20}$$

This choice makes the realization of the decoupler easy. This ensures two independent SISO control loops. However the diagonal transfer matrix $Q(s)$ becomes of higher order and complicated. This may require an approximation of each term in Equation (4.20) by a simpler lower order transfer function in order to facilitate easier controller $C(s)$ tuning.

4.4.1 Decoupled concentration loop transfer function derivation

In this work, simpler approximations are made possible by representing $Q(s)$ in the zero/pole/gain form and then designing the controllers based on these approximations. The approximated effective transfer functions for the process are then found to be:

$$Q_{11}(s) = G^*_{11}(s) = G_{11}(s) - \frac{G_{12}(s)G_{21}(s)}{G_{22}(s)}$$

$$= \frac{0.0087s^6 + 0.156s^5 + 1.37s^4 + 7.363s^3 + 24.5s^2 + 48.3s + 47.25}{0.94s^7 + 30s^6 + 386.5s^5 + 2900s^4 + 13750s^3 + 42190s^2 + 78000s + 71200}$$

$$= \frac{0.009238(s^2 + 5.99s + 17.58)^3}{(s + 13.93)(s^2 + 5.99s + 17.58)^3} \quad (4.21)$$

Equation (4.21) is the zero/pole/gain form of the transfer function. From the derived transfer function $Q_{11}(s)$, it is noticed that the zeros in the numerator polynomials represented by $(s^2 + 5.99s + 17.58)^3$ cancel with the poles of the denominator polynomials of the transfer function represented by $(s^2 + 5.99s + 17.58)^3$ resulting in a simplified transfer function as illustrated in Equation (4.22).

$$G^*_{11}(s) \approx \frac{0.009238}{(s + 13.93)} \quad (4.22)$$

4.4.2 Decoupled temperature loop transfer function derivation

Similarly,

$$Q_{22}*(s) = G_{22}*(s) = G_{22}(s) - \frac{G_{12}(s)G_{21}(s)}{G_{11}(s)}$$

$$= \frac{-0.0087s^6 - 0.156s^5 - 1.4s^4 - 7.36s^3 - 24.5s^2 - 48.3s - 47.3}{0.00924s^7 + 0.14s^6 + 1.008s^5 + 3.6s^4 + 3.8s^3 - 22.9s^2 - 96s - 143}$$

$$= \frac{-0.9413(s^2 + 5.99s + 17.58)^3}{(s - 2.85)(s^2 + 5.99s + 17.58)^3} \quad (4.23)$$

Also Equation (4.23) is the zero/pole/gain form of the transfer function $Q_{22}(s)$. From the derived transfer function, it is noticed that the zeros in the numerator polynomial represented by $(s^2 + 5.99s + 17.58)^3$ cancel with the poles of the denominator polynomials of the transfer function represented by $(s^2 + 5.99s + 17.58)^3$ resulting in a simplified transfer function of first order as illustrated in Equation (4.24).

$$G_{22}*(s) \approx \frac{-0.9413}{(s - 2.85)} \quad (4.24)$$

The Equations (4.22) and (4.24) combined into a matrix form result in $Q(s)$ as:

$$Q(s) = \begin{bmatrix} \dfrac{0.009238}{s+13.93} & 0 \\ 0 & \dfrac{-0.943}{s-2.85} \end{bmatrix} \tag{4.25}$$

The matrix $Q(s)$ is used for design of the parameters of the PI controllers for the individual loops in the process.

4.5 PI Controller design by Pole Placement technique

Two independent PI controllers are designed for each apparent loop using pole placement technique. The relationship between the location of the closed loop poles and the various time-domain specifications are considered. The design objective is to maintain the plant outputs close to the desired values by driving the errors to zero at steady state for step inputs with minimum settling times (reference tracking). To have no steady state error a controller must have an integral action. It is therefore natural to use a PI controller which has the ideal transfer function of the form:

$$C(s) = K_P(1 + K_I \frac{1}{s}) \tag{4.26}$$

Where K_P and $\mathrm{K_I}$ are the controller tuning parameters representing the controller gain constant and the integral gain constant respectively. The process of determining these parameters to achieve consistent performance specifications is known as a controller tuning. The pole placement design method simply attempts to find controller settings that give the desired closed loop poles. The closed loop poles can be chosen arbitrarily by a suitable choice of the gains K_P and $\mathrm{K_I}$ of the controller. Thus the controller transfer matrix $C(s)$ of the system under consideration is given by:

$$C(s) = \begin{bmatrix} C_1(s) & 0 \\ 0 & C_2(s) \end{bmatrix} = \begin{bmatrix} K_{P1}(1 + K_{I1} \dfrac{1}{s}) & 0 \\ 0 & K_{P2}(1 + K_{I2} \dfrac{1}{s}) \end{bmatrix} \tag{4.27}$$

The block diagram of the decoupled TITO CSTR system incorporating the two diagonal PI controllers is shown in Figure 4.4.

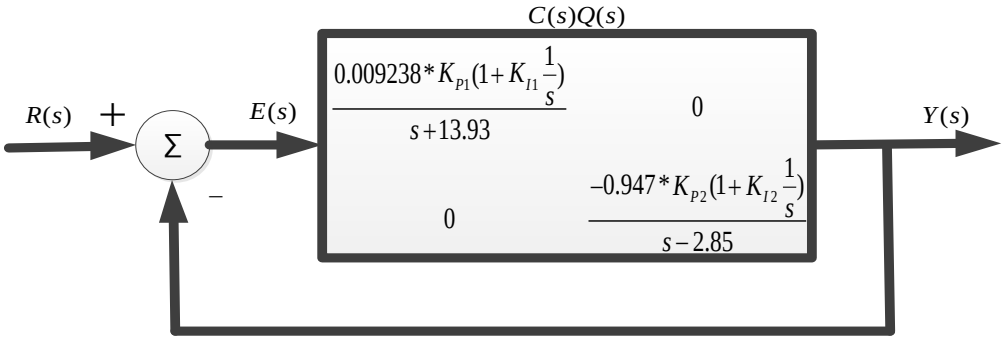

Figure 4.4: Block diagram of the decoupled closed loop system.

From Figure 4.4, the following can be derived.

$$Y(s) = C(s)Q(s)E(s), \text{ and } E(s) = R(s) - Y(s)$$

Therefore,

$$Y(s) = C(s)Q(s)R(s) - C(s)Q(s)Y(s) \tag{4.28}$$

From Equation (4.28) the expression for the outputs may be written as:

$$\begin{aligned} Y_1(s) &= C_1(s)Q_{11}(s)R_1(s) - C_1(s)Q_{11}(s)Y_1(s) \\ Y_2(s) &= C_2(s)Q_{22}(s)R_2(s) - C_2(s)Q_{22}(s)Y_2(s) \end{aligned} \tag{4.29}$$

Solving for the output $Y_1(s)$ by inserting $Q_{11}(s)$ and $C_1(s)$ from Equation (4.22) for $Q_{11}(s)$ and (4.27) for $C_1(s)$ gives:

$$Y_1(s) = \frac{0.009238(K_{P1}s + K_{P1}K_{I1})}{s^2 + s(13.93 + 0.00923K_{P1}) + 0.009238K_{P1}K_{I1}} R_1(s) \tag{4.30}$$

Similarly, it can be shown that using Equations (4.24) and (4.27);

$$Y_2(s) = \frac{-0.947(K_{P2}s + K_{P2}K_{I2})}{s^2 + s(-2.85 - 0.947K_{P2}) + (-0.947K_{P2}K_{I2})} R_2(s) \tag{4.31}$$

Equations (4.30 and (4.31) are the expressions for the outputs from the two separate non-interacting loops developed with the help of two PI controllers.

4.5.1 PI Controller design for the concentration loop

Consider the Equation (4.30) for the concentration control. This closed loop system is of a second order and its characteristic polynomial equation is:

$$s^2 + s(13.93 + 0.00923K_{P1}) + 0.009238K_{P1}K_{I1} = 0 \tag{4.32}$$

Thus, the closed loop system poles can be given arbitrary values by choosing the parameters K_{P1} and $\mathrm{K_{I1}}$ properly. The procedure is to re-parameterize the characteristic equation to be of the desired standard dimensionless form:

$$s^2 + 2\zeta\omega_n s + \omega_n{}^2 = 0 \tag{4.33}$$

To achieve this, the relationship between the location of the closed loop poles and the various time domain specifications are considered. Assuming that the desired poles are characterised by their relative damping ζ and their frequency ω_n and identifying the coefficients of the powers of the variable s in the polynomials (4.32) and (4.33), the controller parameters can be found as:

$$K_{P1} = \frac{2\zeta\omega_n - 13.93}{0.009328}$$
$$K_{P1}K_{I1} = \frac{\omega_n^{\,2}}{0.009238} \qquad (4.34)$$

where ω_n and ζ are the un-damped natural frequency and damping factor respectively. The parameter ω_n determines the speed of response and ζ determines the shape of response (damping). It is necessary to specify the values of ω_n and ζ

The specifications for system's step response that are often used are the percentage overshoot and the settling time. If the performance specifications for the concentration control are such that the settling time should be $0.2 \le T_s \le 1$ (minutes) and an overshoot of $5\% \le M_p \le 15\%$ and the frequency of oscillation in the step response $\omega_d \le 12 rad/s$ are selected then the poles can be placed in the locations that ensures good response, hence the controller settings K_{P1} and $\mathrm{K_{I1}}$ can be calculated with ease. The objective is to determine the region in the s-pane where the closed loop poles must lie in order to satisfy the performance specifications. Since the system is under damped, the closed loop poles are complex conjugates, therefore only the one of the poles is considered. The values for the overshoot and settling time are related to the damping ratio and the un-damped natural frequency. The overshoot is controlled by the damping coefficient whereby low overshoot implies high damping and vice versa.

The relationship between the settling time and the closed loop poles is given by:

$$T_s = \frac{4}{\zeta\omega_n},\ \mathrm{Re}[p_1] = -\zeta\omega_n \Rightarrow T_s = \frac{4}{\left|\mathrm{Re}[p_1]\right|} \Leftrightarrow \left|\mathrm{Re}[p_1]\right| = \frac{4}{T_s} \qquad (4.35)$$

Where p_1 is one of the closed loop poles. Thus, a settling time specification imposes a limit on the real part of the complex conjugate closed loop poles. Since there is an inverse relationship between the settling time and the real part of the pole, that means that increasing the settling time reduces the absolute value of the real part of the closed loop pole and vice versa. Imposing the upper and lower limits of the

settling time guarantees the position upon which the poles must lie. From the specifications therefore the constraints on the real part require that the closed loop poles must be:

$$T_{s-\max} = 1 \Rightarrow \mathrm{Re}[p_1] = \frac{-4}{T_s} = -4$$
$$T_{s-\min} = 0.2 \Rightarrow \mathrm{Re}[p_1] = \frac{-4}{T_s} = -20 \quad (4.36)$$

Therefore the closed loop poles must lie in the region between -4 and -20 on the real part of the s-plane. The percentage overshoot is only a function of the damping. The angle that the closed loop pole makes relative to the negative real axis is also a function of the damping ratio. For any given percent overshoot, the damping ratio and the angle can be computed from the formulae (Ogata, K., 1990):

$$\zeta = \sqrt{\frac{(\ln \frac{M_P}{100\%})^2}{\pi^2 + (\ln \frac{M_P}{100\%})^2}}, \quad \beta = \cos^{-1}(\zeta) \quad (4.37)$$

Where the percentage overshoot is M_P and β is the angle in the clockwise direction from a negative real axis. Thus, from the specifications provided

$$M_{P\max} = 15\% \Rightarrow \zeta = 0.5169 \Rightarrow \beta = 58.9^\circ$$
$$M_{P\min} = 5\% \Rightarrow \zeta = 0.6901 \Rightarrow \beta = 46.4^\circ \quad (4.38)$$

Thus, for each allowed value of the overshoot, constraints on the damping ratio and the angle can be imposed. This implies that the constraints on the damping ratio and the angle are as given by Equation (4.39).

$$0.6901 \geq \zeta \geq 0.5169$$
$$46.4 \leq \beta \leq 58.9^\circ \quad (4.39)$$

The relationship between the real and the imaginary parts of the closed loop pole is given by the tangent of the angle and therefore the real and the imaginary parts of p_1 must satisfy the expression:

$$\tan(46.4^\circ) = 1.0501 \leq \frac{\mathrm{Im}[p_1]}{\mathrm{Re}[p_1]} \leq 1.6577 = \tan 58.9^\circ$$

The damped frequency of oscillation is directly a specification on the imaginary part of the closed loop pole p_1 and the relationship is given by:

$$\omega_d = \omega_n \sqrt{1-\zeta^2} = \mathrm{Im}[p_1] \quad (4.40)$$

The final overall requirements on the locations of the closed loop poles are determined by the consideration that all the constraints specified are satisfied. Choosing a pole at $-8.8 + j11.8$ gives the settling time to be 0.453 minutes as from

equation (4.32). This is within the acceptable specification range. The angle of the radial line through this pole is $\tan^{-1} 11.83/8.83 = 53.37^{\circ}$ so that the damping ratio is $\zeta = 0.598$. This yields an overshoot of 9.58%. The next design specification is to determine ω_n in order to finish the requirements of the second order system. The settling time and the frequency of oscillation are related by the equation:

$$T_s \approx \frac{4}{\zeta\omega_n} = 0.453$$

This implies that $\omega_n = 14.77 rad/s$.

Similarly it can be calculated from $\omega_d = \omega_n\sqrt{1-\zeta^2} \Rightarrow \omega_n = \frac{\omega_d}{\sqrt{1-\zeta^2}} = 14.77 rad/s$

Thus from Equation (4.34) the values of the unknown controller parameters are calculated as:

$$K_{P1} = \frac{2\zeta\omega_n - 13.93}{0.009238} = \frac{(2*0.598*14.77) - 13.93}{0.009238} = 400$$
$$K_{I1} = \frac{\omega_n{}^2}{0.009238K_{P1}} = \frac{14.77^2}{0.009238*400} = 58.978 \quad (4.41)$$

The flow chart of the procedure for the selection of the poles adopted is illustrated in Figure 4.5.

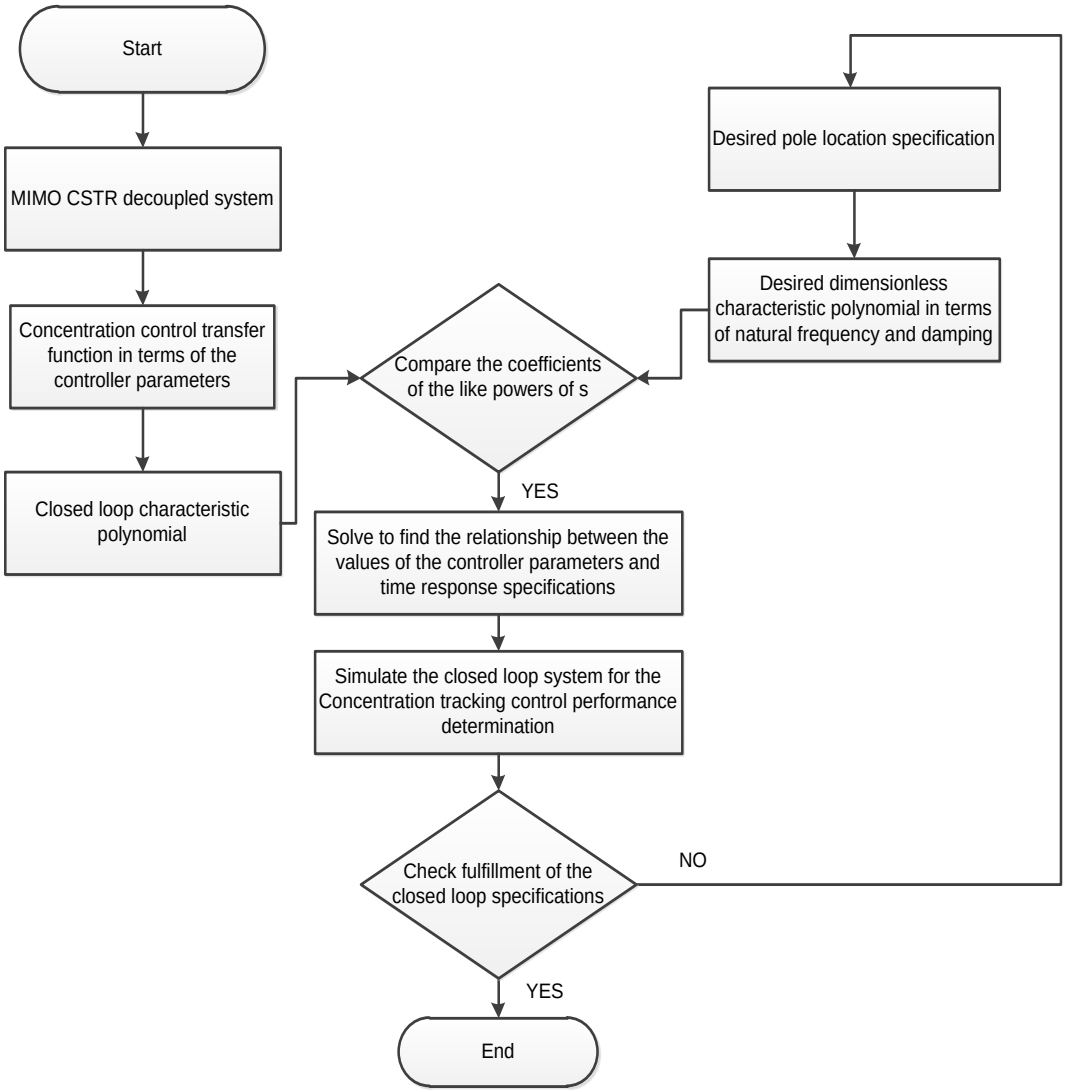

Figure 4.5: Flow diagram of the summary of the pole selection procedure.

Thus the designed controller settings achieve tracking control of the concentration set point as depicted by the time domain responses of the Figure 4.8 below.

4.5.2 PI Controller design for the temperature loop

Similar procedure is used for the design of the second loop PI controller settings as described below.

Consider the Equation (4.31) for the temperature control, then the closed loop system is of second order and its characteristic equation is:

$$s^2 + s(-2.85 - 0.947K_{P2}) + (-0.947K_{P2}K_{I2}) = 0 \quad (4.42)$$

Thus, the closed loop system poles can also be given arbitrary values by choosing the parameters K_{P2} and K_{I2} of the second PI controller settings. The procedure adopted is the same as the one for the concentration control. First is to re-parameterize the characteristic equation in terms of the desired standard dimensionless form:

$$s^2 + 2\zeta\omega_n s + \omega_n{}^2 = 0 \tag{4.43}$$

The relationship between the location of the closed loop poles and the various time domain specifications are considered. The controller parameters can be found as:

$$\begin{aligned} K_{P2} &= \frac{2\zeta\omega_n + 2.85}{-0.947} \\ K_{I2} &= \frac{\omega_n{}^2}{-0.947 K_{P2}} \end{aligned} \tag{4.44}$$

If the performance specifications for the temperature control are such that the settling time should be $0.2 \le T_s \le 1$ (minutes) and an overshoot of 25%, the poles can be placed in the arbitrary locations that ensure good temperature tracking and hence the controller settings K_{P2} and K_{I2} can be calculated using Equations (4.35-4.37). The problem is then to determine the region in the s-pane where the closed loop poles must lie in order to satisfy the performance specifications. With a choice of a settling time of 0.5 minutes which is within the specification range implies that the real part of the pole must be at:

$$T_{s2} = 0.5 \Rightarrow \mathrm{Re}[p_2] = -4 / T_{s2} = -4 / 0.5 = -8$$

For a 25% overshoot, this implies that the damping ratio can be calculated from the Equation (4.39) as:

$$\zeta = \sqrt{\frac{(\ln \frac{M_P}{100\%})^2}{\pi^2 + (\ln \frac{M_P}{100\%})^2}} = \sqrt{\frac{(\ln 0.25)^2}{\pi^2 + (0.25)^2}} = 0.403 \tag{4.45}$$

The imaginary part of the pole is then calculated from the expression:

$$\tan(\beta^\circ) = \frac{\mathrm{Im}[p_1]}{\mathrm{Re}[p_1]} = \cos^{-1}(\zeta) = \tan 66.2^\circ \Rightarrow \mathrm{Im}[p_2] = 18.2 \tag{4.46}$$

Therefore placing the second pole at the point $-8.0 + j18.2$ ensures the desired overshoot and the damping ratio are achieved. The next design specification is to determine ω_n as:

$$T_s \approx \frac{4}{\zeta\omega_n} = 0.5 \Rightarrow \omega_n = \frac{4}{0.403 * 0.5} = 19.85 rad / s \tag{4.47}$$

Thus from Equation (4.44) the values of the unknown controller parameters are calculated as:

$$\begin{aligned} K_{P2} &= \frac{2\zeta\omega_n + 2.85}{-0.947} = \frac{(2 * 0.403 * 19.85) + 2.85}{-0.947} = -19.9 \\ K_{I2} &= \frac{\omega_n{}^2}{-0.947 K_{P1}} = \frac{19.85^2}{-0.947 * (-19.9)} = 20.9 \end{aligned} \tag{4.48}$$

The flow chart of the procedure for the selection of the poles for the temperature control is the same as the one given in Figure 4.5. Thus the designed controllers setting for the proportional gain constant of $K_{P2} = -19.9$ and the integral gain constant of $K_{I2} = 20.9$ achieve tracking control of the temperature set point.

4.6 Simulated Results

Simulation results are used to verify the performance of these control laws. The Simulink block diagram and time response characteristics of the closed loop MIMO CSTR designed using dynamic decoupling technique in which the interaction within the loops are compensated and then two SISO PI controllers are tuned using pole placement techniques to achieve various set-point tracking for the concentration control and temperature control are illustrated below.

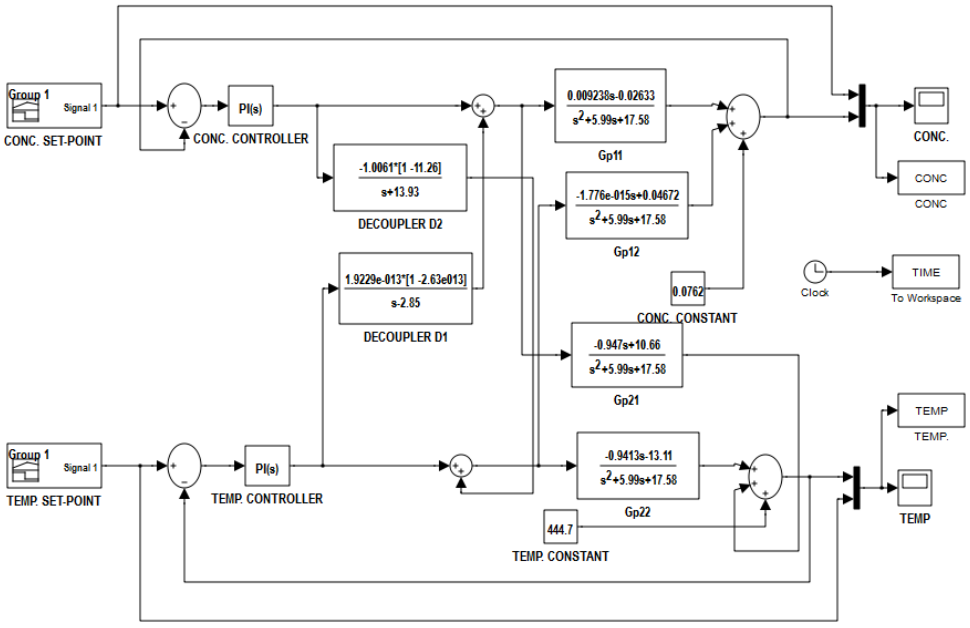

Figure 4.6: Dynamic decoupling control implemented in Simulink

Figure 4.6 represents the closed loop block diagram of the dynamic decoupling control scheme of the CSTR process implemented in the Simulink environment.

4.6.1 Concentration loop simulated results

The designed controller settings achieve tracking control of the concentration set point are used to simulate the concentration control loop as depicted by the time domain response of the Figure 4.7.

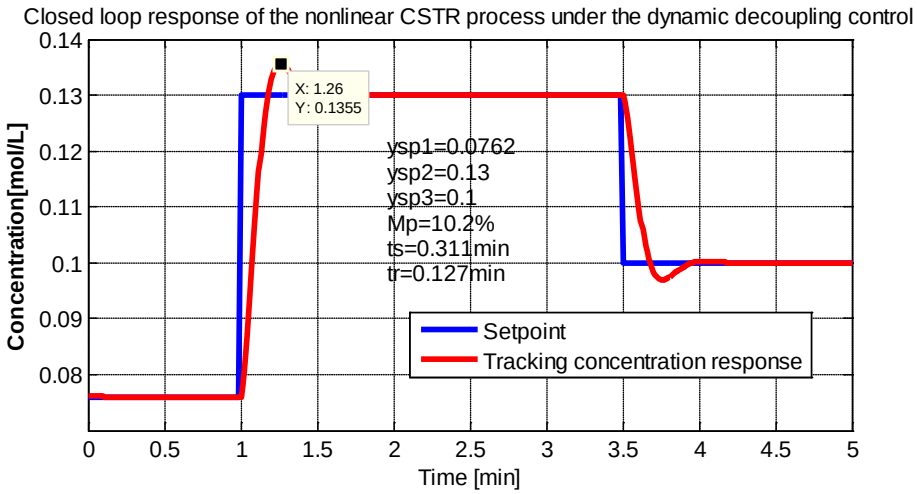

Figure 4.7: Set-point tracking concentration response.

The set-points for the concentration control is varied from $0.0762 mol/l$ to $0.13 mol/l$, then from to $0.13 mol/l$ to $0.1 mol/l$ with time. Figure 4.8 shows the tracking characteristics.

4.6.1.1 Investigation of performance for variations in concentration set-point

Several other variations in the set-point are investigated to evaluate the time response performance indices as illustrated by the following figures.

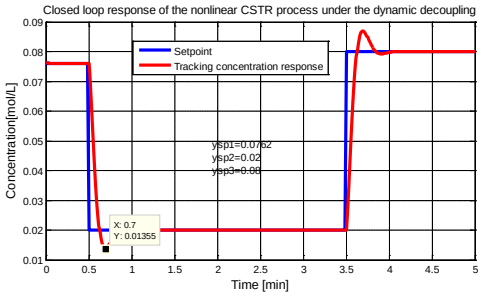

Figure 4.8: response of $0.02 mol/l$

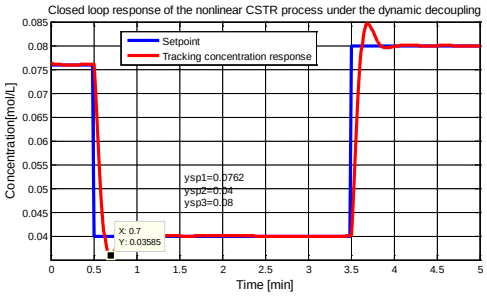

Figure 4.9: response of $0.04 mol/l$

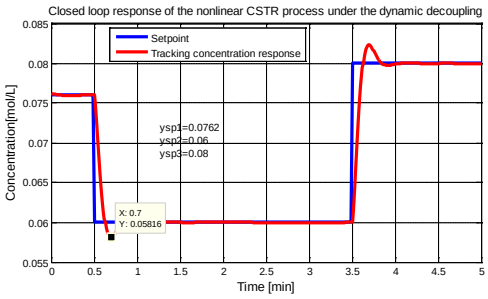

Figure 4.10: response of $0.06 mol/l$

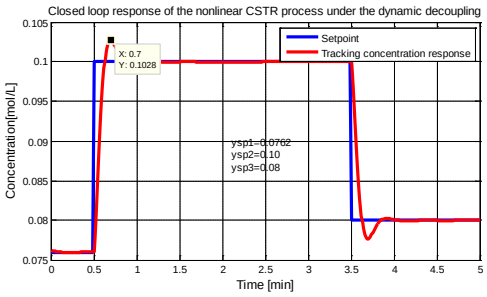

Figure 4.11: response of $0.10 mol/l$.

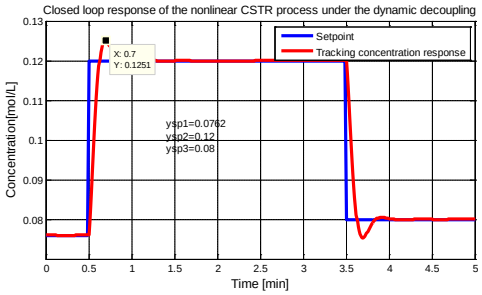

Figure 4.12: response of $0.12 mol/l$

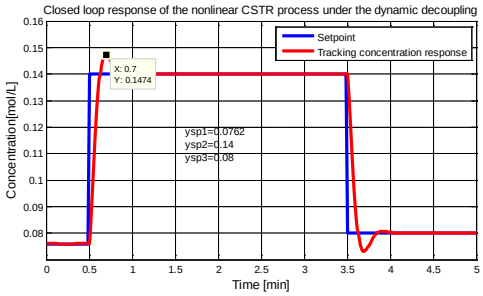

Figure 4.13: response of $0.14 mol/l$.

Table 4.1: Analysis of the different set-points influence over the concentration response performance indicators

Set-point value	Rise time t_r (sec)	Settling time t_s (sec)	Peak over shoot M_p (%)	Steady state error e_{ss} (%)
0.02 Moles/litre.	7.62	27.18	9.58	0
0.04 Moles/litre	7.62	27.18	9.58	0
0.06 Moles/litre	7.62	27.18	9.58	0
0.08 Moles/litre	7.62	27.18	9.58	0
0.1Moles/litre	7.62	27.18	9.58	0
0.12 Moles/litre	7.62	27.18	9.58	0
0.14 Moles/litre	7.62	27.18	9.58	0

Table 4.1 gives the various performance indices for concentration response when the set-point is varied. The investigation derived is that the indices remains constant throughout the set-point variations hence this shows that the dynamic decoupling control design is good irrespective of the set-point variations. Frequency response analysis using Bode plot is also investigated for the decoupled concentration control performance. This is illustrated in Figure 4.14.

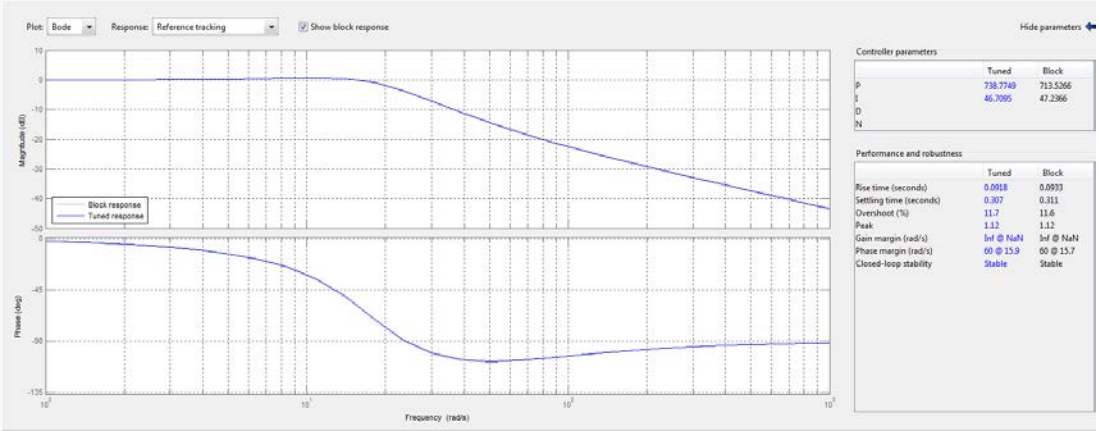

Figure 4.14 Frequency response analyses for the concentration control

The figure shows the open loop gain and the open loop phase plots for the decoupled concentration control system. The closed loop gain margin is infinity and the phase margin indicated is 60 degrees implying that the closed loop concentration control system is stable.

4.6.1.2 Investigation of the process performance for disturbances in the concentration control loop

Similarly, the effects of disturbances are investigated. The disturbances are injected to the concentration output as well as to the control input as illustrated in the Simulink block of Figure 4.15.

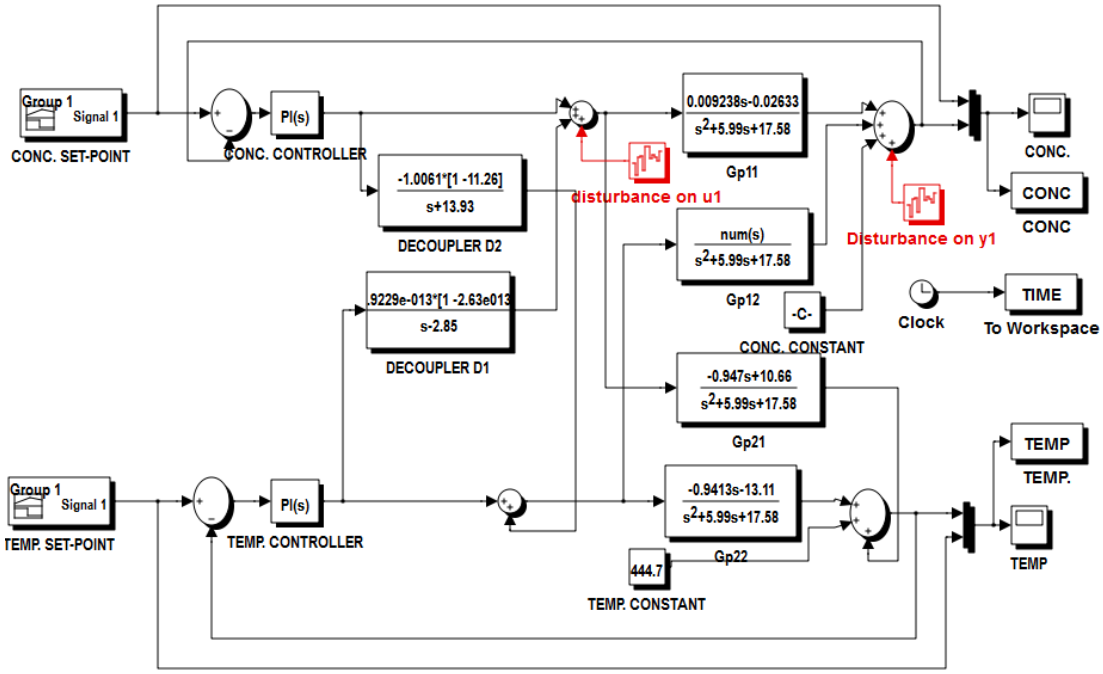

Figure 4.15 Dynamic decoupling controls subject to disturbances at the output (y_1) and the interaction junction (u_1)

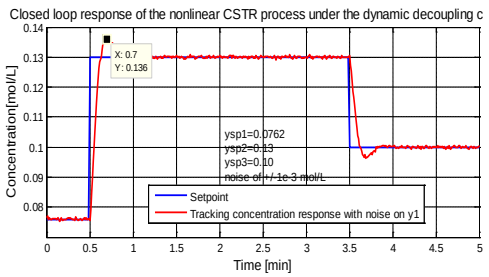

Figure 4.16: Response under $1e^{-3}\text{mol/l}$ noise

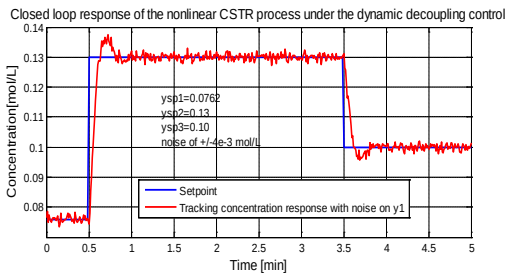

Figure 4.17: Response under $4e^{-3}\text{mol/l}$ noise

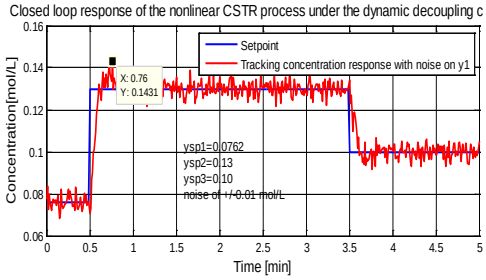

Figure 4.18: Response under $0.01mol/l$ noise.

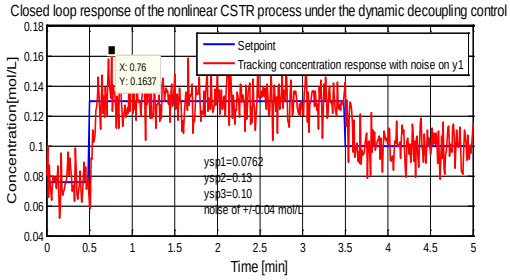

Figure 4.19: Response under $0.04mol/l$ noise.

The designed dynamic control system performance is checked for different varying magnitudes of random disturbances (white noise) added to the output signal y_1 on the main concentration loop. The responses are represented in Figures 4.16 to 4.19. Good tracking control is still achieved in respect to the various performance indices. However as the magnitude of the disturbance is increased, the response becomes noisy.

Similarly, the disturbances at the interaction junction for the control signal u_1 is considered. This is investigated by adding some random noise of vaious magnitudes to the control signal u_1. Figures 4.20 to 4.23 represent the responses for the concentration set-point tracking under the influence of the disturbances for the considered cases. The results of simulation show that the magnitude of the disturbance is important for smooth set-point tracking. However the concentration control system loop can still able to follow the set-point variations implying that the designed decoupling systems is good at rejecting the random variations in the control signal u_1.

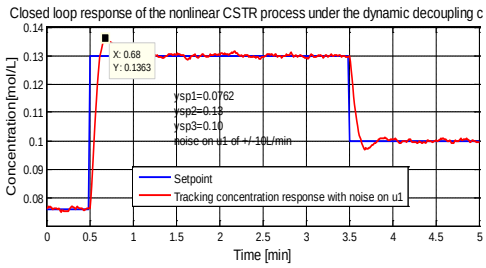

Figure 4.20: Response under $\pm 10l/\min$ .noise

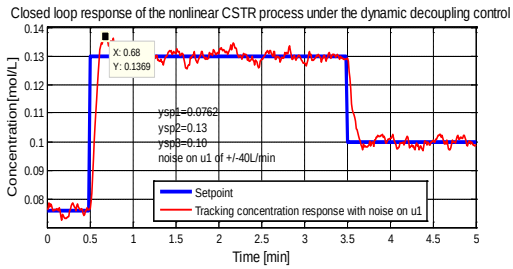

Figure 4.21: Response under $\pm 40l/\min$ noise

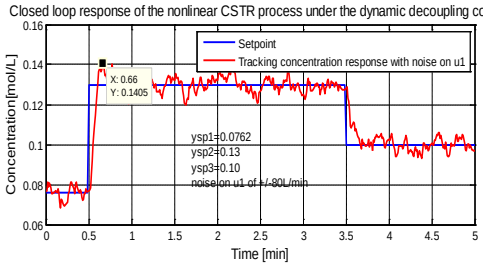

Figure 4.22: Response under $\pm 80l/\min$ .noise.

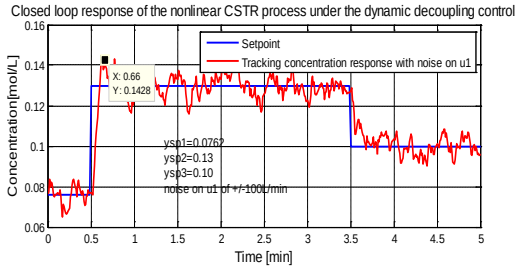

Figure 4.23: Response under $\pm 100l/\min$ noise.

Similarly, the performances of the temperature control loop signal y_2 when the disturbances are in y_1 and u_1 are investigated. This is important because of the interactions that exist in the closed loop system. Figures 4.24-4.27 are the graphs for the responses of the temperature control loop signal y_2 when there are disturbances on y_1 of different magnitudes.

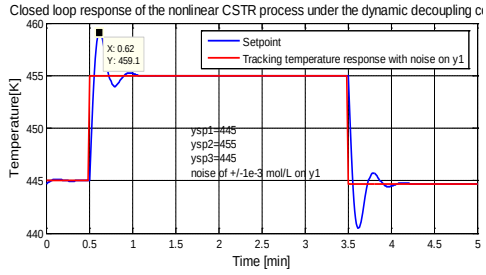

Figure 4.24: Temperature response under $\pm 1e^{-3}\text{mol/l}$ .noise on y_1

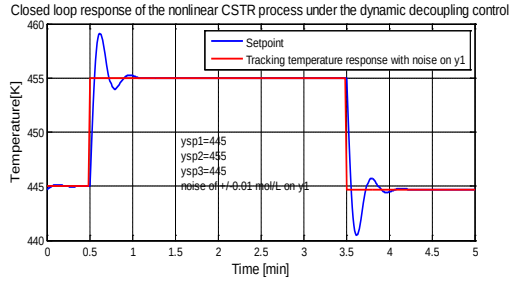

Figure 4.26: Temperature response under $\pm 0.01\text{mol/l}$ .noise on y_1 .

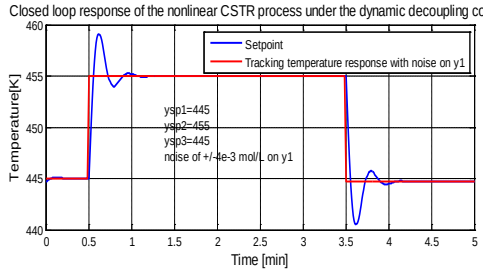

Figure 4.25: Temperature response under $\pm 4e^{-3}\text{mol/l}$ .noise on y_1 .

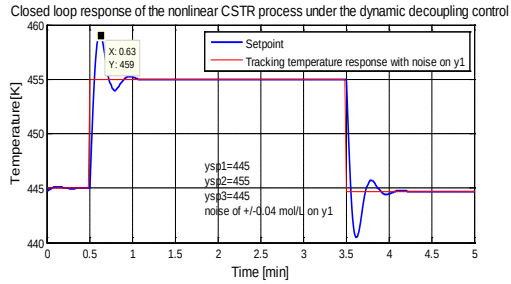

Figure 4.27: Temperature response under $\pm 0.04\text{mol/l}$ .noise on y_1 .

The results from Figures 4.24-4.27 show that there is very little influence of the disturbance effect on y_1 to the temperature control loop signal y_2 . This implies that the decoupling control design is good. Next, the investigation on the influence of the

effect of disturbance on u_1 to the temperature control loop signal y_2 .is done. Figures 4.28-4.31 are the graphs of the responses of the temperature control loop signal y_2 when there are disturbances of different magnitudes on u_1 .

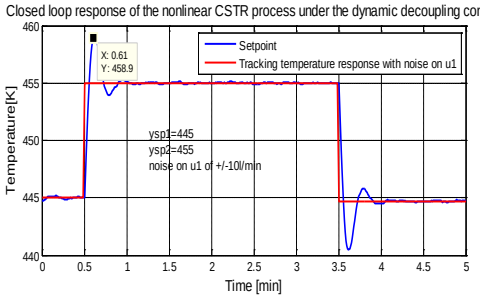

Figure 4.28: Temperature response under $\pm 10l / \min$ .noise on u_1

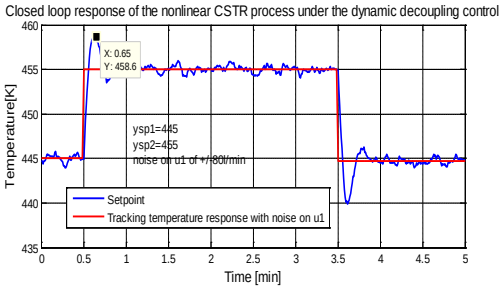

Figure 4.30: Temperature response under $\pm 80l / \min$ .noise on u_1

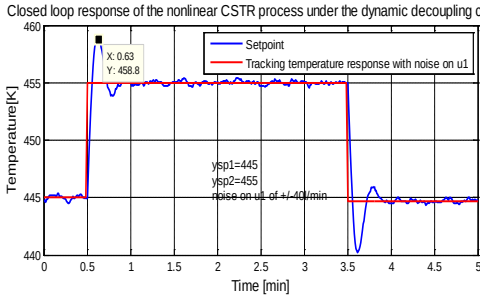

Figure 4.29: Temperature response under $\pm 40l / \min$ .noise on u_1

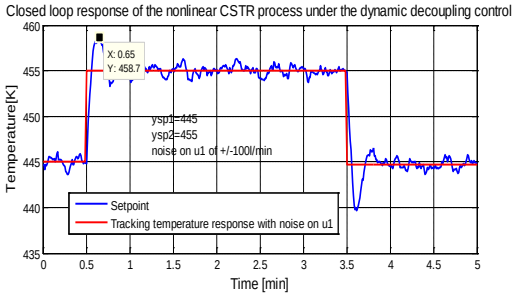

Figure 4.31: Temperature response under $\pm 100l / \min$ noise on u_1

From these responses of Figures 4.28-4.31, it can be seen that as the magnitude of the disturbance u_1 increase, the response on y_2 becomes noisy. This implies that there are still some elements of interactions in the system.

4.6.2 Investigation of the process performance in the temperature control loop

Similarly, simulation to investigate the process performance in the temperature control loop is performed. The same procedure adopted for the concentration control is used. First, the control algorithm derived earlier is used to simulate the temperature control loop for set-point tracking. Figure 4.32 presents the result of simulation

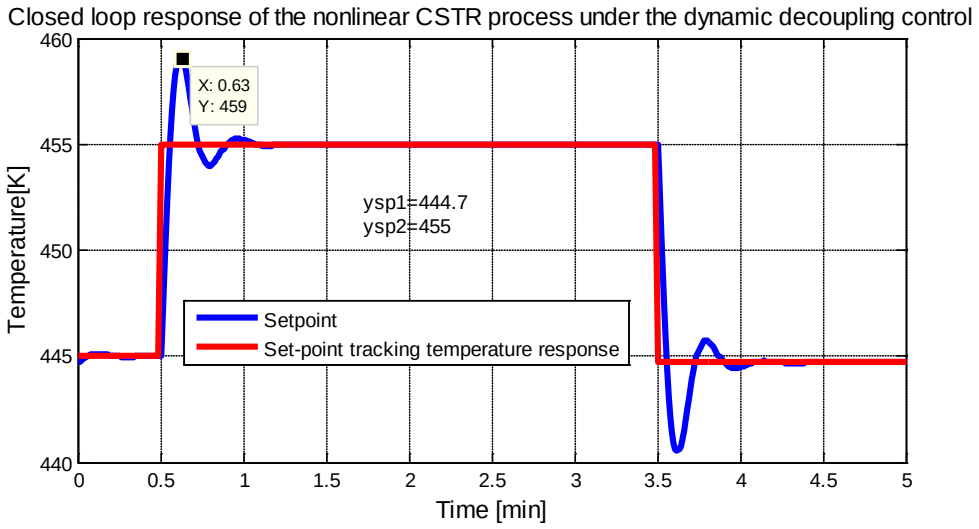

Figure 4.32: Set-point tracking temperature response

The set-points for the temperature control loop is varied from $444.7K$ to $460K$, then from $460K$ to $444.7K$ with time. A part from high percentage overshoot, the other performance indices are good, hence successful temperature set-point tracking is achieved with this control law. Several other variations in set-points are investigated to calculate the changes in the time response performance indices as illustrated by the following Figures 4.33 to 4.38.

4.6.2.1 Investigation of the process performance for variations in the temperature set-point

The variation of set-points magnitude influence over the temperature response performance indices is investigated. This is varied when the concentration loop's set point is maintained at $0.0762mol/l$ to $0.13mol/l$, then from to $0.13mol/l$ to $0.1mol/l$ with time.

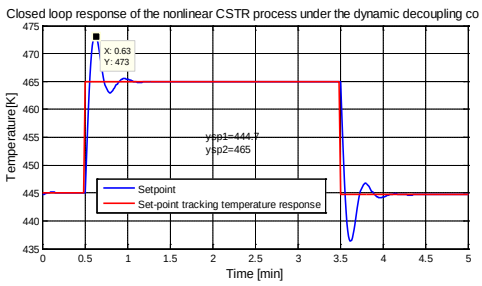

Figure 4.33: Temperature set-point tracking at $465K$.

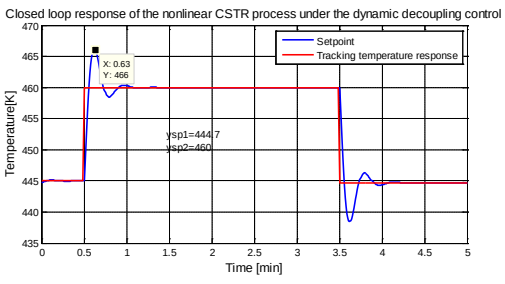

Figure 4.34: Temperature set-point tracking at $460K$.

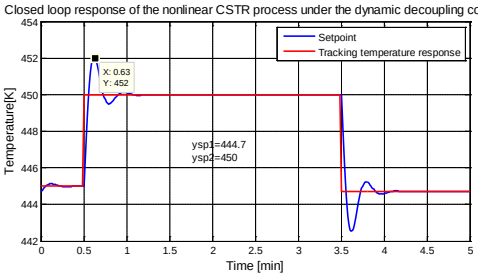

Figure 4.35: Temperature set-point tracking at $450K$.

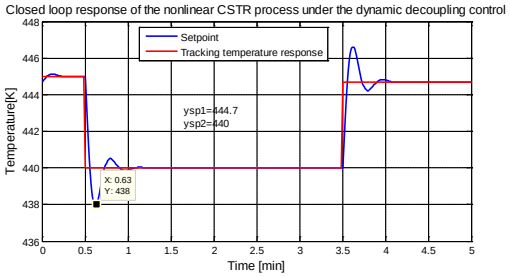

Figure 4.37: Temperature set-point tracking at $440K$.

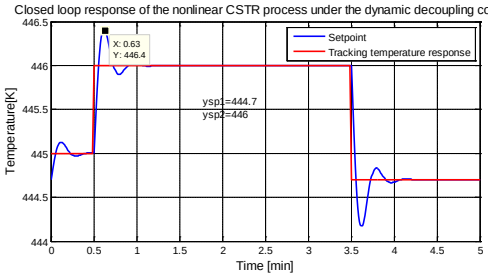

Figure 4.36: Temperature set-point tracking at $446K$.

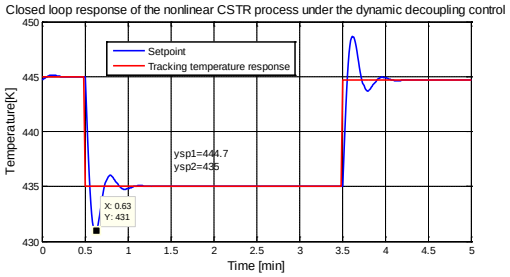

Figure 4.38: Temperature set-point tracking at $435K$

The results show that a part from high percentage overshoots; the other performance indices are good, hence successful temperature set-point tracking is achieved with this control law.

Table 4.2: Analysis of the different set-points influence over the temperature response performance indicators.

Set-point value	Rise time t_r (sec)	Settling time t_s (sec)	Peak over shoot M_p (%)	Steady state error e_{ss} (%)
435K.	2.79	30	28.2	0
440K	2.79	30	28.2	0
446K	2.79	30	28.2	0
450K	2.79	30	28.2	0
455K	2.79	30	28.2	0
460K	2.79	30	28.2	0
465K	2.79	30	28.2	0

The investigation shows that the performance indices such as rise time, settling time peak overshoot, steady state error remains the same no matter the value of set-point. This further shows that the dynamic decoupling control design for the temperature loop is good irrespective of the set-point value.

4.6.2.2 Investigation of the process performance for disturbances in the temperature control loop

Next, the effects of disturbances are investigated for the temperature control loop. The procedure adopted is the same as that for the concentration control loop. The disturbances

are injected to the main temperature control loop at the output y_2 as well as to the control inputs u_2. The effects of the disturbances at y_2 are as illustrated on the responses as represented in Figures 4.39 to 4.42 for the main temperature control loop and at u_2 in Figures 4.43 to 4.46 for the control input u_2.

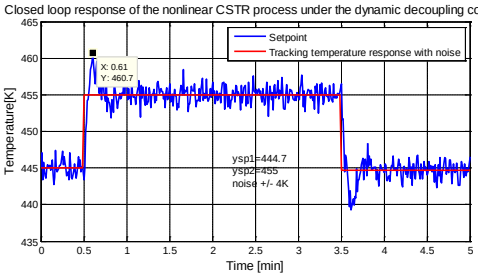

Figure 4.39: Temperature response under $\pm 4K$ .noise.

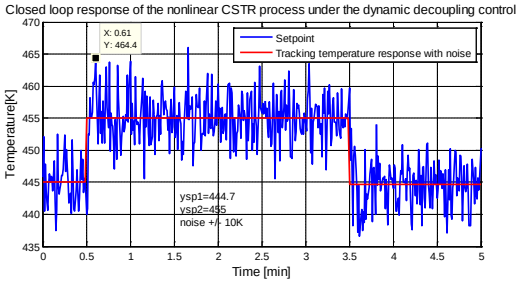

Figure 4.41: Temperature response under $\pm 10K$ noise

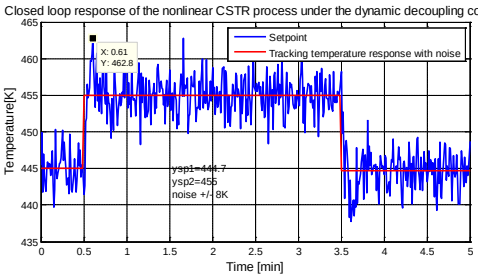

Figure 4.40: Temperature response under $\pm 8K$ noise

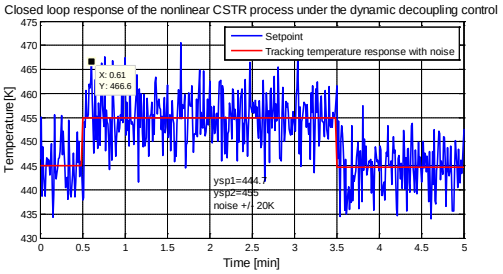

Figure 4.42: Temperature response under $\pm 20K$ noise

The results of simulation shows that the magnitudes of the disturbance is important for smooth set-point tracking. However the temperature control system can still track the set-point variations implying that the designed decoupling systems is good.

Similarly, the disturbances at the interaction junction for the control signal u_2 is considered. The is investigation is done by adding some random noise of various magnitudes to the control signal u_2. Figures 4.43 to 4.46 represent the responses for the temperature set-point tracking under the disturbances for the considered cases. The results of simulation shows that the effects of this kind of the disturbance does not quite affect the set-point tracking. The temperature control system can still track the set-point variations implying that the designed decoupling systems is good at rejecting the random variations in the control signal u_2.although the responses become noisy as the magnitude of this disturbance is increased

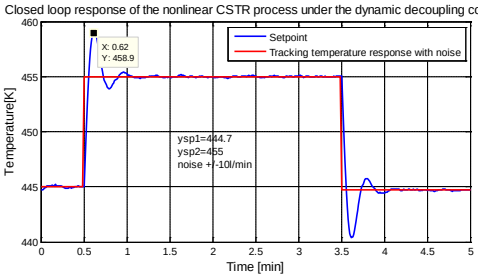

Figure 4.43: Temperature response under $\pm 10l / \min$ noise on u_2.

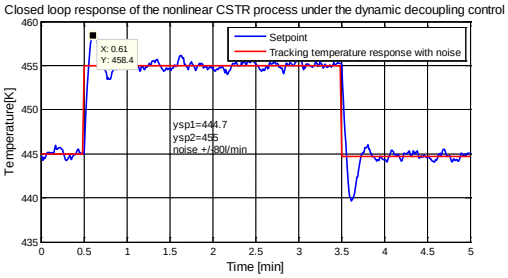

Figure 4.45: Temperature response under $\pm 80l / \min$ noise on u_2.

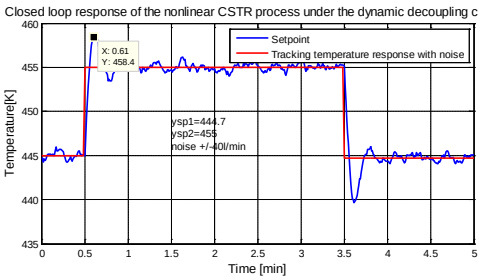

Figure 4.44: Temperature response under $\pm 40l / \min$ noise on u_2

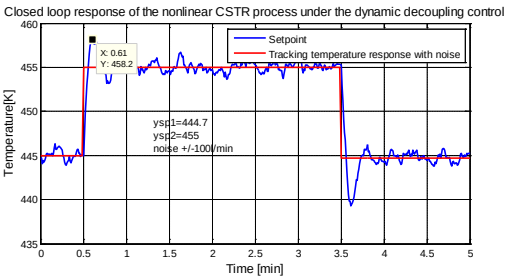

Figure 4.46: Temperature response under $\pm 100l / \min$ noise on u_2

4.6.2.3 Investigation of the process performance in the concentration loop for disturbances in the temperature control loop

Lastly, the behaviour of the concentration loop when the set-point is changing in y_2 is investigated. The graphs of this case are illustrated below. Lastly, the behaviour of the concentration loop when there are disturbances on y_2 and the control signal u_2 .is investigated.

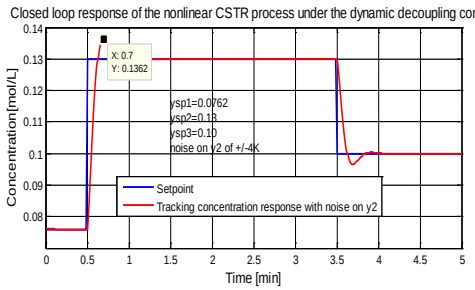

Figure 4.47: Concentration response under $\pm 4K$ noise on y_2.

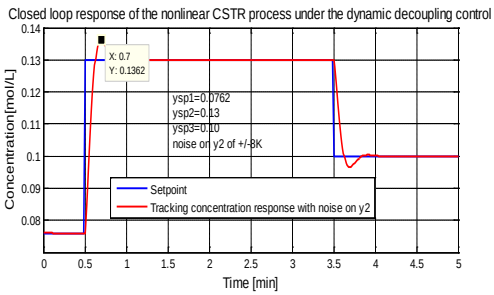

Figure 4.48: Concentration response under $\pm 8K$ noise on y_2

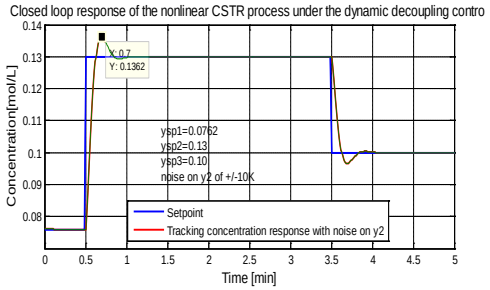

Figure 4.49: Concentration response under $\pm 10K$ noise on y_2.

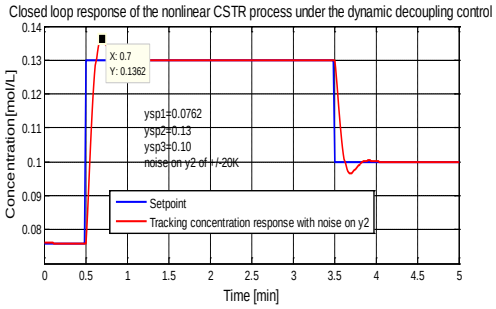

Figure 4.50: Concentration response under $\pm 20K$ noise on y_2

The graphs of these cases are illustrated in the following. Figures 4.47 to 4.50 are the concentration behaviour for changes in y_2. Investigation is done on the responses of Figures 4.47 to 4.50 shows the influences of the disturbances on y_2 to the concentration performance y_1 for the considered cases

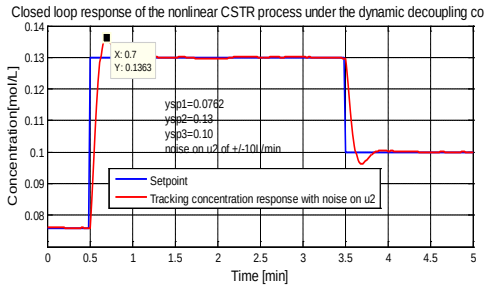

Figure 4.51: Concentration response under $\pm 10l / \min$ noise on u_2.

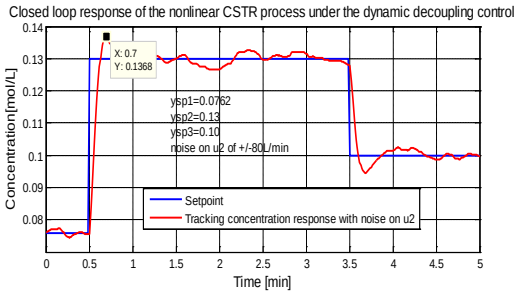

Figure 4.53: Concentration response under $\pm 80l / \min$ noise on u_2.

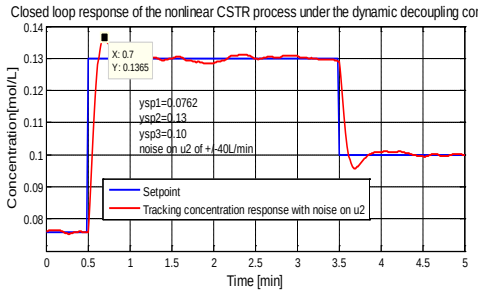

Figure 4.52: Concentration response under $\pm 40l / \min$ noise on u_2

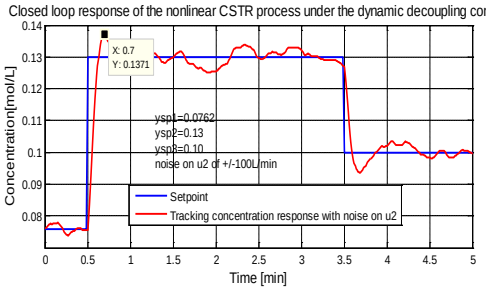

Figure 4.54: Concentration response under $\pm 100l / \min$ noise on u_2

It is shown that the responses on y_1 do not change. This measured by changing the magnitude of the disturbance on y_2 and then monitoring the responses of y_1. Therefore this confirms that the decoupling control design is good. Next, the disturbance effect on y_1 when noise is added on the control signal u_2 is investigated. Figures 4.51 to 4.54 are the concentration behaviour for changes in control signal u_2

Figures 4.51 to 4.54 represent the responses for the concentration set-point tracking under the disturbances for the considered cases. The results from the simulation shows that the effects of this kind of the disturbance does not quite affect the set-point tracking performance of the concentration loop. The concentration control system can still track the set-point variations implying that the designed decoupling systems is good at rejecting the random variations in the control signal u_2 although the responses become sluggish as the magnitude of this disturbance is increased.

Appendix D provides The file that simulates the dynamic decoupling control response of the closed loop MIMO CSTR model for various magnitudes of the set-point step changes, as well as disturbances at the outputs (y1),y(2) and the interaction junctions (u1) and (u2). The Simulink closed loop model to be simulated is *dyn_dec_2015* and is presented in appendix F.

4.6.3 Discussion of the Results

Simulation results are used to verify the performance of the control laws to find whether the effective set-point tracking control and disturbance effect minimisation for the output variables can be achieved. The concentration closed loop simulation study is first investigated for set-point tracking capability. This is done by varying the set-points for the concentration from $0.0762 mol/l$ to $0.13 mol/l$, and then from to $0.13 mol/l$ to $0.1 mol/l$ with time and the responses verified the set-point tracking capability of the designed control scheme. Several other variations in set-points are investigated for the time response performance indices as documented in this chapter. Good tracking control is still achieved.

Similarly, the effects of disturbances are investigated. The process performance is analysed for different varying magnitudes of random disturbances (white noise) added to the main concentration control loop. Good tracking control is still achieved. However as the magnitude of the disturbance is increased, the concentration step response becomes noisy. Similarly, the influence of the disturbances at the interactions point is considered. This is investigated by adding some some random noise of vaious magnitudes to the control signal. The responses for the concentration

set-point tracking with these disturbances for the considered cases show that the magnitude of the disturbance is important for smooth set-point tracking. However the concentration control system is still able to track the set-point variations implying that the designed decoupling systems is good at rejecting the random variations.

Similarly, the performances of the temperature control loop signal y_2 when the disturbances are in y_1 and u_1 are investigated. This is important because of the interactions that exist in the closed loop system. The results show that there is very little influence of the disturbance effect on y_1 to the temperature control loop signal y_2. This implies that the decoupling control design is good. Next, the investigation on the influence of the effect of disturbance on u_1 to the temperature control loop signal y_2 .is also done. It is found that as the magnitude of the disturbance u_1 increase, the response on y_2 becomes sluggish and noisy. This implies that there are still some elements of interactions in the system.

The next simulation investigation performed is on the control performance on the temperature control loop. The same procedure adopted for the concentration control is used. First, the control algorithm derived earlier is used to simulate the temperature control loop for set-point tracking. The set-point is varied from $444.7K$ to $455K$, then from $445K$ to $444.7K$ with time. A part from the high percentage overshoot, the other performance indices are good, hence successful temperature set-point tracking is achieved with this control law. Several other variations in set-points are investigated too. Then, the effects of disturbances are investigated for the temperature control loop. The procedure adopted is the same as that for the concentration control loop. The results of simulation shows that the magnitudes of the disturbance is important for smooth set-point tracking. However the temperature control system is able to track the set-point variations in the presence of the noise disturbances implying that the designed decoupling systems is good.

Analysis is done if the behaviour of one loop influences the behaviour of the other loop. If not influenced then the designed decoupling control is good. This is on the basis of introducing disturbances in one of the loops and simulating the whole system to see if the behaviour of the other loop changes. The results of the analyses show that this kind of decoupling control design is good.

4.7 Conclusion

Difficulties caused by the interacting loops for the MIMO systems are the major obstacle to the design of controllers for such systems. Interactions occur when there

are coupling between the control variables and between the process variables thereby affecting the states of the controlled variables. To address the problem of loop interactions in the $2x2$ MIMO CSTR process under study at one of the operating point, a simple dynamic decoupling mechanism is designed to compensate for the loop interactions. After this two SISO PI controllers for the resulting decoupled system are designed directly and independently using pole placement technique to tune the individual loops for tracking control of the output variables namely, the reactor concentration and the reactor temperature. The results of simulation studies show that the dynamic decoupling control scheme together with the SISO PI control algorithms are capable of achieving effective set-point tracking control in the presence of noise disturbances, implying that the designed decoupling systems is good.

In the following chapter, decentralized controller design method is presented for the $2x2$ MIMO CSTR process under study. In order to design decentralized diagonal controllers, input output pairing is performed based on the Relative Gain Array (RGA) technique, and then Internal Model Control PID controller tuning is developed.

CHAPTER FIVE
DECENTRALIZED CONTROLLER DESIGN FOR THE CSTR

5.1 Introduction

In this chapter, the design of a decentralized controller for the linearized $2x2$ MIMO CSTR model at the given operating point is presented. The decentralized controller design is based on the judicious choice of single loop parings that reduces the effects of process interactions based on the Relative Gain Array (RGA) method proposed by (Bristol, 1966), and on the Inverse model based (IMC) PID controller tuning of the individual paired diagonal loops. The preliminary theory of the method is presented, and then the details of the design procedure are described. The closed loop system is tested by simulation in the Matlab/Simulink environment in terms of the performance specifications to show the suitability of the control strategy.

The chapter is organized as follows: In section 5.2 the approach of the decentralized control design is presented with the motivation for the need of the control. Section 4.3 presents the derivation procedure for the RGA for the linearized $2x2$ MIMO CSTR model. Section 4.4 applies the general theory of the Inverse Model Control (IMC) adopted for the linear PID control design. In section 4.5, the IMC-based feedback PID controller design is presented. Section 4.6 presents the simulation of the closed loop system. Section 4.7 discusses the obtained results from the simulation, and finally section 4.8 gives the conclusion of the chapter.

5.2 Decentralized control approach

In spite of the advancement in the controller design methodologies for the multivariable processes, the decentralized controllers are still popular in chemical industries because of: the ease to which the technique is implemented, the simplicity of operation, and easiness in the controller parameters tuning. Decentralized control of multivariable plants is based on suitable decomposition of the control system into single input single output (SISO) control loops. The main obstacle to decentralize the control design for MIMO systems is the interactions that exist between the control loops. Controller design is based on two steps; judicious choice of single loop parings, and the controller tuning in the individual paired loops. For the design of decentralized controllers, input-output pairing of the variables is performed based on the Relative Gain Array (RGA) method proposed by (Bristol, 1966). The method provides two types of useful information for the multivariable controller design; the measure of the process interactions and the recommendations about the best pairing such that the effects of the interactions are reduced. The method however requires

knowledge of the steady state gains, but not the process dynamics. The main idea around RGA is to assess the effect of the interactions if a controller is designed for each output variable on a specific input variable. It determines how the controlled and the manipulated variables should be coupled to yield control loops with minimal interactions. It is a matrix of the gains which measures the steady state effects of coupling. The RGA method is defined and explained in the following subsection:

5.3 The Relative Gain Array (RGA)

For an nxn process, each component in the RGA matrix is the fraction of the open loop gain of the particular loop in the case with all other loops opened, to the closed loop gain of that loop with all other loops closed. Mathematically each element in the matrix is described by Equation (5.1) as:

$$\lambda_{ij} = \frac{\text{open-loop gain between } y_i \text{ and } u_j}{\text{closed-loop gain between } y_i \text{ and } u_j}; i = \overline{1,N} \text{ and } j = \overline{1,N}$$
$$= \frac{(\partial y_i / \partial u_j)_u}{(\partial y_i / \partial u_j)_y} \quad (5.1)$$

where N is the number of the loops in the process. The subscript u denotes constant values for all control variables except u_j (i.e., all loops open), while subscript y indicates that all outputs except y_i are kept constant by the control loops (i.e., all loops are closed). λ_{ij} is a dimensionless quantity. The relative-gain array matrix is then given by:

$$\Lambda = \begin{bmatrix} \lambda_{11} & \lambda_{12} & .... & \lambda_{1N} \\ \lambda_{21} & \lambda_{22} & .... & \lambda_{2N} \\ .. & .. & .... & .. \\ \lambda_{N1} & \lambda_{N2} & .... & \lambda_{NN} \end{bmatrix} \quad (5.2)$$

Entries of Λ satisfy the following two properties:

$\sum_{i=1}^{N} \lambda_{ij} = 1 \text{ for } j = 1, 2, ..., N$ Summation in a column

$\sum_{j=1}^{N} \lambda_{ij} = 1 \text{ for } i = 1, 2, ..., N$ Summation in a row

For the considered $2x2$ process, the matrix transfer function is of the process is of the form:

$$G(s) = \begin{bmatrix} G_{11}(s) & G_{12}(s) \\ G_{21}(s) & G_{22}(s) \end{bmatrix} \quad (5.3)$$

Under steady state conditions Equation (5.3) is called the steady state process gain matrix as:

$$G(0)=\begin{bmatrix} G_{11}(0) & G_{12}(0) \\ G_{21}(0) & G_{22}(0) \end{bmatrix}=\begin{bmatrix} K_{11} & K_{12} \\ K_{21} & K_{22} \end{bmatrix} \tag{5.4}$$

The RGA of the steady state gain matrix $G(0)$, (Skogestad and Postlethwaite, 2005) is then defined as:

$$\Lambda=\begin{bmatrix} \lambda_{11} & \lambda_{12} \\ \lambda_{21} & \lambda_{22} \end{bmatrix}=G(0).*(G(0)^{-1})^{T} \tag{5.5}$$

Where $(G(0)^{-1})^{T}$ is the transpose of $G(0)^{-1}$. The operator '*' in Equation (5.5) denotes element by element multiplication.

The corresponding relative-gains can be computed as follows

$$\Lambda=\begin{bmatrix} \lambda_{11} & \lambda_{12} \\ \lambda_{21} & \lambda_{22} \end{bmatrix}=\begin{bmatrix} \lambda_{11} & 1-\lambda_{11} \\ 1-\lambda_{11} & \lambda_{11} \end{bmatrix}$$

Where, $\lambda_{11}=\lambda_{22}=\dfrac{1}{1-\dfrac{K_{12}K_{21}}{K_{11}K_{22}}}=\dfrac{K_{11}K_{22}}{K_{11}K_{22}-K_{12}K_{21}}, \lambda_{12}=1-\lambda_{11}=\lambda_{21}$

With regards to the steady state gains, the RGA matrix is obtained as:

$$\Lambda=\begin{bmatrix} \dfrac{K_{11}K_{22}}{K_{11}K_{22}-K_{12}K_{21}} & \dfrac{-K_{12}K_{21}}{K_{11}K_{22}-K_{12}K_{22}} \\ \dfrac{-K_{21}K_{12}}{K_{11}K_{22}-K_{12}K_{21}} & \dfrac{K_{11}K_{22}}{K_{11}K_{22}-K_{12}K_{21}} \end{bmatrix} \tag{5.6}$$

The recommended parings corresponds to the $\lambda_{ij}, i=\overline{1,N}$ and $j=\overline{1,N}$ which have the largest positive values that are closest to one. The RGA element of one indicates that for this pairing, the other control loops do not affect the current one and this is thus the ideal pairing. A RGA element of 0 means that the corresponding input does not affect the output directly at all. Pairings which correspond to values of λ_{ij} which are negative should not be chosen. Thus, for the $2x2$ CSTR model under consideration where the manipulated variables are the process feed flow rate and process coolant flow rate respectively, while the controlled variables are the reactor concentration and the reactor temperature, the steady state gain matrix is:

$G(0)=\begin{bmatrix} -0.0015 & 0.0027 \\ 0.6063 & -0.7457 \end{bmatrix}$, and evaluating its RGA yields

$$\Lambda=\begin{bmatrix} -2.2577 & 3.2577 \\ 3.2577 & -2.2577 \end{bmatrix} \tag{5.7}$$

Given that loops are not be formed with relative gains which are negative to ensure closed loop stability, this implies that a perfect pairing for independent single loops

should be $y_1 - u_2$ and $y_2 - u_1$ for the purposes of the decentralized control. This means that the pairing should be such that:

$$\begin{bmatrix} Y_1(s) \\ Y_2(s) \end{bmatrix} = \begin{bmatrix} G_{12}(s) & G_{11}(s) \\ G_{22}(s) & G_{21}(s) \end{bmatrix} \begin{bmatrix} U_2(s) \\ U_1(s) \end{bmatrix} \tag{5.8}$$

The steady state input-output relation for the recommended pairing should then be:

$$\begin{bmatrix} Y_1(0) \\ Y_2(0) \end{bmatrix} = \begin{bmatrix} 0.0027 & -0.0015 \\ -0.7454 & 0.6063 \end{bmatrix} \begin{bmatrix} U_2(s) \\ U_1(s) \end{bmatrix} \tag{5.9}$$

The RGA pairing rule does not consider the stability of the resulting control structure. Therefore, it is necessary to check the resulting control structure stability and which is done according to the Niederlinski index (Niederlinski, 1971). The Niederlinski Index is calculated from the full gain matrix of the steady-state and is defined as:

$$NI = \frac{|G(0)|}{\prod_i G(0)_{ii}}$$

Here $|G(0)|$ implies the determinant of the full gain matrix of the steady-state and

$$\prod_i G(0)_{ii} = G_{11}(0)G_{22}(0)$$

$$NI = \frac{[(0.00270)(6063)] - [(-0.7454)(-0.0015)]}{(0.0027)(0.6063)} = 0.3169 \tag{5.10}$$

Since $NI \succ 0$ for the recommended pairing, the multivariable decentralized control system under consideration may be integrally stable. Thus, the effluent concentration should be controlled by the coolant flow rate while the reactor temperature is to be controlled by the feed flow rate. This is based on the RGA matrix of Equation (5.9). This implies that two independent diagonal controllers can be designed while disregarding the coupling between the two input pairs. After that an interaction measure is designed to factor in the off-diagonal elements effects on the stability and performance. Figure 5.1 represents the block diagram for the decentralized control that is developed.

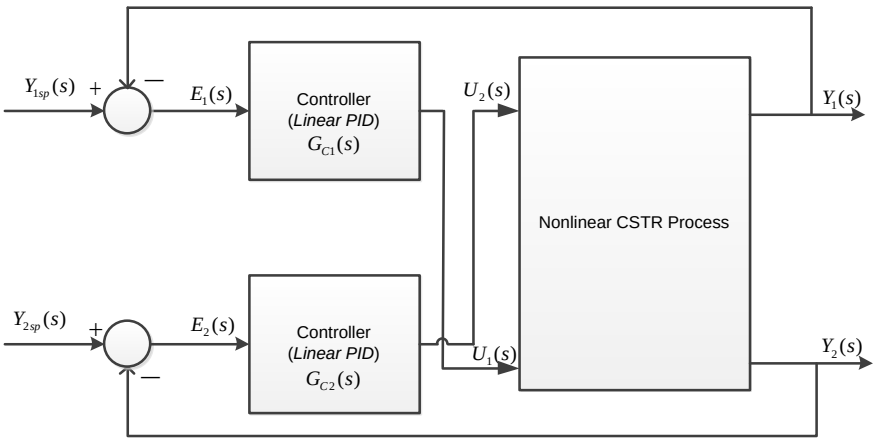

Figure 5.1: The decentralized control block diagram for the MIMO CSTR.

In this case, the difference between $Y_{sp2}(s)$ and $Y_2(s)$ (the errors in output 2) is used to adjust the input for the concentration control (input 1 of the CSTR) using a linear controller $G_{C2}(s)$. Similarly, the difference between $Y_{sp1}(s)$ and $Y_1(s)$ (the errors in output 1) is used to adjust the input for the temperature control (input 2 of the CSTR) using a linear controller $G_{C1}(s)$ as illustrated in Figure 5.1. Ignoring the off-diagonal elements, first, the diagonal controllers are designed in line with the theory for the Inverse Model Control (IMC). Appendix G provides the PID controller settings based on IMC.

5.4 IMC-based PID feedback control design theory

IMC-based PID feedback control design procedure that makes use of the model inverse for control system philosophy as proposed in (Chien and Fruehauf, 1990; Bequette, B.W. 2003) is applied to design the two independent PID controllers. This is explained using the following two block diagrams in Figures 5.2 and 5.3.

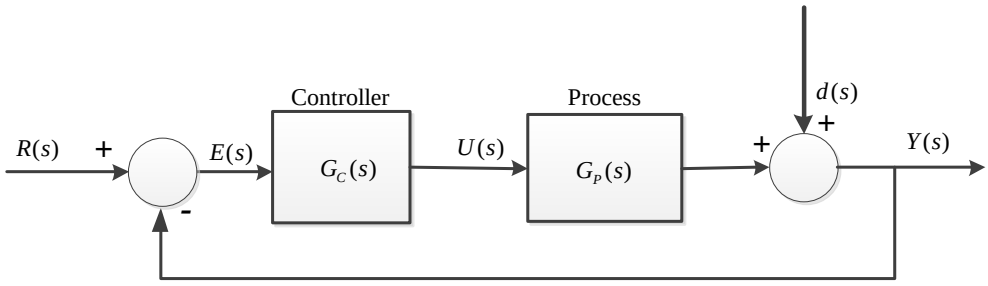

Figure 5.2: Classical feedback control scheme

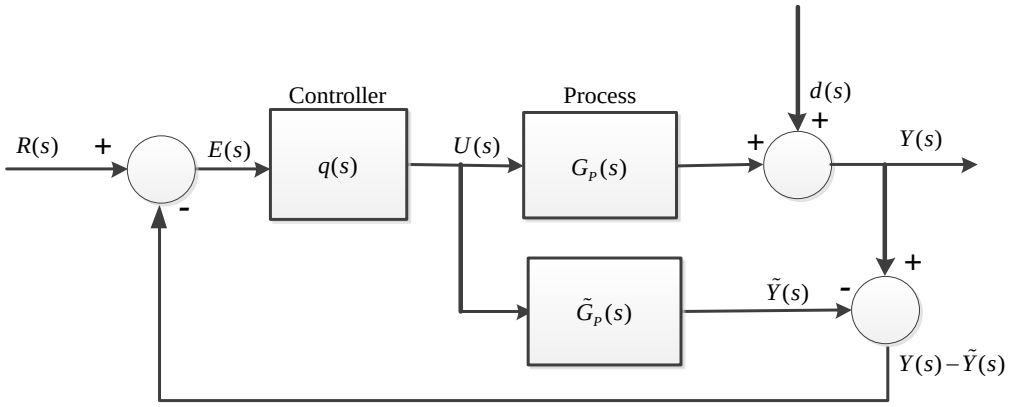

Figure 5.3: Inverse model control scheme

The IMC controller is designed based on Figure 5.3. The model of the process $\tilde{G}_P(s)$ and the output $U(s)$ of the controller are required in order to calculate the model output $\tilde{Y}(s)$. The response of the model is subtracted from the actual response of the process and the error $Y(s)-\tilde{Y}(s)$ is applied to the IMC controller $q(s)$ as an input. Figure 5.2 is the block diagram for the conventional feedback control. Using the limiting case that based on the block diagram reduction techniques, it can be shown that the two block diagrams (Figures 5.2 and 5.3) are identical if $\mathrm{G_C(s)}$ and $\mathrm{q(s)}$ satisfy the relation

$$G_C(s)=\frac{q(s)}{1-\tilde{G}_P(s)q(s)}. \tag{5.11}$$

Thus any IMC controller $q(s)$ is equivalent to a standard feedback controller $G_C(s)$ and vice versa.

The design procedure is summarized in the following steps:

- The IMC controller transfer functions, $q(s)$ which including a filter $f(s)$ is determined. The controller $q(s)$ may be half proper or even improper to result in the desired PID controller derivative action. For good set-point tracking, a filter with the following form is generally used $f(s)=\frac{1}{(\gamma s+1)^z}$ where γ is the adjustable filter factor similar to the closed loop time constant to vary the closed loop system's speed of response and z is the order of the filter.
- The IMC-based PID controller parameters are determined by using the transformation: $G_C(s)=\frac{q(s)}{1-\tilde{G}_P(s)q(s)}$ where $\tilde{G}_P(s)$ is the plant model.

- Express the transformation in the standard PID form and determine the controller tuning parameters K_P, τ_I, τ_D where K_P is the proportional gain constant, τ_I is the integral time constant and τ_D is the derivative time constant.
- Perform closed loop simulations. Adjust the value of γ as a trade-off between performance and robustness.

5.4.1 IMC-based PID feedback control design for the concentration loop

The relationship between the effluent concentrations to the coolant flow rate $(y_1 - u_2)$ in transfer function form is:

$$G_{12}(s) = \left[\frac{0.04672}{s^2 + 5.99s + 17.58}\right] = \left[\frac{0.00266}{0.0569s^2 + 0.34073s + 1}\right] \tag{5.12}$$

This transfer function is of the form

$G_{12}(s) = \dfrac{K_1}{\tau_1^2 s^2 + 2\zeta_1\tau_1 s + 1}$ Where K_1 represents the system's steady state gain and τ_1 represents the system time constant.

According to the proposal by (Chien and Fruehauf, 1990; Bequette, 2003); the IMC controller can be designed based on the inverse of the process model with a low pass filter $f(s)$ placed in series Therefore the IMC controller transfer function for the concentration control loop as illustrated in Figure 5.1 is derived as:

$$q_{12}(s) = G_{12}^{-1}(s) f(s) = \frac{\tau_1^2 s^2 + 2\zeta_1\tau_1 s + 1}{K_1} \frac{1}{(\gamma_1 s + 1)} \tag{5.13}$$

Where $q_{12}(s)$ is the IMC controller transfer function for the concentration loop. Assuming Figure 5.3 is used for the derivation, then the equivalent standard feedback controller after some transformation is thus;

$$G_{C12}(s) = \frac{q_{12}(s)}{1 - G_{12}(s)q_{12}(s)} = \frac{\dfrac{\tau_1^2 s^2 + 2\zeta_1\tau_1 s + 1}{K_1}\dfrac{1}{(\gamma_1 s + 1)}}{1 - [(\dfrac{K_1}{\tau_1^2 s^2 + 2\zeta_1\tau_1 s + 1})(\dfrac{\tau_1^2 s^2 + 2\zeta_1\tau_1 s + 1}{K_1}\dfrac{1}{(\gamma_1 s + 1)})]} = \tag{5.14}$$

$$= \frac{\tau_1^2 s^2 + 2\zeta_1\tau_1 s + 1}{K_1\gamma_1 s} = \left[\frac{2\zeta_1\tau_1}{K_1\gamma_1}\right]\frac{\tau_1^2 s^2 + 2\zeta_1\tau_1 s + 1}{2\zeta_1\tau_1 s}$$

The general transfer function for an ideal PID controller is of the form

$$G_{C12}(s) = K_{P12}(1 + \frac{1}{s\tau_I} + s\tau_D) = K_{P12}\left[\frac{\tau_I\tau_D s^2 + \tau_I s + 1}{\tau_I s}\right] \tag{5.15}$$

Rearranging Equation (5.14) in the form of the Equation (5.15) to find how the model parameters and γ_1 are related to the PID controller parameters, the following IMC-based PID controller relationships are found:

$$K_{P12}\left[\frac{\tau_I\tau_D s^2+\tau_I s+1}{\tau_I s}\right]=\left[\frac{2\zeta_1\tau_1}{K_1\gamma_1}\right]\frac{\tau_1^{\,2}s^2+2\zeta_1\tau_1 s+1}{2\zeta_1\tau_1 s} \tag{5.16}$$

Expressing the like terms in terms of K_1,τ_1 and γ or the controller parameters then Equation (5.17) is derived.

$$\begin{aligned}
&\rightarrow K_{P12}=\frac{2\zeta_1\tau_1}{K_1\gamma_1};\\
&\tau_I s=2\zeta_1\tau_1 s\rightarrow\tau_I=2\zeta_1\tau_1\\
&\tau_I\tau_D s^2=\tau_I^{\,2}s^2\rightarrow\tau_I\tau_D=\tau_1^{\,2}\\
&\tau_D=\frac{\tau_1^{\,2}}{\tau_I}=\frac{\tau_1^{\,2}}{2\zeta_1\tau_1}=\frac{\tau_1}{2\zeta_1}
\end{aligned} \tag{5.17}$$

From Equation (5.12) it is found that the various process model parameters are:

$$\begin{aligned}
&K_1=0.00266\\
&\tau_1=\sqrt{0.0569}=0.2385\\
&\zeta_1=\frac{0.34073}{2\tau_1}=0.71432
\end{aligned} \tag{5.18}$$

The PID controller tuning parameters designed as per Equations (5.17) and (5.18) are the derived, as follows,

$$\begin{aligned}
&K_{P12}=\frac{2\zeta_1\tau_1}{K_1\gamma_1}=426.98\\
&\tau_I=0.340728\Rightarrow K_I=2.935\\
&\tau_D=\frac{\tau_1}{2\zeta_1}=0.1556\\
&\gamma_1=\frac{1}{5}=0.3
\end{aligned} \tag{5.19}$$

With calculation of the PID controller representing the loop y_1-u_2, the concentration loop controller design process is completed.

5.4.2 IMC-based PID feedback control design for the temperature loop

Next the relationship between the reaction temperatures to the feed flow rate (y_2-u_1) transfer function form is considered for the second PID controller design:

$$G_{21}(s)=\left[\frac{-0.947s+10.66}{s^2+5.99s+17.58}\right]=\left[\frac{0.6063(-0.08885s+1)}{0.0569s^2+0.34073s+1}\right] \tag{5.20}$$

Equation (5.20) shows that the transfer function has a right hand (RH) zero at $s=1/0.08885$.This will result in an inverse response in the process transfer function. The process model zeros becomes the controller poles, if the model inverse is applied for the control system design, and may result in an unstable controller. It is therefore recommended that this zero be factored out before using the model inverse

for the controller design. The proposed control design procedure is in the following steps:

- The process model is factored into non-invertible and invertible portions using an all-pass factorization as follows:

$$G_{21}(s) = G_{21+}(s)G_{21-}(s) = \left[\frac{0.6063(-0.08885s+1)}{0.0569s^2+0.34073s+1}\right] \tag{5.21}$$

Where $G_{21-}(s)$ contains the invertible elements and $G_{21+}(s)$ contains the noninvertible elements such that;

$$G_{21-}(s) = \frac{0.6063}{0.0569s^2+0.34073s+1} = \frac{K_2}{{\tau_2}^2 s^2 + 2\zeta_2 \tau 2_s + 1}$$

And $G_{21+}(s) = -0.08885s+1 = -\beta s+1$

where K_2 is the system's steady state gain and β gives the time constant of the noninvertible element.

- The idealized controller constructed from the invertible elements plus filter is then of the form:

$$\begin{aligned} q_{21}(s) &= {G_{21-}}^{-1}(s)\, f(s) = \frac{{\tau_2}^2 s^2 + 2\zeta_2\tau_2 s + 1}{K_{P2}} \frac{1}{(\gamma_2 s+1)} \\ &= \frac{0.0569s^2+0.34073s+1}{0.6063} \frac{1}{(\gamma_2 s+1)} \end{aligned} \tag{5.22}$$

- The PID equivalent is then found by the transformation as in Equation (5.14):

$$G_{C21}(s) = \frac{q_{21}(s)}{1-G_{21}(s)q_{21}(s)} = \frac{q_{21}(s)}{1-G_{21-}(s)G_{21+}(s)q_{21}(s)} =$$

$$= \frac{\dfrac{{\tau_2}^2 s^2 + 2\zeta_2\tau_2 s + 1}{K_2} \dfrac{1}{(\gamma_2 s+1)}}{1-\left[\left(\dfrac{K_2}{{\tau_2}^2 s^2 + 2\zeta_2\tau_2 s + 1}\right)\left(\dfrac{{\tau_2}^2 s^2 + 2\zeta_2\tau_2 s + 1}{K_2} \dfrac{1}{(\gamma_2 s+1)}\right)(-\beta s+1)\right]} \tag{5.23}$$

Following the procedure described in Bequette (2003); the IMC-based PID controller design and implementation parameters to yield good set-point tracking are as follows:

$$\begin{aligned} K_{P21} &= \frac{2\zeta_2\tau_2}{K_2(\beta+\gamma_2)} \\ \tau_{I2} &= 2\zeta_2\tau_2 \\ \tau_{D2} &= \frac{\tau_2}{2\zeta_2} \end{aligned} \tag{5.24}$$

From Equation (5.20), by comparing the denominator polynomial to the standard second order dimensionless Equation, $s^2 + 2\zeta\omega_n s + {\omega_n}^2$ and assuming that $\omega_n = 1/\tau$, the model parameters are:

$$
\begin{aligned}
K_2 &= 0.6063 \\
\beta &= -0.08885 \\
\tau_2 &= 0.2385 \\
\zeta_2 &= 0.71432
\end{aligned}
\qquad (5.25)
$$

Using Equations (5.24) and (5.25) the PID controller tuning parameters for the second loop are found as follows:

$$
\begin{aligned}
K_{P21} &= \frac{2(0.71432)(0.2385)}{0.6063(-0.08885+0.4)} = 1.606 \\
\tau_{I2} &= 2(0.71432)(0.2385) = 0.3407 \\
\tau_{D2} &= \frac{0.2385}{2(0.74132)} = 0.1608 \\
\gamma_2 &= 0.45
\end{aligned}
\qquad (5.26)
$$

After the design of the individual diagonal decentralized controllers for each independent loop, two detuning factors, each for an individual loop and which are equivalent to the interaction measures of the off-diagonal matrices of the process are factored into the controller tuning parameters to compensate for the interactions. A detuning factor F of typical values varying between 2 and 5 (Luyben, 1986) is normally chosen to adjust the proportional controller gain constant so that $K_P^* = K_P / F$ and the integral time constant adjusted to $\tau_I^* = \tau_I F$, so that the effects of the interactions are minimised The stability of each loop is determined by the detuning factor F the and the bigger the magnitude of F , the more stable the system is. However the detuned closed loop system's response becomes more sluggish to set-point changes and disturbances, therefore the detuning factor serves as a compromise between stability and performance.

5.5 Simulation results

Simulation results are used to show the performance of the designed controllers. First the performances with independent designed diagonal controllers are tested. Figures 5.4 and 5.5 show the Simulink block diagrams used to implement the two feedback PID decentralized diagonal controllers for the $2x2$ MIMO CSTR process under study as a first step in the implementation of the closed loop control for the $2x2$ MIMO CSTR process by ignoring the off-diagonal elements. The design procedure adopted is by using IMC-based PID feedback control that makes use of the model inverse for control system philosophy to design the two independent diagonal PID controllers.

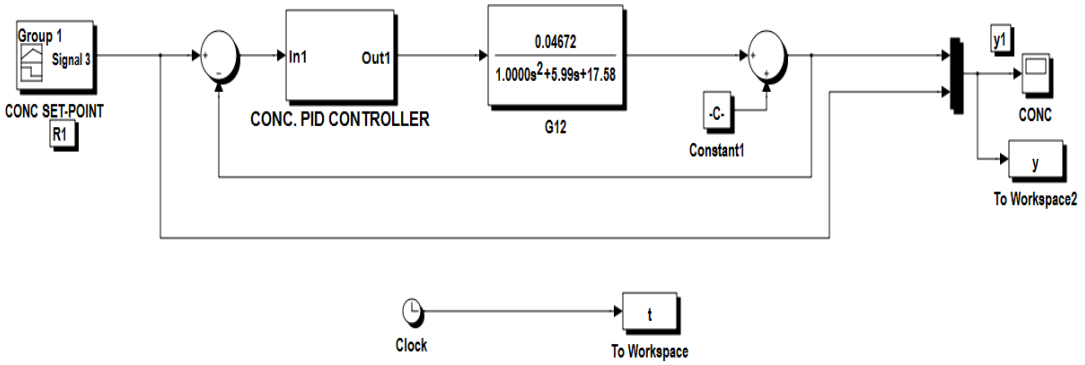

Figure 5.4: Fully decentralized closed loop control scheme for the concentration

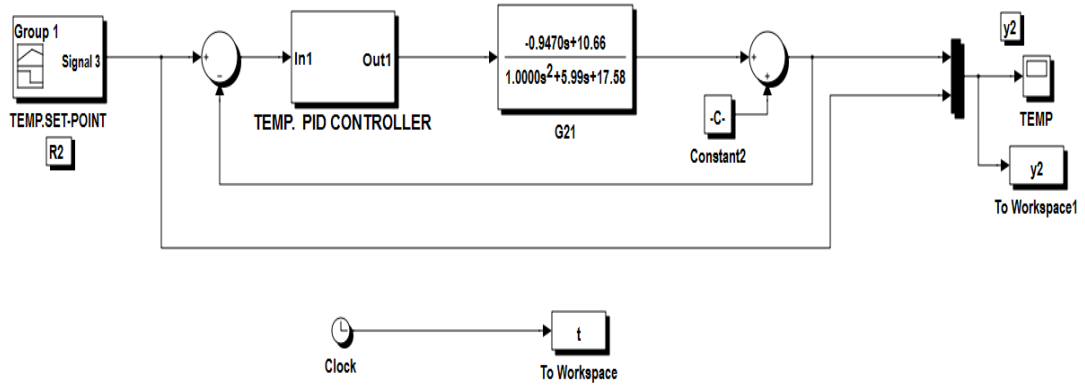

Figure 5.5: Fully decentralized closed loop control scheme for the temperature

5.5.1 Concentration loop transition behaviour

Figure 5.6 show the time response for set-point tracking characteristic of the concentration for varying set-point values. The set-point is varied in steps from 0.0762mol/l to 0.13mol/l, and then to 0.06mol/l, as illustrated. The PID controller tuning parameters of Equation 5.19 are used. As can be seen in Figure 5.6, the concentration response tracking capabilities for the designed decentralized controller are good. Calculated indices such as the peak overshoot, Peak time, settling time, steady state error and rise time for the designed controller are then obtained for a number of set-point values as illustrated in Table 5.1. These are for the Figures 5.7-5.11. A maximum overshoot of 5.5263% is attained with 0% steady state error for a maximum set-point of 0.08mol/l

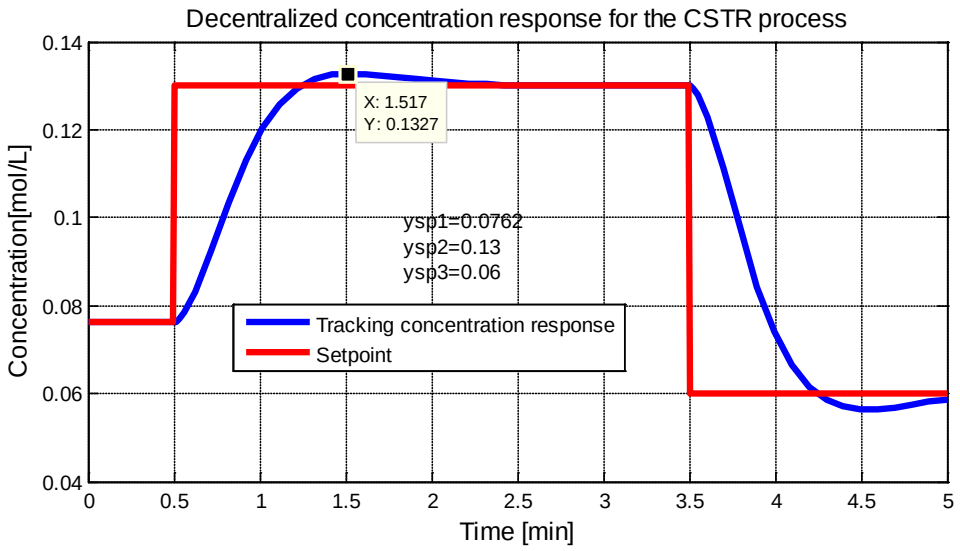

Figure 5.6: Decentralized concentration set-point tracking

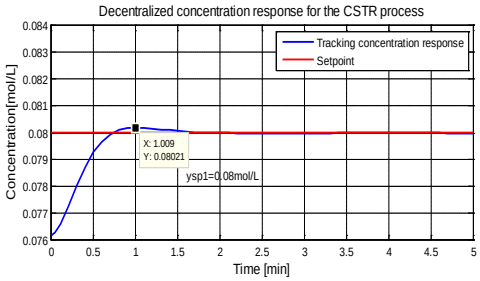

Figure 5.7: Set-point tracking for 0.08mol/l

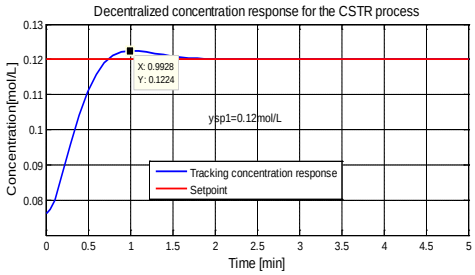

Figure 5.9: Set-point tracking for 0.12mol/l

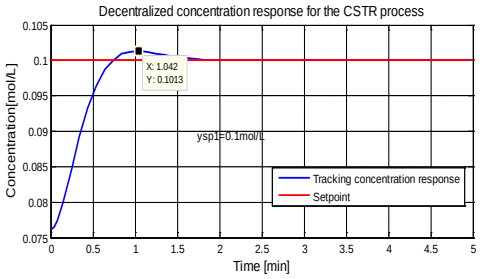

Figure 5.8: Set-point tracking for 0.1mol/l

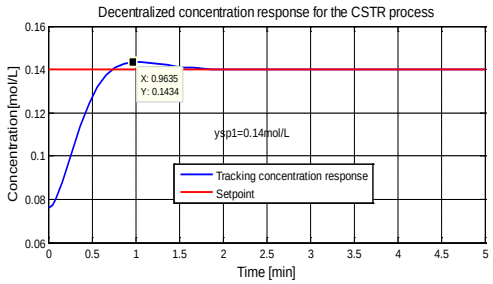

Figure 5.10: Set-point tracking for 0.14mol/l

Table 5.1: Performance indices for the concentration control loop

Set-point value	Settling time t_s (sec)	Peak over shoot M_p (%)	Peak time t_s (sec)	Steady state error e_{ss} (%)
0.08mol/l	78.534	5.5263	60.534	0
0.1mol/l	79.534	5.4622	62.544	0
0.12mol/l	78.534	5.4794	59.568	0
0.14mol/l	78.534	5.3291	59.01	0

5.5.2 Temperature loop transition behaviour

Figure 5.7 shows the time response for set-point tracking characteristic of the temperature for varying set-point values. The set-point is varied in steps from $444.77K$ to $455K$, and then to $440K$, as illustrated. The PID controller tuning parameters of Equation 5.26 are used. As can be seen in Figure 5.11, the temperature response tracking capabilities for the designed decentralized controller are good. Calculated indices such as the peak overshoot, Peak time, settling time, steady state error and rise time for the designed controller are then obtained for a number of set-point values, as illustrated in Table 5.2. These are for the Figures 5.12-5.15. A maximum overshoot of 8.9% is attained with 0% steady state error for a maximum set-point of $460K$

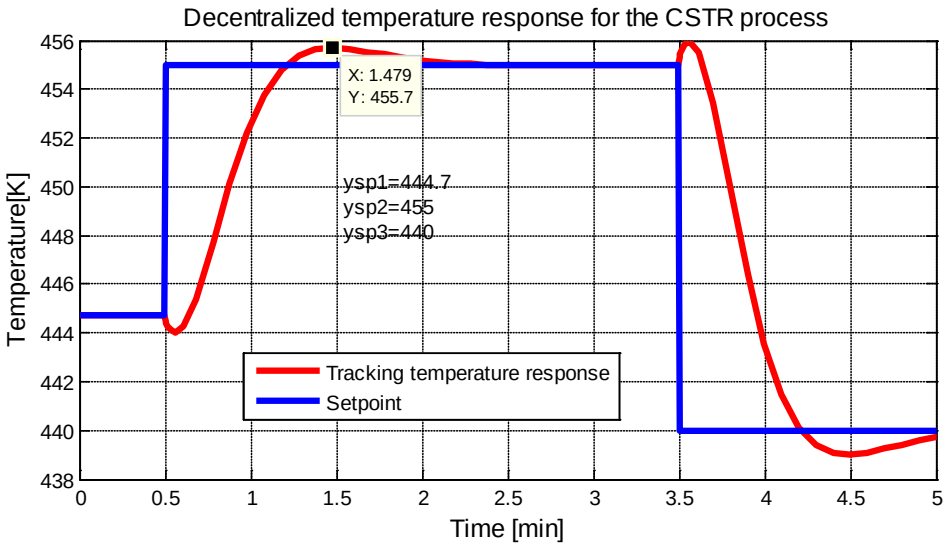

Figure 5.11: Decentralized temperature set-point tracking

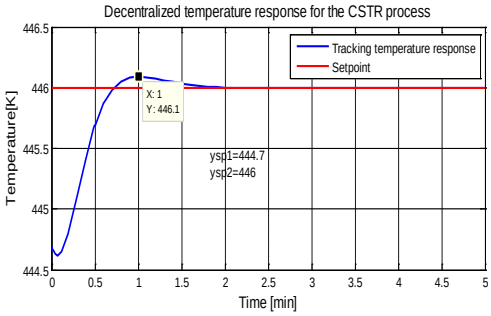

Figure 5.12: Set-point tracking for $446K$

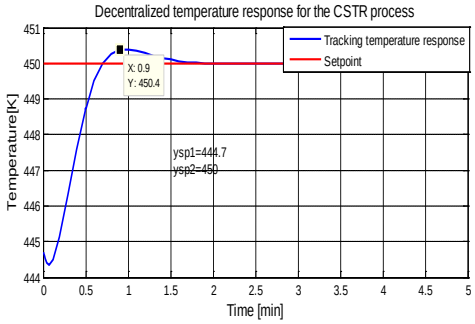

Figure 5.13: Set-point tracking for $450K$

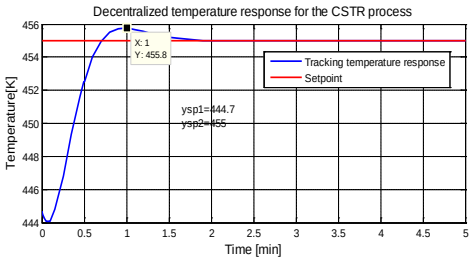

Figure 5.14: Set-point tracking for $455K$

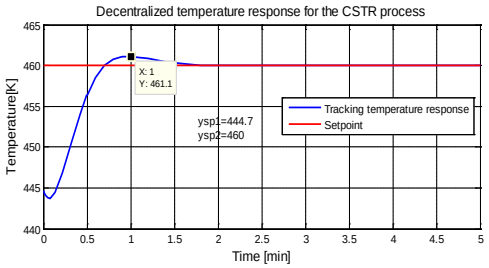

Figure 5.15: Set-point tracking for $460K$

Table 5.2: Performance indices for temperature control loop

Set-point value	Settling time t_s(min)	Peak over shoot M_p(%)	Peak time t_s(sec)	Steady state error e_{ss}(%)
446K	1.3089	8.1300	60.5340	0
450K	1.3424	7.6481	60.000	0
455K	1.3228	7.8201	60.000	0
460K	1.3235	8.9000	60.000	0

5.5.3 Simulation of the decentralized closed loop MIMO system

Figure 5.16 represents the block diagram the MIMO closed loop CSTR system based on the two independently designed decentralized controllers, described in the preceding sections. This block diagram was simulated for different step set-points for the case where the calculated settings of the decentralized controllers are used in order to see the effects of the interactions. The following closed loop responses are obtained both for the concentration loop as well as for the temperature loop.

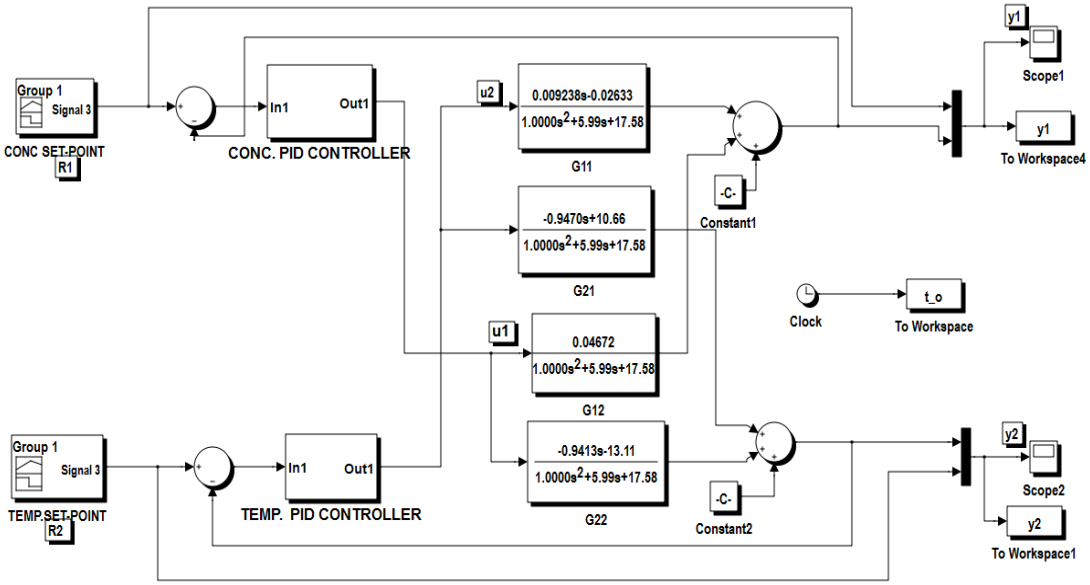

Figure 5.16: Decentralized control implemented in Simulink.

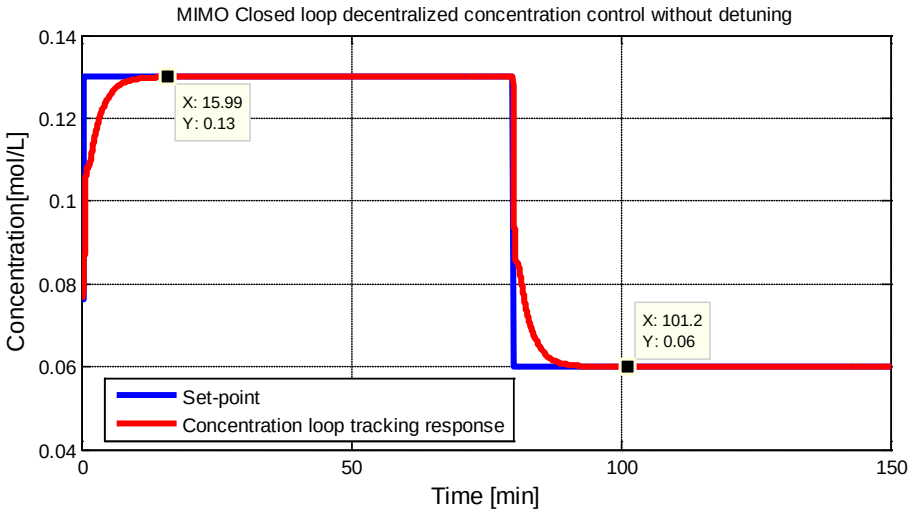

Figure 5.17: Concentration set-point tracking under decentralized control

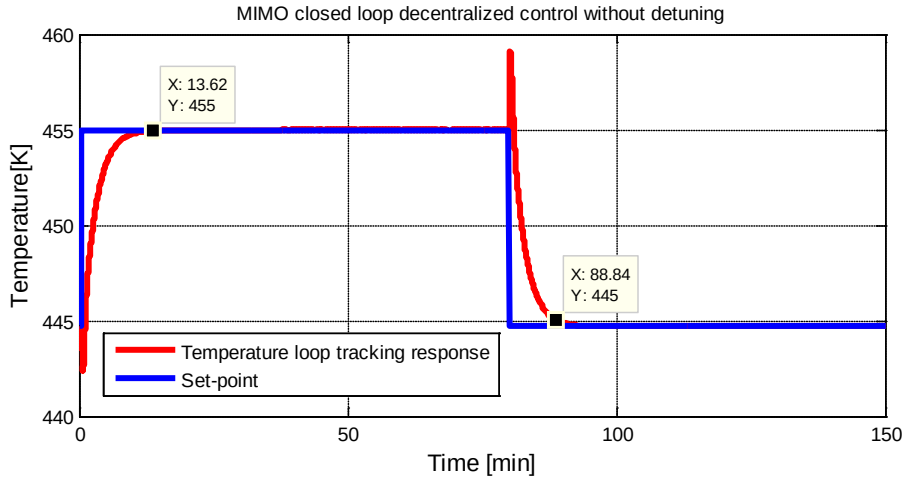

Figure 5.18: Temperature set-point tracking under the decentralized control

Figures 5.17 and 5.18 are the responses of the concentration control loop and the temperature control loop respectively for the MIMO system. The set-point tracking response capabilities for both outputs are achieved though the responses are sluggish. It takes the concentration loop to reach the steady state value of 0.13mol/l in 15.99 minutes whereas the temperature loop's steady state value of $455K$ is reached after a time of 13.62 minutes.

Investigations on the influences over the process output step response for various magnitudes of disturbances are also investigated for the developed scheme and presented in the following subsection.

5.5.4 Investigation on the disturbance influence on the concentration output y_1

Figure 5.19 is the block diagram of the closed loop system with disturbance at the concentration output y_1

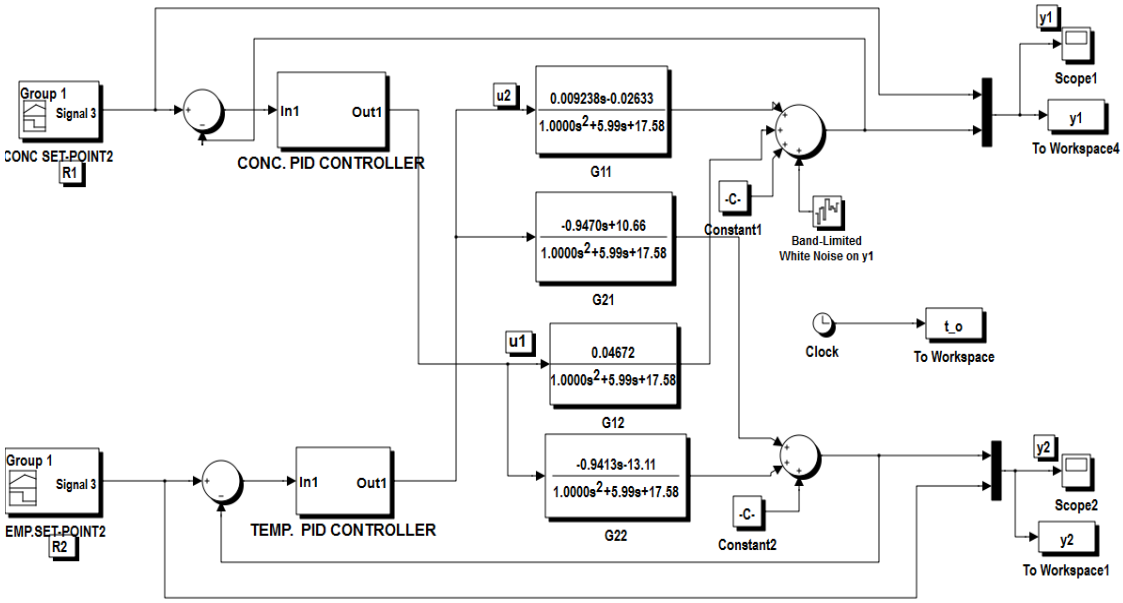

Figure 5.19: Closed loop control with disturbances at the concentration output y_1

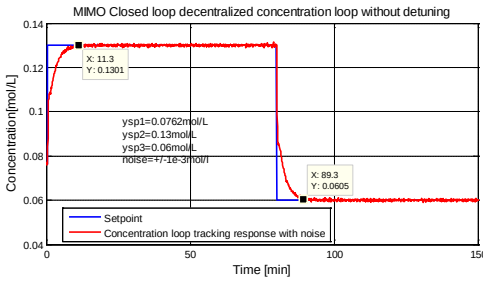

Figure 5.20: Response under $\pm 1e^{-3}\text{mol/l}$ noise

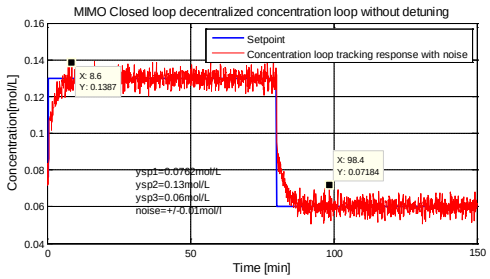

Figure 5.22: Response under $\pm 0.01\text{mol/l}$ noise

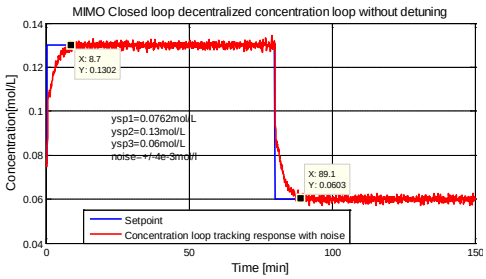

Figure 5.21: Response under $\pm 4e^{-3}\text{mol/l}$ noise

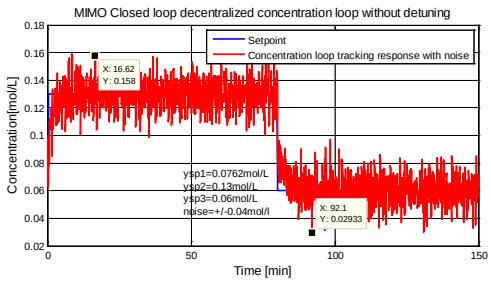

Figure 5.23: Response under $\pm 0.04\text{mol/l}$ noise

The designed decentralized control system performance is checked for different varying magnitudes of random disturbances (white noise) added to the output signal

y_1 on the main concentration loop. The responses are represented in Figures 5.20 to 5.23. Good tracking control is still achieved. However as the magnitude of the disturbance is increased, the response becomes noisy.

Figures 5.24-5.27 are the responses that shows the influences on the output temperature as a result of the disturbances on the concentration loop y_1

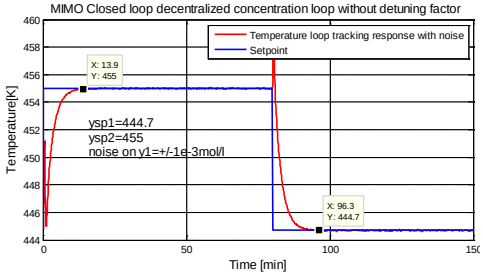

Figure 5.24: Response under $\pm 0.01 \text{mol/l}$ noise

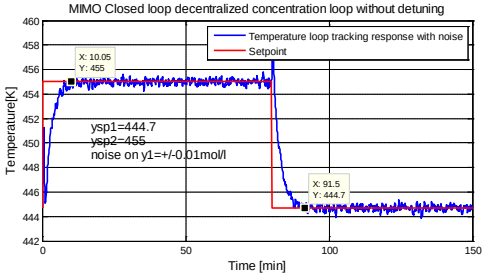

Figure 5.26: Temperature response under $\pm 0.01 \text{mol/l}$ noise on y_1

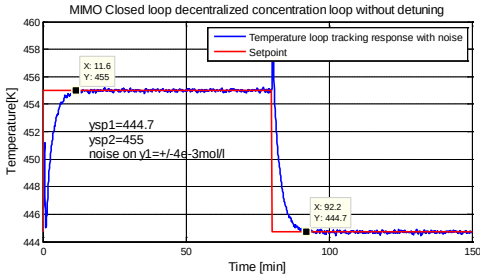

Figure 5.25: Temperature response under $\pm 4e^{-3} \text{mol/l}$ noise on y_1

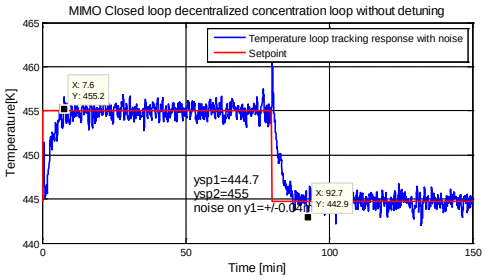

Figure 5.27: Temperature response under $\pm 0.04 \text{mol/l}$ noise on y_1

Similarly, it can be seen that the disturbance at the concentration output influences the second loop (temperature loop) too, but the magnitude of the effect is smaller between the loops. Decentrarized control scheme can not eliminate completely the efeects of the loop interactions. The results of simulation shows that the magnitude of the disturbance is important for smooth set-point tracking. However the temperature control system is still able to track the set-point variations implying that the designed decentralized systems is good even in the presence of the random disturbances, but full independence of the control loops can not be achieved.

5.5.5 Investigation on the disturbance interference over the temperature output y_2

Figure 5.28 is the block diagram of the closed loop MIMO system with disturbance on the temperature output y_2. The same type of experiments as in point 5.5.4 are performed.

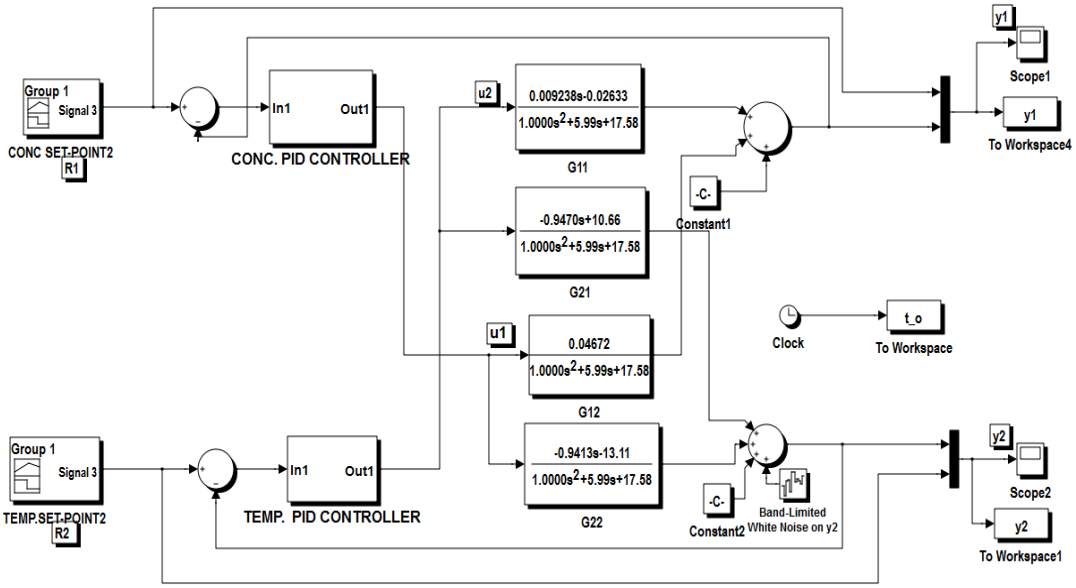

Figure 5.28: Closed loop control with disturbances on y_2 output.

The responses are represented in Figures 5.29 to 5.32. Good tracking control but sluggish responses are still achieved. However as the magnitude of the disturbance is increased, the response becomes noisy.

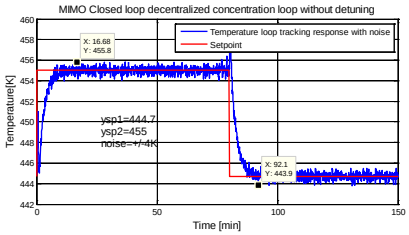

Figure 5.29: Temperature response under $\pm 4K$ noise

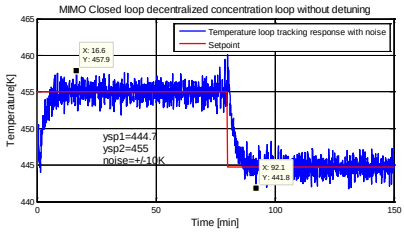

Figure 5.31: Temperature response under $\pm 10K$ noise

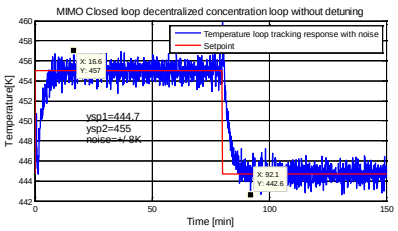

Figure 5.30: Temperature response under $\pm 8K$ noise

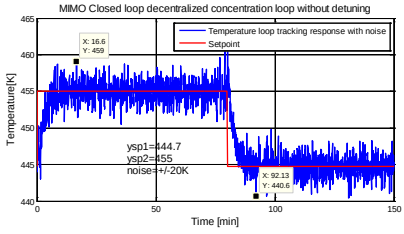

Figure 5.32: Temperature response under $\pm 20K$ noise

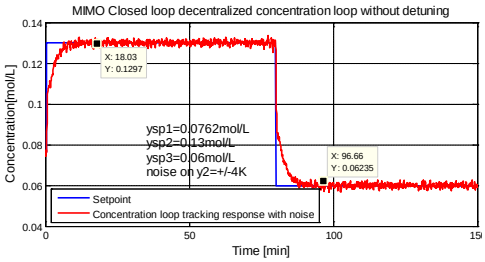

Figure 5.33: Concentration response under $\pm 4\text{K noise}$ on y_2

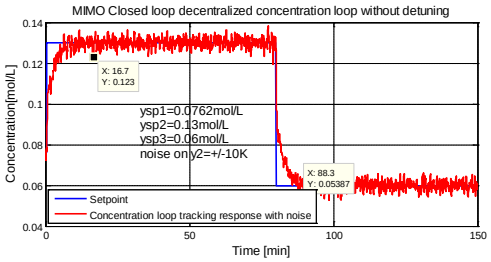

Figure 5.35: Concentration response under $\pm 10\text{K noise}$ on y_2

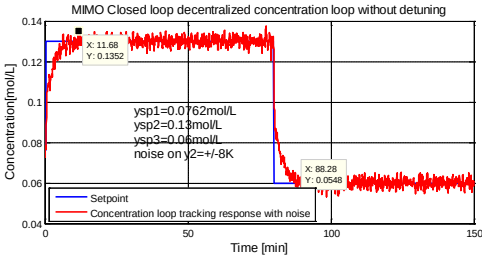

Figure 5.34: Concentration response under $\pm 8\text{K noise}$ on y_2

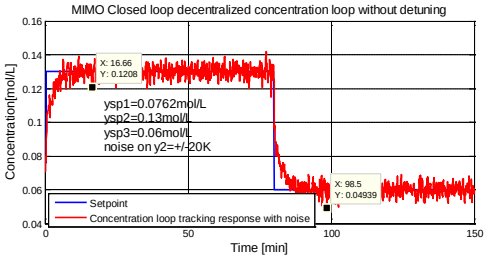

Figure 5.36: Concentration response under $\pm 20\text{K noise}$ on y_2

Figures 5.33-5.36 show the responses of the output concentration as a result of the disturbances on the temperature loop at y_2 output. Similarly, this disturbance influences the first loop (concentration loop) as illustrated .This is due to the interactions of the loops. Decentrarized control scheme can not eliminate completely the effects of the loop interactions. The results of simulation shows that the magnitude of the disturbance is important for the smooth set-point tracking. However the concentration system for the concentration is still able to track the set-point variations, implying that the designed decentralized systems is good even in the presence of the random disturbances.

Next the detunining factors are considered to improve the performances of the designed decentralized control schemes.

5.6 Decentralized control with detuning factors

After the design of the individual diagonal controllers for each independent loop, two detuning factors, each for the separate individual loops are factored into the controller tuning parameters to compensate for the interactions. A detuning factor F of typical values varying between 2 and 5 (Luyben, 1986) is normally chosen to adjust the proportional controller gain constant so that $K_P^* = K_P / F$ and the integral time

constant adjusted so that $\tau_I^* = \tau_I F$ so that the effects of the interactions are minimised The stability of each loop is determined by the detuning factor F, and the bigger the magnitude of F, the more stable the system is. However the result is a closed loop system whose response becomes more sluggish to the set-point changes and the disturbance influences, therefore the detuning factor serves as a compromise between the performance and the stability of the system.

For the designed controllers, it is found that the concentration control with a detuning factor of $F_1 = 2$ gives the best performance for:

$K_{P12}^* = K_{P12} / F_1 = 426.98 / 2 = 213.49$,and

$\tau_{I12}^* = \tau_{I12} F_1 = 0.340728(2) = 0.681456$.

Similarly, for the temperature control loop a detuning factor $F_2 = 1.4$ of gives the best performance:

$K_{P21}^* = K_{P21} / F_2 = 1.556 / 1.4 = 1.11143$, and

$\tau_{I12}^* = \tau_{I12} F_2 = 0.340728(1.4) = 0.4770192$.

The corresponding closed loop responses for the detuned loops are illustrated in Figures 5.37 and 5.38 for the concentration control and the temperature control respectively.

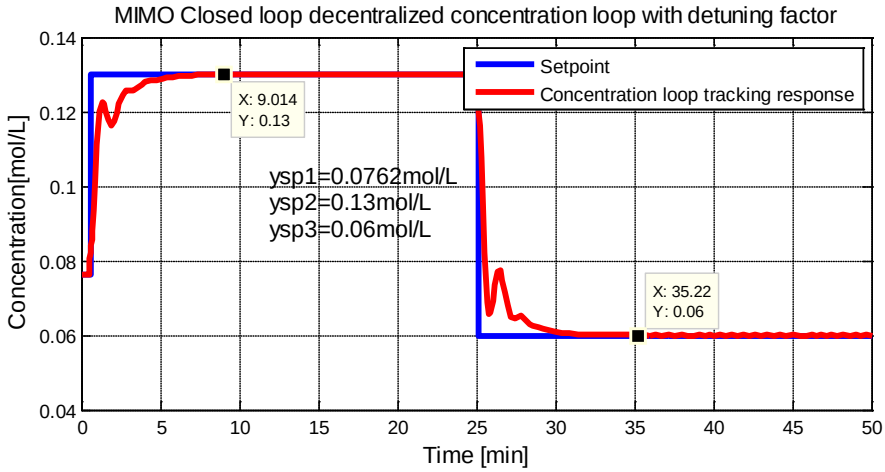

Figure 5.37: Concentration closed response using the detuning factor

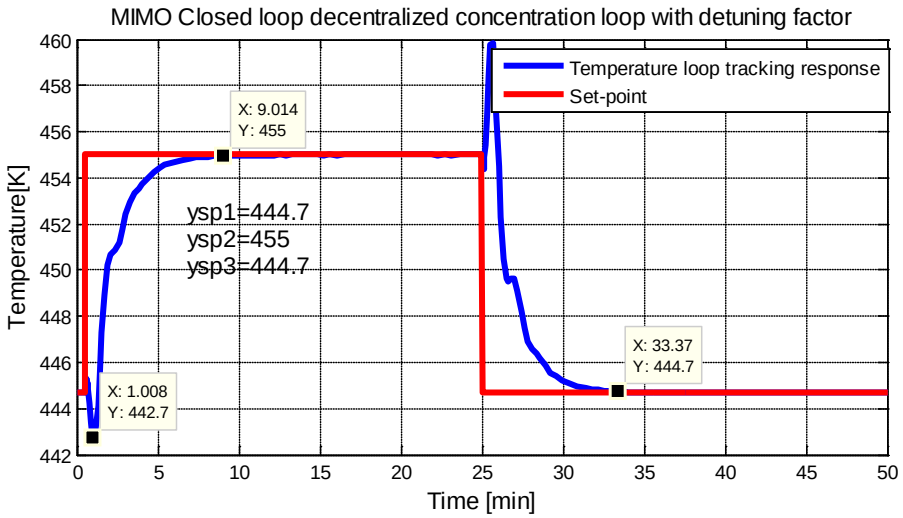

Figure 5.38: Temperature loop closed response using the detuning factor

Figures 5.37 and 5.38 are the responses of the concentration control loop and the temperature control loop respectively for the MIMO system with independent detuning factors. The set-point tracking response capabilities for both the outputs are achieved though the responses are sluggish. It takes the concentration loop to reach the steady state value of 0.13mol/l in 9 minutes whereas the temperature loop's steady state value of 455K is reached after the same time of. 9 minutes This is a significant improvement when compared to the responses without detuning factors presented in the preceding section.

5.6.1 Comparison of closed loop performance between decentralized control with and without detuning factors

A comparison is made between the responses of the decentralized control under detuning and without detuning factors in terms of performance specifications in order to see which system performs better and why. Table 5.3 gives the various specifications for both the concentration and the temperature responses

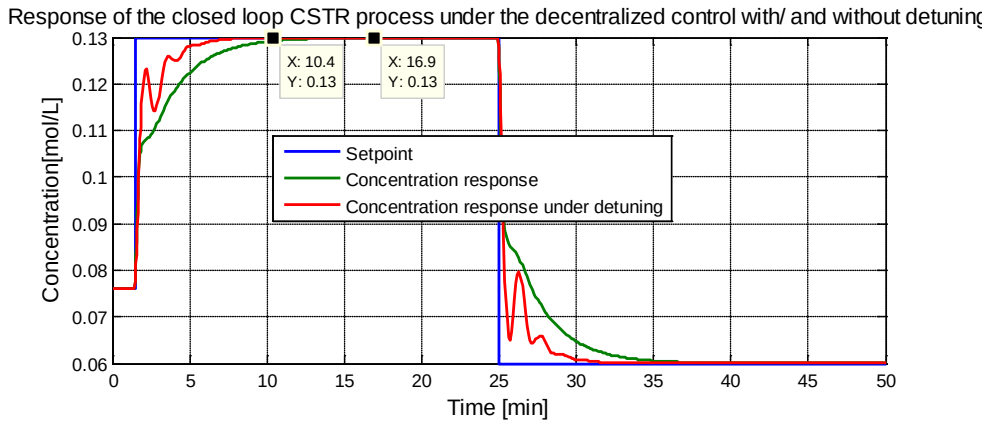

Figure 5.39: Comparison for the concentration response without and with the detuning factor

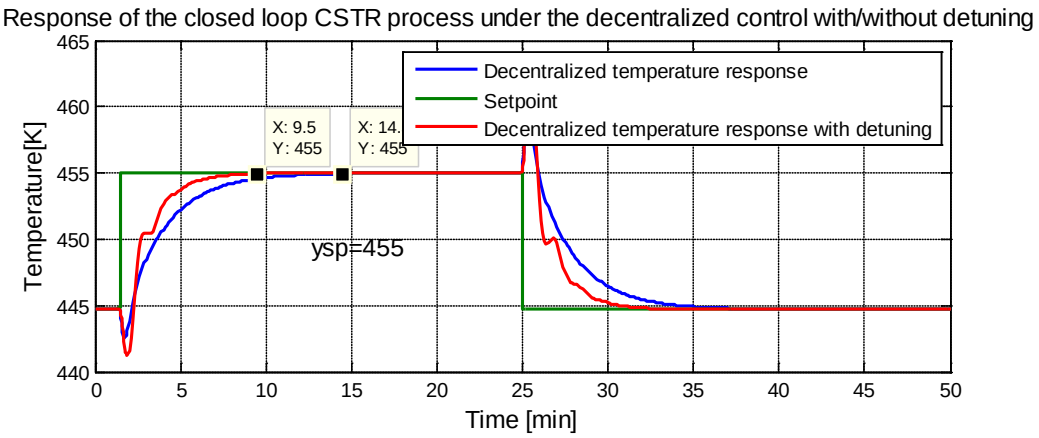

Figure 5.40: Comparison for the temperature response without and with the detuning factor

Table 5.2: Performance indices for the concentration and the temperature with and without detuning

Approach	**Set-point value**	Settling time $t_s(\min)$	Peak over shoot $M_P(\%)$	Peak time $t_p(\min)$	Steady state error $e_{ss}(\%)$
Decentralized control	0.13mol/l	15.4	0	15.4	0
	455K	9.0	0	9.0	0
Decentralized control with detuning factor	0.13mol/l	13	0	13	0
	455K	8.0	0	8.0	0

The investigation is done for the concentration tracking response to step changes in set-point from 0.0762mol/l then to $0.13\text{mol/l},$ then to 0.06mol/l, as illustrated in Figure 5.39. From the Figure 5.39, it can be seen that the concentration performance with detuning factor outperforms the one without detuning when a comparison is made in terms of speed of response and the time it takes to reach the steady state value. However the response is still sluggish. Similar analysis is done for the temperature control response for to step changes in set-point from 444.77K to 455K and then to 444.77K and it is seen from Figure 5.40, that the temperature response under detuned decentralized control is much faster in terms of the speed of response to reach the steady state. It is therefore concluded that the detuning factors incorporated have enhanced the performance of the system.

Responses to various magnitudes of disturbances are also investigated for the schemes developed with the help of the detuning factors and the performances of the various loops are as illustrated in the following.

5.6.2 Investigation on the disturbance interference in the decentralized system with detuning factor over the concentration output y_1

This investigation is done to show that the influence of the interaction is reduced if the detuning factor is used. This is checked for different varying magnitudes of random disturbances (white noise) added to the output signal y_1 on the main concentration loop. The responses are represented in Figures 5.41 to 5.44 are responses of the concentration output signal y_1 .when the magnitude of the disturbance on y_1 is varied in the range of $\pm 1e^{-3}$ moles/litre to 0.04 moles/litre. As can be seen in the responses, the effect of noise is drastically reduced. Set-point tracking controlled is achieved.

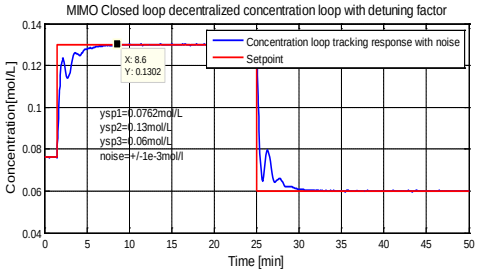

Figure 5.41: Response under $\pm 1e^{-3}\text{mol/l}$ noise

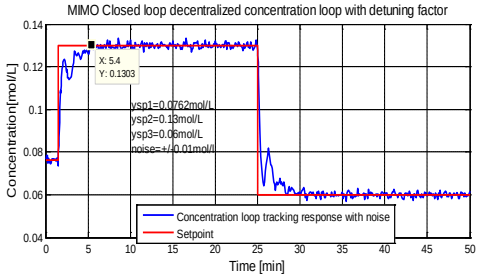

Figure 5.43: Response under $\pm 0.01\text{mol/l}$ noise

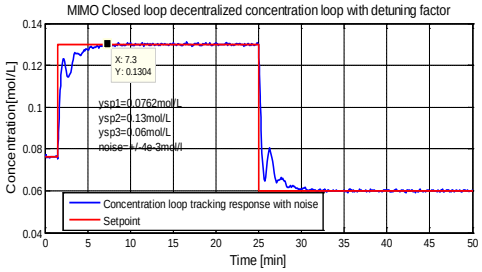

Figure 5.42: Response under $\pm 4e^{-3}\text{mol/l}$ noise

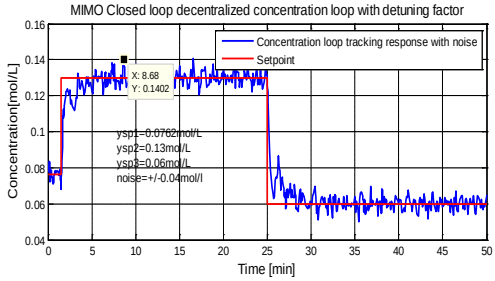

Figure 5.44: Response under $\pm 0.04\text{mol/l}$ noise

Figures 5.45 to 5.48 are responses of the temperature output signal y_2 .when the magnitude of the disturbance on y_1 is varied in the range of $\pm 1e^{-3}$ moles/litre to ± 0.04 moles/litre. This is to show that the influence of the interactions is significantly reduced as a result of the detuning factor used. As can be seen in the responses, the effect of noise is drastically reduced. Smooth temperature set-point tracking controlled is achieved.

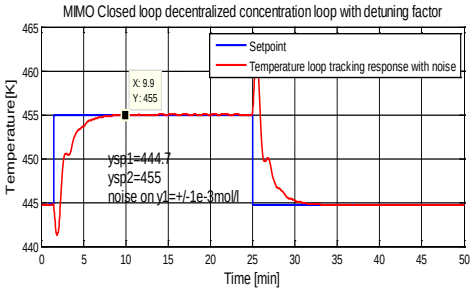

Figure 5.45: Response under $\pm 0.01 mol/l$ noise on y_1

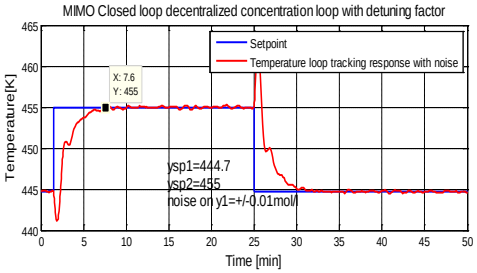

Figure 5.47: Response under $\pm 0.01 mol/l$ noise on y_1

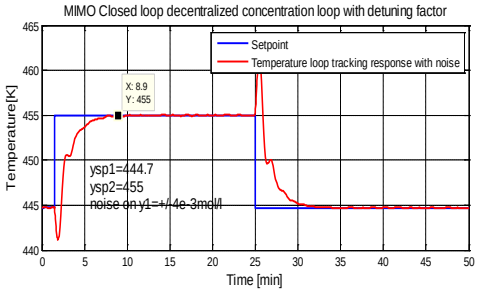

Figure 5.46: Response under $\pm 0.04 mol/l$ noise on y_1

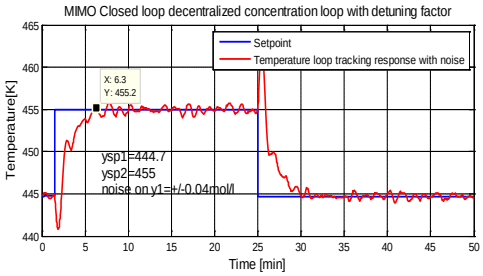

Figure 5.48: Response under $\pm 0.04 mol/l$ noise on y_1

Next, the influence of disturbances on y_2 is investigated.

5.6.3 Investigation on the disturbance interference in the decentralized system with detuning factor over the temperature output y_2

Figures 5.49 to 5.52 are responses of the temperature output signal y_2 .when the magnitude of the disturbance on y_2 is varied in the range of $\pm 4K$ to $\pm 20K$. Set-point tracking control is achieved but the responses are sluggish. Similarly, the magnitude of the disturbance has significant effect on the shape of response.

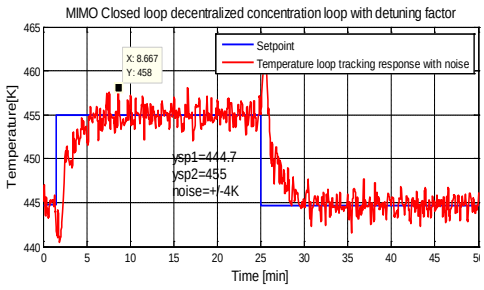

Figure 5.49: Response under $\pm 4K$ noise

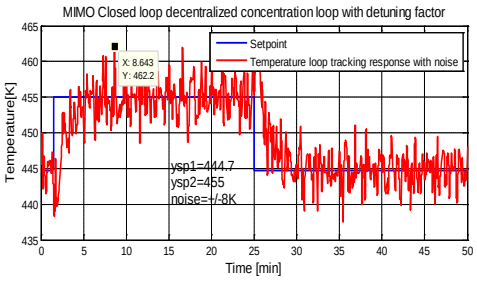

Figure 5.50: Response under $\pm 8K$ noise

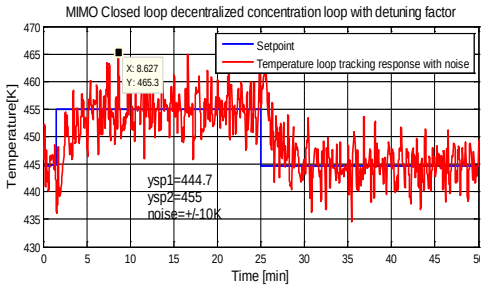

Figure 5.51: Response under ±10K noise

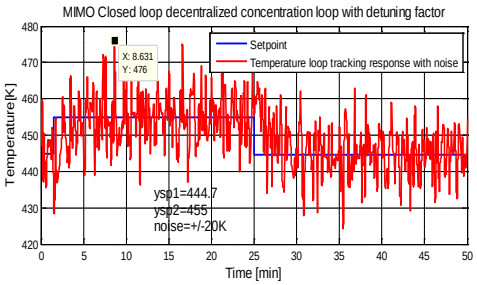

Figure 5.52: Response under ±20K noise

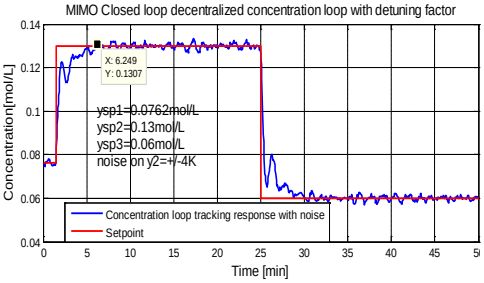

Figure 5.53: Response under ±10K noise

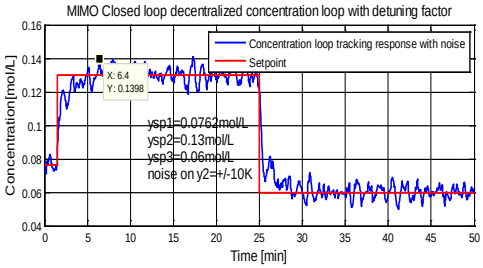

Figure 5.54: Response under ±20K noise

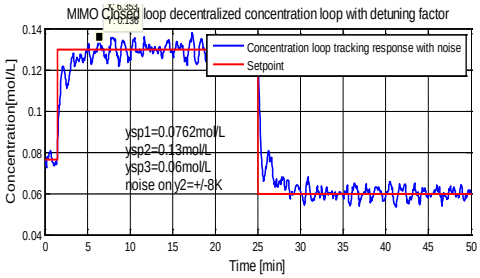

Figure 5.55: Response under ±10K noise

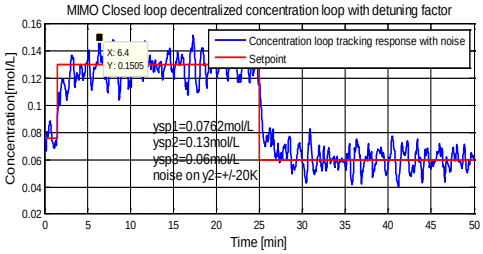

Figure 5.56: Response under ±20K noise

Similarly, Figures 5.53-5.56 are responses of the concentration loop to see the influence of the interactions as a result of disturbances on the temperature loop. From the figures, it is noted that the influence is not much if the detuning factor is used. Good concentration set-point tracking is still achieved.

Appendix E1 presents the file that simulates the diagonal decentralized closed loop system response for various magnitudes of the set-point step changes, as well as disturbances at the output (y1) and the interaction junction (u1). The Simulink closed loop models to be simulated are *diag_decent_temp'* and *'decentconc_2015'* These are provided in appendix F**.** Appendix E2 provides the file that simulates the decentralized control response of the closed loop MIMO CSTR with and without detuning, for various magnitudes of set-point step changes as well as disturbances. The Simulink closed loop model to be simulated is *decent1_2015* The model is provided in appendix F**.**

5.7 Discussion of the Results

Simulation studies are used to verify the performance of the designed decentralized controllers. First the performances with independent designed diagonal controllers are tested as a first step in the implementation of the closed loop control of the $2x2$ MIMO CSTR process by ignoring the off-diagonal elements. The design procedure adopted is by using IMC-based PID feedback control Good set-point tracking capabilities for the proposed decentralized controller is achieved for the outputs (concentration and temperature). Lastly, the closed loop system with the off-diagonal elements is considered using the designed decentralized controllers used so as to see the effects of the interactions. The set-point tracking response capabilities for both outputs are achieved though the responses obtained are sluggish.

Investigations on the influences over the process output step response for various magnitudes of disturbances are also investigated by varying magnitudes of random disturbances (white noise) added to the outputs Good tracking control is still achieved though, as the magnitude of the disturbance is increased, the response becomes noisy. Similarly, the disturbance influences due to intearctions on the loops are also investigated and it is found that. the magnitude of the effect is smaller between the loops implying that the designed decentralized systems is good even in the presence of the random disturbances. Decentrarized control scheme can not eliminate completely the efeects of the loop interactions. The results of simulation shows that the magnitude of the disturbance is important for smooth set-point tracking. Next the detunining factors are considered to better the performances of the designed decentralized control schemes. A detuning factor serves as a compromise between performance and stability of the process. It is found by comparison that there is a significant improvement in the performances without detuning factors in the designed decentralized control system. The investigation is also done for responses to various magnitudes of disturbances. This investigation is done to show that the influence of the interaction is reduced if the detuning factor is used and, it is found the effect of noise is drastically reduced. Good concentration set-point tracking is still achieved.

5.8 Concluding remarks on the developed decentralized design method.

The design and implementation of decentralized PID controller for the MIMO CSTR system are performed. For the design of the controllers, pairing among the input-output variables is done using the RGA analysis. The results of this analysis required that the concentration be controlled by the coolant flow rate while the temperature to be controlled by the feed flow rate for minimum interaction and for optimal tracking

response. Then two SISO PID controllers are designed directly for the diagonal transfer functions of the process model and independently using internal model control (IMC) principles to tune the diagonal loops for tracking control of the output variables namely, concentration and temperature. After the independent tuning of the individual loops, a detuning factor for each individual loop is proposed to compensate for the off-diagonal matrix transfer function interactions Simulation results demonstrate the effectiveness of the proposed control law in achieving tracking control with good disturbance rejection capabilities.

The next method developed for the control of the MIMO CSTR process is the input/output feedback nonlinear linearizing controller design method as presented in Chapter six

CHAPTER SIX
INPUT/OUTPUT FEEDBACK LINEARIZATION CONTROLLER DESIGN FOR THE CSTR PROCESS

6.1 Introduction

This chapter discusses the input/output feedback linearization controller design strategy applicable to the nonlinear Multi-Input Multi-Output (MIMO) control of the reactor temperature and concentration in a CSTR process. Input/output Feedback linearization technique is a control design methodology that uses feedback signal to cancel the inherent nonlinear dynamics in a system and to create a linear differential relation between the output and a newly defined synthetic input. The most fundamental property of a linear system from the control point of view is the validity of the principle of superposition. The outputs of such systems are proportional to the inputs. Systems with this property are governed by linear differential equations. It is on the account of the superposition property that it can be guaranteed that the linear system designed to perform satisfactorily when excited by a standard test signal, will exhibit satisfactory output behaviour under any operating condition. This is not true with the nonlinear systems because they do not obey the superposition principle. The nonlinearity applies to more real-world systems, because all real control systems are nonlinear. It is on this context that many different approaches have been proposed for the analysis and control design for nonlinear systems. One of these approaches is the feedback linearization technique.

The chapter is structured in the following sections: In section 6.2 the preliminary theory of the feedback linearization method is presented. Section 6.3 presents the details of the design of the input/output feedback linearization control schemes for the linearized $2x2$ MIMO CSTR process. Section 6.4 presents the linear PI control design strategy applied to aid the input/output feedback linearization control schemes.. Section 6.5 presents the simulation of the closed loop linearized system in the Matlab/Simulink environment in terms of the performance specifications. Section 6.6 discusses the obtained results. Section 6.7, a comparison with the other conventional methods developed in Chapters 4 and 5 for the control of the nonlinear MIMO CSTR process is made and finally section 6.8 concludes the chapter.

6.2 Feedback linearization control schemes

There is no general technique that can be used for the design of a nonlinear controller. However there are many alternatives and complementary techniques, that

can be applied to the solutions of certain classes of nonlinear control problems. In this section, feedback linearization nonlinear control design technique is developed.

Feedback linearization is a strategy used for nonlinear control design that algebraically converts the nonlinear system characteristics to full or partial linear systems in order for linear control methods to be used. The approach is quite different from the conventional (Jacobian) linearization technique because the feedback linearization is realized using exact state conversion and feedback, instead of the linear approximations of the characteristics. The conventional concept of linearization implies the approximation of the nonlinear system using a linear counterpart in the neighbourhood of a steady state operating point. In comparison to the conventional method, the novelty of this method is that linearization is valid for larger operating space rather than single operating point. There are basically two distinct strategies for of feedback linearization can be identified. These are: input/output feedback linearization and I/O feedback linearization (Hedrick and Girard, 2005). In both cases the idea is to find feedback and coordinate transformations in order that the resulting system becomes linear in some way.

The I/O feedback linearization technique is used in this work, The I/O feedback linearization technique's objective is to find a linear input-output behaviour of the resulting system so that any linear control methodology may be applied for the controller design. Equations (3.12) and (3.13) presented earlier may be re-written as follows:

$$\dot{x} = f(x) + g(x)u \quad u = \begin{bmatrix} q \\ q_c \end{bmatrix}$$
$$y = h(x) \qquad (6.1)$$
$$x(0) = x_o$$

The case considered is for a system where the number of inputs variables is the same as the number of output variables, therefore dimension vectors $l = m$ where: x is the n-vector of the state variables; u is the m-vector of the manipulated input variables; y is the m-vector of the controlled output variables; $f(x)$ is the n-vector of the nonlinear functions; $g(x)$ is the nxm-matrix of the nonlinear functions; $h(x)$ is the l-vector of the nonlinear functions and $x(0) = x_o$ is the vector of initial state. The model of Equation (6.1) is called the control *affine*, since the control input signal u appears linearly in the state space equation. This model can be modified as much as required in order to satisfy more complex nonlinear processes encountered like those with disturbances and/or time delays.

6.3 I/O Feedback linearization control design technique

Input/output controller design by feedback linearization is a control technique where the controlled output $y = h(x)$ of the dynamic system is differentiated until the physical input u appears in the r^{th} derivative of the controlled output (Slotine and Li, 1991). A key concept of the feedback linearization theory for nonlinear control affine systems is the relative degree feature r. If r, is less than n, then there will be internal dynamics in the system. If, $r = n$, then Input/output and Input/State linearization are the same. The relative degree r is the number of times the output y has to be differentiated in order to have at least one component of the control vector in it. Consider a scalar function h and a vector field f. The Lie derivative of h with respect to f denoted by $L_f h$ is given by

$L_f h(x) = \frac{\partial h(x)}{\partial x} f(x)$ and the Lie derivative of h with respect to g denoted by $L_g h$ is given by $L_g h(x) = \frac{\partial h(x)}{\partial x} g(x)$. The idea of using the Lie derivative formulation is to determine a control methodology that renders a linear deferential equation from the virtual input v to the output y. This concept of feedback linearization theory can also be applied for MIMO systems. By diffentiating the nonlinear Equation of (6.1), for every component of the output vector, the following is achieved.

$$\dot{y}_i = L_f h_i(x) + \sum_{j=1}^{m} (L_{gj} h_i) u_j, i = 1, ..., i \tag{6.2}$$

The key point is that if, $L_{gj} L_f^{r_i - 1} h_i(x) = 0$ for all j, then the input vector u does not appear explicitly in Equation (6.2) and further differentiation is continued until, for some integer $r \le n$

$$y_i^{(r_i)} = L_f{}^{r_i} h_i(x) + \sum_{j=1}^{m} L_{gj} L_f{}^{(r_i - 1)} h_i(x) u_j, i = 1, ..., l \tag{6.3}$$

such that $L_{gj} L_f{}^{(r_i - 1)} h_i(x) \neq 0$, for at least one parameter j in the neighbourhood of the steady state point x_o. The procedure is repeated for every output y_i and results in a number of l equations expressed in Equation (6.4):

$$\begin{bmatrix} y_1^{(r_1)} \\ . \\ y_m^{(r_i)} \end{bmatrix} = \begin{bmatrix} L_f^{r_1} h_1(x) \\ . \\ L_f^{r_m} h_l(x) \end{bmatrix} + B(x) \begin{bmatrix} u_1 \\ . \\ u_m \end{bmatrix} \tag{6.4}$$

Where $B(x)$ is a lxm matrix expressed as:

$$B(x) = \begin{bmatrix} L_{g1}L_f^{r_1-1}h_1 & . & . & L_{gm}L_f^{r_1-1}h_1 \\ . & . & . & . \\ . & . & . & . \\ L_{gl}L_f^{r_l-1}h_l & . & . & L_{gm}L_f^{r_l-1}h_l \end{bmatrix} \quad (6.5)$$

The $B(x)$ matrix realized is known as a decoupling matrix for the multi-input multi-output system. When this matrix is non-singular then the vector u of the control signal can be expressed in Equation (6.5):

$$u = -B^{-1}(x)\begin{bmatrix} L_f^{r_1}h_1(x) \\ . \\ . \\ L_f^{r_l}h_l(x) \end{bmatrix} + B^{-1}(x)\begin{bmatrix} v_1 \\ . \\ . \\ v_m \end{bmatrix} \quad (6.6)$$

The vector $\begin{bmatrix} v_1 & . & . & v_m \end{bmatrix}^T$ is the vector for the synthetic (virtual) set of inputs or the synthetic controls that the control designer defines. The characteristics of the new controls are then obtained by substitution of Equation (6.6) in Equation (6.4) to obtain:

$$\begin{bmatrix} y_1^{(r_1)} \\ . \\ . \\ y_m^{(r_m)} \end{bmatrix} = \begin{bmatrix} v_1 \\ . \\ . \\ v_m \end{bmatrix} \quad (6.7)$$

The transformed system of Equation (6.7) is called a decoupling control law and shows a linear MIMO decoupled relationship. As can be seen, the transformation leads to a linearized system in the form of integrators. Thus, the system in Equation (6.4) possesses relative degrees $(r_1, r_2, ...r_m)$ at x_o and the scalar value r which is equal to $r_1 + r_2 + ... + r_m$ is termed as the total relative degree of the system at x_o. The order of relative degree for the system allows for the verification whether a nonlinear system can be input/output linearized (Isidori, A., 1991; Slotine and Hedrick, 1993). After performing the input/output linearization, the characteristics of the nonlinear system is split into external input/output portion and an internal (unobservable) portion as demonstrated by (Slotine and Li, 1991). Because the external portion comprises of a linear relation between the output y and the synthetic input v, any linear controller design methods can be used to design a controller with the help of control implemented through the synthetic input v so that the output tracks any given set point trajectory assuming the internal dynamics remain bounded). The control law involving tracking of a desired output is then obtained in the form:

$$v = y_d - k_o e - k_1 \dot{e} - ..... + k_{n-1} e^{(n-1)} \quad (6.8)$$

Where, the reference or desired output signal is y_d and the tracking error is $e(t) = y(t) - y_d(t)$. The exponentially convergent tracking error is then achieved. The k_i constants are chosen so that the roots of the polynomial $s^n + k_{n-1}s^{n-1} + ... + k_o$ are placed in the left hand side of the complex plane.

6.4 I/Output Feedback linearization control design for the CSTR process

The block diagram of the arrangement for the considered case of the CSTR process is illustrated in Figure 6.1.

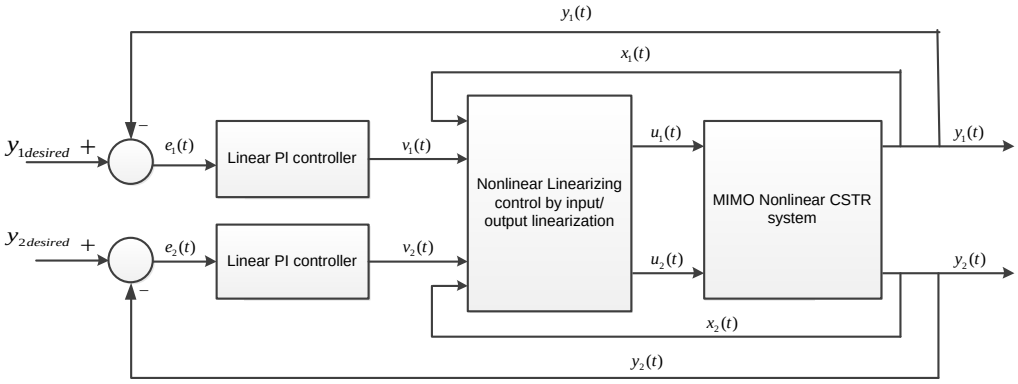

Figure 6.1: Input-output feedback linearization control structure

As illustrated in Figure 6.1, the system comprises of three parts namely, linear controllers (two), the nonlinear linearizing controller using input/output linearization methodology that maps the nonlinear system to a linear and decoupled system and lastly the nonlinear plant model. In order to design of the controllers, v_1 and v_2 are chosen in a way so that a stable MIMO closed loop system results and the desired set-points are achieved. Two different controllers, one for each output are then designed.

Application of the described above input/output linearization and linear controller design for the considered CSTR is described below. Substitution of q with u_1 and q_c with u_2 also C_{AO} with x_1 and T with x_2, the CSTR model Equations, (3.12) and (3.13) can be modified to the standard state space affine form as:

$$\dot{x}_1 = \frac{u_1}{V}(C_{AO} - x_1) - k_o x_1 \exp(-a_1 / x_2) \tag{6.9}$$

$$\dot{x}_2 = \frac{u_1}{V}(T_O - x_2) - a_2 x_1 \exp(-a_1 / x_2) + a_3 u_2 (1 - \exp(-a_4 / x_2)(T_{CO} - x_2) \tag{6.10}$$

Where, $a_1 = E/R$, $a_2 = \frac{(-\Delta H)k_o}{\rho C_p}$, $a_3 = \frac{\rho_c C_{pc}}{\rho C_p V}$, and $a_4 = \frac{-hA}{\rho c_p}$, and $x = [x_1 \ x_2]^T = [C_A \ T]^T$ denotes the state vector as well as the output vector while $u = [u_1 \ u_2]^T = [q \ q_c]^T$ denotes the input vector. Equations (6.9) and (6.10) can be written in the standard affine form as:

$$\begin{aligned}
\dot{x}_1 &= f_1(x_1, x_2) + g_{11}(x_1, x_2)u_1 \\
\dot{x}_2 &= f_2(x_1, x_2) + g_{21}(x_1, x_2)u_1 + g_{22}(x_1, x_2)\bar{u}_2 \\
y_1 &= x_1 = h_1(x_1) \\
y_2 &= x_2 = h_2(x_2)
\end{aligned} \tag{6.11}$$

Where,

$$\begin{aligned}
f_1(x_1, x_2) &= -k_o x_1 \exp(-a_1 / x_2) \\
f_2(x_1, x_2) &= a_2 x_1 \exp(-a_1 / x_2) \\
g_{11}(x) &= \frac{1}{V}(C_{AO} - x_1) \\
g_{21}(x) &= \frac{1}{V}(T_O - x_2) \\
g_{22}(x) &= a_3(T_{CO} - x_2) \\
\bar{u}_2 &= u_2(1 - \exp(-a_4 / u_2))
\end{aligned} \tag{6.12}$$

Here, $\bar{u}_2 = u_2(1 - \exp(-a_4 / u_2))$ from which the control input can be deduced as:

$$\begin{aligned}
\ln \bar{u}_2 &= \ln u_2 - \ln u_2 + a_4 / u_2) \\
\ln \bar{u}_2 &= a_4 / u_2 \\
u_2 &= a_4 / \ln \bar{u}_2
\end{aligned} \tag{6.13}$$

The output vector is $y = h(x) = [x_1 \ x_2]^T = [C_A \ T]^T$ and for the application of the input/output feedback linearization technique, this output must be differentiated several for the input parameters to appear in the outputs or their derivatives. Thus,

$L_f h(x) = \frac{\partial h(x)}{\partial (x)} f(x)$ and $L_g h(x) = \frac{\partial h(x)}{\partial (x)} g(x)$, from which,

$$
\begin{aligned}
L_{f1}h_1(x_1) &= \frac{\partial h_1(x_1)}{\partial(x_1)} f_1(x_1,x_2) = f_1(x_1,x_2)\\
L_{f2}h_1(x_2) &= \frac{\partial h_1(x_2)}{\partial(x_2)} f_2(x_1,x_2) = f_2(x_1,x_2)\\
L_{g11}h_1(x_1) &= \frac{\partial h_1(x_1)}{\partial(x_1)} g_{11}(x_1,x_2) = g_{11}(x_1,x_2)\\
L_{g12}h_1(x_1) &= \frac{\partial h_1(x_1)}{\partial(x_1)} g_{12}(x_1,x_2) = g_{12}(x_1,x_2)\\
L_{g21}h_2(x_2) &= \frac{\partial h_2(x_2)}{\partial(x_2)} g_{21}(x_1,x_2) = g_{21}(x_1,x_2)\\
L_{g22}h_2(x_2) &= \frac{\partial h_1(x_2)}{\partial(x_2)} g_{22}(x_1,x_2) = g_{22}(x_1,x_2)
\end{aligned}
\tag{6.14}
$$

Then,

$$
\begin{bmatrix}\dot{y}_1\\ y_2\end{bmatrix} = \begin{bmatrix}\dot{x}_1\\ \dot{x}_2\end{bmatrix} = \begin{bmatrix}L_{f1}h_1(x_1)\\ L_{f2}h_2(x_2)\end{bmatrix} + \begin{bmatrix}L_{g11}h_1(x_1) & L_{g12}h_1(x_1)\\ L_{g21}h_1(x_1) & L_{g22}h_1(x_1)\end{bmatrix}\begin{bmatrix}u_1\\ \bar{u}_2\end{bmatrix}
$$

$$
\begin{bmatrix}\dot{y}_1\\ y_2\end{bmatrix} = \begin{bmatrix}f_1(x_1,x_2)\\ f_2(x_1,x_2)\end{bmatrix} + \begin{bmatrix}g_{11}(x_1,x_2) & g_{12}(x_1,x_2)\\ g_{21}(x_1,x_2) & g_{22}(x_1,x_2)\end{bmatrix}\begin{bmatrix}u_1\\ \bar{u}_2\end{bmatrix} \tag{6.15}
$$

This implies that:

$$
\begin{aligned}
\dot{y}_1 &= \dot{x}_1 = f_1(x_1,x_2) + g_{11}u_1 = v_1;\ r_1 = 1\\
\dot{y}_2 &= \dot{x}_1 = f_2(x_1,x_2) + g_{21}u_1 + g\bar{u}_{22} = v_2;\ r_2 = 1
\end{aligned}
\tag{6.16}
$$

Thus, the total degree of this system is 2 and the following are obtained.

$$
B(x) = \begin{bmatrix}g_{11}(x_1,x_2) & g_{12}(x_1,x_2)\\ g_{21}(x_1,x_2) & g_{21}(x_1,x_2)\end{bmatrix} = \begin{bmatrix}\dfrac{(C_{AO}-x_1)}{V} & 0\\ \dfrac{(T_O-x_2)}{V} & a_3(T_{CO}-x_2)\end{bmatrix}, \text{ and,}
$$

$$
\begin{bmatrix}\dot{y}_1\\ \dot{y}_2\end{bmatrix} = \begin{bmatrix}-k_o x_1 \exp(-a_1/x_2)\\ -a_2 x_1 \exp(-a_1/x_2)\end{bmatrix} + \begin{bmatrix}\dfrac{C_{AO}-x_1}{V} & 0\\ \dfrac{T_O-x_2}{V} & a_3(T_{CO}-x_2)\end{bmatrix}\begin{bmatrix}u_1\\ \bar{u}_2\end{bmatrix} = \begin{bmatrix}v_1\\ v_2\end{bmatrix} \tag{6.17}
$$

From Equation (6.17) it implies that the two nonlinear linearizing controllers resulting from the input-output linearization are:

$$
u_1 = \frac{v_1(x) - L_{f1}(x_1)}{L_{g11}(x_1)} = \frac{v_1(x) - \left[-k_o x_1 \exp(-a_1/x_2)\right]}{\left[(C_{AO}-x_1)/V\right]} \tag{6.18}
$$

and,

$$
\begin{aligned}
\bar{u}_2 &= \frac{v_2 - L_{f2}(x_2) - L_{g21}(x_2)u_1}{L_{g22}(x_2)}\\
&= \frac{v_2 - \left[-a_2 x_1 \exp(-a_1/x_2)\right] - \left[(T_O-x_2)/V\right]u_1}{\left[a_3(T_{CO}-x_2)\right]};\ u_2 = a_4/\ln\bar{u}_2
\end{aligned}
\tag{6.19}
$$

Equations (6.18) and (6.19) represent the components of the vector of the nonlinear control sent to the CSTR process. Additional linear controllers are then necessary to be designed. The reason is that the nonlinear control depends on the parameters of the process, which normally are non-stationary; also various disturbances can influence the process. These are two causes that can make the system non stable and the linearization not fulfilled. To overcome such possibility an additional linear control is needed to make the closed loop system stable and to improve its performance.

6.5 Linear PI controller design

The linear controller part is then designed. The procedure for the design by pole placement used is as summarised in the following. On the basis of Equation (6.17) it can then be written as:

$$\begin{aligned} \dot{y}_1 &= v_1 \rightarrow sY_1(s) = V_1(s) \\ \dot{y}_2 &= v_2 \rightarrow sY_2(s) = V_2(s) \end{aligned} \tag{6.20}$$

Then if the linear controls v_1 and v_2 are determined using PI controllers, the equations governing them would be:

$$\begin{aligned} v_1 &= k_{11}(y_{1sp} - y_1) + k_{12}\int_0^t (y_{1sp} - y_1)dt \\ v_2 &= k_{21}(y_{2sp} - y_2) + k_{22}\int_0^t (y_{2sp} - y_2)dt \end{aligned} \tag{6.21}$$

Assuming that the desired output's rate of change is specified as;

$$\begin{bmatrix} \dot{y}_{1sp} \\ \dot{y}_{2sp} \end{bmatrix} = \begin{bmatrix} v_1 \\ v_2 \end{bmatrix} = \begin{bmatrix} k_{11}(y_{1sp1} - y_1) + k_{12}\int_0^t (y_{1sp} - y_1)dt \\ k_{21}(y_{2sp} - y_2) + k_{22}\int_0^t (y_{2sp} - y_2)dt \end{bmatrix} \tag{6.22}$$

where k_{11}, k_{12}, k_{21} and k_{22} are the linear PI controller tuning parameters. The goal is to make $\begin{bmatrix} \dot{y}_1 \\ \dot{y}_2 \end{bmatrix} = \begin{bmatrix} \dot{y}_{1sp} \\ \dot{y}_{2sp} \end{bmatrix}$ by choosing v appropriately, then the input-output linearized closed loop system results when:

$$\begin{bmatrix} \dot{y}_1 \\ \dot{y}_2 \end{bmatrix} = \begin{bmatrix} k_{11}(y_{sp1} - y_1) + k_{12}\int_0^t (y_{sp1} - y_1)d\tau \\ k_{21}(y_{sp2} - y_2) + k_{22}\int_0^t (y_{sp2} - y_2)d\tau \end{bmatrix} \tag{6.23}$$

The linearized system is represented by the following transfer functions:

$$G_{C1}(s)=\frac{Y_1(s)}{V_1(s)}=\frac{1}{s}$$
$$G_{C2}(s)=\frac{Y_2(s)}{V_2(s)}=\frac{1}{s} \quad (6.24)$$

Equation (6.24) is applied for the closed loop transfer functions derivation as:

$$G_{C1CL}(s)=\frac{Y_1(s)}{Y_{1sp}(s)}$$
$$G_{C2CL}(s)=\frac{Y_2(s)}{Y_{2sp}(s)} \quad (6.25)$$

Where G_{C1CL} and G_{C2CL} are the individual closed loop transfer functions. These transfer functions are derived for the considered cases as follows:

6.5.1 Linear PI controller design for the concentration loop

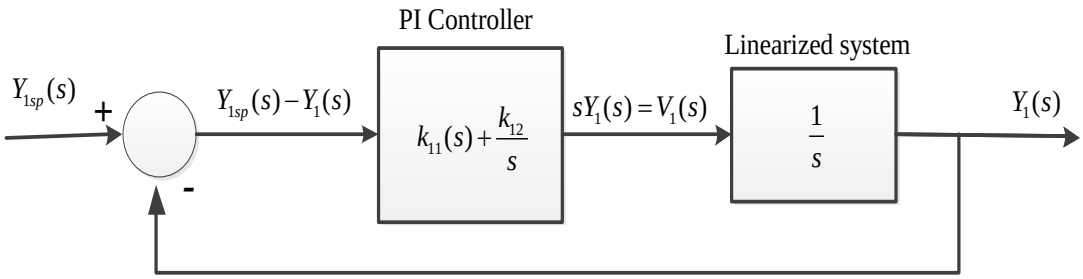

Figure 6.2: Desired closed loop Input-output feedback linearization for concentration

First, the concentration loop is considered. Figure 6.2 is the desired closed loop Input-output feedback linearized control structure for the concentration control, where the linearized part transfer function is given by the Equation $\frac{Y_1(s)}{V_1(s)}=\frac{1}{s}$; hence with the help of Figure 6.2, the derived closed loop transfer function is.

$$\frac{Y_1(s)}{Y_{1sp}(s)}=\frac{(k_{11}+k_{12}/s)\,1/s}{1+(k_{11}+k_{12}/s)\,1/s}=\frac{\frac{k_{11}s+k_{12}}{s^2}}{\frac{s^2+k_{11}s+k_{12}}{s^2}}=\frac{k_{11}s+k_{12}}{s^2+k_{11}s+k_{12}}$$

This closed loop transfer function is then presented in the form:

$$\frac{Y_1(s)}{Y_{1sp}(s)} = \frac{k_{11}s + k_{12}}{s^2 + k_{11}s + k_{12}}$$

$$= \frac{2\tau_1\zeta_1 s + 1}{\tau_1{}^2 s^2 + \tau_1\zeta_1 s + 1} \quad (6.26)$$

where, $\tau_1 = \frac{1}{\sqrt{k_{12}}}$, $\zeta_1 = \frac{k_{11}}{2\sqrt{k_{12}}}$ or, $k_{11} = \frac{2\zeta_1}{\tau_1}$, $k_{12} = \frac{1}{\tau_1{}^2}$

τ_1, τ_2, ζ_1 and ζ_2 are the time constants and damping parameters that determine the shape of the step responses for concentration and temperature respectively. If the roots of the characteristic equation: $s^2 + k_{11}s + k_{12}$ are appropriately selected, then asymptotic tracking of the desired closed loop response can be realised. According to Slotine and Li, (1990); Henson and Seborg, (1991) the controller tuning parameters k_{11}, and k_{12} may be selected to provide the required closed loop response. To guarantee smaller overshoots, the conditions $k_{11}{}^2 \geq 4k_{12}$ .and $k_{21}{}^2 \geq 4k_{22}$ should be fulfilled. The problem is then to find the appropriate parameters k_{11}, and k_{12}. According to Wilson (2014), the algorithm for appropriate values of k_{11}, and k_{12} is as follows:

1. Choose the appropriate values of the damping factors. For tight control, with little overshoot, $\zeta_1 \approx 3$ or higher.is recommended.
2. Specify the time scale by choosing appropriate values of time constant τ_1. Often it is convenient to specify the rise time.
3. From the specified values of ζ_1 and τ_1, the scalar values of parameters are evaluated for each output. From Equation (6.26) therefore,

$$k_{11}{}^{2,} \geq 4k_{12} \rightarrow (\frac{2\zeta_1}{\tau_1})^2 \geq \frac{1}{\zeta_1^2}$$

$$(\frac{2\zeta_1}{\tau_1})^2 - \frac{1}{\zeta_1^2} \geq 0 \rightarrow 2\zeta_1^2 - 1 \geq 0 \quad (6.27)$$

$$\zeta_1 \geq \sqrt{\frac{1}{2}} \rightarrow \zeta_1 \geq 0.707 \text{ is selected}$$

From Equation (6.26), assuming that the specific transient controller requirements for the damping factor should be 1.2 and the time constant to be 0.3 min, as per Equation (6.27), the controller tuning parameters for the concentration loop are calculated as follows:

$$k_{11} = \frac{2\zeta_1}{\tau_1} = \frac{2(1.2)}{0.3} = 8$$
$$k_{12} = \frac{1}{\tau_1^2} = \frac{1}{(0.3)^2} = 11.11 \quad (6.28)$$

Thus the PI controller tuning parameters designed as per Equations (6.27) and (6.28) are implemented for the concentration control loop: The designed controlled system's performance is discussed at the end of this chapter.

6.5.2 Linear PI controller design for the temperature loop

Similarly, the temperature closed loop is considered. Figure 6.3 is the desired closed loop I/O feedback linearization control structure for the temperature control, where the linearized part transfer function is given by the Equation $\frac{Y_2(s)}{V_2(s)} = \frac{1}{s}$;

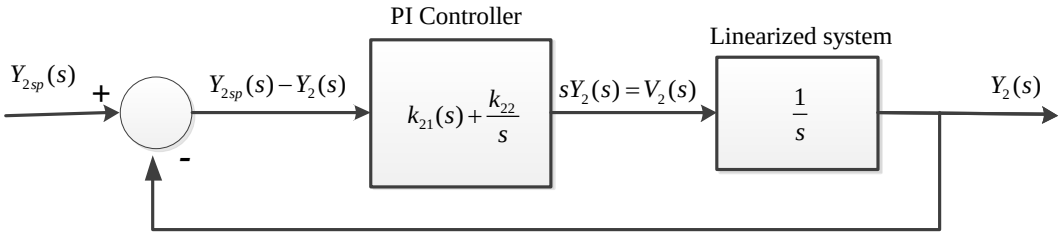

Figure 6.3: Desired closed loop Input-output feedback linearization for temperature

Hence with the help of Figure 6.3, the transfer function of the closed loop is derived.

$$\frac{Y_2(s)}{Y_{2sp}(s)} = \frac{(k_{21} + k_{22}/s)\,1/s}{1 + (k_{21} + k_{22}/s)\,1/s} = \frac{\frac{k_{21}s + k_{22}}{s^2}}{\frac{s^2 + k_{21}s + k_{22}}{s^2}} = \frac{k_{21}s + k_{22}}{s^2 + k_{21}s + k_{22}}$$

This closed loop transfer function can be presented in the form:

$$\frac{Y_2(s)}{Y_{sp2}(s)} = \frac{k_{21}s + k_{22}}{s^2 + k_{21}s + k_{22}}$$

$$= \frac{2\tau_2\zeta_2 s + 1}{\tau_2^2 s^2 + \tau_2\zeta_2 s + 1}$$

$$\text{where, } \tau_2 = \frac{1}{\sqrt{k_{22}}}, \quad \zeta = \frac{k_{21}}{2\sqrt{k_{22}}} \text{ or, } k_{21} = \frac{2\zeta_2}{\tau_2},\ k_{22} = \frac{1}{\tau_2^2} \quad (6.29)$$

Here, ζ_2 and τ_2 ,are the time constant and damping parameter that determine the shape of the step responses for the temperature. If the roots of the characteristic equation s $s^2 + k_{21}s + k_{22}$, are appropriately selected, then asymptotic tracking of the desired closed loop response can be realized. According to Slotine and Li, (1990);

Henson and Seborg, (1991) the controller tuning parameters k_{21} and k_{22} can be selected to provide the response of the desired closed loop. To guarantee smaller overshoots, the conditions $k_{21}{}^2 \geq 4k_{22}$ should be fulfilled. The problem is then to find the appropriate parameters k_{21} and k_{22}. According to Wilson (2014), the algorithm for appropriate values of k_{21} and k_{22} is as follows:

1. Choose the appropriate values of the damping factors. For tight control, with little overshoot, $\zeta_2 \approx 3$ or higher.is recommended.
2. Specify the time scale by choosing appropriate values of time constant τ_2. Often it is convenient to specify the rise time
3. From the specified values of ζ_2 and τ_2, the scalar values of parameters are evaluated for each output. From equation (6.29) therefore,

$$k_{21}{}^{2,} \geq 4k_{22} \rightarrow (\frac{2\zeta_2}{\tau_2})^2 \geq \frac{1}{\zeta_2^2}$$

$$(\frac{2\zeta_2}{\tau_2})^2 - \frac{1}{\zeta_2^2} \geq 0 \rightarrow 2\zeta_2^2 - 1 \geq 0 \qquad (6.30)$$

$$\zeta_2 \geq \sqrt{\frac{1}{2}} \rightarrow \zeta_2 = 1.1 \text{ is selected}$$

Similarly, the controller tuning parameters for the temperature control loop are subsequently calculated by choosing the damping factor ζ_2 and time constant τ_2 that ensures that the condition $k_{21}{}^2 \geq 4k_{22}$ is fulfilled. From equation (6.29), assuming that the specific transient controller requirements for the damping factor should be 1.1 and the time constant to be 0.14 min, then:

$$k_{21} = \frac{2\zeta_2}{\tau_2} = \frac{2(1.1)}{0.075} = 29$$

$$k_{22} = \frac{1}{\tau_2^2} = \frac{1}{(0.14)^2} = 51 \qquad (6.31)$$

Thus the PI controller tuning parameters are designed as per equations (6.30) and (6.31). The controller is for the temperature control loop:

6.6 Simulation results

Simulation results are used to show the performance of the designed controllers. The Simulink block diagrams used to implement this control scheme are illustrated in the following figures.

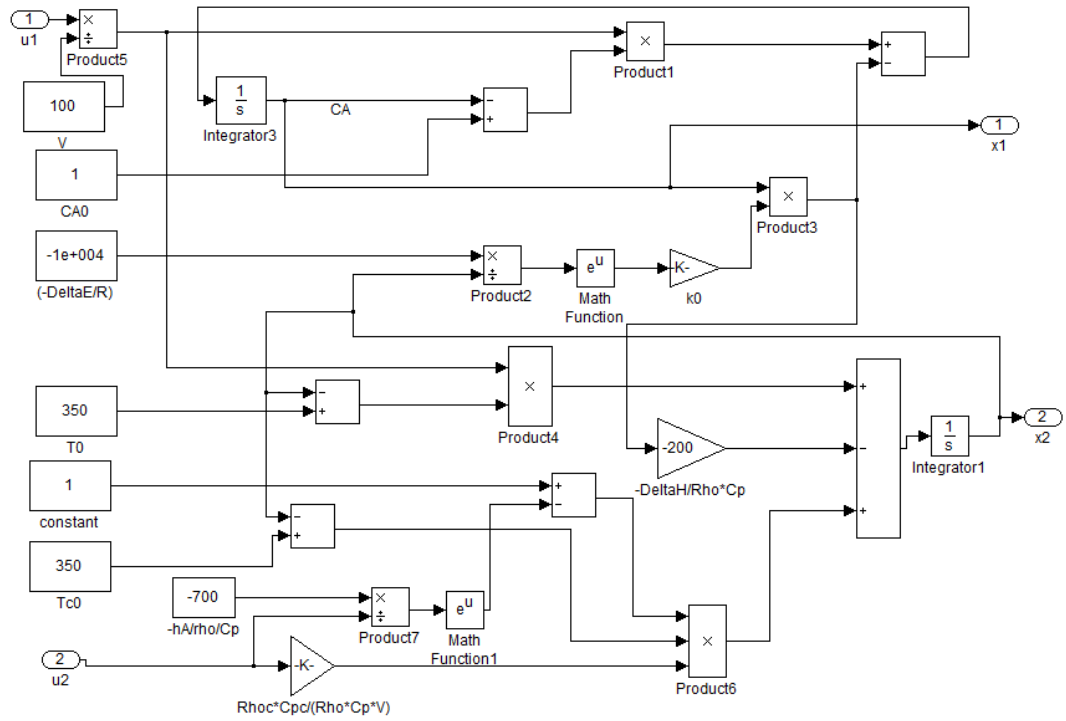

Figure 6.4: Simulink CSTR process model.

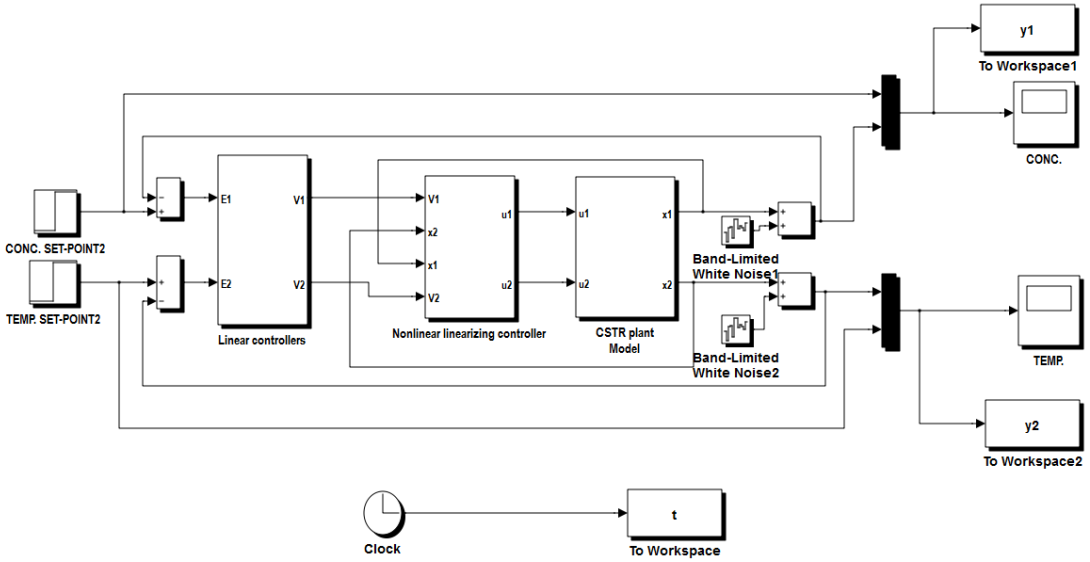

Figure 6.5: Control structure using input-output feedback linearization

Figure 6.4 is the Simulink block diagram for the nonlinear CSTR process model used for the design of the I/O feedback linearization control algorithm. Figure 6.5 illustrates the Simulink block diagram of the complete set-up consisting of the linear controllers, the nonlinear linearizing controller and the CSTR model implemented in the Simulink environment. Then Figure 6.6 is the Simulink block diagram for the nonlinear linearizing controller implemented with the help of Equations (6.18) and (6.19) derived earlier.

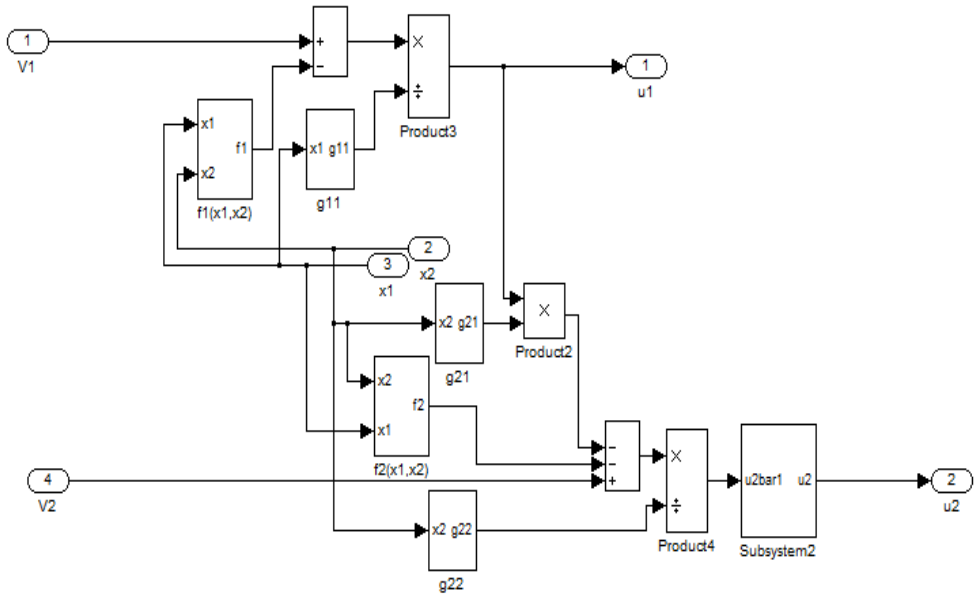

Figure 6.6: Simulink block for the I/O feedback linearization controller

The set-point tracking performance capabilities for both outputs with different values of magnitudes are tested based on simulations of the closed loop system of Figure 6.5 under various set-point and disturbance situations. The results of the simulations are presented as follows.

6.6.1.1 Concentration loop results from simulation for various set-points

Figure 6.7 presents the time response for set-point tracking characteristics for the concentration control for varying set-points. The PI controller tuning parameters of Equation (6.29) are used. The set-point is varied in steps from 0.0762mol/l to 0.13mol/l, then to 0.06mol/l, as illustrated. Analysis of this plot for various time response indices indicates that the rise time is 0.9 min, the settling time of 1.98 min, the percentage overshoot is 10.5947%, the time to peak overshoot is 0.56 min, and steady state error of 0%. This therefore implies that the simulated response tracking capabilities for the designed concentration control loop by the I/O feedback linearization methodology is good.

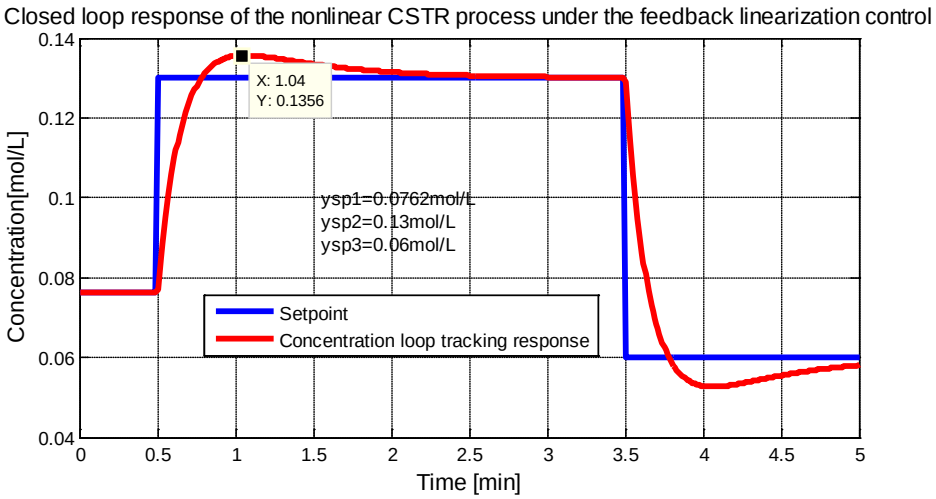

Figure 6.7: Input-output feedback linearization controlled concentration set-point tracking

Simulations are also performed for different set-point conditions. Figures 6.8 to 6.13 show the concentration responses for the set-point tracking when the magnitudes are varied as $0.08mol/l$, $0.09mol/l$, $0.10mol/l$, $0.11mol/l$, $0.12mol/l$ and $0.13mol/l$, then in Table 6.1 the various time response specifications are compared. From Table 6.1, it is deduced that the simulated responses for various set-points have good tracking capability for the input-output feedback linearizing control of the concentration loop of the MIMO system.

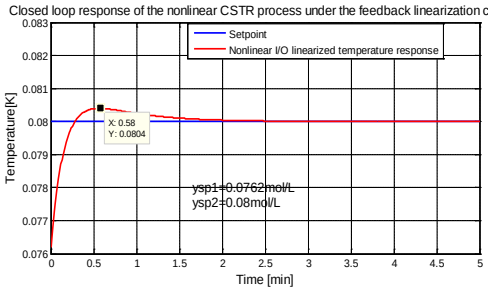

Figure 6.8: Response for a set-point of $0.08mol/l$

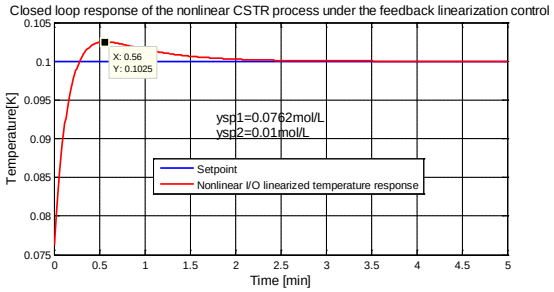

Figure 6.10: Response for a set-point of $0.1mol/l$

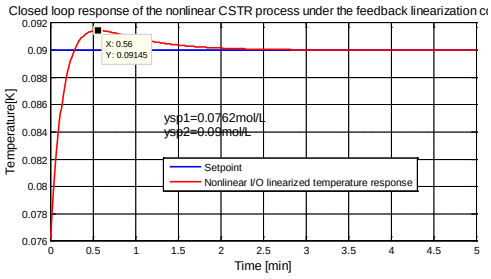

Figure 6.9: Response for a set-point of $0.09mol/l$

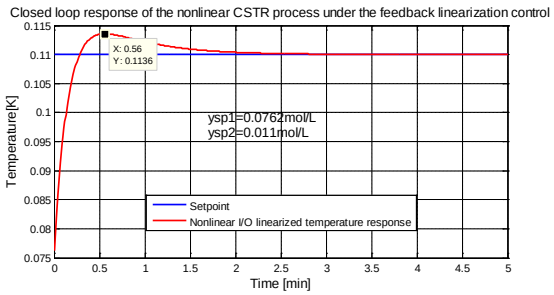

Figure 6.11: Response for a set-point of $0.11mol/l$

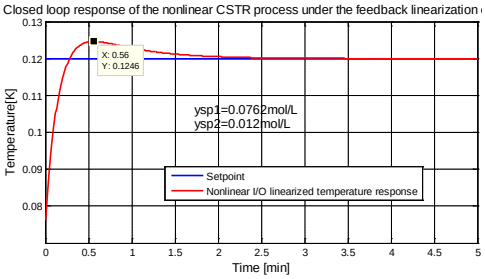

Figure 6.12: Response for a set-point of $0.12mol/l$

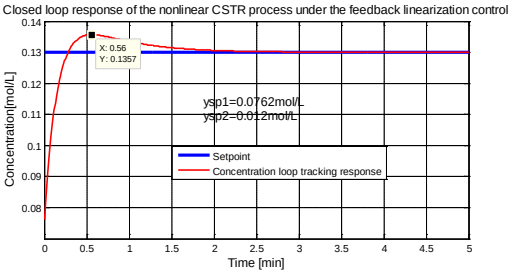

Figure 6.13: Response for a set-point of $0.13mol/l$.

Table 6.1: Performance indices for the concentration control loop using I/O linearization-based control

Set-point value	Settling time $t_s(\min)$	Rise time $t_r(\min)$	Peak over shoot $M_p(\%)$	Peak time $t_s(\min)$	Steady state error $e_{ss}(\%)$
0.08mol/l	1.9800	0.900	10.5263	056	0
0.09mol/l	1.9800	0.900	10.5075	0.56	0
0.10mol/l	1.9800	0.900	10.5042	0.56	0
0.11mol/l	1.9800	0.900	10.6508	0.56	0
0.12mol/l	1.9800	0.900	10.5022	0.56	0
0.13mol/l	1.9800	0.900	10.5947	0.56	0

As can be seen Table 6.1, the maximum peak overshoot of 10.65081% is attained with 0% steady state error. This implies that the designed control is good at tacking the set-point values. Next the influence of disturbances is investigated.

6.6.1.2 Investigation of the process performance for a disturbance on concentration control loop

The designed I/O feedback linearization control system's performance is checked for different magnitudes of random disturbances (white noise) added to the output signal y_1 on the main concentration loop. The responses are represented in the following Figures 6.14-6.17.

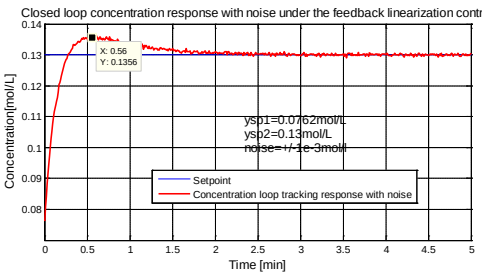

Figure 6.14: Concentration response under $\pm 1e^{-3}$mol/l disturbance magnitude

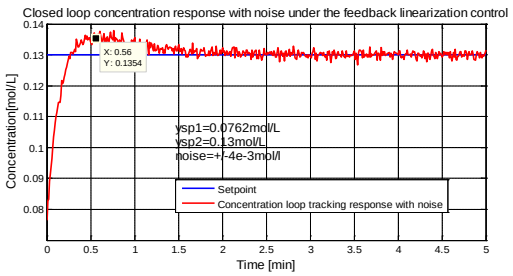

Figure 6.15: Concentration response under $\pm 4e^{-3}$mol/l disturbance magnitude

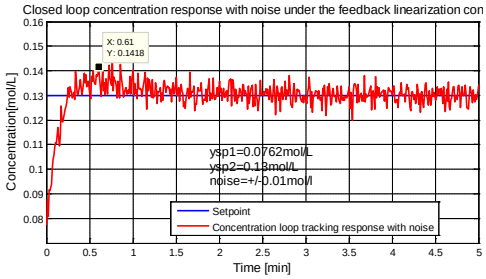

Figure 6.16: Concentration response under $\pm 0.01 \text{mol/l}$ disturbance magnitude

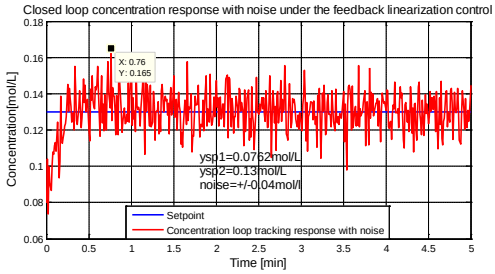

Figure 6.17: Concentration response under $\pm 0.04 \text{mol/l}$ disturbance magnitude

The responses from the simulations including the disturbances suggest that good tracking control is still achieved. However, as the magnitude of the disturbance is increased, the response becomes noisy and therefore the performance is degraded. Simulation of the temperature loop output signal is also investigated when the disturbance is on the y_1 output. These are illustrated in Figures 6.18-6.22 below.

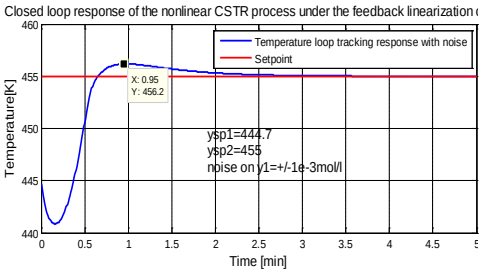

Figure 6.18: Temperature response under $\pm 1e^{-3} \text{mol/l}$ disturbance magnitude

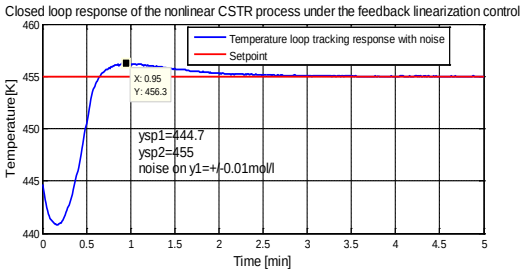

Figure 6.20: Temperature response under $\pm 0.01 \text{mol/l}$ disturbance magnitude

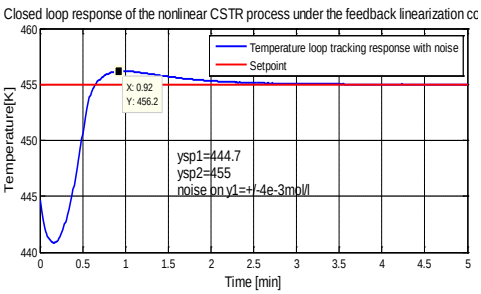

Figure 6.19: Temperature response under $\pm 4e^{-3} \text{mol/l}$ disturbance magnitude

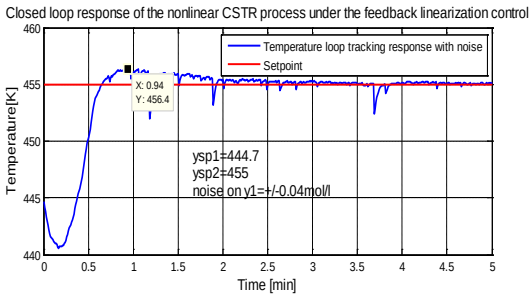

Figure 6.21: Temperature response under $\pm 0.04 \text{mol/l}$ disturbance magnitude

The responses from the simulations show that the influence of disturbances on y_1 is very minimal in the temperature control loop y_2 though the magnitude of such disturbances has an effect on the performance of the system as can be seen in Figure 6.21.

6.6.2.1 Temperature loop results from simulation for various set-points

Next, the temperature control loop's performance is checked for set-point tracking using I/O feedback linearization control with the help of the control law developed in Equation (6.13) for the PI controller tuning parameters. This is checked for different set-point values in terms of the various performance indices such as the peak overshoot, peak time, settling time, steady state error, and rise time. Figures 6.22-6.25 are the set-point tracking characteristics. The set-point values tested are varied as, $447K$ $450K$, $455K$ and $460K$.

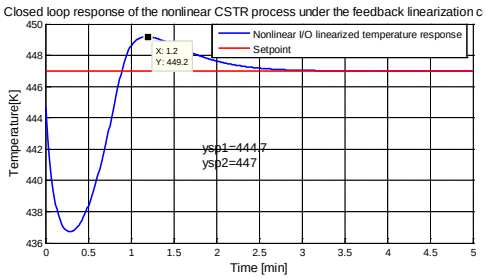

Figure 6.22: Response for $447K$ set point

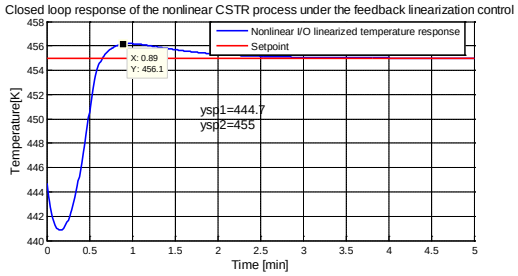

Figure 6.24: Response for $455K$ set point

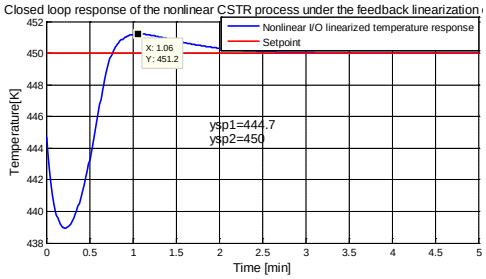

Figure 6.23: Response for $450K$ set point

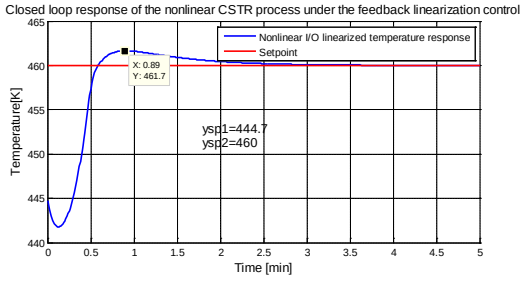

Figure 6.25: Response for $460K$ set point

Table 6.2 summarises the various performance characteristics for the temperature control loop with the I/O feedback linearizing control. The results show that even though set-point tracking for the temperature control loop is achieved, the inverse response as a result of the zero in the transfer function of the process is much evident and the performance is sluggish and depends on the set-point.

Table 6.2: **Performance indices for the temperature control loop using I/O linearizing control**

Set-point value	Settling time t_s (min)	Rise time t_r (min)	Peak over shoot M_p (%)	Peak time t_s (min)	Steady state error e_{ss} (%)
$447K$	2.5000	0.800	56.603	1.2	0
$450K$	2.0000	0.800	22.621	1.06	0
$455K$	1.6800	0.680	10.68	0.89	0
$460K$	1.6800	0.620	10.11	0.89	0

The performance indices vary and are not constant. This could be due to the lack of robustness in the controller design since the fixed PI controller has only limited tuning parameters. Further analysis of this design is thus needed in order to improve of the performance of this loop. Next an investigation on the system's response to disturbances is carried out as, outlined in the following.

6.6.2.2 Investigation of process performance for a disturbance on the temperature control loop

The designed I/O feedback linearization control system's performance is checked for different magnitudes of random disturbances (white noise) added to the output signal y_2 on the main temperature loop. The responses are represented in the following Figures 6.26-6.29.

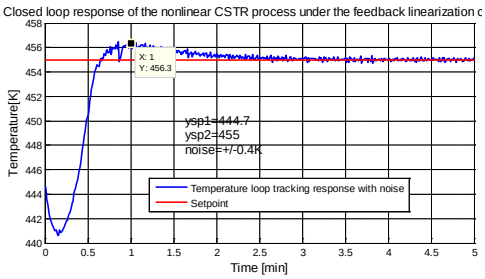

Figure 6.26: Response under a disturbance magnitude $\pm 0.4K$

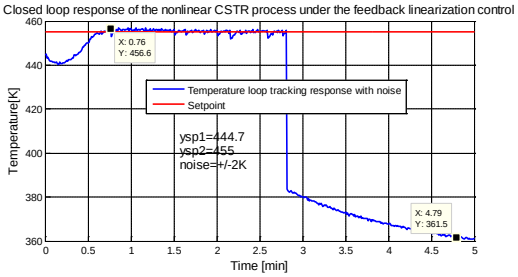

Figure 6.28: Response under a disturbance magnitude $\pm 2K$

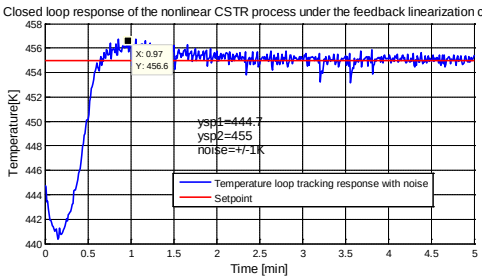

Figure 6.27: Response under a disturbance magnitude $\pm 1K$

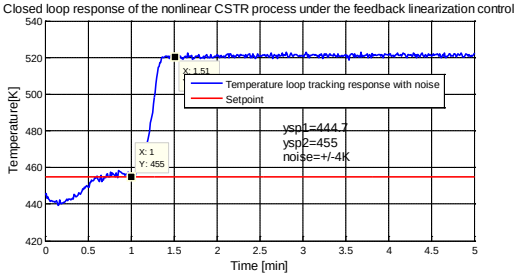

Figure 6.29: Response under a disturbance magnitude $\pm 4K$

The effects of disturbance in this case have significant contribution in the performance degradation of this particular control loop. The disturbance magnitudes are varied in the ranges $\pm 0.4K$, $\pm 1K$, $\pm 2K$, $\pm 4K$, as illustrated. The responses are more sluggish and the disturbance changes tend to make the system less stable thereby forcing a break down in the response of the system resulting in instability as can be seen in Figures 6.28 and 6.29 for the disturbance magnitudes of $\pm 2K$, $\pm 4K$, and therefore the designed fixed PI controller for this loop is not able to prevent the temperature runaway effectively. Therefore further analysis of the design is needed.

Next, the influence of this disturbance on the concentration control output is investigated because of the interaction relationships that exist between the two control loops. Figures 6.30-6.33 are the diagrams of the simulations y_1 of when the disturbance is on y_2

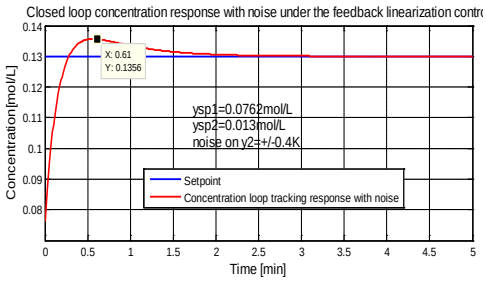

Figure 6.30: Concentration response under a disturbance magnitude $\pm 0.4K$

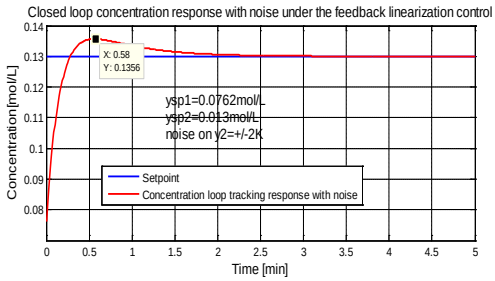

Figure 6.32: Concentration response under a disturbance magnitude $\pm 2K$

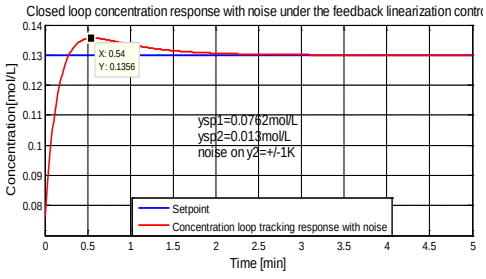

Figure 6.31 Concentration response under a disturbance magnitude $\pm 1K$

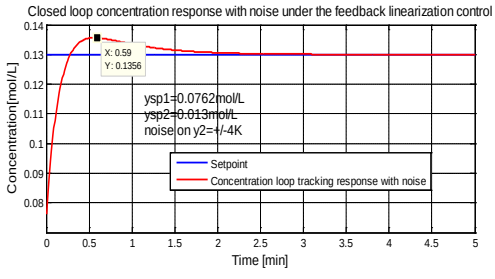

Figure 6.33: Concentration response under a disturbance magnitude $\pm 4K$

Analysis of Figures 6.30-6.33 shows that the concentration responses for set point tracking are perfect. This implies that when the disturbance is on the temperature y_2 ,

there is no effect on the concentration loop y_1 .Good set point tracking control for y_1 is achieved.

6.7 Discussion of the Results

Simulation results are used to show the performance of the designed controllers based on the I/O feedback linearizing control law and the independent PI controllers designed based on the pole placement principles. First, the set-point tracking performance capabilities for the concentration control loop with different values of the magnitudes are tested. Analysis of various time response indices indicates that the simulated response tracking capabilities for the designed concentration control loop is good. The designed I/O feedback linearization control system's performance is checked for different varying magnitudes of random disturbances (white noise) perturbed to the concentration loop and the simulated responses with disturbances suggest good tracking control though the magnitude of the disturbance matters because higher magnitudes of disturbances causes the performance to be degraded. Simulation of the temperature loop output signal is also investigated when the disturbance is on the concentration loop output. The responses from the simulations indicate that the effect of disturbances on the concentration loop output is very minimal in the temperature control loop though the magnitude of such disturbances has an influence on the performance of the system.

Next, the temperature control loop's performance is also analysed This is checked for different set-point values in terms of the various performance indices The results show that even though set-point tracking for the temperature control loop is achieved, the inverse response due to the zero in the transfer function of the process is much evident and the performance is sluggish and depends on the magnitude of the set-point. The performance indices vary and are not constant. This could be due to the fact that the PI controller design in the loop is with only limited tuning parameters. It further suggests that a temperature upset is a difficult disturbance to control with this technique. Further analysis of the design is thus needed for the improvement of the loop performance. In terms of performance due to the effects to disturbances, it is shown that the effects have significant contribution in the performance degradation of this particular control loop. The result is a sluggish and less stable, forcing a break down in the response. Therefore further analysis of the design is needed. The performance of concentration control output is investigated for the influence of the disturbance of the temperature control loop. This is done on the basis of the interaction relationships that exist between the two control loops. Analysis shows that the concentration responses for set point tracking are perfect. This implies that when

the disturbance is on the temperature loop, there is no effect on the concentration loop. Good set point tracking control for the concentration control is achieved.

6.8 Concluding remarks on the I/O feedback linearization method designed

The design and simulation of the input-output feedback linearization control design for the nonlinear MIMO CSTR system are investigated. This control technique uses feedback signal to cancel the inherent nonlinear dynamics in a system by creating linear differential relationship between the system's outputs and the newly proposed synthetic inputs. The nonlinear controller is first designed on the basis of the input-output linearization to control the concentration and the reactor temperature in a CSTR process. Then two linear PI controllers for the respective loops are independently designed using the pole-placement techniques. Finally closed loop simulations are performed to verify the suitability of the proposed controllers. Moreover, the suitability is checked with noisy disturbances on the control loops. The results of this analysis show the suitability of the proposed control law in achieving set-point tracking for the concentration control as well as for the reactor temperature control. Similarly, the proposed control exhibits satisfactory performance in the presence of disturbances with limited magnitudes.

Chapter seven that follows introduces an approach to block diagram transformation between the Matlab/Simulink environments to Beckhoff Twin3.1 environment for real-time implementation based on number of the philosophies of the IEC 61499 standard

CHAPTER SEVEN
FUNCTION BLOCK TRANSFORMATION FROM MATLAB/SIMULINK TO BECKHOFF TwinCAT 3 FOR REAL-TIME SIMULATION AND CONTROL

7.1 Introduction

The chapter presents a methodology for transforming the developed continuous time controller blocks as well as the complete closed loop systems application from Matlab/Simulink environment to the Beckhoff Embedded PC-based PLC automation software using the capabilities of TwinCAT 3.1 simulation environment for real-time control. Real-time control specializes in the development of hardware and software algorithms for integrating a closed loop control system application that has a tight time window to gather data, process that data and update the system. In this chapter the concepts of real-time control is used for the simulation of the nonlinear multivariable CSTR process in real-time. The Beckhoff CX5020 Programmable Logic Controller is used for the closed loop real-time control system simulation to show the effectiveness of the control laws developed in Chapters 4, 5 and 6. TwinCAT 3.1 software allows for the control set up by programming in Matlab/Simulink and then downloading to TwinCAT 3.1 runtime simulation environments for real-time implementation. The communication between the embedded PC and the Beckhoff CX5020 PLC is ensured by the EtherCAT communication protocol which is an open real-time Ethernet developed by Beckhoff.

The chapter is structured as follows: In section 7.2, the background of the TwinCAT 3.1 software as a tool for real time control is presented. In section 7.3 the methodology for integration of TwinCAT 3.1 with Matlab/Simulink software is presented. In section 7.4 the steps for TwinCAT module generation from a Simulink model is outlined in order to implement real-time control simulations of the developed control algorithms. Section 7.5 presents closed loop control transformations from Matlab/Simulink to TwinCAT 3.1 and results of real-time simulations. In section 7.6, discussions of the results from the simulations are presented. Section 7.7 gives the conclusion of the chapter.

7.2 The Beckhoff TwinCAT 3.1 Software for Automation Technology (Overview)

The Windows Control and Automation Technology (TwinCAT 3.1) is new PC-based PLC automation software developed by Beckhoff automation that enables control engineers to model and simulate complex, distributed control applications in real-time. It partly supports the IEC 61499 standard in terms of interoperability concept. The software turns almost any PC-based system into a real-time control with multiple PLC's and/or runtime systems. In support to interoperability between different

platforms, this new software supports the development of control applications in Matlab/Simulink environment and generates executable PLC code based on the models applied to it. The TwinCAT 3.1 software is divided into TWO components, namely the extended automation Engineering components (XAE) and the extended automation Runtime components (XAR). The Engineering components enable the Configuration, Programming and Debugging of applications. This engineering environment is called the PLC control. The runtime environment consists of further components that are used for execution of the created control modules and algorithms in real-time. This runtime system is called the System Manager. Any Windows programs can access TwinCAT data via Microsoft interfaces. The software supports IEC 61131 programming languages, object-oriented programming, C/C++ and Matlab/Simulink among other languages thereby enabling interoperability with other software vendors. Where support for Matlab/Simulink is concerned, a Simulink block is available in the TwinCAT interface for Matlab/Simulink that establishes an Automation Device Specification (ADS) connection to the real-time variables. No specific Beckhoff modules or other modifications to the original model are required to create Matlab/Simulink modules. The Matlab and Simulink coders generate C++ code, which is then compiled in a TwinCAT 3.1 module. The use of this new software reduces programming time and various new functionalities are available. The architecture of TwinCAT 3.1.1 software, (Beckhoff.com, 2015) is as illustrated in Figure 7.1.where the various blocks functionalities are subsequently explained.

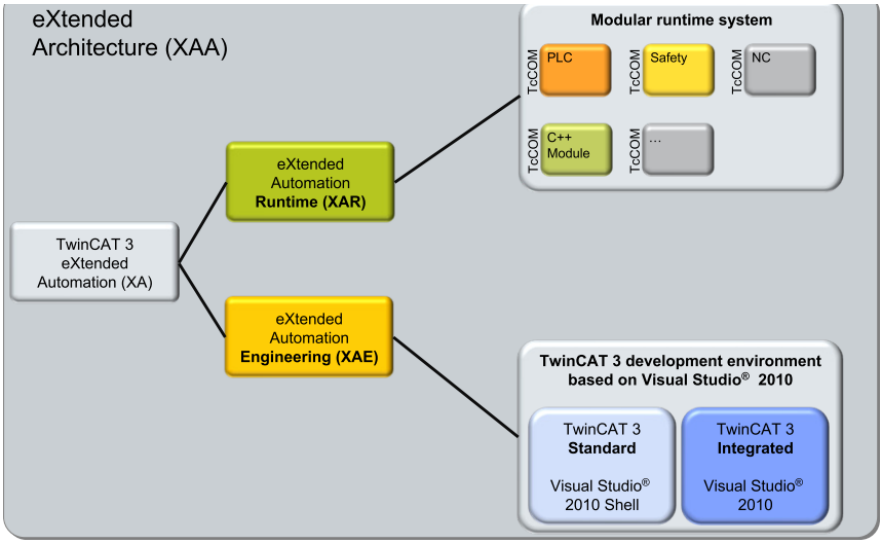

Figure 7.1: TwinCAT 3.1 eXtended Automation (http://www.beckhoff.com/english.,2015)

7.2.1 The Beckhoff TwinCAT 3.1.1 Software Automation Engineering platform

In the Engineering platform components, the major highlights are: the Integration of software tools in the Microsoft Visual studio 2010 or higher version as the

development environment. This environment in addition to the Integrated TwinCAT System Manager is all that is needed to configure, parameterize, program and to fault-find the automation devices, Programming can be done according to IEC 61131-3 standard languages, or the usage of C and C++ for real-time programming, and/or linkage to Matlab/Simulink or other options for links to third party Software-tools. Figure 7.2 (Beckhoff.com, 2015) illustrates the block diagram of the set-up

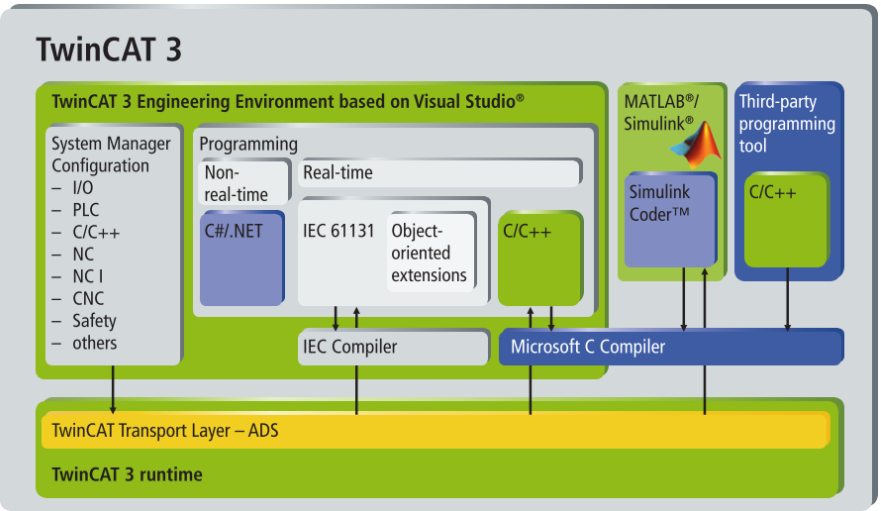

Figure 7.2: TwinCAT 3.1. Engineering platform (http://www.beckhoff.com/english.,2015)

7.2.2 The Beckhoff TwinCAT 3.1.1 Software Automation Runtime

This platform offers a real-time environment, where TwinCAT modules can be loaded, executed and administered. The generated modules can be called cyclically from tasks or by other modules (generated by using C/C++ or out of the Matlab/Simulink environment). The TwinCAT 3.1 runtime environment can be used to distribute functional units such as human machine interface (HMI), programmable logic controllers (PLC) runtimes or motion control (MC) to dedicated cores. All the real-time components are encapsulated in modules which are managed by the runtime system. TwinCAT 3.1 uses the concepts from the Component Object Model (COM) to define the characteristics and behavior of the modules. TwinCAT COM (TcCOM) allows modules implemented in different languages to interact seamlessly in the real-time context. The block diagram of a Modular TwinCAT 3.1 runtime platform is as illustrated in Figure 7.3.

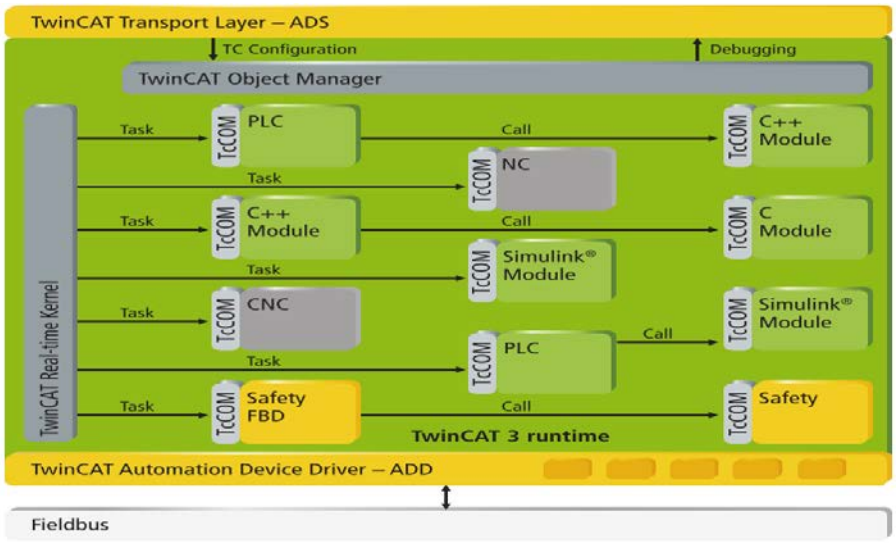

Figure.7.3: Modular TwinCAT 3.1. Runtime platform (http://www.beckhoff.com/english.,2015)

7.2.3 Overview of the Programmable Logic Controller (PLC)

The PLCs are embedded computers built specifically for industrial environment and used for the automation of industrial processes. They form the backbone of most present day industrial automation. A PLC is a computer based controller which continuously checks the state of input devices in a system and makes decisions for the actions to be taken. Based upon programs in the system, the state of the output devices is then controlled. This implies that PLCs are examples of real-time systems since the outputs must are activated as a result of the input conditions within bounded time spans. Generally, the PLC consists of Central Processing Unit (CPU), the memory units (both the Random Access Memory (RAM) and the Read Only Memory (ROM), the power supply unit and other auxiliary devices including I/O units. The heart of the PLC is the CPU unit. This unit comprises microprocessor(s) which is used for the execution of arithmetic and logical operations, connection to local area networks, interfacing the computer and other peripherals. The CPU executes programs by checking the states of the input unit and outputs information through the output unit for the external field devices. The output unit is used to communicate between the CPU of the PLC and the external field devices where the PLC provides the signals for control. Present day PLCs have become very attractive for controlling real-time industrial processes mainly because they are increasingly more versatile in terms of performance and standardization. The real-time control software is written in more languages and the embedded operating system can run more applications which are some of the requirements of the IEC 61499 standard. The Beckhoff CX5020 PLC is one such real-time control software that meets the requirements for real-time control. This thesis has utilized the Beckhoff CX5020 PLC for the implementation of the closed loop real-time control for the CSTR process. The novelty of this PLC is discussed in the following.

7.2.3.1 The Beckhoff CX5020 PLC

This PLC is an embedded PC from the CX5000 series-based PLCs developed by Beckhoff Automation Inc., and is packaged with all of the necessary communication and I/O options to make it a fully functional PLC. Because of the modular structure, it allows for flexible extension and modification and consists of independent modules that can be freely added and removed from the system. The Beckhoff CX5020 is based on a 1.6 GHz Intel Atom Z530 processor (CPU), 1 GB of RAM and a flashcard serving as persistent memory. It is Beckhoff proprietary software that makes it operates as a PLC or for implementation of other Control projects depending on TwinCAT runtime environment. There is also an integrated uninterrupted power supply (UPS) embedded within it to provide emergency power for around two seconds and allows a secure shutdown of the device in case of power failure. The Z530 features hyper threading technology, i.e. it has two virtual CPU cores for more effective execution of the software (Beckhoff.com, 2015). The extended operating temperature range between -25 and +60 °C enables application in climatically demanding situations. The block diagram of the Beckhoff CX5020 PLC is illustrated in Figure 7.4.

Figure 7.4: Beckhoff CX5020 PLC (www.beckhoff.com/CX5000)

The CX5020 is DIN rail mountable with durable and compact magnetic housing, fanless (without rotating components), embedded PC with direct connection for Beckhoff Bus Terminals or EtherCAT terminals. Table 7.1 gives the technical datasheet for the CX5020 PLC.

Table 7.1: Embedded CX5020 PLC Technical data sheet (www.beckhoff.com/CX5000)

Technical data	CX5020-x1xx
Processor	processor Intel® Atom™ Z530, 1.6 GHz clock frequency (TC3: 40)
Flash memory	128 MB Compact Flash card (optionally extendable)
Internal main memory	512 MB RAM (optionally 1 GB installed ex-factory)
Persistent memory	integrated 1-second UPS (1 MB on Compact Flash card)
Interfaces	2 x RJ45, 10/100/1000 Mbit/s, DVI-D, 4 x USB 2.0, 1 x optional interface
Diagnostics LED	1 x power, 1 x TC status, 1 x flash access, 2 x bus status
Clock	internal battery-backed clock for time and date (battery exchangeable)
Operating system	Microsoft Windows CE 6 or Microsoft Windows Embedded Standard 2009
Control software	TwinCAT 2 PLC runtime or TwinCAT 2 NC PTP runtime
Power supply	24 V DC (-15 %/+20 %)
Current supply E-bus/K-bus	2 A
Max. power loss	12.5 W (including the system interfaces)
Dimensions(W x H x D)	100 mm x 106 mm x 92 mm
Operating/storage temperature	-25…+60 °C/-40…+85 °C
Relative humidity	95 %, no condensation
Vibration/shock	resistance conforms to EN 60068-2-6/EN 60068-2-27
EMC immunity/emission	conforms to EN 61000-6-2/EN 61000-6-4
Protection class	IP 20
TC3 performance class	performance class 40

In addition to the technical data sheet there are quite a variety of PLC versions of CX5020 and these depend on the plant to be controlled as well as the communication protocol to be used to link the controller to the plant.

7.2.3.2 The Beckhoff CX5020 PLC Communication with Ethernet for real-time control

To be able to control a synthetic model from the Matlab/Simulink environment with a PLC, a communication connection is required to interface the PLC and the embedded PC. The communication protocol Ethernet/IP is used. The block diagram of such an arrangement is shown in Figure 7.5.

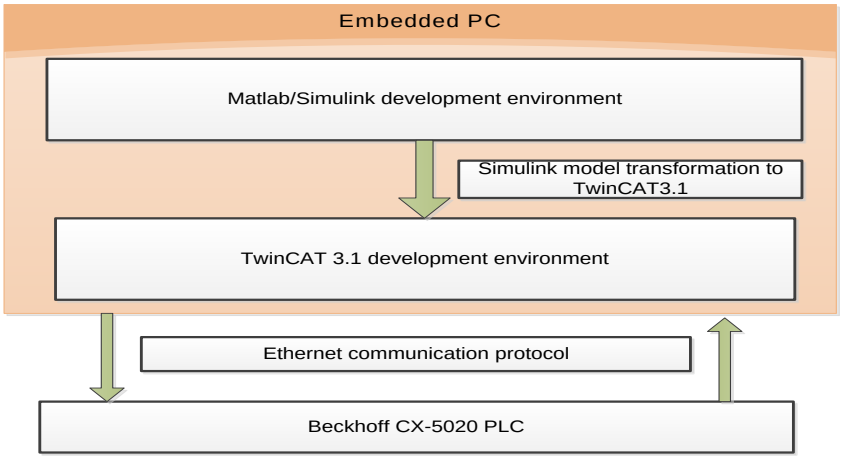

Figure 7.5: Real-time control communication with Ethernet

In this case, the CX5020 PLC acts as a real-time platform for execution of the applications downloaded from the TwinCAT 3.1 development environment through the Ethernet communication platform. Through this connection, real-time communication between the Matlab/Simulink, the TwinCAT 3.1 developed algorithms and the PLC is provided.

7.3 Matlab/Simulink Integration with TwinCAT 3.1

To use control programs and controllers designed in Matlab/Simulink with real machine after successful tests in simulation, the developed algorithms can be programmed in real-time capable languages like C++ or PLC code. For example, Matlab/Simulink software is capable of generating codes from the Simulink models to the various targets by using the Embedded Simulink Coder (formerly “Real-Time Workshop). With the Simulink Embedded Coder and the supplementary software from Beckhoff automation, called the TwinCAT 3.1 Target for Matlab/Simulink (TE1400), makes it possible for the generation of C++ code which is then encapsulated in a standard TwinCAT 3.1 module format. This code may be instantiated or loaded into the TwinCAT 3.1 development platform. The TE1400 software acts as the interface for the automatic generation of real-time capable modules, which can be executed on the TwinCAT 3.1 runtime environment. In general, to enable full transformation from Matlab/Simulink to TwinCAT 3.1, two licences must be available (TwinCAT 3.1 Target for Matlab/Simulink and TwinCAT 3.1 Interface for Matlab/Simulink). The TwinCAT 3.1 offers system target files of Matlab/Simulink coder to be used on the TwinCAT 3.1 target. It allows for the generation of the TwinCAT 3.1 runtime modules. The TwinCAT 3.1 Interface Matlab/Simulink enables for the communication interface between Matlab/Simulink and the TwinCAT 3.1 runtime. It provides for the real-time parameter acquisition and visualisation. Both the hardware simulation and the controller simulation are made possible by this TwinCAT 3.1 Interface for Matlab/Simulink. The real-time capable module is termed the TwinCAT Component Object Model (TcCOM). This module can be imported in the TwinCAT 3.1 environment and contains the input and output of the Simulink model. TcCOM facilitates the implementation of modules from different languages to interact with easiness in the real-time context. The block diagram of Figure 7.6 represents the transformation procedure between Matlab/Simulink to TwinCAT 3.1.

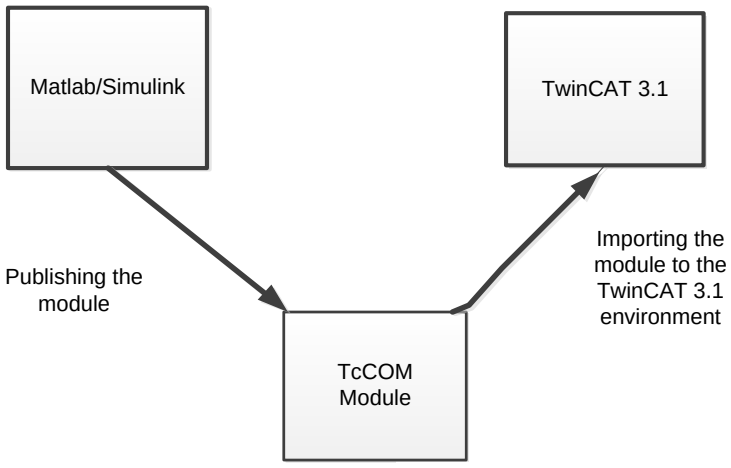

Figure 7.6: TcCOM module operation

The transformation between the two platforms (Matlab/Simulink and TwinCAT 3.1) can be explained as follows.

In the Simulink platform, the build process for the model is started by first generating the code for the TwinCAT target platform. Once the code generation for the model is completed the TcCOM modules set of information are published. The module is imported to the TwinCAT 3.1 target platform (RT) implying the publish procedure completed successfully for TwinCAT Real-Time environment. After starting the TwinCAT 3.1 runtime, the module is executed in real-time and can thus be integrated into a real machine controller. The TwinCAT 3.1 has the capability for visual presentation and navigation of the Simulink block diagrams that include the monitoring of the parameters and signals values and/or the capability of modification at run-time without change to the original model (interoperability).

7.4 Steps for TwinCAT module generation from a Simulink model

The following is a general procedure for the steps involved in transforming the model developed in the Matlab/Simulink environment to a TwinCAT function block module for real-time control simulation.

1. The Simulink model is opened in the main Simulink platform and the model explorer tab is started under the view menu. Beneath the explorer pop-up window, the model configuration is selected, upon which the generation code tub is activated. This will result in another pop-up window containing the system target files. Then the TwinCAT.tlc file for the TwinCAT target is selected. The model explorer pop-up window is then closed.
2. The code generation process is then started via the Simulink through menu, tool, code generation, and build in that order. The building process then starts and the progress can be monitored on the Matlab workspace.

On completion of the build process, all the model files required for transformation are ready and can be used in the TwinCAT platform. Thus, the generated TwinCAT module can be used. The following steps are then applied for the TwinCAT environment.

3. The TwinCAT Engineering platform (XAE) is opened. The visual studio platform will pop-up asking for the creation of a new TwinCAT project. Upon activating this tab, the solution explorer windows will pop-up. In the solution explorer, the node “System” when expanded, a selection of “Add an item-TcCOM objects” is activated. This leads to the selection of the generated Simulink module with its default settings to append to this task. A task is then added to this module. In the context menu of. To check this, selection of the object node *of the module* and opening the tab “*Context”*. The resulting table contains the object ID and the object name of the task. Now the configuration of the model is completed and can be activated on the target system.
4. Upon selection of the target system, the configuration is activated for executing of the Simulink generated module on the target system.
5. Activating the configuration on the target system, the TwinCAT system is started and the target status icon changes its colour from blue to green implying the system is running real-time.
6. If the block diagram tab is selected, the block diagram “*online*” status can be monitored.

Figures 7.7 to 7.16; presents snapshots of the procedures adopted for Simulink block transformation to the TwinCAT function blocks.

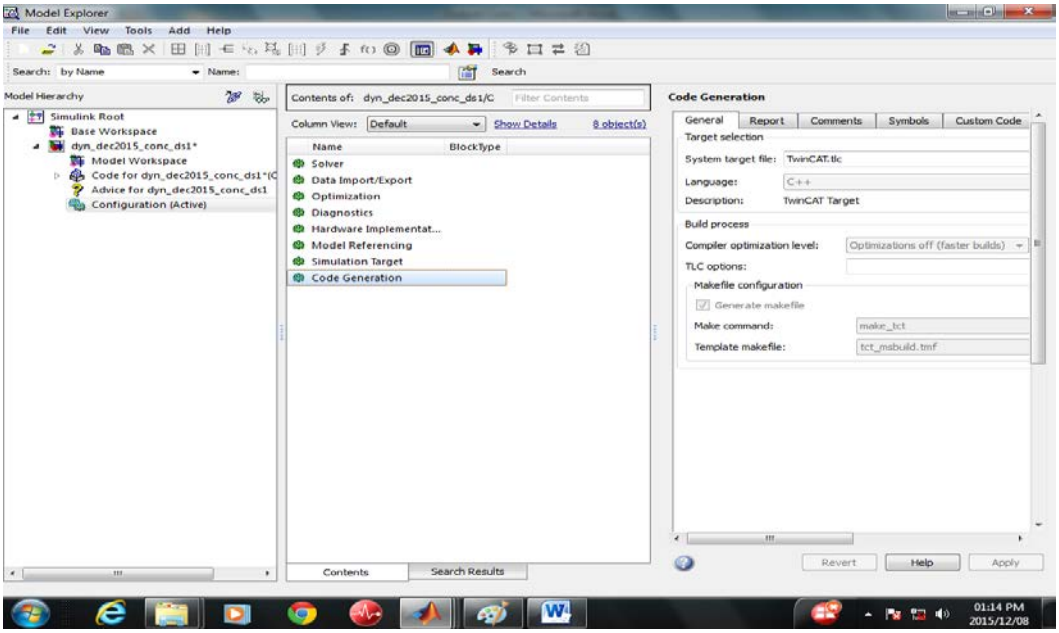

Figure 7.7: Snapshot of the Code generation in Simulink platform

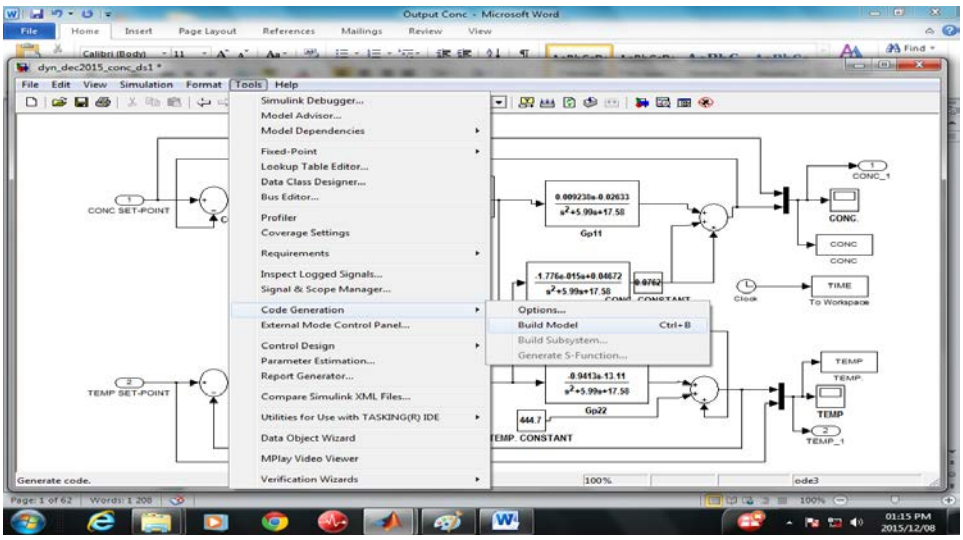

Figure 7.8: Snapshot of the model building in Simulink platform

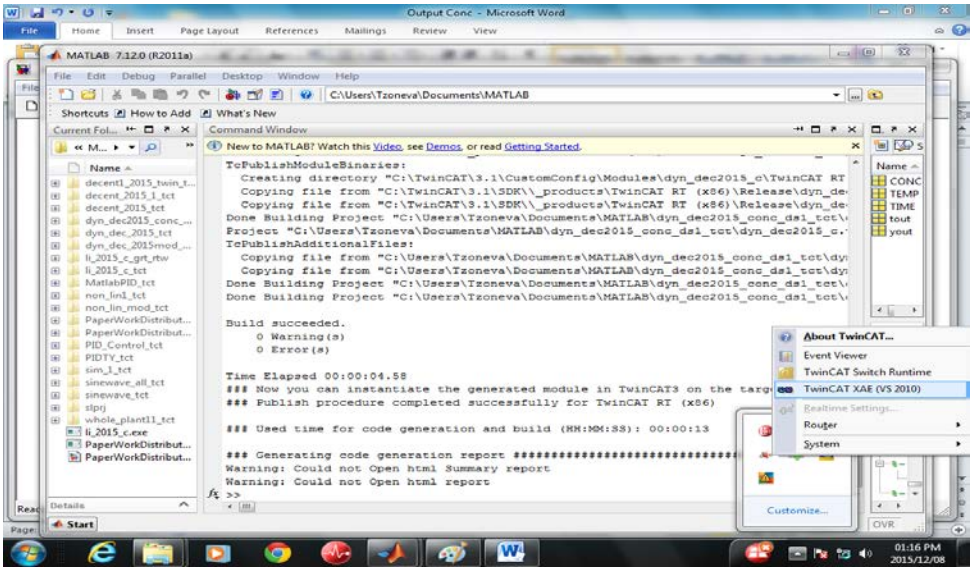

Figure 7.9: Snapshot of the Code generated in Simulink platform

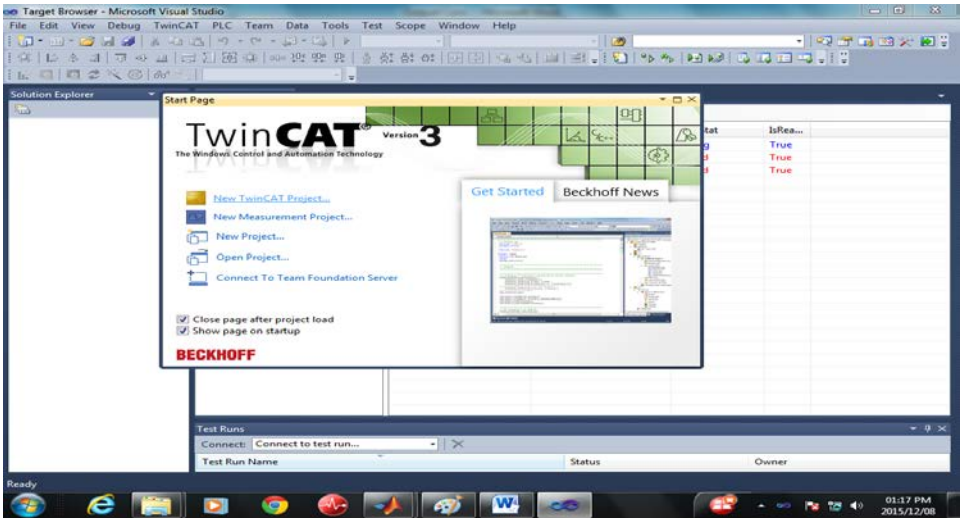

Figure 7.10: Snapshot of the TwinCAT Microsoft visual studio platform

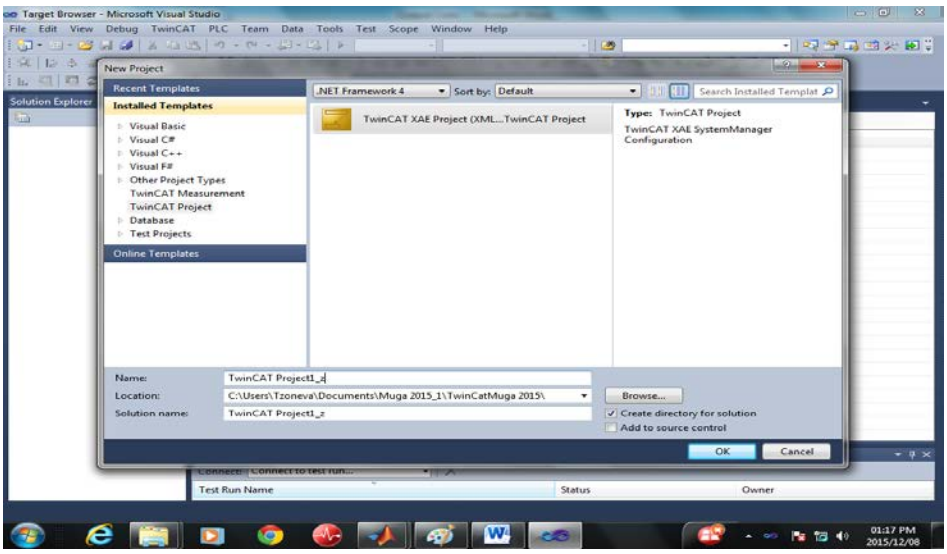

Figure 7.11: Snapshot for creating new TwinCAT project in the visual studio platform

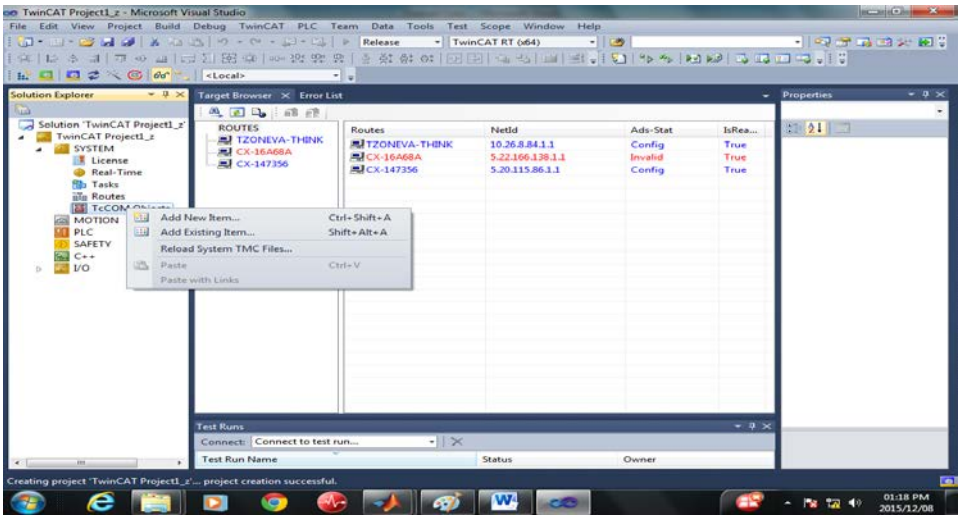

Figure 7.12: Snapshot for adding new TcCOM object

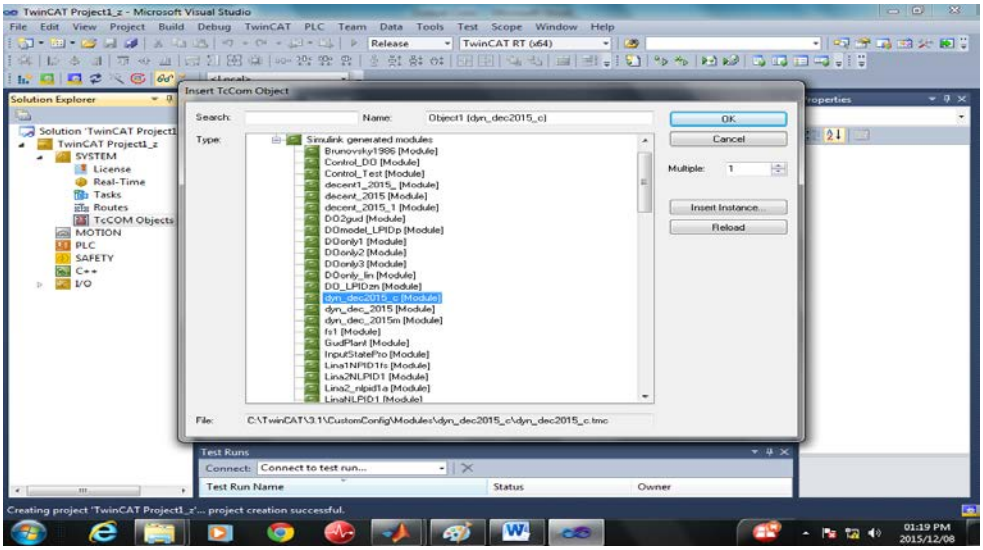

Figure 7.13: Snapshot for test running TcCOM object

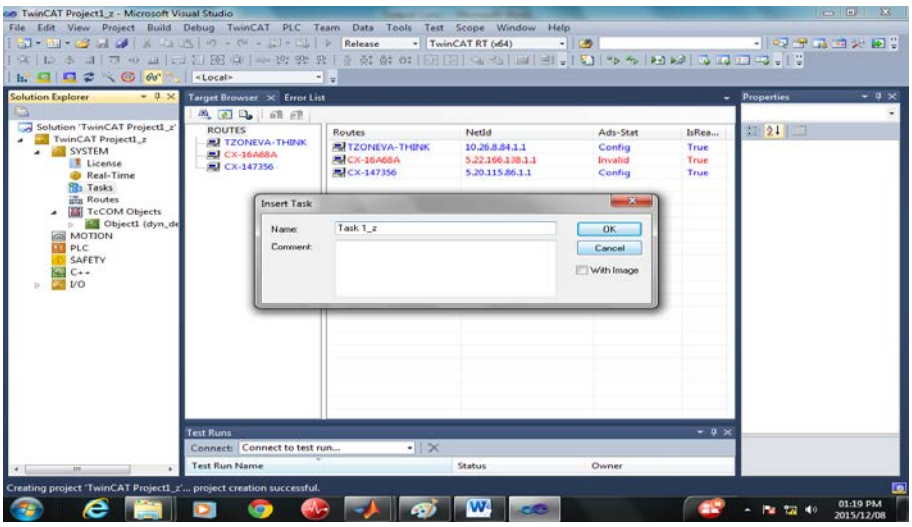

Figure 7.14: Snapshot for linking the TcCOM object to the local PLC

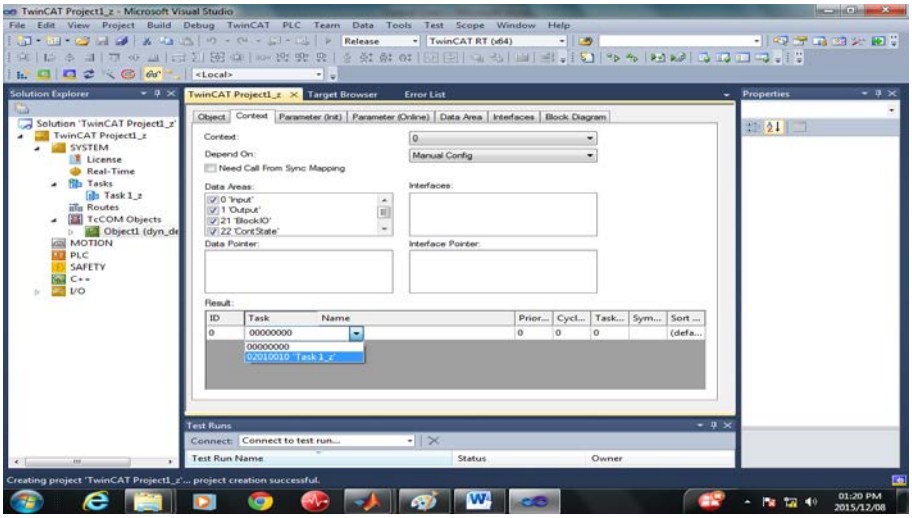

Figure 7.15: Snapshot for linking the TcCOM object to the task

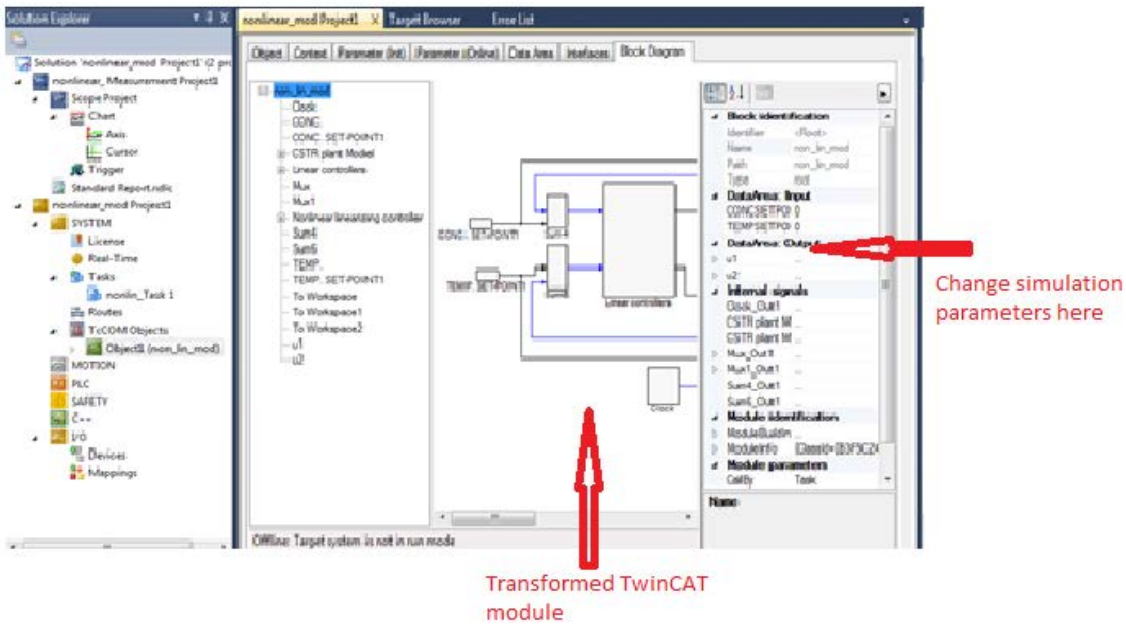

Figure 7.16: Snapshot of the TwinCAT project in Microsoft visual studio platform

In the following, results from the block diagram transformation between the Matlab/Simulink environments to Beckhoff TwinCAT 3.1 environment for the real-time implementation of the developed algorithms of Chapters4, 5, and 6 is presented

7.5 Closed loop control transformations and results of real-time simulations

The main aim of this chapter is to show how the closed loop control systems for the $2x2$ MIMO CSTR process developed in Chapters 4, 5, and 6 could be transformed to TwinCAT 3.1 software environment and then to be deployed to the Beckhoff CX5020 PLC for real-time execution of the control applications under various set point conditions and/or disturbances. Simulation results are used to show the performance of the designed controllers in real-time situations. First the performances of the decoupling controllers are tested. Then the performances of the decentralized controllers are presented, followed by the input-output linearization controller, and finally a comparison of the methods is presented.

7.5.1 Dynamic decoupling control simulation in Real-time environment

In line with the steps listed in section 7.4 above, the control algorithms of the dynamic decoupling developed in Chapter 4 are used for real-time implementation by downloading the algorithms closed loop system to the Beckhoff CX5020 PLC for real-time execution to verify the effectiveness of the control schemes under real-time environment. The following are the real-time simulation results from the experiments investigated.

7.5.1.1 Model transformation and set-point tracking control for the decoupling closed loop system with the decoupling controllers

Figure 7.17 shows the transformed Simulink closed loop MIMO CSTR process under dynamic control to the corresponding TwinCAT 3 function blocks (modules). The transformation technique shows that the data and parameter connection are the same in these two platforms and therefore there is a one to one correspondence of function blocks between Simulink and TwinCAT 3.1.

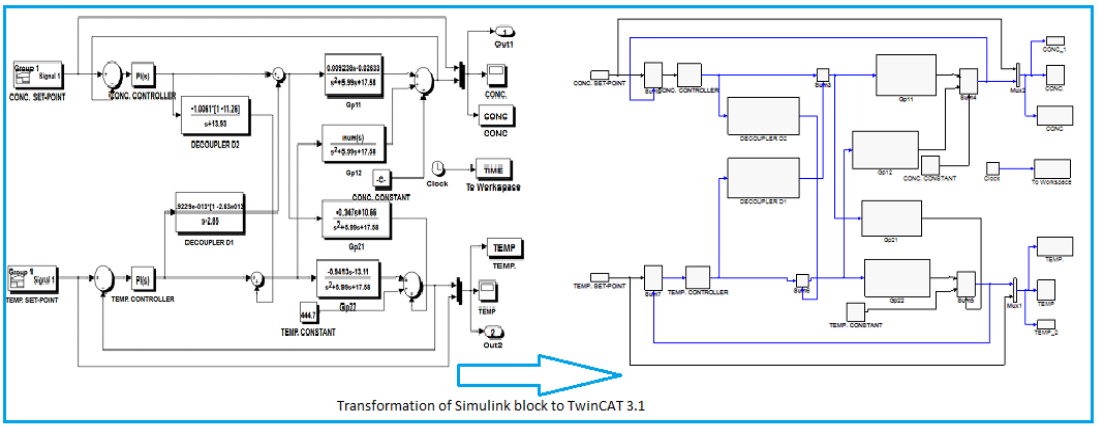

Figure 7.17: Transformed Simulink closed loop model under dynamic decoupling to TwinCAT 3 function blocks

Next, investigations are made for set point tracking for both the concentration and the temperature responses respectively. Figures 7.18-7.23 are the various step responses for the concentration set-point tracking control when the set point is varied from 0.08 moles/litre to 0.13 moles/litre.

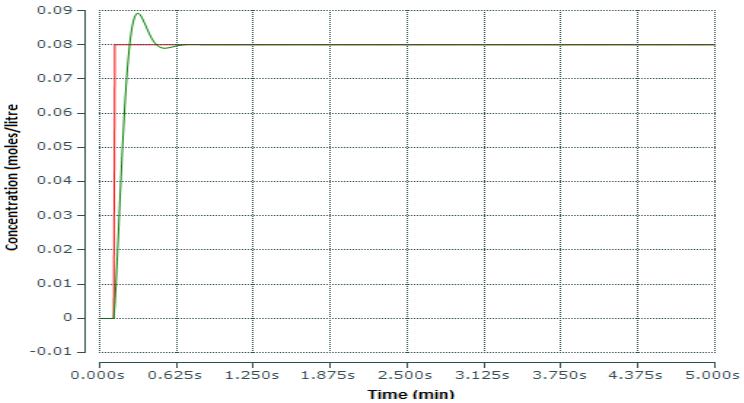

Figure 7.18: Concentration tracking of a set-point of 0.08 moles/litre

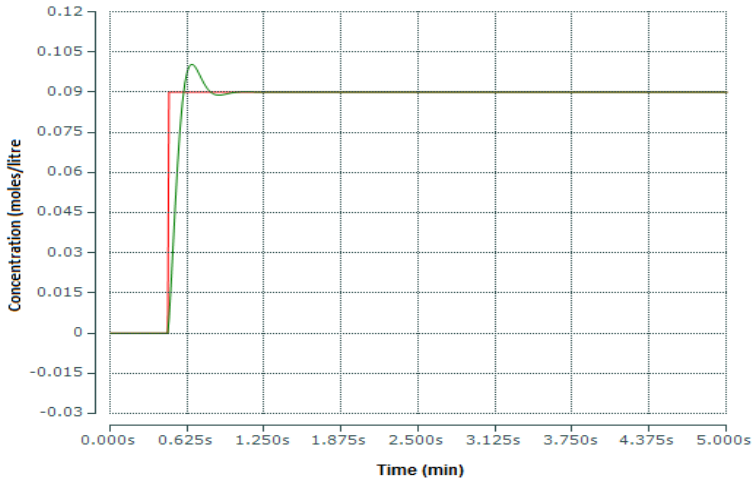

Figure 7.19: Concentration tracking of a set-point of 0.09 moles/litre

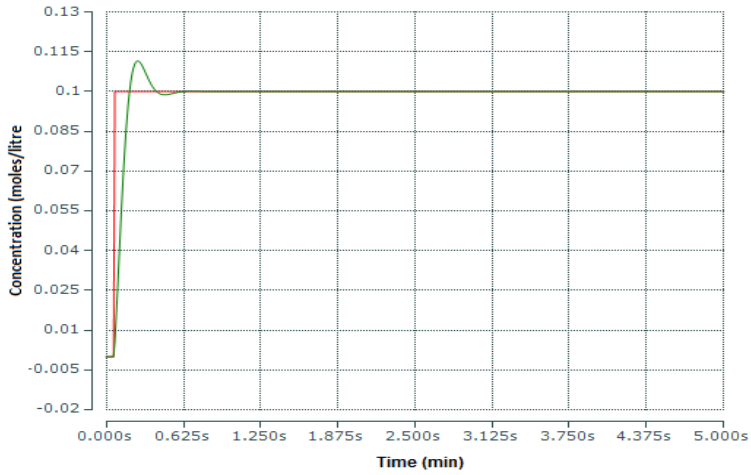

Figure 7.20: Concentration tracking of a set-point of 0.1 moles/litre

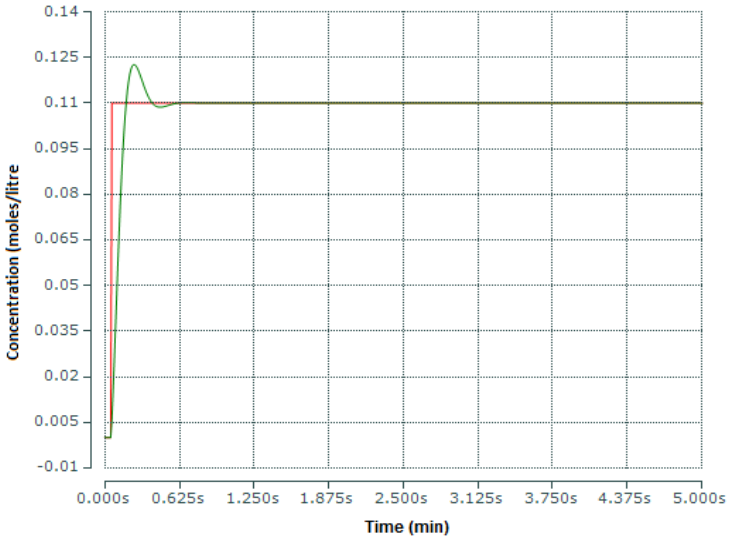

Figure 7.21 Concentration tracking of a set-point of 0.11 moles/litre

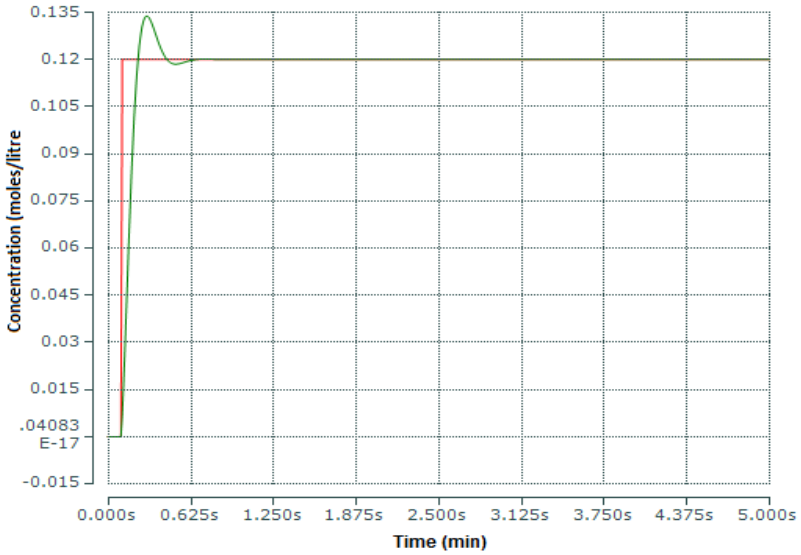

Figure 7.22: Concentration tracking of a set-point of 0.12 moles/litre

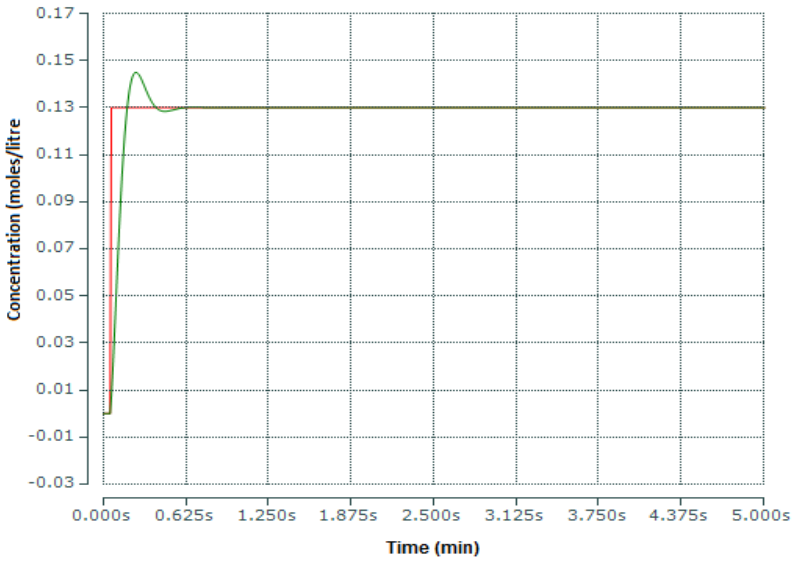

Figure 7.23 Concentration tracking of a set-point of 0.13 moles/litre

Analyses of the obtained figures, further confirms that the designed dynamic decoupling controller settings achieve tracking control of the concentration set point in real-time situation and therefore the control design is good.

7.5.2.1 Investigation of the process performance for a disturbance on the concentration control loop

Next, the effects of disturbances are investigated for the concentration control loop in real-time. The procedure adopted is the same as that for the concentration control loop in Chapter 4. The difference is that this time the investigation is done on a real-time platform. The disturbances are injected to the main concentration control loop at the output y_1 as well as to the control inputs u_1 The TwinCAT functional block diagram with a disturbance at the output y_1 is llustrated in Figure 7.24. Figures 7.25-7.32 are the responses when the effects of the disturbances are at y_1.

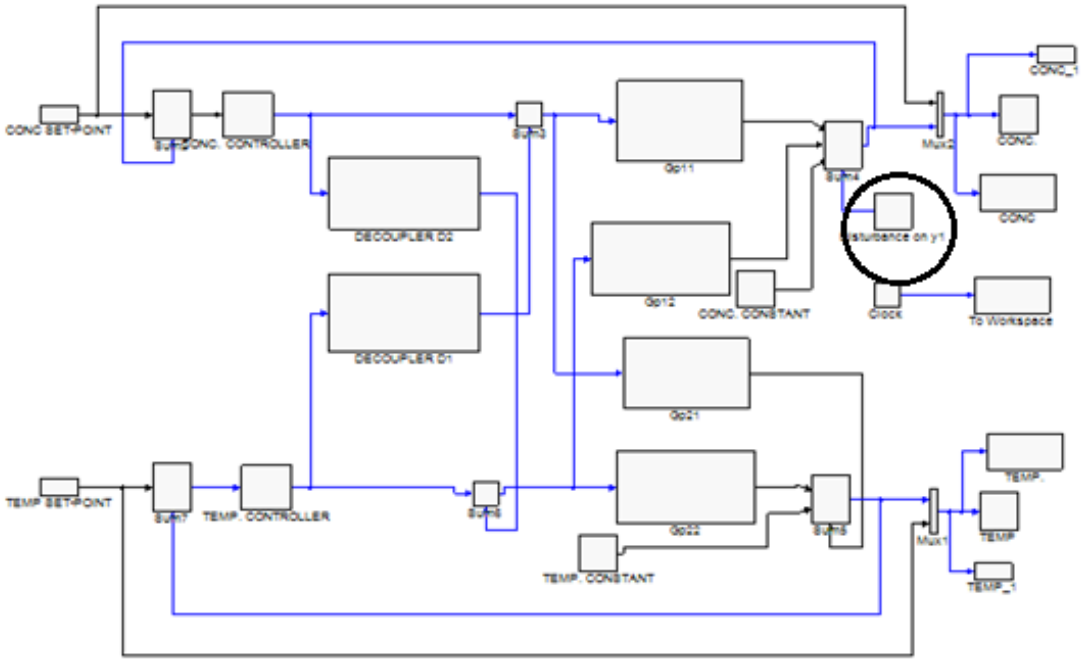

Figure 7.24: TwinCAT 3 dynamic function blocks module for the CSTR closed loop with decoupled control system with disturbance on y_1

The set-point selected for the investigation is 0.13 moles/litre.

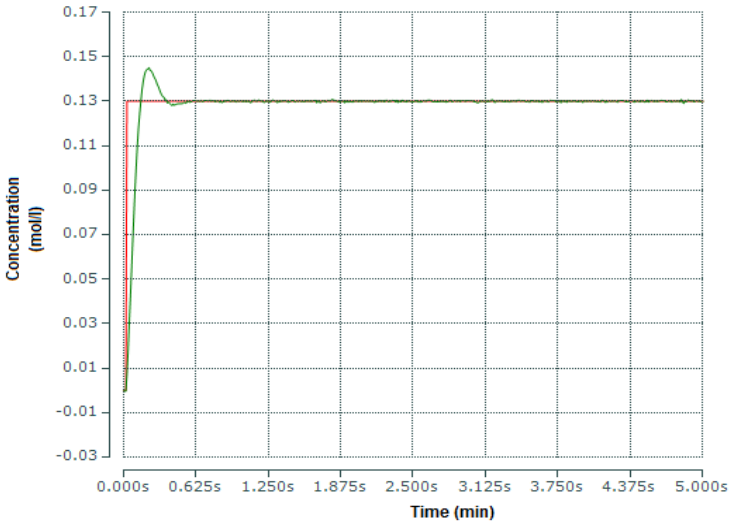

Figure 7.25: Set-point tracking under $\pm 1e^{-3}$ moles/litre disturbance on y_1

Figure 7.26: Set-point tracking under $\pm 4e^{-3}$ moles/litre disturbance on y_1

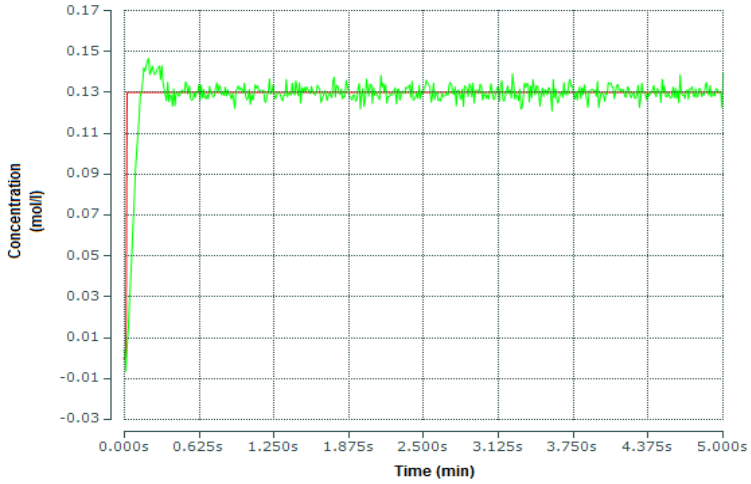

Figure 7.27: Set-point tracking under ± 0.01 moles/litre disturbance on y_1

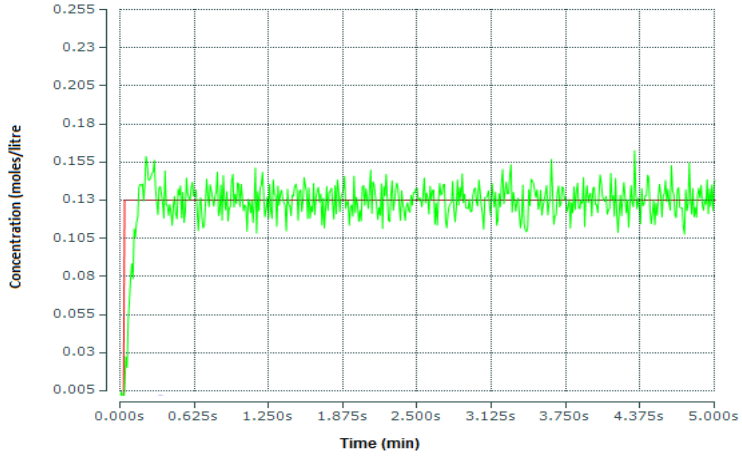

Figure 7.28: Set-point tracking under ± 0.04 moles/litre disturbance on y_1

As can be seen from the responses, good tracking control is still achieved. However as the magnitude of the disturbance is increased, the response becomes noisy. This correlates very well with the findings reported in Chapter 4. Next, the effect of disturbances on u_1 is considered.

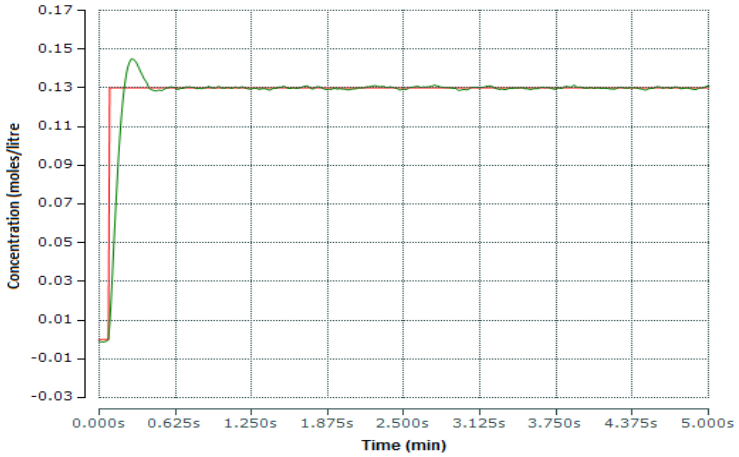

Figure 7.29 Concentration Set-point tracking under ± 10 litres/min disturbance on u_1

Figure 7.30: Concentration Set-point tracking under ± 40 litres/min disturbance on u_1

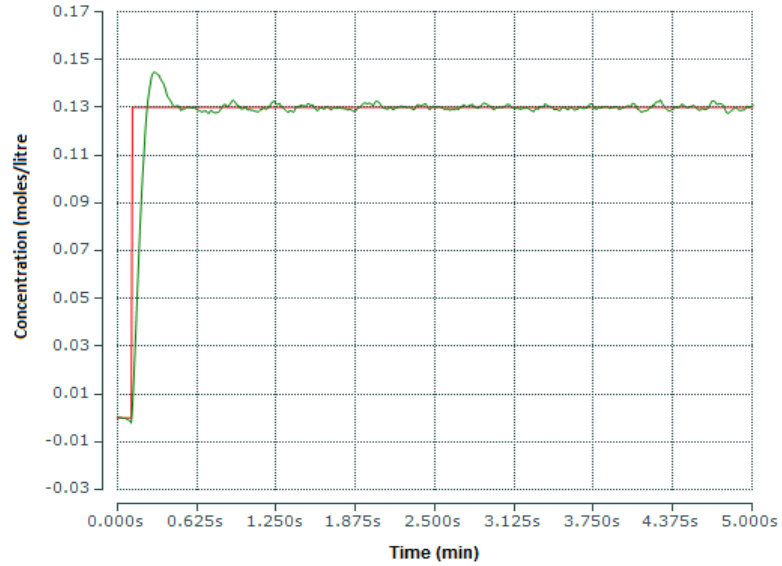

Figure 7.31: Concentration Set-point tracking under ± 80 litres/min disturbance on u_1

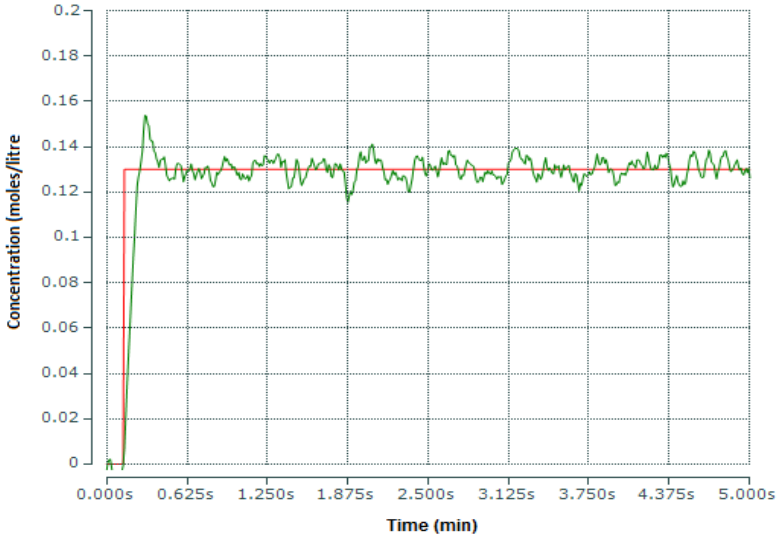

Figure 7.32: Concentration Set-point tracking under ± 100 litres/min disturbance on u_1

Figures 7.33 to 7.36 represent the responses for the concentration set-point tracking under the influence of the disturbances on u_1 for the considered cases. The results of the real-time simulation show that the magnitude of the disturbance is important for smooth set-point tracking. However the concentration control system is still capable of tracking the set-point variations implying that the designed decoupling systems is good at rejecting the random variations in the control signal u_1 when the CSTR closed loop system is run on real-time.

Similarly, the performances of the concentration control loop signal y_1 real-time when the disturbances are in u_2 and y_2 are investigated. Figures 7.33-7.36 are the graphs

of the responses of the concentration control loop signal y_1 when there are disturbances of different magnitudes on y_2.

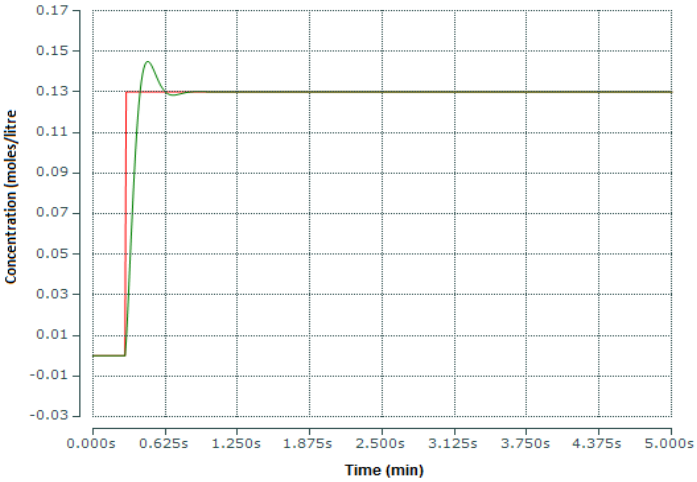

Figure 7.33: Concentration Set-point tracking under $\pm 4K$ disturbance on y_2

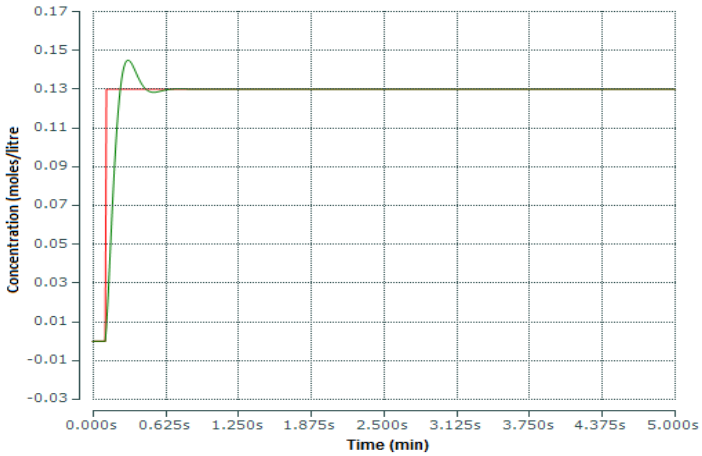

Figure 7.34: Concentration Set-point tracking under $\pm 8K$ disturbance on y_2

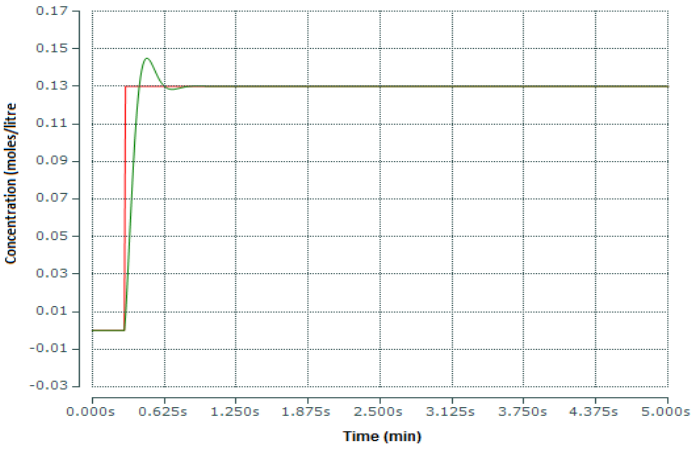

Figure 7.35: Concentration Set-point tracking under $\pm 10K$ disturbance on y_2

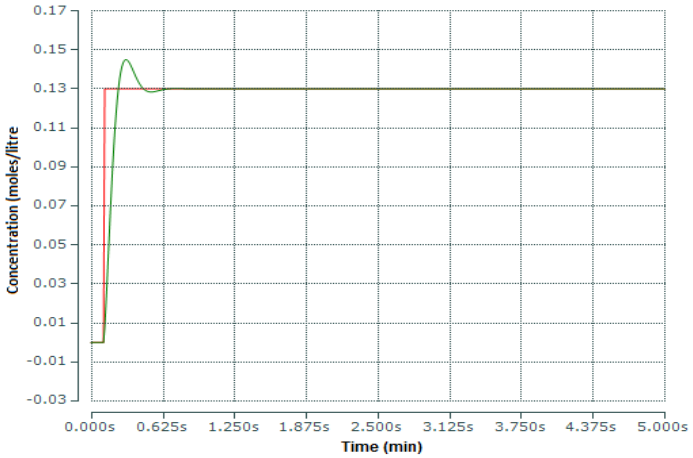

Figure 7.36: Concentration Set-point tracking under $\pm 20K$ disturbance on y_2

From the real-time simulations, as represented by Figures 7.33-7.36, disturbances on the output y_2 have negligible effect on the concentration real-time set-point tracking. Good results are achieved. Similarly, the performances of the concentration control loop signal y_1 in real-time when the disturbances are in u_2 are investigated. Figures 7.37-7.40 show the graphs of the responses of the concentration control loop signal y_1 when there are disturbances of different magnitudes on u_2.

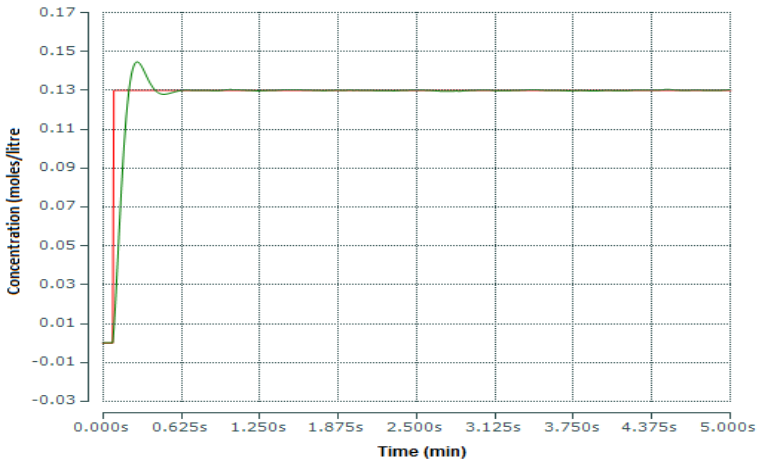

Figure 7.37: Concentration Set-point tracking under ± 10 litres/min disturbance on u_2

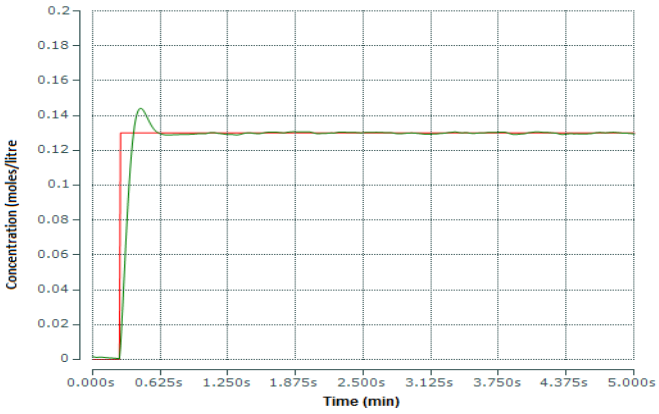

Figure 7.38: Concentration Set-point tracking under ± 40 litres/min disturbance on u_2

Figure 7.39: Concentration Set-point tracking under ± 80 litres/min disturbance on u_2

Figure 7.40: Concentration Set-point tracking under ± 100 litres/min disturbance on u_2

Next the results for temperature loop real-time simulation are presented in the section that follows.

7.5.2.2 Temperature loop results from simulation for various set-points and disturbances

The variation of set-points magnitude influence over the temperature response performance indices is investigated. The set-point is varied from $450K$ to $465K$ in steps of $5K$

The responses are illustrated in Figures 7.41-7.44 below.

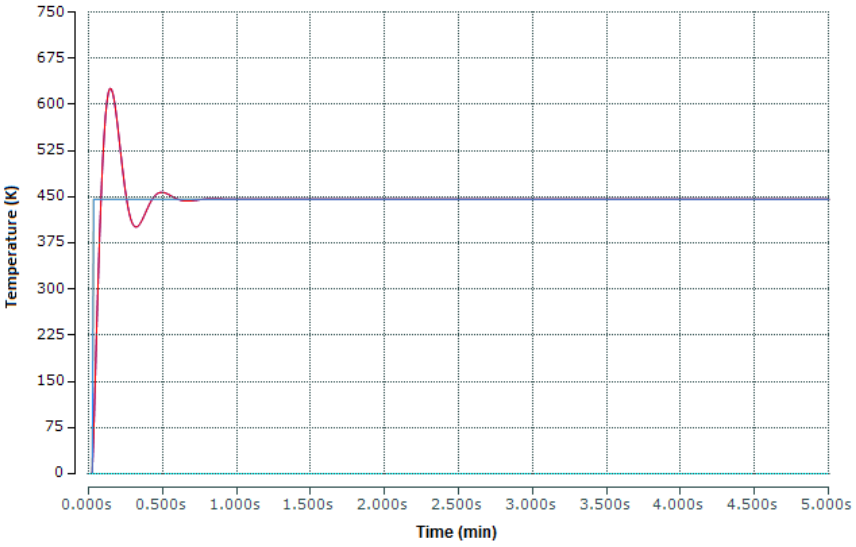

Figure 7.41: Temperature Set-point of $450K$ tracking

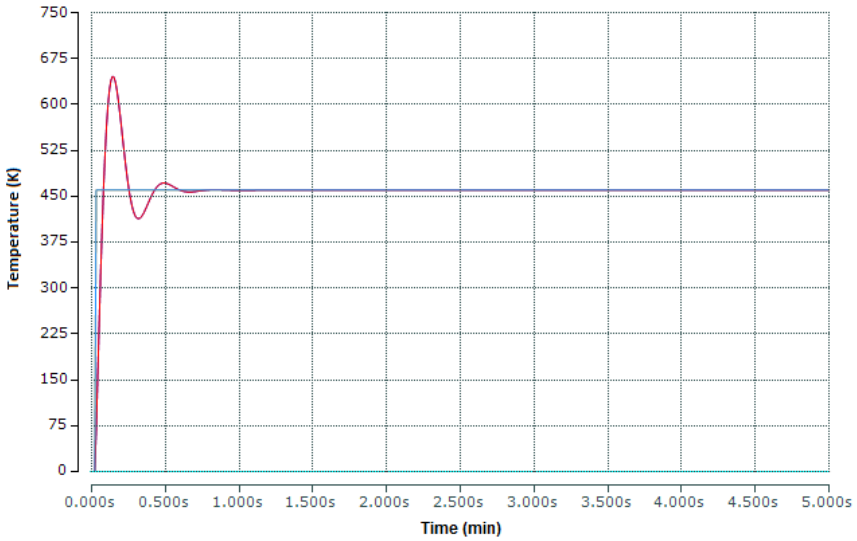

Figure 7.42: Temperature Set-point of $455K$ tracking

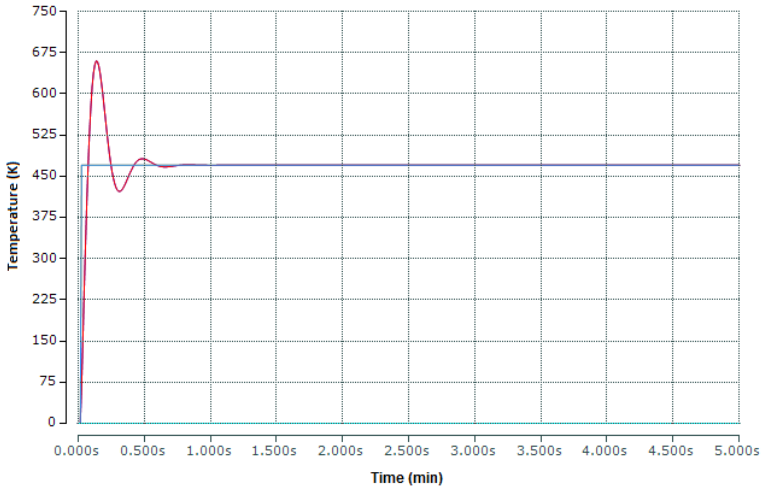

Figure 7.43: Temperature Set-point of $460K$ tracking

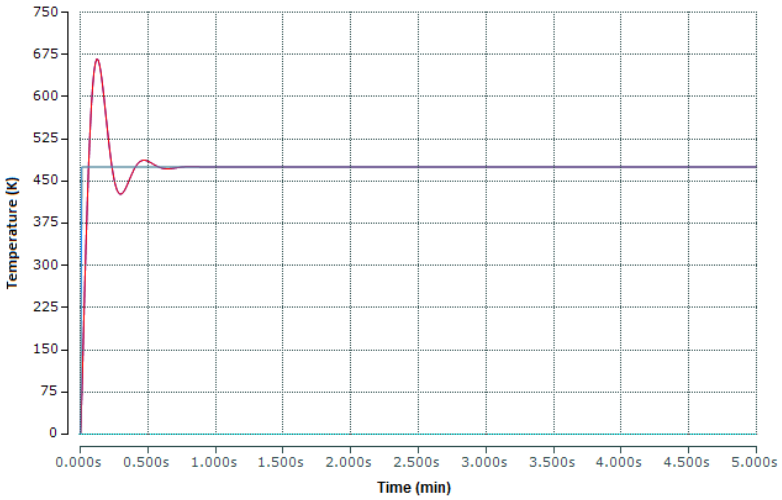

Figure 7.44: Temperature Set-point of $465K$ tracking

The results show that a part from high percentage overshoots; the other performance indices are good, hence successful temperature set-point tracking is achieved for real-time simulation. A comparative analysis with the results presented in Chapter 4 for the closed loop system under decoupling control, shows that the overshoot has increased but the performance indices remain the same. The results of comparison is given in Table 7.2

Table 7.2: Comparison between the performance indicators of the closed loop concentration and temperature responses under the Matlab/Simulink and the TwinCAT PLC real-time for various magnitudes

closed loop concentration performance indices								
	Matlab/Simulink				TwinCAT PLC real-time			
Set-point value	Rise time t_r (sec)	Settling time t_s (sec)	Peak over shoot M_p (%)	Steady state error e_{ss} (%)	Rise time t_r (sec)	Settling time t_s (sec)	Peak over shoot M_p (%)	Steady state error e_{ss} (%)
0.02 Moles/litre.	7.62	27.18	9.58	0	4.25	33	11.0	0
0.04 Moles/litre	7.62	27.18	9.58	0	4.25	33	11.0	0
0.06 Moles/litre	7.62	27.18	9.58	0	4.25	33	11.0	0
0.08 Moles/litre	7.62	27.18	9.58	0	4.25	33	11.0	0
0.1Moles/litre	7.62	27.18	9.58	0	4.25	33	11.0	0
0.12 Moles/litre	7.62	27.18	9.58	0	4.25	33	11.0	0
0.14 Moles/litre	7.62	27.18	9.58	0	4.25	33	11.0	0
closed loop temperature performance indices								
	Matlab/Simulink			TwinCAT PLC real-time				
Set-point value	Rise time t_r (sec)	Settling time t_s (sec)	Peak over shoot M_p (%)	Steady state error e_{ss} (%)	Rise time t_r (sec)	Settling time t_s (sec)	Peak over shoot M_p (%)	Steady state error e_{ss} (%)
435K.	2.79	30	28.2	0	2.79	30	41.9	0
440K	2.79	30	28.2	0	2.79	30	41.9	0
446K	2.79	30	28.2	0	2.79	30	41.9	0
450K	2.79	30	28.2	0	2.79	30	41.9	0
455K	2.79	30	28.2	0	2.79	30	41.9	0
460K	2.79	30	28.2	0	2.79	30	41.9	0
465K	2.79	30	28.2	0	2.79	30	41.9	0

Next, the performance of the temperature loop under the influence of the disturbances on, y_1, u_1 and u_2 are considered because of the interactions that exist in the closed loop system. Figures 7.45-7.48 present the temperature responses for disturbance on y_1. The set-point to be tracked is $450K$ for all considered disturbances

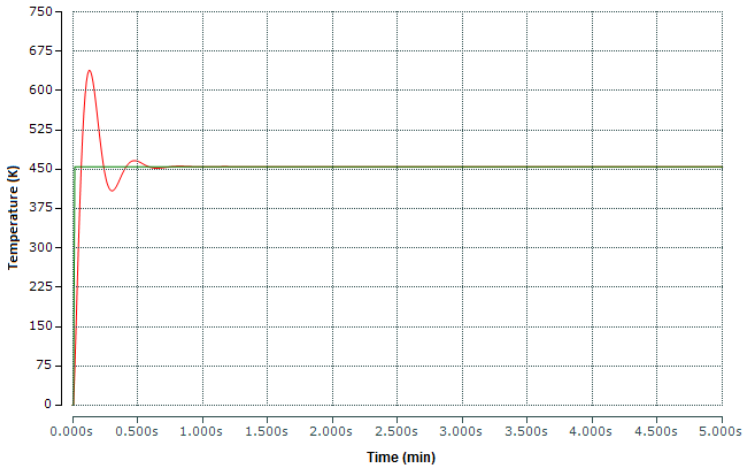

Figure 7.45: Temperature Set-point tracking under $\pm 1e^{-3}$ mole/litre disturbance on y_1

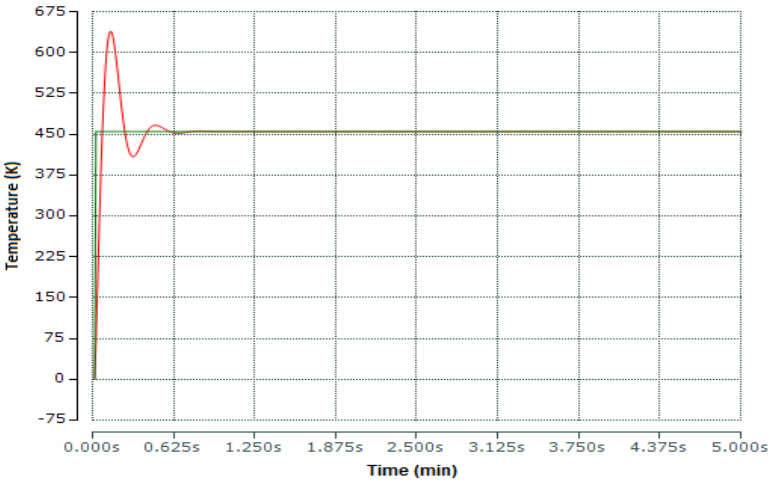

Figure 7.46: Temperature Set-point tracking under $\pm 4e^{-3}$ mole/litre disturbance on y_1

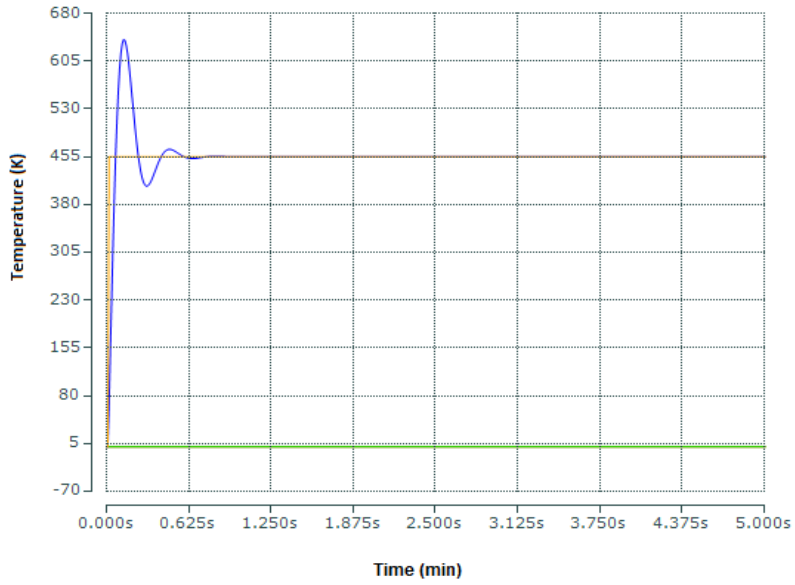

Figure 7.47: Temperature Set-point tracking under ± 0.01 mole/litre disturbance on y_1

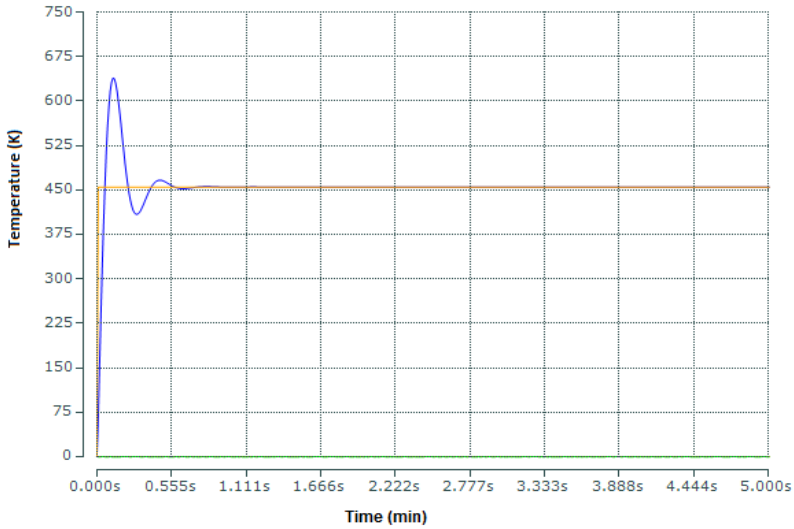

Figure 7.48: Temperature Set-point tracking under ± 0.04 mole/litre disturbance on y_1

Good set-point tracking control is realised in real-time. The disturbance on y_1 do not degrade the performance of the temperature loop y_2. Similarly, the performances of the temperature control loop signal (y_2) when the disturbances are in the junction u_1 are investigated. Figures 7.49-7.52 show the graphs of the responses of the temperature control loop signal y_2 when there are disturbances on u_1 of different magnitudes.

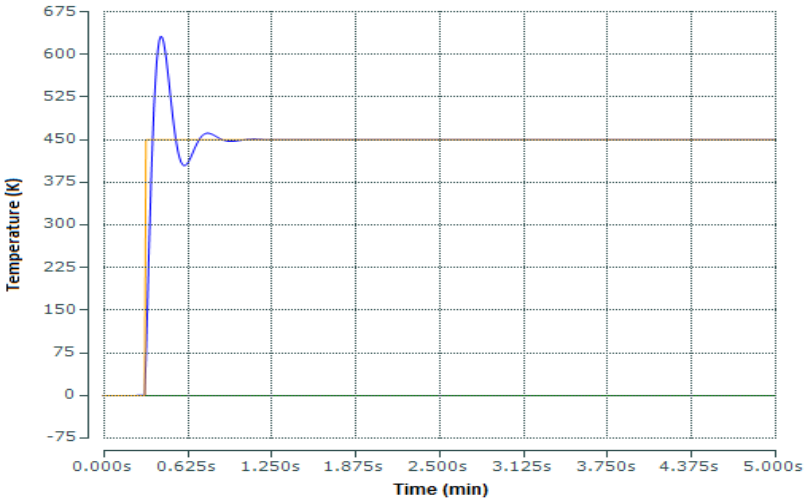

Figure 7.49: Temperature Set-point tracking under ± 10 litres/min disturbance on u_1

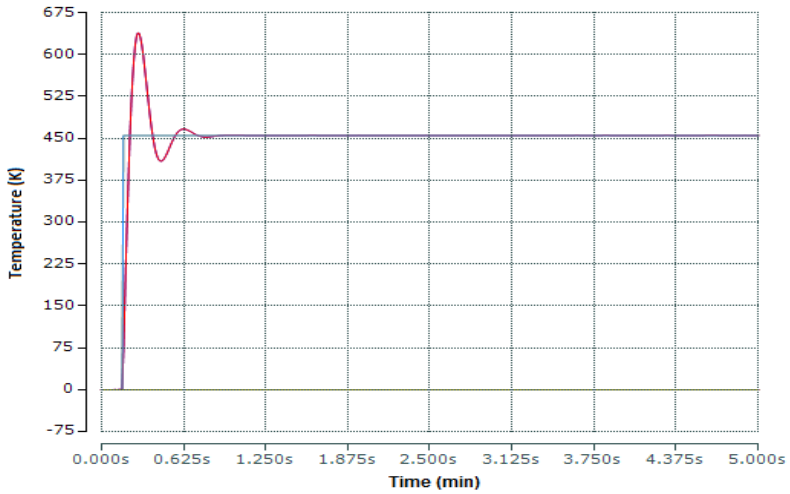

Figure 7.50: Temperature Set-point tracking under ± 40 litres/min disturbance on u_1

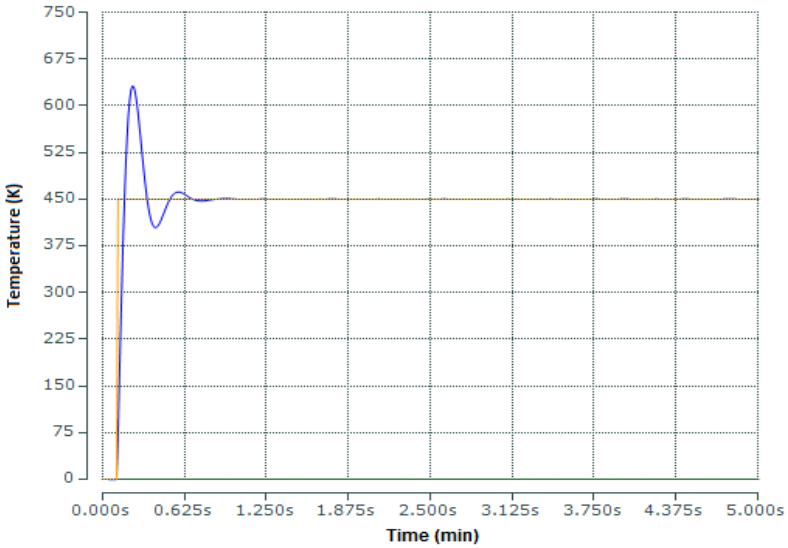

Figure 7.51: Temperature Set-point tracking under ± 80 litres/min disturbance on u_1

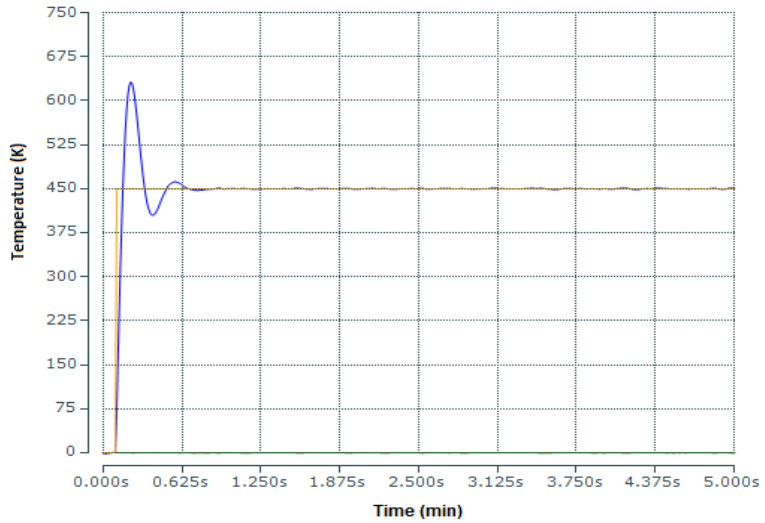

Figure 7.52: Temperature Set-point tracking under ± 100 litres/min disturbance on u_1

Figures 7.49-7.52 present the graphs of the real-time responses of the temperature control loop signal y_2 when there are disturbances on u_1 of different magnitudes. Good tracking response is achieved.

Next the disurbance on the temperature loop effects over the temperature loop real-time behaviour is presented in the section that follows. The first investigation done is when the disturbance is on the main loop output signal y_2

The responses of Figures 7.53-7.56 show the set point tracking performance of the temperature for various settings of the disturbance magnitudes.

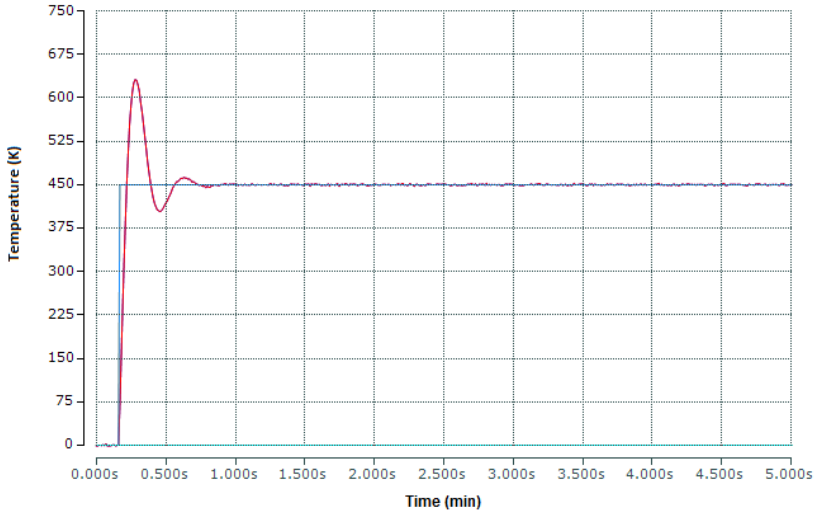

Figure 7.53: Temperature Set-point tracking under $\pm 4K$ disturbance on y_2

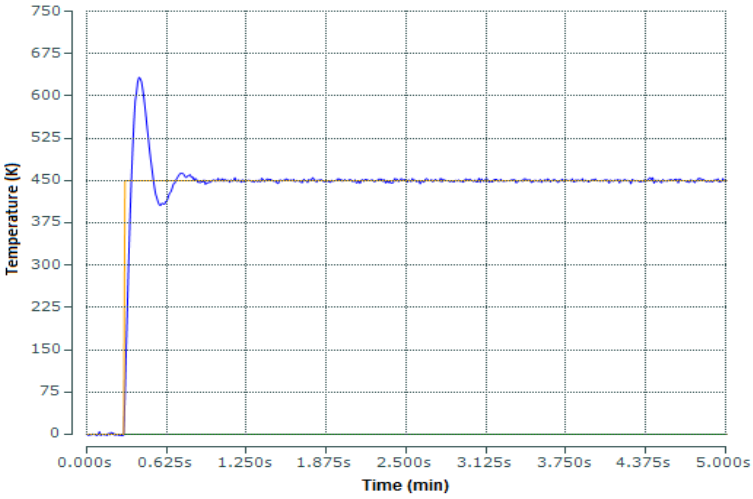

Figure 7.54: Temperature Set-point tracking under $\pm 8K$ disturbance on y_2

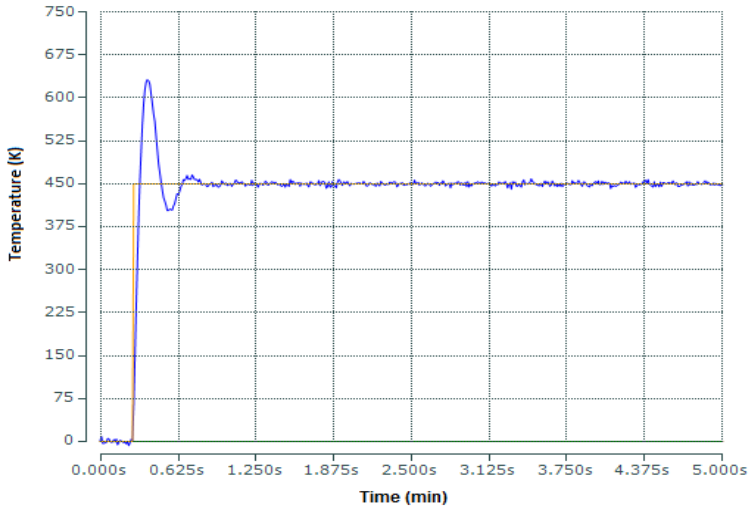

Figure 7.55: Temperature Set-point tracking under $\pm 10K$ disturbance on y_2

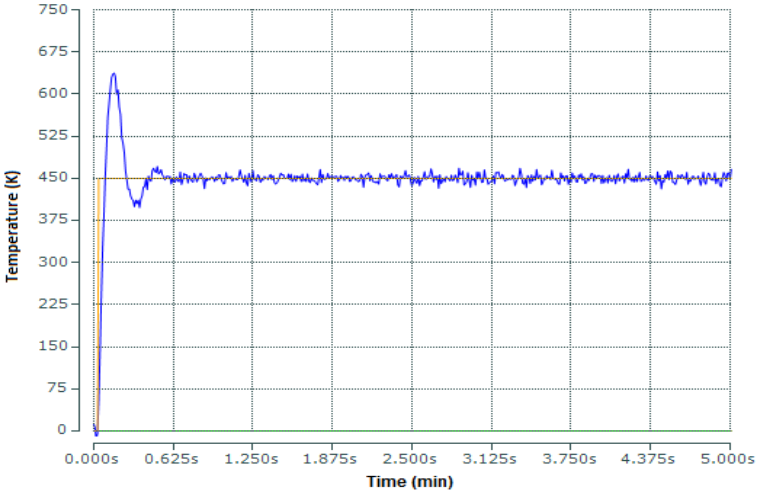

Figure 7.56: Temperature Set-point tracking under $\pm 20K$ disturbance on y_2

Good set-point tracking in real-time control is still achieved. However as the magnitude of the disturbance is increased, the response becomes noisy.

Similar investigation is done for disturbances on the control signal u_2 and the real-time responses as a result of real time simulations are illustrated in Figures 7.57-7.60 below.

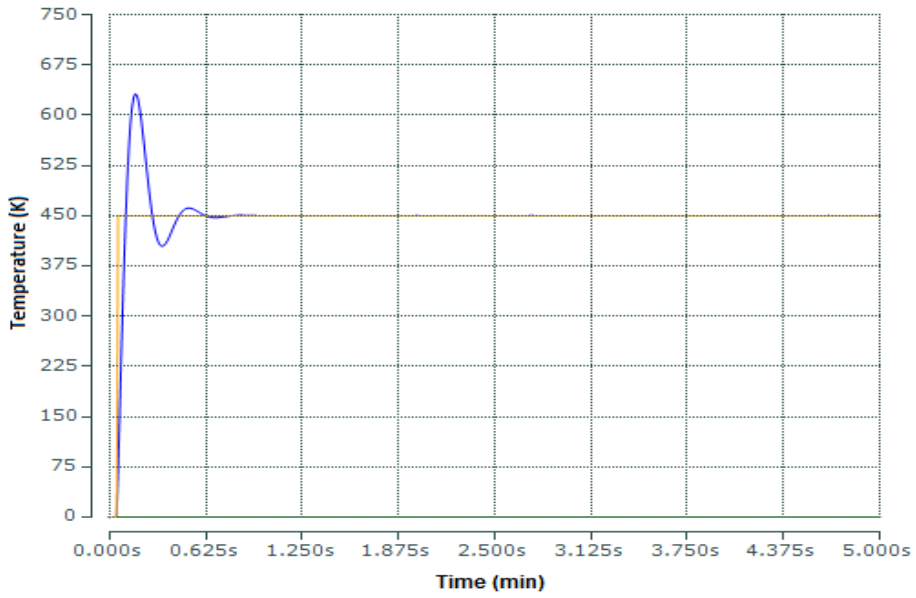

Figure 7.57: Temperature Set-point tracking under ± 10 litres/min disturbance on u_2

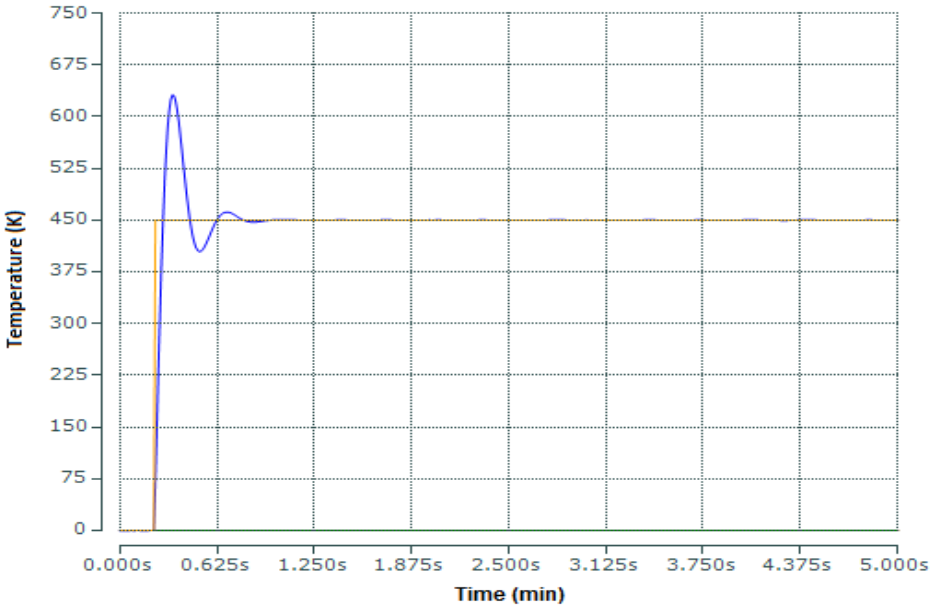

Figure 7.58: Temperature Set-point tracking under ± 40 litres/min disturbance on u_2

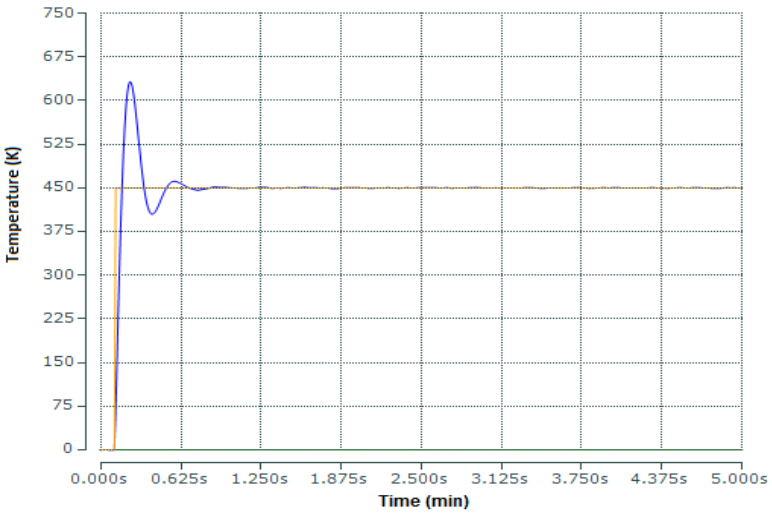

Figure 7.59: Temperature Set-point tracking under ± 80 litres/min disturbance on u_2

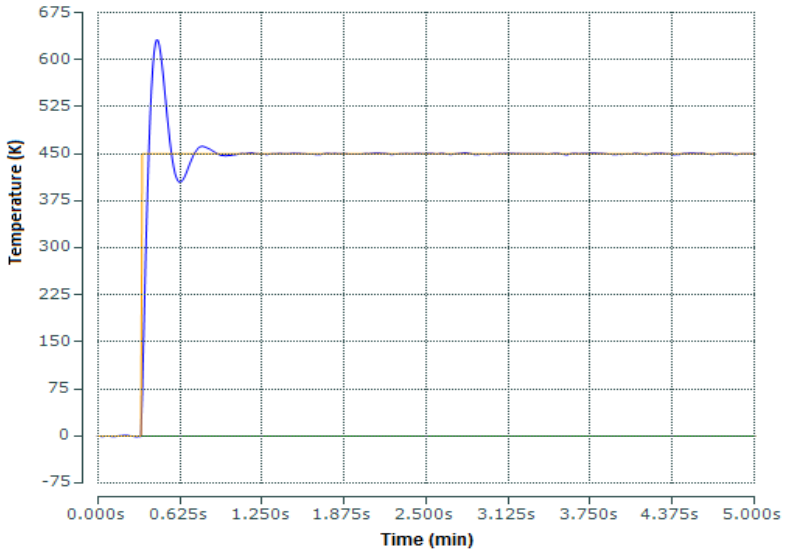

Figure 7.60: Temperature Set-point tracking under ± 100 litres/min disturbance on u_2

Very little effect of disturbance is observed in the performance characteristics of the temperature tracking response during the real-time simulation. Good tracking capability is observed. The only limitation is the percentage overshoot.

7.5.3 Decentralized control simulation in Real-time

Based on the transformation algorithm listed in section 7.4 above, the algorithms of the decentralized control methodology developed in Chapter 5 are used for real-time implementation by downloading the algorithms to the Beckhoff CX5020 PLC for real-time execution to verify the effectiveness of the control schemes under real-time environment.

7.5.3.1 Model transformation and set-point tracking control for the decentralized closed loop system

Figure 7.61: shows the transformed Simulink closed loop MIMO CSTR process under decentralized control to the corresponding TwinCAT 3 function blocks (modules). The transformation technique shows that the data and parameter connection are the same in these two platforms and therefore there is a one to one correspondence of function blocks between Simulink and TwinCAT platforms.

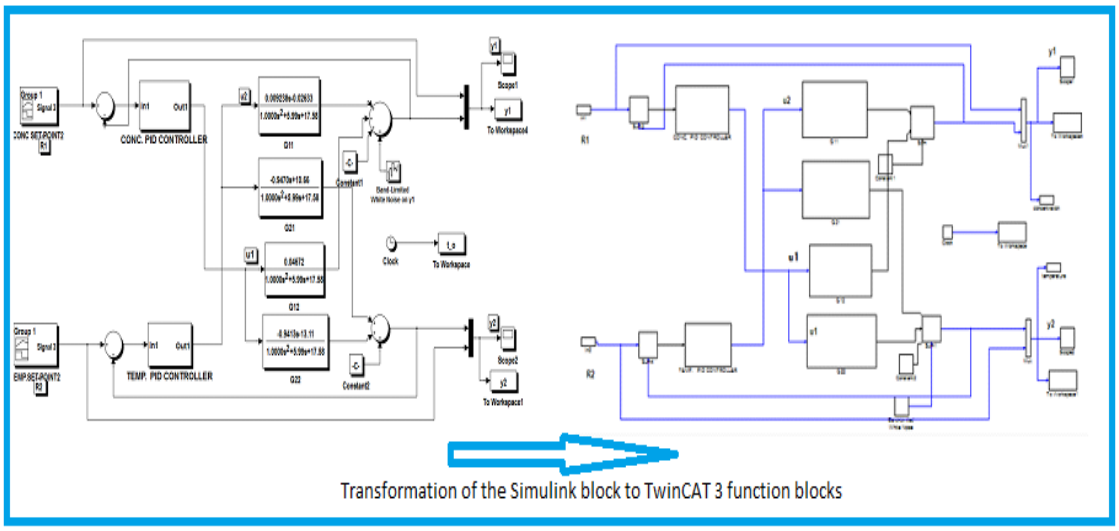

Figure 7.61: Transformed Simulink decentralized closed loop control system to TwinCAT 3 function blocks

Next, investigations are made of set point tracking control for both the concentration and the temperature respectively. Figures 7.62-7.66 present the various step responses for the concentration set-point tracking when the set point is varied from 0.09 moles/litre to 0.13 moles/litre

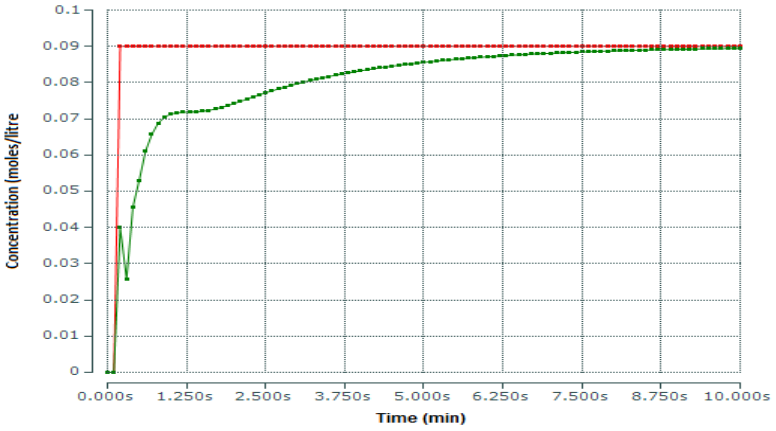

Figure 7.62: Concentration set-point of 0.09 moles/litre tracking

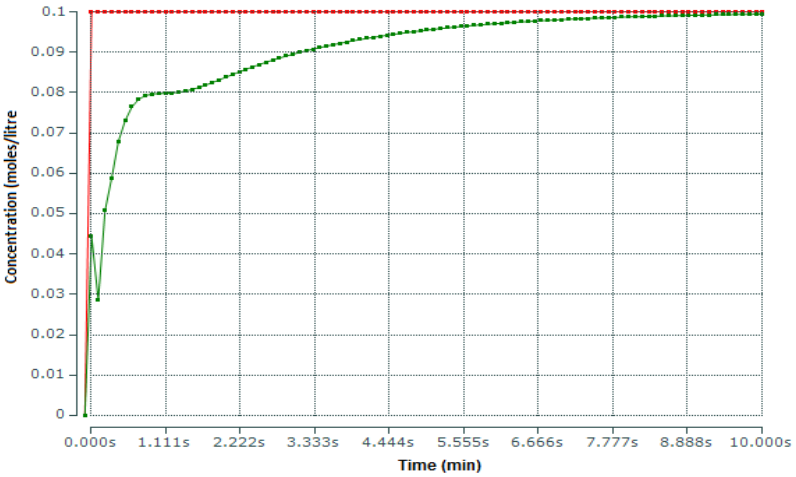

Figure 7.63: Concentration set-point of 0.1 moles/litre tracking

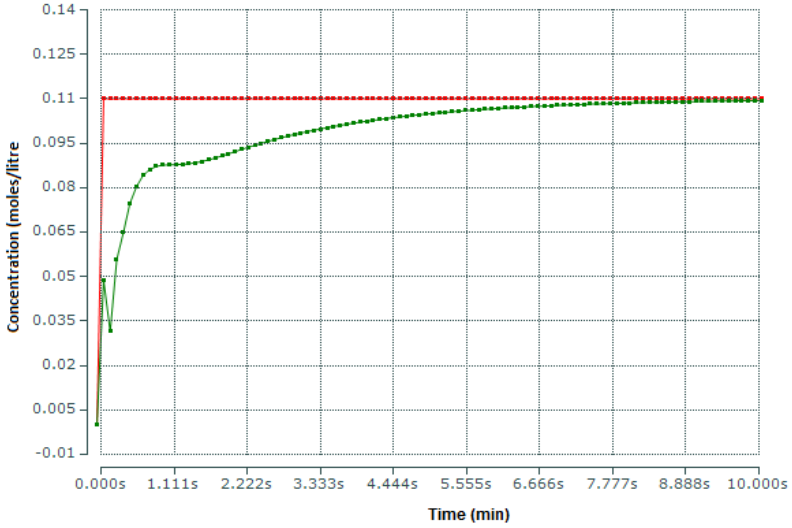

Figure 7.64: Concentration set-point of 0.11 moles/litre tracking

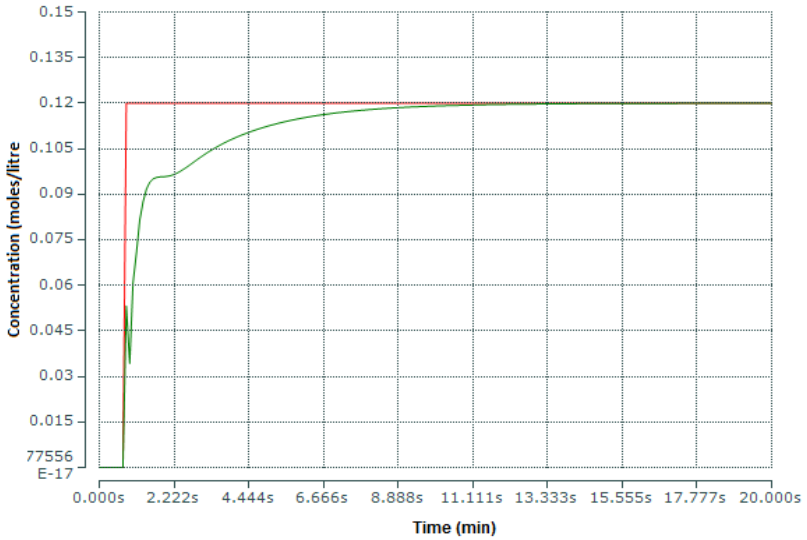

Figure 7.65: Concentration set-point of 0.12 moles/litre tracking

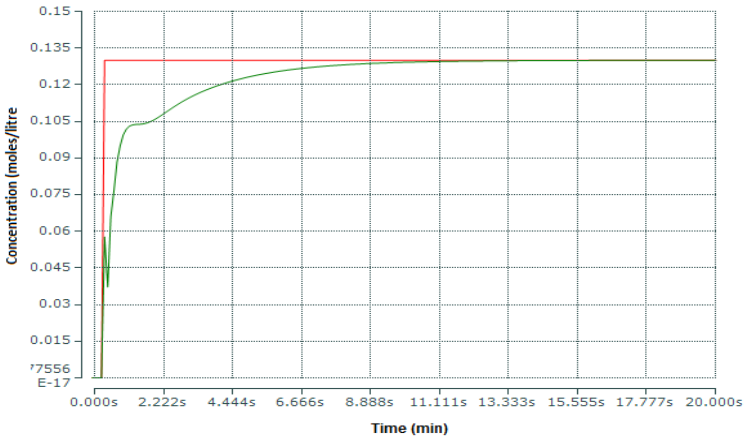

Figure 7.66: Concentration set-point of 0.13 moles/litre tracking

Analyses of the obtained transition behaviours, further confirms that the designed decentralized controller settings achieve tracking control of the concentration set point in real-time and therefore the control design is good. As can be seen the set-point tracking response capabilities for the concentration outputs at different set-point settings are achieved, though the responses are sluggish. Investigations on the influences of various magnitudes of disturbances over the process output step response in real-time are also performed for the developed scheme and presented in the following subsection

7.5.3.2 Investigation of the process performance for a disturbance on concentration control loop.

Next, the effects of disturbances are investigated for the concentration control loop in real time. The procedure adopted is the same as that for the concentration control loop in Chapter 5. The difference is that, this time the investigation is done on a real-time platform. The disturbances are injected to the main concentration control loop at the outputs y_1. Figures 7.67-7.70 show the real-time responses of the concentration when the disturbances are at y_1. The set-point is 0.13 moles/litre.

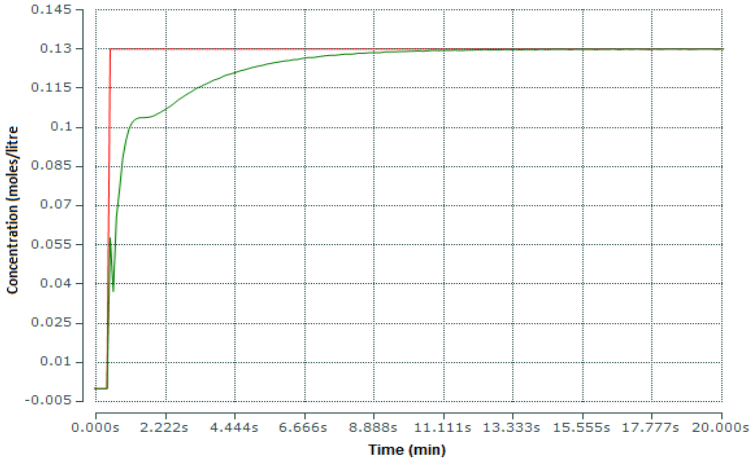

Figure 7.67: Concentration Set-point tracking under $\pm 1e^{-3}$ moles/litre disturbance on y_1

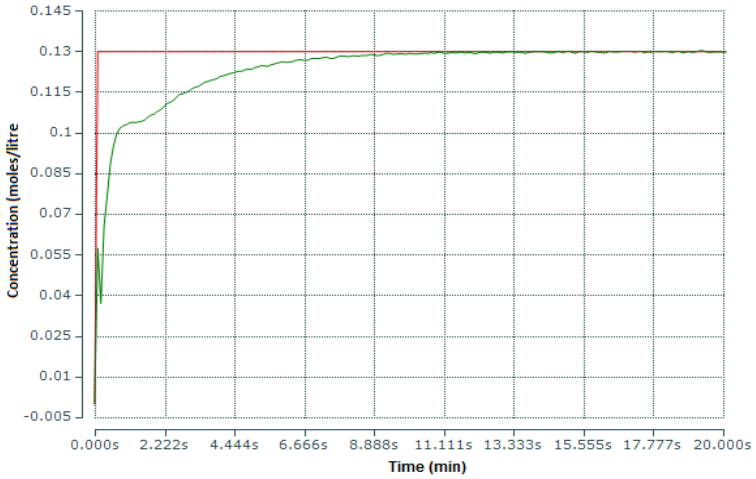

Figure 7.68: Concentration Set-point tracking under $\pm 4e^{-3}$ moles/litre disturbance on y_1

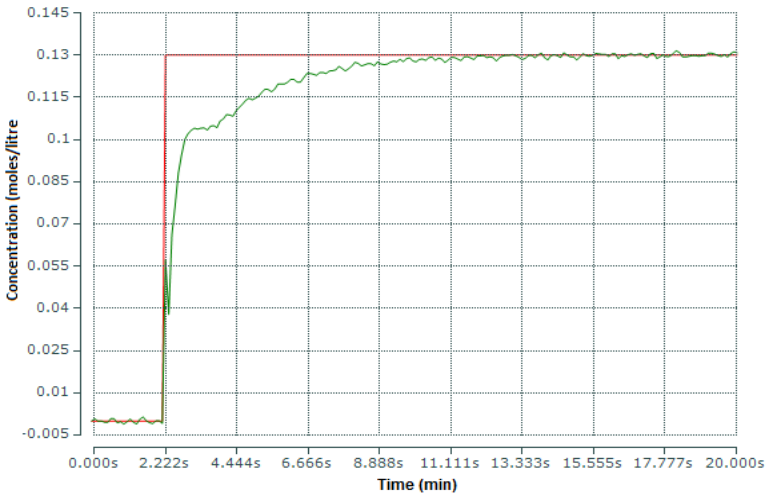

Figure 7.69: Concentration Set-point tracking under ± 0.01 moles/litre disturbance on y_1

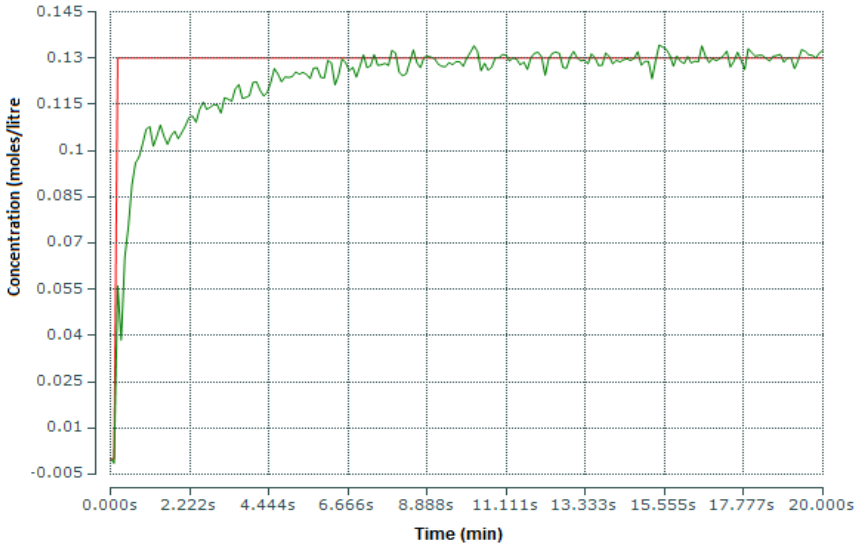

Figure 7.70: Concentration Set-point tracking under ± 0.04 moles/litre disturbance on y_1

Good tracking control is still achieved in the real-time simulation results. However as the magnitude of the disturbance is increased, the response becomes noisy as was investigated in Chapter5.

Next, the effects of the disturbances acting on the temperature output y_2 are investigated. Figures 7.71-7.74 show the real-time responses.

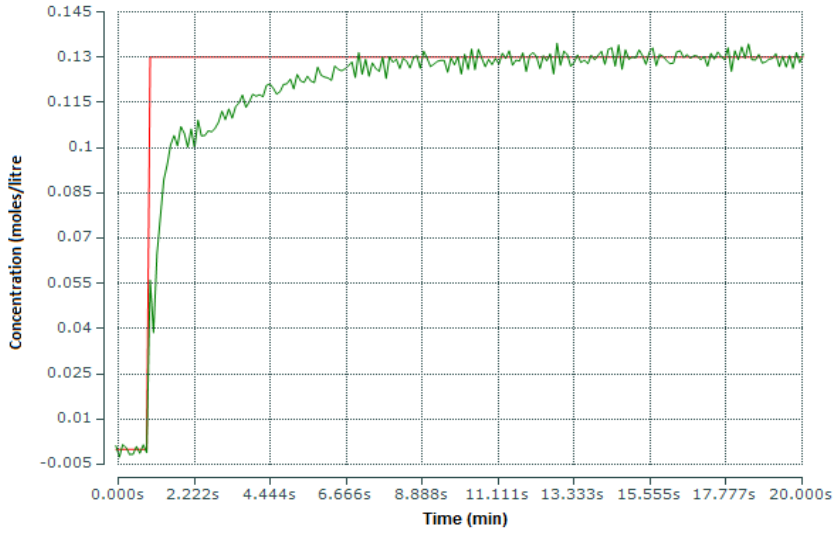

Figure 7.71: Concentration Set-point tracking under $\pm 4K$ disturbance on y_2

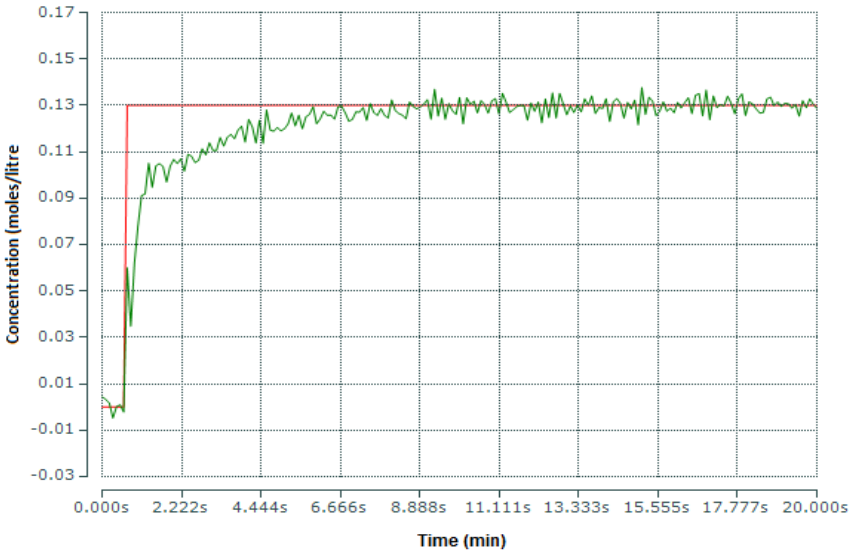

Figure 7.72: Concentration Set-point tracking under $\pm 8K$ disturbance on y_2

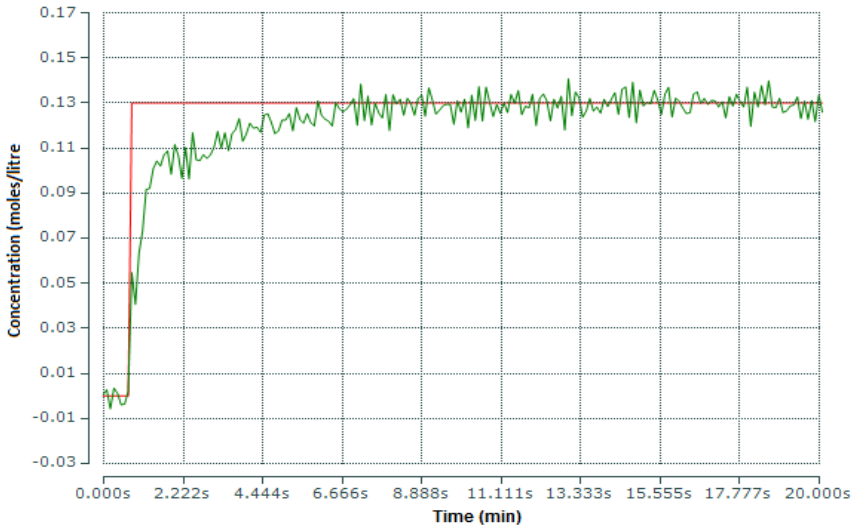

Figure 7.73: Concentration Set-point tracking under $\pm 10K$ disturbance on y_2

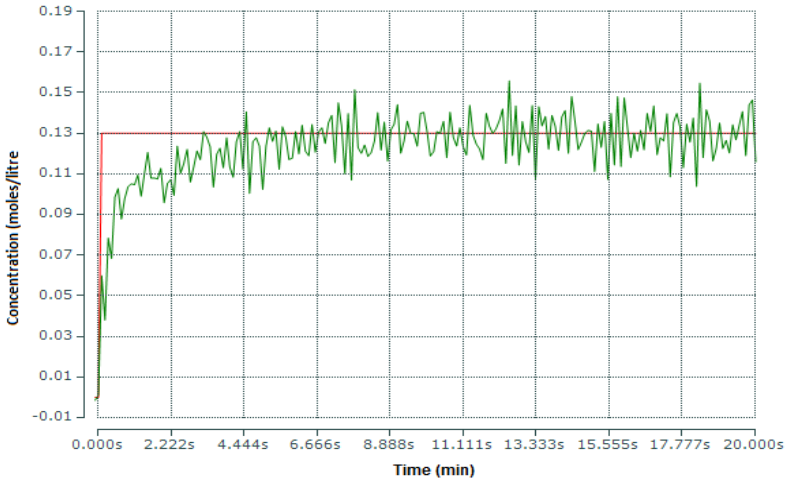

Figure 7.74: Concentration Set-point tracking under $\pm 20K$ disturbance on y_2

Decentrarized control scheme can not eliminate completely the effects of the loop interactions. The results of real-time simulation shows that the magnitude of the disturbance is important for the smooth set-point tracking. However the concentration system for the concentration response under real-time simulations is still able to track the set-point variations, implying that the designed decentralized systems can achieve its main requirement but needs further improvement.

7.5.3.3 Temperature loop results from simulation for various set-points and disturbances

The variation of set-points magnitude influence over the temperature response performance indices is investigated. The set-point is varied from $450K$ to $465K$ in steps of $5K$. The responses are illustrated in Figures 7.75-7.78 below.

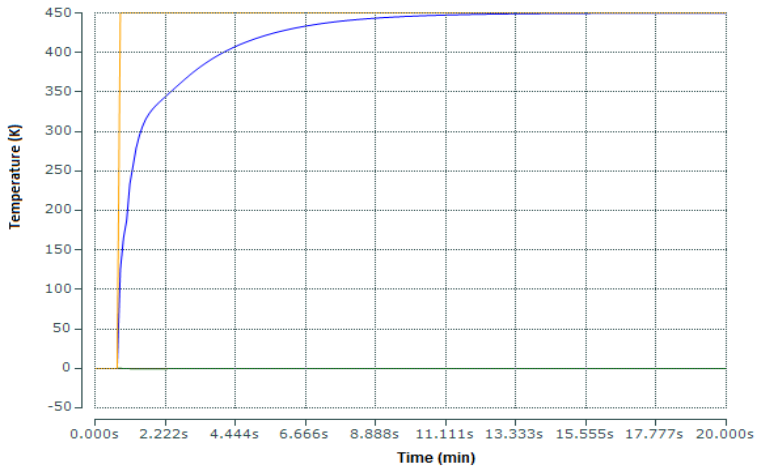

Figure 7.75: Temperature Set-point of $450K$ tracking

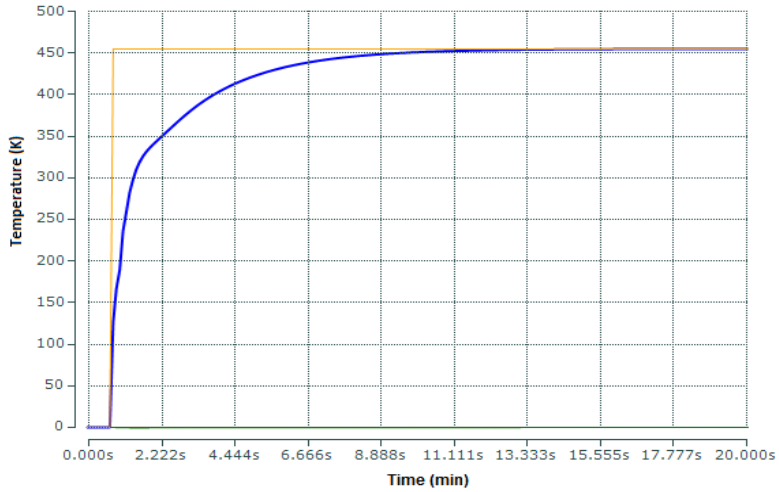

Figure 7.76: Temperature Set-point of $455K$ tracking.

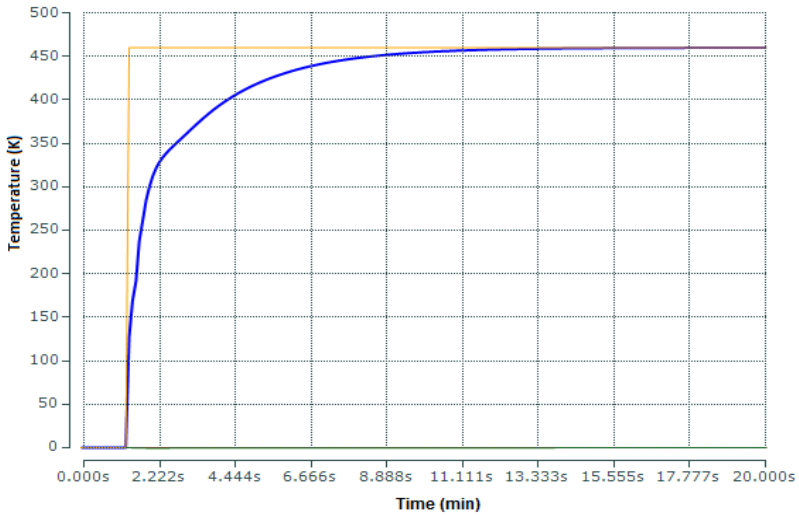

Figure 7.77: Temperature Set-point of $460K$ tracking

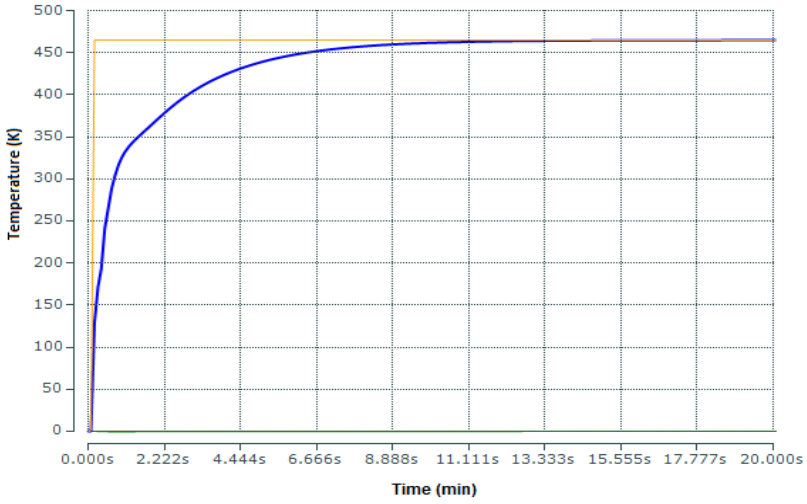

Figure 7.78: Temperature Set-point of $465K$ tracking

The results show that a part from the sluggish responses; successful temperature set-point tracking under real-time simulation is obtained.

Next, the effects of disturbances are investigated for the temperature control loop in real-time. The procedure adopted is the same as that for the temperature control loop investigated in Chapter 5. The difference is that, this time the investigation is done on real-time platform. Figures 7.79-7.82 present real-time temperature the responses when the actions of the disturbances are at y_2.

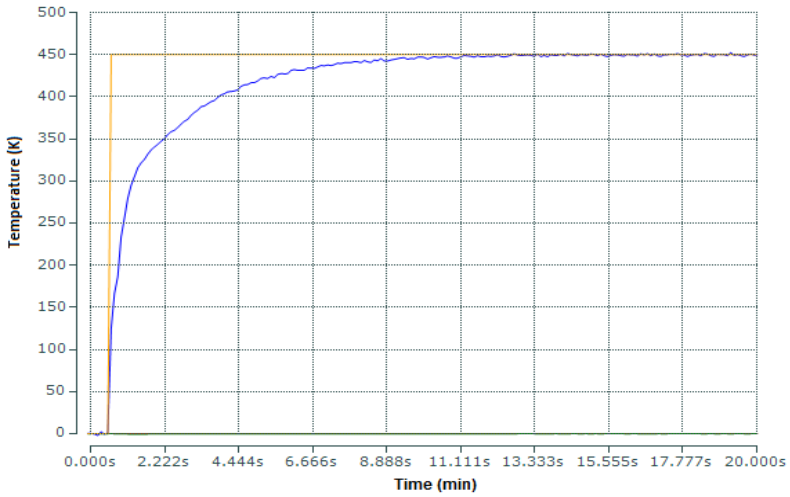

Figure 7.79: Temperature Set-point tracking under $\pm 4K$ disturbance on y_2

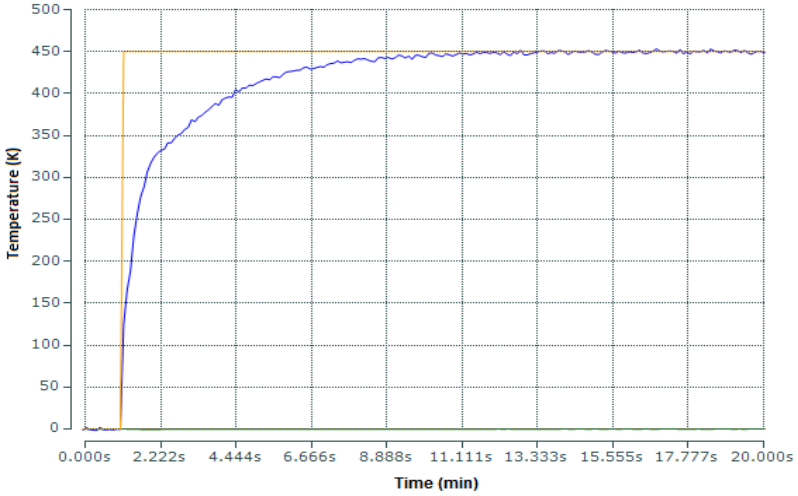

Figure 7.80: Temperature Set-point tracking under $\pm 8K$ disturbance on y_2

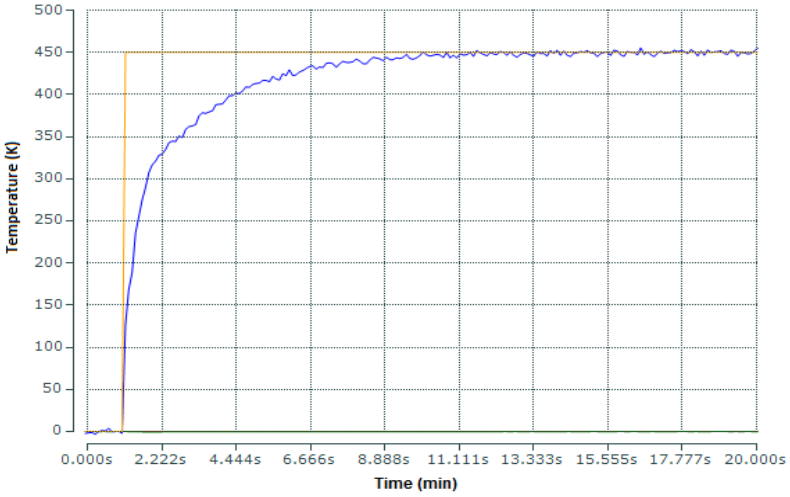

Figure 7.81: Temperature Set-point tracking under $\pm 10K$ disturbance on y_2

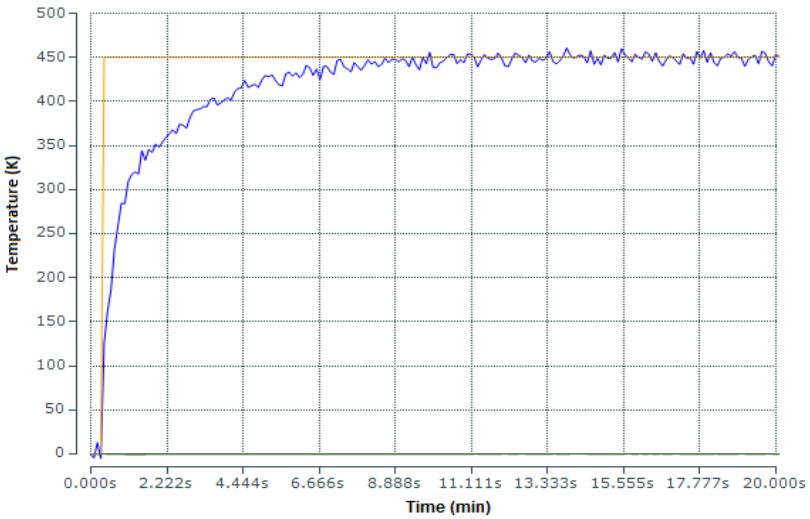

Figure 7.82: Temperature Set-point tracking under $\pm 20K$ disturbance on y_2

The results of simulation show that the magnitude of the disturbance is important for the smooth set-point tracking. However the real-time simulation results for the temperature show the capability to track the set-point variations, implying that the designed decentralized systems is good even in the presence of the random disturbances. Figures 7.83-7.86 are the temperature responses when the actions of the disturbances are at concentration output y_1.

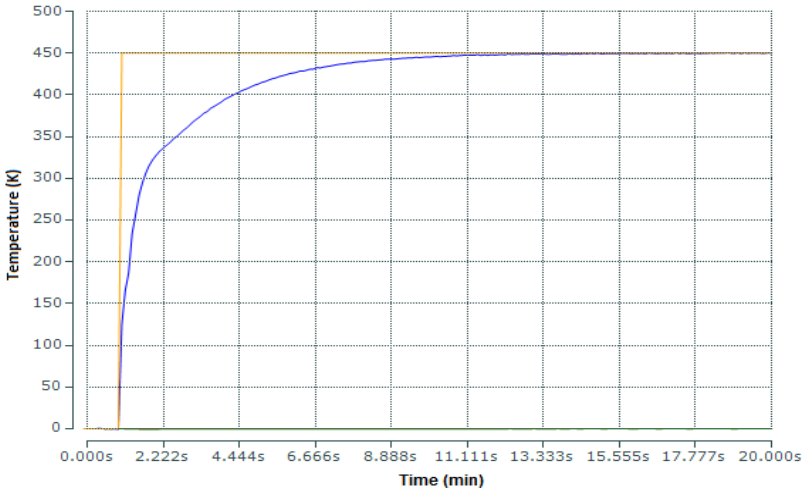

Figure 7.83: Temperature Set-point tracking under $\pm 1e^{-3}$ moles/litre disturbance on y_2

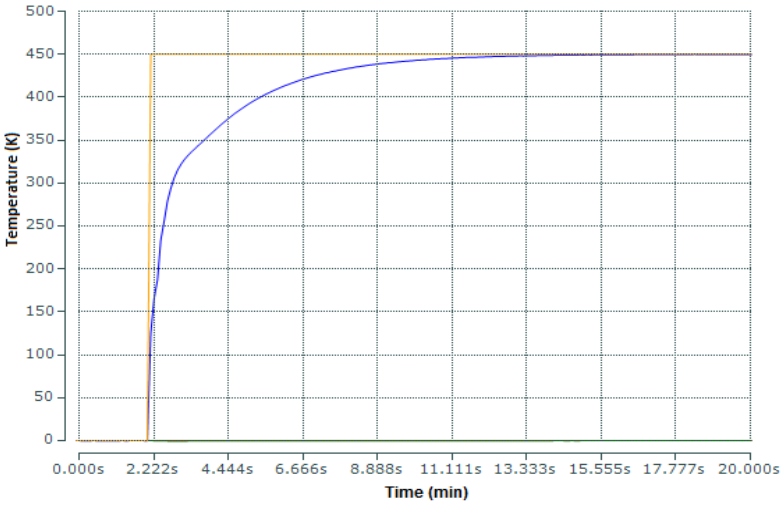

Figure 7.84: Temperature Set-point tracking under $\pm 4e^{-3}$ moles/litre disturbance on y_1

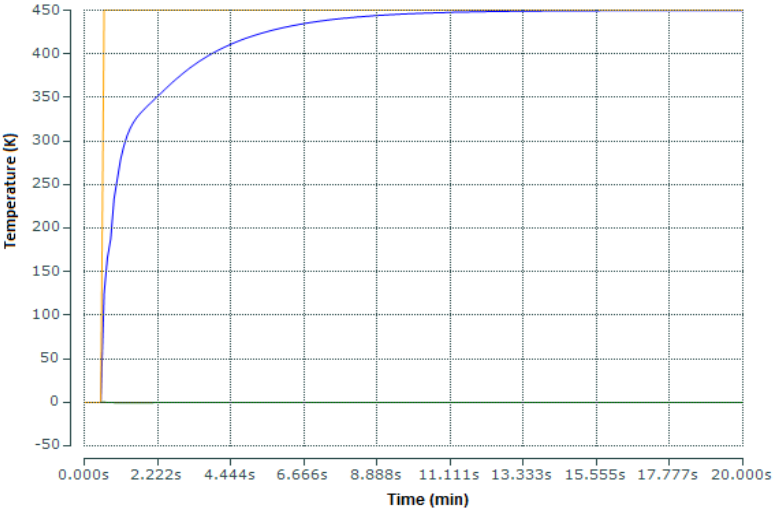

Figure 7.85: Temperature Set-point tracking under ± 0.01 moles/litre disturbance on y_1

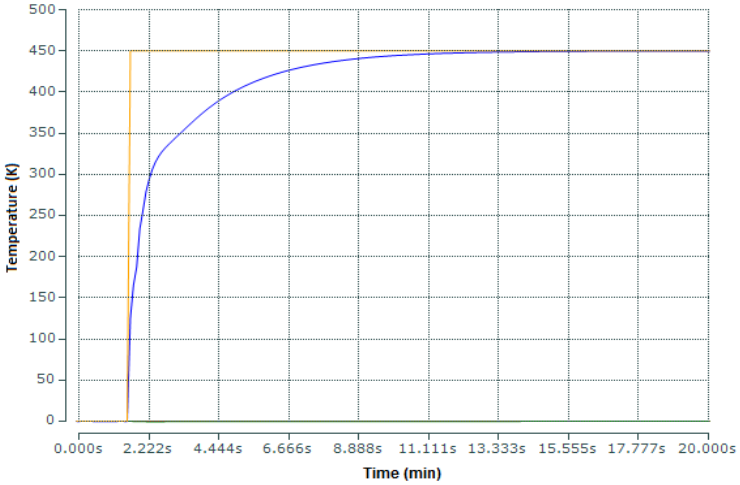

Figure 7.86: Temperature Set-point tracking under ± 0.04 moles/litre disturbance on y_1

Good set-point tracking control is realised in real-time. The disturbance effects at y_1 do not degrade on the performance of the temperature loop apart from the sluggish response. The decentralized control in this case performs well.

A comparative analysis with the results presented in Chapter 5 for the closed loop system under decentralized control, shows that the overshoot has reduced to but the time it takes to settle has increased. The results of comparison are given in Table 7.3.

Table 7.3: Comparison between the performance indicators of the closed loop concentration and temperature responses under the Matlab/Simulink and the TwinCAT PLC real-time for various step magnitudes in decentralized control

closed loop concentration performance indices								
	Matlab/Simulink				TwinCAT PLC real-time			
Set-point value	Settling time $t_s(\min)$	Peak over shoot $M_P(\%)$	Peak time $t_p(\min)$	Steady state error $e_{ss}(\%)$	Settling time $t_s(\min)$	Peak over shoot $M_P(\%)$	Peak time $t_p(\min)$	Steady state error $e_{ss}(\%)$
0.08mol/l	1.3089	5.5263	1.0089	0	8.778	0	8.778	0
0.1mol/l	1.3089	5.4622	1.0424	0	8.778	0	8.778	0
0.12mol/l	1.3089	5.4794	0.9928	0	8.778	0	8.778	0
0.14mol/l	1.3089	5.3291	0.9835	0	8.778	0	8.778	0
closed loop temperature performance indices								
	Matlab/Simulink			TwinCAT PLC real-time				
Set-point value	Settling time $t_s(\min)$	Peak over shoot $M_P(\%)$	Peak time $t_p(\min)$	Steady state error $e_{ss}(\%)$	Settling time $t_s(\min)$	Peak over shoot $M_P(\%)$	Peak time $t_p(\min)$	Steady state error $e_{ss}(\%)$
446K	1.3089	8.1300	1.0089	0	8.778	0	8.778	0
450K	1.3424	7.6481	1.0	0	8.778	0	8.778	0
455K	1.3228	7.8201	1.0	0	8.778	0	8.778	0
460K	1.3235	8.9000	1.0	0	8.778	0	8.778	0

7.5.4 Input-Output feedback linearization control simulation in Real-time

Based on the transformation algorithm in section 7.4 above, the algorithms of the Input-Output control methodology developed in Chapter 6 are used for real-time implementation. This is done by downloading the algorithms to the Beckhoff CX5020 PLC for real-time execution to verify the effectiveness of the control schemes under real-time environment. The following are the real-time simulation results from the experiments investigated.

7.5.4.1 Model transformation and set-point tracking control for the input-output feedback linearization closed loop system

Figure 7.87: shows the transformed Simulink closed loop MIMO CSTR process under the I/O feedback linearization control to the corresponding TwinCAT 3 function blocks (modules). The transformation technique shows that the data and parameter connection are the same in these two platforms and therefore there is a one to one correspondence of function blocks between Simulink and TwinCAT platforms.

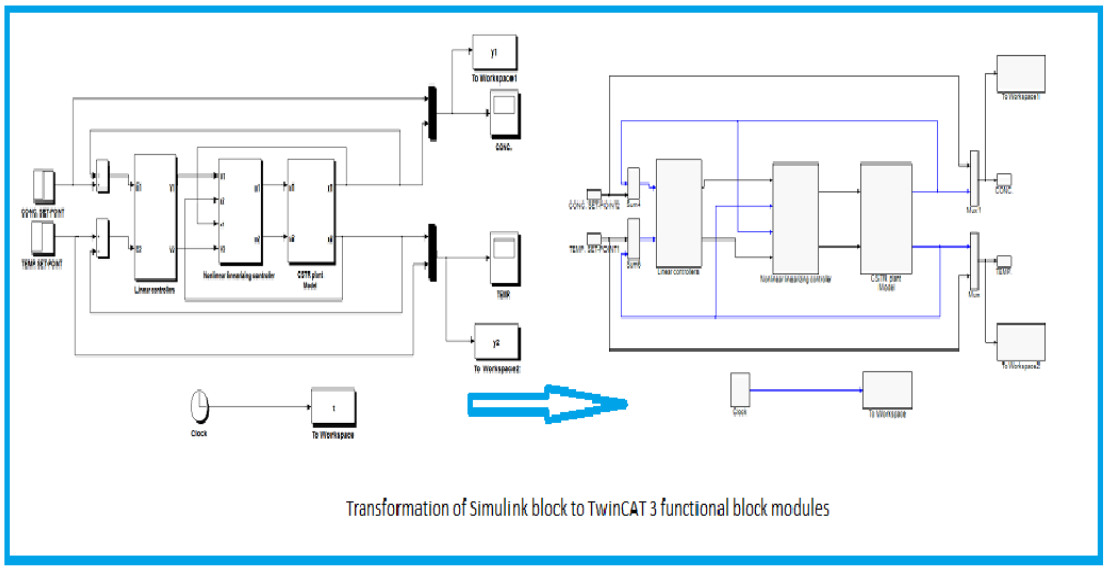

Figure 7.87: Transformed Simulink Input-Output linearized closed loop to TwinCAT 3 function blocks.

Investigations are done for real-time set point tracking control for both the concentration and the temperature responses. Figures 7.88-7.93 show the various step responses for the concentration under the I/O linearized closed loop when the set point is varied from 0.08 moles/litre to 0.13 moles/litre.

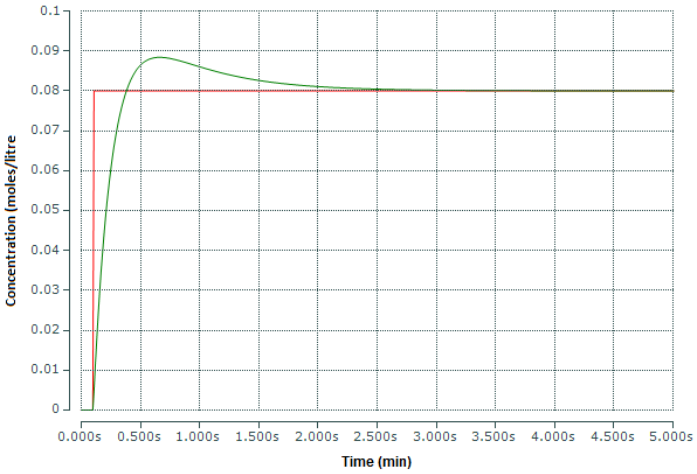

Figure 7.88: Concentration Set-point of 0.08 moles/litre tracking

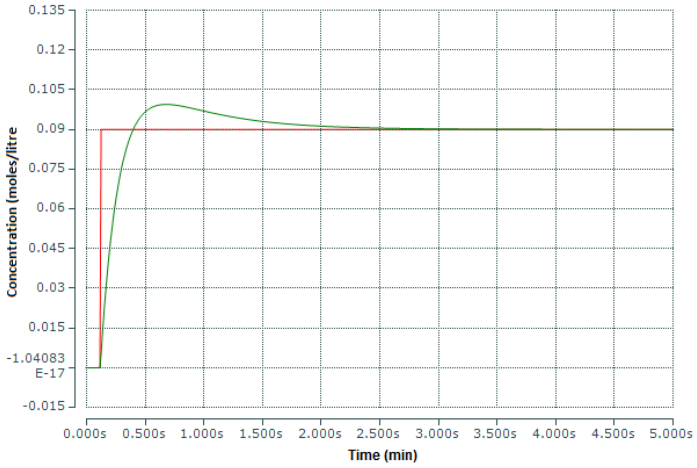

Figure 7.89: Concentration Set-point of 0.09 moles/litre tracking

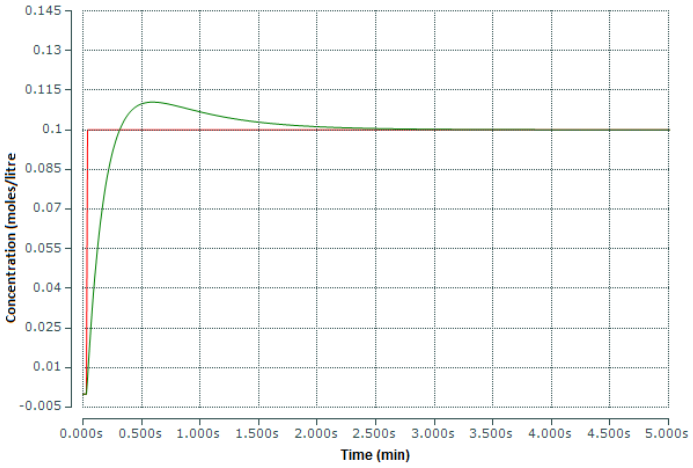

Figure 7.90: Concentration Set-point of 0.1 moles/litre tracking

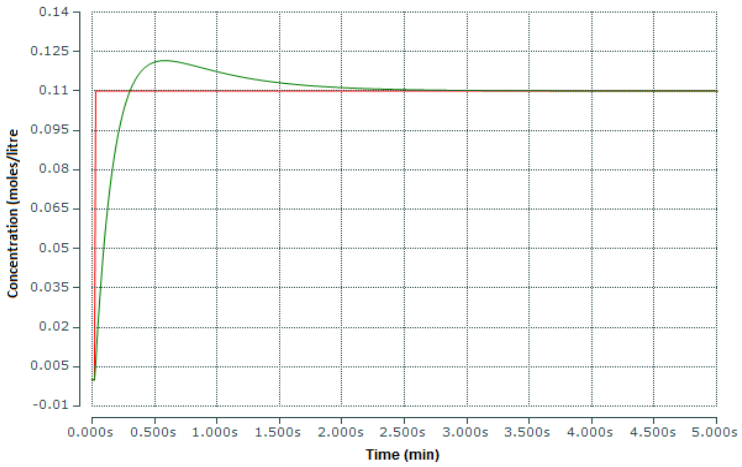

Figure 7.91: Concentration Set-point of 0.11 moles/litre tracking

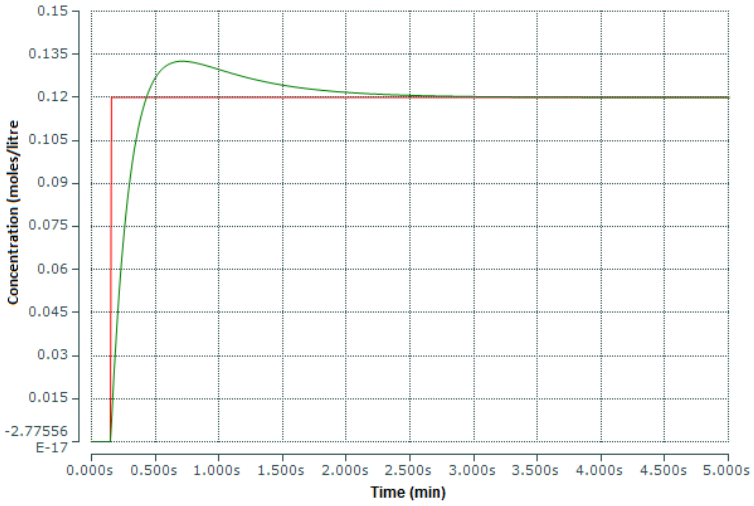

Figure 7.92: Concentration Set-point of for 0.12 moles/litre tracking

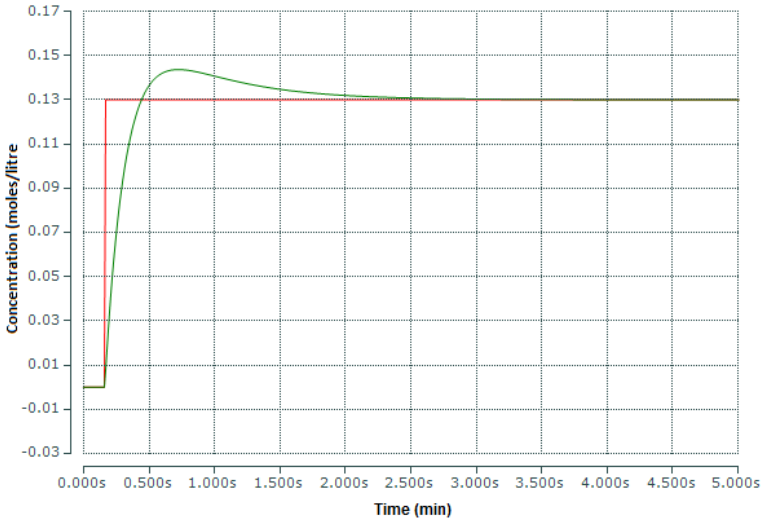

Figure 7.93: Concentration Set-point of for 0.13 moles/litre tracking

Analyses of the concentration real-time behaviour, further confirms that the designed I/O feedback linearization controller settings achieve good tracking control of the concentration set point in real-time situation, and therefore the control design is good. The influences over the real-time process output step response of various magnitudes of disturbances are also investigated for the developed scheme for the concentration control loop. The procedure adopted is the same as that for the concentration control loop in Chapter 6. The difference is that, this time the investigation is done on a real-time platform. The disturbances are injected to the main concentration control loop at the outputs y_1.

7.5.4.2 Investigation of the concentration real-time performance for a disturbance on the concentration output y_1

Figures 7.94-7.97 are the responses when the effects of the disturbances are at y_1

Analyses of the responses, further confirms that the designed I/O feedback linearization controller settings achieve good tracking control of the concentration set point in real-time situation as well as rejecting disturbances and therefore the I/O feedback linearization control design for the concentration loop is good though the magnitude of disturbance results in a noisy response.

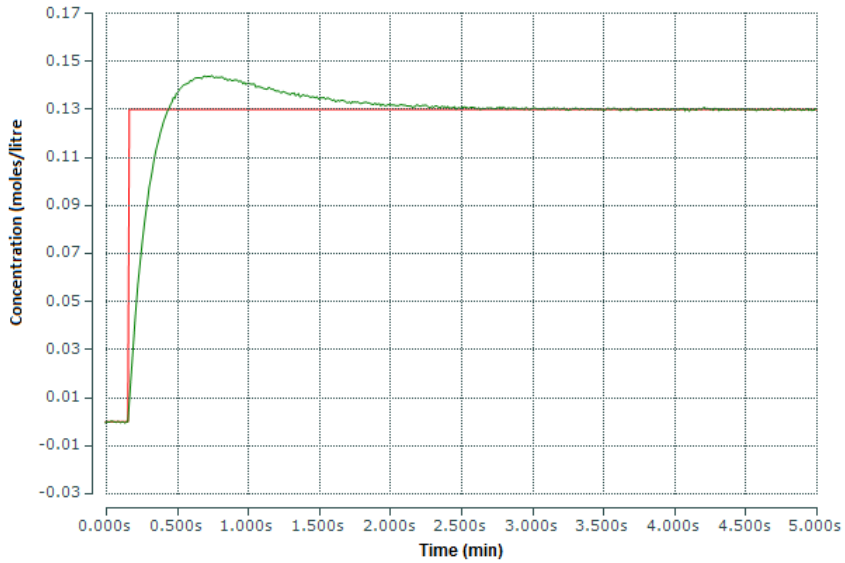

Figure 7.94: Concentration Set-point tracking for $\pm 1e^{-3}$ moles/litre disturbance on y_1

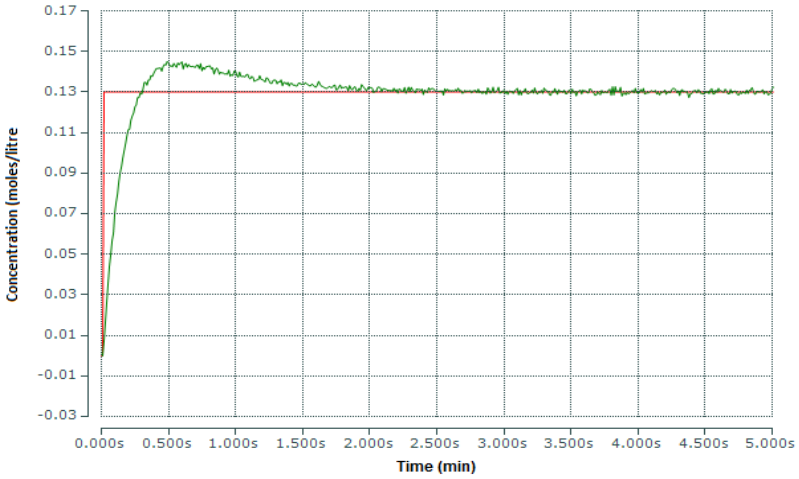

Figure 7.95: Concentration Set-point tracking for $\pm 4e^{-3}$ moles/litre disturbance on y_1

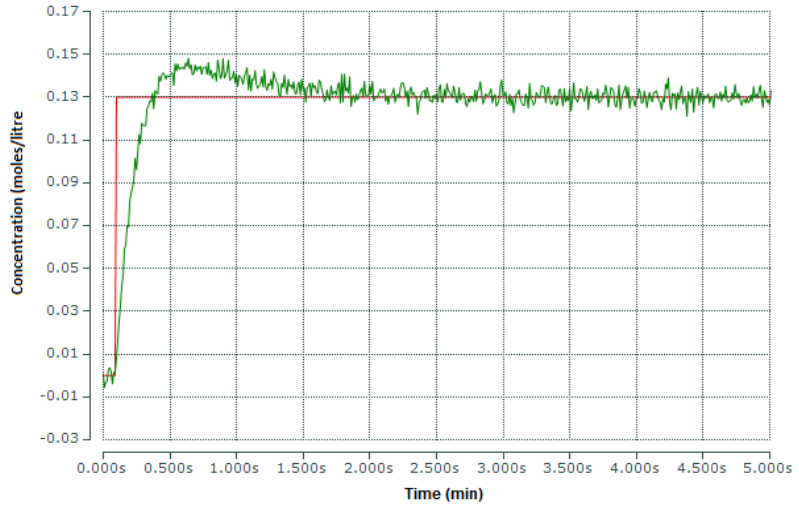

Figure 7.96: Concentration Set-point tracking for ± 0.01 moles/litre disturbance on y_1

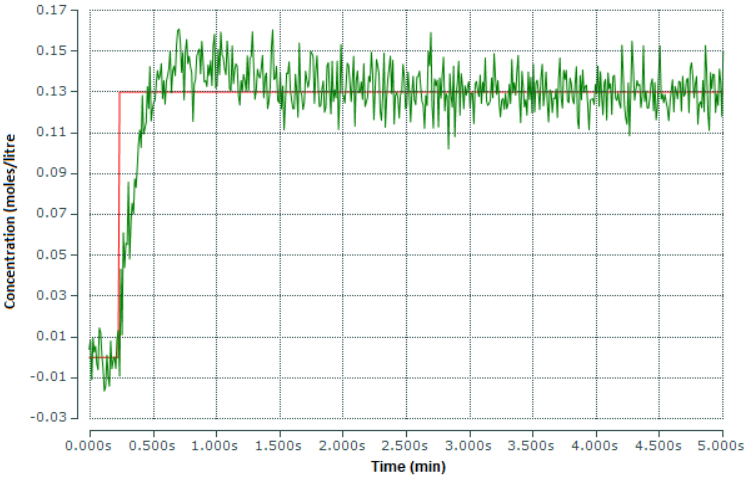

Figure 7.97: Concentration Set-point tracking for ± 0.04 moles/litre disturbance on y_1

In appendix C, the algorithm that simulates the nonlinear linearizing feedback control response of the closed loop MIMO CSTR model for various magnitudes of set-point step changes, as well as disturbances at the outputs (y1) and (y2) is provided. The Simulink closed loop model to be simulated is *li_2015*.and provided in appendix F.

A comparative analysis with the results presented in Chapter 6 for the closed loop system under I/O feedback linearization control, shows that the various performance indicators are almost similar. The results of comparison are given in Table 7.4.

Table 7.4: Comparison between the performance indicators of the closed loop concentration responses under the Matlab/Simulink and the TwinCAT PLC real-time for various step magnitudes in I/O feedback linearization control

closed loop concentration performance indices										
	Matlab/Simulink					TwinCAT PLC real-time				
Set-point value	Settling Time t_s(min)	Rise time t_r(min)	Peak over shoot M_P(%)	Peak time t_s(min)	Steady state error e_{ss}(%)	Settling Time t_s(min)	Rise time t_r(min)	Peak over shoot M_P(%)	Peak time t_s(min)	Steady state error e_{ss}(%)
0.08mol/l	1.9800	0.900	10.5263	056	0	2.1	0.3	10.0	0.6	0
0.09mol/l	1.9800	0.900	10.5075	0.56	0	2.1	0.3	10.0	0.6	0
0.10mol/l	1.9800	0.900	10.5042	0.56	0	2.1	0.3	10.0	0.6	0
0.11mol/l	1.9800	0.900	10.6508	0.56	0	2.1	0.3	10.0	0.6	0
0.12mol/l	1.9800	0.900	10.5022	0.56	0	2.1	0.3	10.0	0.6	0
0.13mol/l	1.9800	0.900	10.5947	0.56	0	2.1	0.3	10.0	0.6	0

7.6 Discussion of the Results from the simulations

Based on the steps required for model transformation the between the Matlab/Simulink to the TwinCAT 3 functional blocks, the algorithms of the control design methodologies developed in Chapters 4. 5 and 6, simulation results are used to verify the suitability of the control to find whether the effective set-point tracking control and disturbance effect minimisation for the output variables can be achieved in real-time using the transformed Simulink blocks to the TwinCAT 3 functional blocks, then downloaded to the Beckhoff CX5020 PLC for real-time execution. Good set-point tracking control is achieved for the MIMO closed loop CSTR process for the considered cases of the dynamic decoupling and decentralized control. Similarly, the effects of disturbances are investigated. The CSTR process performance under the input-output feedback linearization transformed TwinCAT functional modules achieved good set-point tracking with these disturbances minimization for the concentration control loop under all the cases considered. In the case of the temperature control loop developed, the objective for real-time control for the particular loop is not achieved at the moment. This implies that further investigation on the control design for this particular loop should be done.

7.7 Conclusion

The simulation results from the investigation done between Simulink and TwinCAT 3 software platforms in the case of the model transformation and closed loop simulation of the process for the considered cases have shown the suitability and the potentials of merging the Matlab/Simulink control function blocks into the TwinCAT 3.1 function blocks in real-time .The merits derived from such integration implies that the existing software and software components can be re-used This is in line with one of the IEC 6144 standard requirements such as portability and interoperability. Similarly, the simplification of programming applications is greatly achieved. The investigation has also shown that the integration the of Matlab/Simulink models running in the TwinCAT 3.1 PLC do not need any modification, hence confirming that the TwinCAT 3.1 development platform can be used for the design and implementation of controllers from different platforms.

CHAPTER EIGHT
CONCLUSION, DELIVERABLES, APPLICATIONS AND FUTURE WORK

8.1 Introduction

This research focuses on the control design strategies for the Continuous Stirred Tank Reactor (CSTR) process. To control such a process a careful design strategy is required because of the nonlinearities, loop interaction and the potentially unstable dynamics. In these systems, linear control methods alone may not perform satisfactorily. The thesis describes the developed methods for the design and implementation of the closed loop system in the Beckhoff PLC Twin CAT 3.1 real-time (Beckhoff Automation) and Matlab/Simulink (*www.mathworks.com)* environment are used to test the effectiveness of the developed models and methods in realizing the thesis objectives. Comparative performance analyses using the two platforms (Matlab/Simulink and TwinCAT 3.1) such as configurability and decentralization assessment are carried out. The main research questions formulated were:

- Whether linear or nonlinear methods for design of controllers for the MIMO nonlinear CSTR processes could contribute to better performance of the closed loop system for various process conditions, as changing set point and disturbances
- The capability of the software TwinCAT 3.1 to be applied for programming of the developed decentralized distributed closed loop systems and to perform real-time simulation and lastly,
- The capability of the real-time Twin CAT 3.1 environment to assure the same results of the closed loop systems through real-time simulation in comparison with the situation in Matlab/Simulink environment.

Three different controller design approaches (dynamic decoupling control, Dentralized and I/O feedback linearization) are investigated. Simulations are used to demonstrate the suitability of the closed loop control systems in line with the functional block programming concepts. It is envisaged that the thesis contributions will provide a platform for understanding the concepts of the TwinCAT 3.1 software environment and its application to practical distributed control systems. The developed guide for the model transformation between the two environments (Matlab/Simulink and TwinCAT 3.1) for modelling, data analysis and real-time simulation can be very useful for further research investigations or engineering project implementation in industry.

The simulation results from the investigations done between Simulink and TwinCAT 3 software platforms in regard to the model transformation and control of the closed loop process for all the considered cases have shown the suitability and the potentials of merging the Matlab/Simulink control function blocks into the TwinCAT

3.1 function blocks in real-time. The merits derived from such integration imply that the existing software and software components can be re-used. This is in line with the IEC 6144 standard requirements such as portability and interoperability. Similarly, the simplification of programming applications is greatly achieved. The investigation has also shown that the integration the of Matlab/Simulink models running in the TwinCAT 3.1 PLC do not need any modification, hence confirming that the TwinCAT 3.1 development platform can be used for the design and implementation of controllers from different vendor platforms.

In this chapter, section 8.2 describes the problems solved in this thesis. In section 8.3 the thesis deliverables are discussed while section 8.4 lists the software algorithms developed in this thesis. In section 8.5, the applications relevant to the deliverables of the thesis are discussed. Section 8.6 and 8.7 presents future research work and the author's publication respectively. Section 8.8 gives the conclusion of the chapter.

8.2 Problems solved in the thesis

These problems can be divided into two main groups:

- Design-based
- Implementation-based.

8.2.1 Design-based

Sub-problem1: Formulation of the mathematical model for the MIMO nonlinear CSTR plant

Sub-problem 2: Development of methods for linearization of the nonlinear Multi-Input Multi-Output (MIMO) CSTR process and methods for analysing the stability of the system

Sub-problem 3: Development of methods for the analysis and design of linear controllers using dynamic decoupling techniques relevant to the MIMO nonlinear CSTR plant model.

Sub-problem 4: Development of methods for the analysis and design of linear controllers using decentralized control techniques relevant to the MIMO nonlinear CSTR plant model.

Sub-problem 5: Development of methods for the analysis and design of nonlinear controllers using I/O feedback linearization techniques relevant to the MIMO nonlinear CSTR plant model.

8.2.2 Implementation-based sub-problem.

Sub-problem1: Development of a software model of the nonlinear MIMO CSTR. This is done in the Matlab/Simulink platform and investigation by simulations

Sub-problem 2: Performance of simulations for the developed decoupled closed loop control system in the Matlab/Simulink environment

Sub-problem: 3 Simulations for the developed decentralized closed loop control system in the Matlab/Simulink environment for various cases of set-points and disturbances.

Sub-problem: 4 Simulations of the developed closed loop input/output feedback linearized control system in the Matlab/Simulink environment for various cases of set-points and disturbances.

Sub-problem: 5.Transformation of the developed software for simulation of the closed loop systems from the Matlab/Simulink platform to the TwinCAT 3 simulation environment (Function blocks).

Sub-problem: 6 .Perform simulations in real-time for the closed loop systems in the TwinCAT PLC platform thereby demonstrating the effectiveness of the transformation.

8.3. The thesis deliverables

The deliverables of this thesis are as follows:

8.3.1 Comprehensive Literature review.

The review on the relevant aspects of the areas of concern to this research is done

A review of the existing literature for the CSTR modelling and the control design is presented and a review on the IEC 61499 standard and the distributed control in process industry is done. Several control strategies and problems are reviewed based on the model-based control concepts. Successful application of these control strategies has been reported with good results. Similarly a number of the review papers on the new IEC 61499 standard as well as its real time applicability are reviewed and discussed. The feasibility to integrate the concepts of the Matlab/Simulink transformation to the Functional block programming environment of TwinCAT 3.1, and utilize them to design and implement nonlinear controllers for the CSTR nonlinear plant are also reviewed.

8.3.2 Mathematical modelling of the nonlinear MIMO CSTR in the Matlab/Simulink platform.

The CSTR process is derived based on the first principles and simulation studies are performed. The CSTR dynamics mathematical model is formulated based on the assumption that the model represents the ideal case, where the feed flow and the coolant flow rates respectively are the considered the inputs and the product concentration and the temperature respectively are the monitored outputs. The simulation results demonstrate that the CSTR process exhibits highly nonlinear dynamic behaviour because of the coupling and the inter-relationships of the states,

the exponential dependence of each state on the reactor temperature, as well as the reaction rate being an exponential function of the temperature.

8.3.3 Design of the dynamic decoupling controller for the MIMO CSTR process

Difficulties caused by the interacting loops for the MIMO systems are the major obstacle to the controllers designed for such systems. Interactions occur when there are coupling between the control variables and between the process variables thereby affecting the states of the controlled variables. To address the problem of loop interactions a simple dynamic decoupling mechanism is designed. After this two SISO PI controllers are designed directly for the resulting decoupled system and independently by applying pole placement technique to tune the individual loops for tracking control of the output variables. The results of simulation studies show that the dynamic decoupling control scheme together with the Single-Input Single-Output (SISO) PI control algorithms are capable of achieving effective set-point tracking control in the situation where noise disturbances are present, implying that the designed decoupling systems is robust towards the disturbances (from the point of view of stability).

8.3.4 Design of the decentralized control for the MIMO CSTR process

The design, implementation and simulation of the decentralized internal model controller (IMC)-based PID for the MIMO CSTR system are performed. For the design of the controllers, pairing among the input-output variables is done using the Relative Gain Array (RGA) analysis. Then two SISO PID controllers are designed directly for the diagonal transfer functions for the developed closed loop control system that consists of the process model and independently using internal model controller. After the independent tuning of the individual loops, a detuning factor for each individual loop is proposed to compensate for the off-diagonal matrix transfer function interactions. Simulation results show the suitability of the developed control law in achieving tracking control with good disturbance rejection capabilities.

8.3.5 Design of the I/O feedback nonlinear linearized control for the MIMO CSTR process

This control technique applies a feedback signal to remove the inherent nonlinear characteristics in a system by creating linear differential relationship between the system's outputs and the newly defined synthetic inputs. The nonlinear linearizing controller, for controlling the concentration and reactor temperature is first designed. Then two linear PI controllers for the respective loops are independently designed using the pole-placement techniques. Finally closed loop simulations are performed

to show the suitability of the developed controllers. Moreover, the performance is checked with noisy disturbances on the control loops. The results of this analysis show the suitability of the developed control law in achieving set-point tracking control. The proposed control exhibits satisfactory performance in the presence of disturbances with limited magnitudes.

8.3.6 Development of transformation procedure for the developed software from the Matlab/Simulink environment to Beckhoff TwinCAT 3 real-time environment for real-time simulation.

An algorithm detailing the steps of the software transformation from the Matlab/Simulink platform to the TwinCAT 3 real-time environment is developed. It can be used as a guide for further research investigations. The real-time simulation results using the Beckhoff PLC in which the transformed to software platforms is downloaded have shown the suitability and the potentials of merging the Matlab/Simulink works into the TwinCAT 3.1 platform .The derived benefits of such integration implies that the interoperability and portability of software components is possible. This is in line with one of the IEC 61499 standard requirements. Similarly, the simplification of the programming applications is greatly achieved. The investigation has also verified the possibility of integrating the Matlab/Simulink models to run in the PLC without any alteration to the model, hence implying that the TwinCAT 3 development platform can be used for the design and implementation of controllers from different platforms

8.6 Future work

Further investigations on how the methods and algorithms can be developed to use of both for the hardware simulation and the controller simulation in real-time is necessary so that real-time distributed control for the process can be achieved.

8.4 Developed software.

The methods and algorithms developed in the thesis and which are used for development of Matlab/Simulink software investigations and simulations of the various models developed are as given in Tables 8.1 for the Matlab script files and in Table 8.2 for the Simulink models.

Table8.1: Matlab m-files developed for the thesis

Script file	Appendix	Function
openloop_cstr.m.	Appendix A1	Presents the function file for the MIMO CSTR process with the parameter values that are used for the development of different models.

		in Simulink
openloop_cstrsim.m	Appendix A2	The main file for the CSTR process model for simulating the function openloop_cstr.m for various magnitudes of perturbations over the initial steady state conditions by a plus or minus 10% from the nominal values.
linearize_mod.m	APPENDIX B	Script file for the linearization of the CSTR process model by finding the Jacobian matrices, the state space matrices and the transfer functions of the state space model
Conc_code_li_2015.m	APPENDIX C	This algorithm simulates the nonlinear linearizing feedback control response of the closed loop MIMO CSTR model for various magnitudes of set-point step changes, as well as disturbances at the outputs (y1) and (y2). The Simulink closed loop model to be simulated is *li_2015*.
dyn_conc_code)	APPENDIX D	This file simulates the dynamic decoupling control response of the closed loop MIMO CSTR model for various magnitudes of the set-point step changes, as well as disturbances at the outputs (y1),y(2) and the interaction junctions (u1) and (u2). The Simulink closed loop model to be simulated is *dyn_dec_2015*.
decentsim.m	APPENDIX E1	This file simulates the diagonal decentralized closed loop response of the system for various values of the set-point changes, as well as disturbances at the output (y1) and the interaction junction (u1). The Simulink closed loop models to be simulated are *diag_decent_temp'* and *'decentconc_2015'.*
conc_code_4.m	APPENDIX E2	This file simulates the decentralized control response of the closed loop MIMO CSTR with and without detuning, for various magnitudes of set-point step changes as well as disturbances. The Simulink closed loop model to be simulated is *decent1_2015.*

Table 8.2: Simulink models developed in the thesis

Simulink models	Appendix	Function
decent_2015.	Model of MIMO closed loop decentralized control	Model for the MIMO closed loop system under decentralized control
dyn_dec_2015	Model of MIMO closed loop dynamic decoupling control	The MIMO closed loop under dynamic decoupling control
decen1_2015	Model of MIMO closed loop decentralized control incorporating the detuning	The closed loop MIMO system under decentralized control incorporating the detuning
li_2015	Model of MIMO closed loop I/O feedback linearization control	The MIMO closed loop system under I/O feedback linearization control
openloop_cstr_mod	Model of MIMO open loop CSTR system	The open loop CSTR process
diag_decent_temp	Model of diagonal temperature closed loop control	The temperature diagonal closed loop control system
decenconc_2015	Model of diagonal concentration closed loop control	The concentration diagonal closed loop control system

The methods and algorithms developed in the thesis and which are used for development of TwinCAT software investigations and simulations of the various models developed are as given in Table 8.3 for the Matlab script files, Table 8.2 for the Simulink models, Table 8.3 the Simulink models for TwinCAT 3 transformation and Table 8.4 the generated TwinCAT function blocks.

Table 8.3: Simulink models transformed to TwinCAT 3 functional blocks

Simulink models for TwinCAT 3 transformation	Appendix	Function
dyn_dec_2015_ds1	Model of MIMO closed loop dynamic decoupling control (Appendix F1)	Transform the MIMO closed loop control by dynamic decoupling to equivalent TwinCAT 3 functional blocks
decen1_2015_twin	Model of MIMO closed loop decentralized control(Appendix F2)	Transform the closed loop MIMO by decentralized block to equivalent TwinCAT 3 functional blocks
li_2015_c	Model of MIMO closed loop I/O feedback linearization l(Appendix F2)	Simulates the closed loop MIMO control by I/O feedback linearization to equivalent TwinCAT 3 functional blocks

Table8.4: TwinCAT 3 models developed

Simulink models for TwinCAT 3 transformation	Appendix	Function
dyn_dec_2015.tcm	Model of MIMO closed loop dynamic decoupling control (Appendix. G1)	Transform the MIMO closed loop control by dynamic decoupling to equivalent TwinCAT 3 functional blocks
decen1_2015.tcm	Model of MIMO closed loop decentralized control (Appendix. G2)	Transform the closed loop MIMO by decentralized block to equivalent TwinCAT 3 functional blocks
li_2015_c.tcm	Model of MIMO closed loop I/O feedback linearization l (Appendix. G3)	Simulates the closed loop MIMO control by I/O feedback linearization to equivalent TwinCAT 3 functional blocks

8.5 Application of the results from this thesis.

The methods and algorithms resulting from this thesis can form a cornerstone for:

- Further research investigations or engineering project implementation in industry
- Use as a guide or algorithm for the transformation of the developed software from Matlab/Simulink environment to the TwinCAT 3.1 simulation environment
- Educational and training institutions in the field of engineering and real-time automation

8.7 Publications

- Muga, J., R. Tzoneva, S. Krishnamurthy (2016). Design, implementation, and real-time simulation of a controller-based decoupled CSTR MIMO closed loop system. *International Journal of Electrical Engineering & Technology (IJEET),* v. 7, Iss. 3, pp. 126-144
- Muga, J., R. Tzoneva (2016) Decentralized controller design and PLC implementation for the TITO CSTR process, *Journal of the South African Institute of Electrical Engineering* (under review)
- Muga J., R. Tzoneva (2015) Design, implementation, and performance comparison of linear and nonlinear control strategies for the TITO CSTR process, *Control Engineering and Technology* (under review)
- Muga, J., R. Tzoneva (2014). Design and Implementation of IEC 61499 Standard-based Neural Networks Nonlinear controllers Using Functional Block Programming In Distributed Control Platform. *A celebration of Research excellence at Cape Peninsula University of Technology.* pp. 60 Research day 27th November, 2014 poster exhibition

8.8 Conclusion

This chapter presents an overview of the thesis deliverables, developed methods and software, the areas applicable to the thesis deliverable, the possible future work to improve on the thesis and the publications resulting from the investigations.

REFERENCES

Allgower F. & Doyle. F.J. 1997. Nonlinear process control–which way to the Promised Land. *5th international conference on chemical process control*, 93: 24-45.

Alvarez-Ramírez, J. 1991. Stability of a class of uncertain continuous stirred chemical reactors with a nonlinear feedback. *Chemical Engineering Science*, 49(11): 1743–1748.

Anitha, P.M. & Subbulekshmi., D. 2011. RNGA algorithm of nonlinear chemical reactor. *2011 International Conference on Emerging Trends in Electrical and Computer Technology*.

Antonelli, R. & Astolfi, A. 2003. Continuous stirred tank reactors: easy to stabilize? *Automatica*, 33: 1817–1827.

Alsafi, Y. & Vyatkin, V. Ontology-based reconfiguration agent for intelligent mechatronic systems in flexible manufacturing. *Robotics and Computer-Integrated Manufacturing*, 26: 381–391.

Aris, R. & Amundson, N.R. 2000. An analysis of chemical reactor stability and control—I. *Chemical Engineering Science*, 7(8): 121–131.

B., V., Ponnusamy, L. & K., T. 2015. Design and optimization of multivariable controller for CSTR system. *2015 International Conference on Robotics, Automation, Control and Embedded Systems (RACE)*, (Article number: 7097271).

Bakosova, M. & Vasickaninova, A. 2009. Simulation Of Robust Stabilization Of A Chemical Reactor. *ECMS 2009 Proceedings edited by J. Otamendi, A. Bargiela, J. L. Montes, L. M. Doncel Pedrera*: 570–576.

Balakotaiah, V., & Luss, D. 1981. Analysis of the Multiplicity Patterns of a CSTR. Chem. Eng. Comm. 13: 111.

Bansode, P. & Jadhav, S.P. 2015. Decoupling based predictive control analysis of a continuous stirred tank reactor. *2015 International Conference on Industrial Instrumentation and Control (ICIC)*: 816–820.

Bartolini, G., Pisano, A. & Usai, E. 2009. On the second-order sliding mode control of nonlinear systems with uncertain control direction. *Automatica*, 45: 2982–2985.

Benenati, R.F. 1973. Process modeling, simulation and control for chemical engineers, William L. Luyben, McGraw-Hill, New York, 1973. 558 pp. *Journal of Polymer Science: Polymer Letters Edition J. Polym. Sci. B Polym. Lett. Ed.*: 289–290.

Bequette, B.W. 2003. Nonlinear control of chemical processes: a review. *Industrial & Engineering Chemistry Research Ind. Eng. Chem. Res.*, 30: 1391–1413.

Black, G. & Vyatkin, V. 2010. Intelligent Component-based Automation of Baggage Handling Systems with IEC 61499. *IEEE Transactions on Automation Science and Engineering*. 7(2): 337-351

Bristol, E. 1966. On a new measure of interaction for multivariable process control. *IEEE Transactions on Automatic Control IEEE Trans. Automat. Contr.*, 11: 133–134.

Cai, W.-J., Ni, W., He, M.-J. & Ni, C.-Y. 2008. Normalized Decoupling [illegible] MIMO Process Control System Design. *Industrial & Engineering Chemistry Research Ind. Eng. Chem. Res.*, 47: 7347–7356.

Campanelli, S., Foglia, P. & Prete, C.A. 2015. An architecture to integrate IEC 61131-3 systems in an IEC 61499 distributed solution. *Computers in Industry*, 72: 47–67.

Chen, J., Yang, W., Luo, A.U. & Wu, X. 2013. The Multi-Point Temperature Decoupling Control Method and its Realization. *AMM Applied Mechanics and Materials*, 321(324): 2237–2240.

Chen, Z.-F. & Zhang, Y. 2014. Robust control of a class of non-affine nonlinear systems by state and output feedback. *Journal of Central South University J. Cent. South Univ.*, 21(4): 1322–1328.

Chen, Z., Zhang, Y., Yang, L., Zeng, Q. & Liu, Z. 2012. Robust Output Tracking Control of a Class of Highly Uncertain Non-affine Nonlinear Systems. *International Journal of Advancements in Computing Technology IJACT*, 4(21): 607–614.

Chen, M., Ge, S.S. & Ren, B. 2011. Adaptive tracking control of uncertain MIMO nonlinear systems with input constraints. *Automatica*, 47(3): 452–465.

Chou, Y.-S. & King, C.-Y. 1996. Two-degree-of-freedom controllers for multivariable model-matching systems: Application to a continuous stirred tank reactor (CSTR). *Optimal Control Applications and Methods Optim. Control Appl. Meth.*, 17: 3–27.

Chi, T.C. & Chyi, S-D., 2001. Robust controller design for a class of nonlinear uncertain chemical processes. *Journal of Process control.* 11: 469-482.

Copot, D., Ionescu, C., Hernandez, A., Thybaut, J. & Keyser, R.D. 2015. Development of a control strategy for efficient operation of a CSTR reactor. *2015 19th International Conference on System Theory, Control and Computing (ICSTCC)*: 717–722.

Czeczot, J., 2006. Balance-based adaptive control methodology and its application to the non-isothermal CSTR, Chemical Engineering and Processing 45: 359–371

Dai, W. & Vyatkin, V. 2010. Redesign distributed IEC 61131-3 PLC system in IEC 61499 function blocks. *2010 IEEE 15th Conference on Emerging Technologies & Factory Automation (ETFA 2010)*.

Dai, W. & Vyatkin, V. 2010. On migration from PLCs to IEC 61499: Addressing the data handling issues. *2010 8th IEEE International Conference on Industrial Informatics*.

Desoer, C. & Wang, Y.-T. 1980. Foundations of feedback theory for nonlinear dynamical systems. *IEEE Trans. Circuits Syst. IEEE Transactions on Circuits and Systems*, 27(2): 104–123.

Dubinin, V., Vyatkin, V., & Pfeiffer, T. 2005. 'Engineering of Validatable Automation Systems Based on an Extension of UML Combined With Function Blocks of IEC 61499**.** *IEEE International Conference on Robotics and Automation.* Proceedings of ICRA 2005, Barcelona. 4007-4012.

Enqvist, M. & Ljung, L. 2004. Estimating nonlinear systems in a neighborhood of LTI-approximants. *Proceedings of the 41st IEEE Conference on Decision and Control, 2002.*: 639–644.

Fruehauf, P.S., Chien, I.-L. & Lauritsen, M.D. 1990. Simplified IMC-PID tuning rules. *ISA Transactions*, 86(33): 43–59.

Fu, Y. & Chai, T. 2011. Robust self-tuning PI decoupling control of uncertain multivariable systems. *Int. J. Adapt. Control Signal Process. International Journal of Adaptive Control and*

Signal Processing, 26(4): 316–332.

Gagnon, E., Pomerleau, A. & Desbiens, A. 1998. Simplified, ideal or inverted decoupling? *ISA Transactions*, 37: 265–276.

Ganesh, P. & Chidambaram, M. 2010. Multivariable controller tuning for non-square systems by genetic algorithm. *Proceedings of 2005 International Conference on Intelligent Sensing and Information Processing,* 24(1): 17–22.

Gao, J., & Budman, H.M. 2005 Design of robust gain-scheduled PI controllers for nonlinear processes. *Journal of Process Control* 15: 807–817.

Garelli, F., Mantz, R. & Battista, H.D. 2006. Limiting interactions in decentralized control of MIMO systems. *Journal of Process Control*, 16(5): 473–483.

Garrido, J., Vázquez, F. & Morilla, F. 2014. Multivariable PID control by decoupling. *International Journal of Systems Science*: 1–19.

Ghosh, A. & Das, S. 2012. Decoupled periodic compensation for multi-channel output gain margin improvement of continuous-time MIMO plants. *IET Control Theory & Applications IET Control Theory Appl.*, 6(11): 1735–1740.

G., L. & Ray, G. 2014. A Set of Stabilizing PID Controllers for Multi input-Multi output Systems. *International Journal of Control and Automation IJCA*, 7(4): 175–190.

Grosdidier, P. & Morari, M. 1987. Interaction measures for systems under decentralized control. *Automatica*, 22: 309–319.

Golubitsky, M. & Keyfitz, B.L. 1980. A qualitative study of the steady-state solutions for continuous flow stirred tank chemical reactor. *Society for Industrial and Applied Mathematics.* 11(2)

Guay, M., Dier, R., Hahn, J. & Mclellan, P. 2005. Effect of process nonlinearity on linear quadratic regulator performance. *Journal of Process Control*, 15: 113–124.

Hadisujoto, B., Refai, R., Chen, D. & Moon, T.J. 2010. Dynamic Thermal Model of PEM Fuel Cells for MIMO Control Design. *ASME 2010 Dynamic Systems and Control Conference, Volume 1*, 1.

Hahn, J., Mönnigmann, M. & Marquardt, W. 2004. A method for robustness analysis of controlled nonlinear systems. *Chemical Engineering Science*, 59: 4325–4338.

Hammer, J. 2014. State feedback control of nonlinear systems: a simple approach. *International Journal of Control*, 87(1): 143–160.

Hanisch, H.M., Lobov, A., Martinez Lastra, J.L., Tuokko, R., & Vyatkin, V. 2006. Formal Validation of Intelligent Automated Production Systems towards Industrial Applications**.** *International Journal of Manufacturing Technology and Management.8*(*1):*75-86

Henson, M.A. & Seborg, D.E. 1990. Input-output linearization of general nonlinear processes. *AIChE Journal AIChE J.*, 36: 1753–1757.

Holobloc, Inc,-Resources for the new generation. *(www.holobloc.com)*

Hovd, M. & Skogestad, S. 1994. Improved independent design of robust decentralized controllers. *Journal of Process Control*, 3(1): 43–51.

Hu, W., Cai, W.-J. & Xiao, G. 2010. Decentralized Control System Design for MIMO Processes with Integrators/Differentiators. *Industrial & Engineering Chemistry Research Ind. Eng. Chem. Res.*, 49(24): 12521–12528.

Jevtović, B.T. & Mataušek, M.R. 2010. PID controller design of TITO system based on ideal decoupler. *Journal of Process Control*, 20: 869–876.

Jiao, X., Yan-Ping, Q., Wan-Cheng, W. & Xiao-Xiao, J. 2015. A nonlinear control method of multi-input multi-output nonlinear non-minimum phase system. *2015 34th Chinese Control Conference (CCC)*: 748–753.

Jin, Q.-B., Wang, Y.-F., Wang, Q., Liu, Q. & Tian, Y.-Q. 2014. Reflexive Decoupling Control Based on Singular Value Decomposition for Multivariable System with Time Delays. *J. Chem. Eng. Japan / JCEJ J. Chem. Eng. Japan jcej Journal Of Chemical Engineering Of Japan*, 47(1): 69–77.

Jones, R. & Tham, M. 2006. Reducing Interactions in Decentralized Control Schemes. *2006 SICE-ICASE International Joint Conference*.

Jouili, K., Charfeddine, S. & Jerbi, H. 2008. An Advanced Geometric Approach of Input-Output Linearization for Nonlinear Control of a CSTR. *2008 Second UKSIM European Symposium on Computer Modeling and Simulation*: 353–358.

Jyothi, S.N., Aravind, S. & Chidambaram, M., 2001. Design on PI/PID Controllers for Systems with a Zero. *Indian Chem. Eng.,* 43: 288-293.

Isidori, A. Nonlinear Control Systems*, 3rd edition, Springer Verlag,* London, 1995.

Kaldmäe, A. & Moog, C.H. 2015. Disturbance Decoupling of Time Delay Systems. *Asian Journal of Control*.

Kamala, N., Thyagarajan, T. & Renganathan, S. 2012. Multivariable control of nonlinear process using soft computing techniques. *Journal of Advances in Information Technology JAIT*, 3(1): 48–56.

Kravaris, C. & Kantor, J.C. 1990. Geometric methods for nonlinear process control. 1. Background. *Industrial & Engineering Chemistry Research Ind. Eng. Chem. Res.*, 29: 2295–2310.

Kravaris, C. & Kantor, J.C. 1990. Geometric methods for nonlinear process control. 2. Controller synthesis. *Industrial & Engineering Chemistry Research Ind. Eng. Chem. Res.*, 29(12): 2310–2323.

Kruger, K. & Basson, A. 2013. Multi-agent Systems vs IEC 61499 for Holonic Resource Control in Reconfigurable Systems. *Procedia CIRP*, (7): 503–508.

Kumar, N. & Khanduja, N. 2012. Mathematical modeling and simulation of CSTR using MIT rule. *2012 IEEE 5th India International Conference on Power Electronics (IICPE)*.

Kurniawan, E., Cao, Z. & Man, Z. 2013. Design of decentralized repetitive control of linear MIMO system. *2013 IEEE 8th Conference on Industrial Electronics and Applications (ICIEA)*, 12(5): 427–432.

Kwon, H.-Y. & Choi, H.-L. 2014. Gain scheduling control of nonlinear systems based on approximate input-output linearization. *International Journal of Control, Automation and Systems Int. J. Control Autom. Syst.*, 12(5): 1131–1137.

Lee, I.H., Choi, J.W. & Kim, M.S. 2011. Studies on the heating capacity control of a multi-type heat pump system applying a multi-input multi-output (MIMO) method. *International Journal of Refrigeration*, 34(2): 416–428.

Lengare, M., Chile, R. & Waghmare, L. 2012. Design of decentralized controllers for MIMO processes. *Computers & Electrical Engineering*, 38(1): 140–147.

Li, D.-J., Zhang, J., Cui, Y. & Liu, L. 2012. Intelligent control of nonlinear systems with application to chemical reactor recycle. *Neural Comput & Applic Neural Computing and Applications*, 23(5): 1495–1502.

Liu, R.-J., Liu, G.-P. & Wu, M. 2012. A novel decoupling control method for multivariable systems with disturbances. *Proceedings of 2012 UKACC International Conference on Control*: 76–80.

Liu, Y.-J. & Wang, W. 2011. Adaptive output feedback control of uncertain nonlinear systems based on dynamic surface control technique. *International Journal of Robust and Nonlinear Control Int. J. Robust Nonlinear Control*, 30(6): 945–958.

Luyben, W.L. 1986. Simple method for tuning SISO controllers in multivariable systems. *Industrial & Engineering Chemistry Process Design and Development Ind. Eng. Chem. Proc. Des. Dev.*, 25: 654–660.

Mulubika, C. & Basson, A. H. 2013. Comparison of IEC 61499 and Agent Based Control for a Reconfigurable Manufacturing Subsystem*. International Conference on Competitive Manufacturing (COMA)*:

Maghade, D. & Patre, B. 2012. Decentralized PI/PID controllers based on gain and phase margin specifications for TITO processes. *ISA Transactions*, 51: 550–558.

Manikandan, R., Vinodha, R., Lincoln, S.A. & Prakash, J. 2014. Design and simulation of model based controllers for 2x2 CSTR process. *2014 International Conference on Green Computing Communication and Electrical Engineering (ICGCCEE)*: 1–6.

Marinescu, B. 2010. Output feedback pole placement for linear time-varying systems with application to the control of nonlinear systems. *Automatica*, 46: 1524–1530.

Mehta, U. & Majhi, S. 2011. On-line relay test for automatic tuning of PI controllers for stable processes. *Transactions of the Institute of Measurement and Control*, 34(7): 903–913.

Mohamed, B., Bachir, D., Abdellah, M. & Mohammed, C. 2012. Journal of the Korean Mathematical Society. *Journal of the Korean Mathematical Society*, 49(3): 641–658.

Nordfeldt, P. & Hägglund, T. 2006. Decoupler and PID controller design of TITO systems. *Journal of Process Control*, 16: 923–936.

Nunes, D.C., Pinto, J.E.M.G., Fonseca, D.G.V., Maitelli, A.L. & Araújo, F.M.U. 2014. Relay Based PID Auto-tuning Applied to a Multivariable Level Control System. *Proceedings of the 11th International Conference on Informatics in Control, Automation and Robotics*, 1(1-2).

Patil, S., Sorouri, M. & Vyatkin, V. 2012. Formal Verification of Intelligent Mechatronic Systems with Decentralized Control Logic**.** *IEEE Conference on Emerging Technologies and Factory Automation, ETFA.* Krakow, Poland

Pottman, M. & Seborg, D.E. 1992. Identification of non-linear processes using reciprocal multiquadric functions. *Journal of Process Control*, 2: 189–203.

Pu, Y. & Yu-Hong, W. 2015. Explicit model predictive control of CSTR system based on PWA model. *2015 34th Chinese Control Conference (CCC)*: 2304–2308.

Rajapandiyan, C. & Chidambaram, M. 2012. Controller Design for MIMO Processes Based on Simple Decoupled Equivalent Transfer Functions and Simplified Decoupler. *Industrial & Engineering Chemistry Research Ind. Eng. Chem. Res.*, 51(38): 12398–12410.

Rehan, M., Tahir, F., Iqbal, N. & Mustafa, G. 2008. Modeling, simulation and decentralized control of a nonlinear coupled tank system. *2008 Second International Conference on Electrical Engineering*.

Rehman, O.U. & Petersen, I.R. 2015. Using Inverse Nonlinearities in Robust Output Feedback Guaranteed Cost Control of Nonlinear Systems. *IEEE Transactions on Automatic Control IEEE Trans. Automat. Contr.*, 60(4): 1139–1144.

Rosinova, D. 2012. Decentralized Robust Control of MIMO Systems: Quadruple Tank Case Study. *9th IFAC Symposium Advances in Control Education*.

Rockwell Automation/Holobloc, Inc (http://www.fb61499.com/tools.html).

Russo, L.P. & Bequette, B.W. 1995. Impact of process design on the multiplicity behavior of a jacketed exothermic CSTR. *AIChE Journal AIChE J.*, Vol. 41(1): 135–147.

Sahoo, N., Panigrahi, B., Dash, P. & Panda, G. 2002. Application of a multivariable feedback linearization scheme for STATCOM control. *Electric Power Systems Research*, 62(2): 81–91.

Saey, P., De Landtsheer, T., Hauspie, W., Jos Knockaert, & Deconinck, G. 2014. Using an industrial hardware target for Matlab generated real-time code to control a torsional drive system. *Onderzoeksgroep Energie & Automatisering (E&A)*, 1-10.

Schweickhardt, T. & Allgower, F. 2005. Linear modelling error and steady-state behaviour of nonlinear dynamical systems. *In Proc. 44th IEEE Conf. Decision Control:* 8150-8155, Seville, Spain

Seborg, D.E. 1994. A perspective on advanced strategies for process control. *MIC Modeling, Identification and Control: A Norwegian Research Bulletin*: 179–189.

Shen, Y., Li, S., Li, N. & Cai, W.-J. 2011. Partial Decoupling Control for Multivariable Processes. *Industrial & Engineering Chemistry Research Ind. Eng. Chem. Res.*, 50(12): 7380–7387.

Sorouri, M., Patil, S. & Vyatkin**,** V. 2012. Distributed Control Patterns for Intelligent Mechatronic Systems**.** *IEEE Conference on Industrial Informatics*, 2012, Beijing, July 24-26

Sujatha, V. & Panda, R.C. 2013. Control configuration selection for multi input multi output processes. *Journal of Process Control*, 23(10): 1567–1574.

Tavakoli, S., Griffin, I. & Fleming, P.J. 2006. Tuning of decentralised PI (PID) controllers for TITO processes. *Control Engineering Practice*, 14: 1069–1080.

Toh, W.K. & Rangaiah, G.P. 2002. A Methodology for Autotuning of Multivariable Systems. *Industrial & Engineering Chemistry Research Ind. Eng. Chem. Res.*, 41(18): 4605–4615.

Ulrich, S. & Sasiadek, J.Z. 2013. Decentralized simple adaptive control of nonlinear systems. *Int. J. Adapt. Control Signal Process. International Journal of Adaptive Control and Signal Processing*, 28: 750–763.

Uppal, A., Ray, W. & Poore, A. 1974. On the dynamic behavior of continuous stirred tank reactors. *Chemical Engineering Science*, 29: 967–985.

Vinodha, R., Abraham Lincoln, S. & Prakash, S. 2010. Multiple Model and Neural based Adaptive Multi-loop Controller for a CSTR Process. *International journal of Electrical and Computing engineering*. 5(4) 251-256.

Vojtesek, J., Novak, J. & Dostal, P. 2005. Effect of External Linear Model's Order on Adaptive Control of CSTR. *Applied Simulation and Modelling*: 591–598.

Vu, T.N.L. & Lee, M. 2010. Independent design of multi-loop PI/PID controllers for interacting multivariable processes. *Journal of Process Control*, 20(8): 922–933.

Vyatkin V., 2006. Modelling and execution of reactive function block systems with Condition/Event nets**.** *4th IEEE Conference on Industrial Informatics (INDIN'06), Proceedings,* Singapore

Vyatkin, V., Christensen, J., Lastra, J.M. & Auinger, F. 2006. OOONEIDA: an open, object-oriented knowledge economy for intelligent distributed automation. *IEEE International Conference on Industrial Informatics, 2003. INDIN 2003. Proceedings.*

Vyatkin, V. & Hanisch, H.M., 2005. Re-use in Formal Modeling and Verification of Distributed Control Systems. *10th IEEE Conference on Emerging Technologies and Factory Automation (ETFA'05)*, *Catania, Italy*, *September*, 2005

Vyatkin, V. & Hanisch, H. M. 2003. Verification of Distributed Control Systems in Intelligent Manufacturing', *Journal of International Manufacturing*. 14(1): 123-136

Vyatkin, V. & Hanisch, H.M. 2001**.** Formal-modeling and Verification in the Software Engineering Framework of IEC61499: a way to self-verifying systems**,** *8th IEEE Conference on Emerging Technologies in Factory Automation, Proceedings ETFA'01*, Nice, France, September, 2001

Wang, J., Li, H. & Wang, J. 2005. Nonlinear PI control of a class of nonlinear singularly perturbed systems. *IEE Proceedings - Control Theory and Applications*, 152(5): 560–566.

Vyatkin, V, Hanisch, H.-M., Pang, C. & Yang, J. 2009. Application of Closed-Loop Modelling in Integrated Component Design and Validation of Manufacturing Automation. IEEE Transactions on Systems, Man and Cybernetics Part C: 39(1) 17-28.

Wang, Y., Zhou, D. & Gao, F. 2007. Robust fault-tolerant control of a class of non-minimum phase nonlinear processes. *Journal of Process Control*, 17: 523–537.

Xiong, Q. & Cai, W.-J. 2006. Effective transfer function method for decentralized control system design of multi-input multi-output processes. *Journal of Process Control*, 16(8): 773–784.

Xudong, Y. 2005. Adaptive output-feedback control of nonlinear systems with unknown nonlinearities. *Automatica*, 41: 1367–1374.

Zhai, J. & Qian, C. 2011. Global control of nonlinear systems with uncertain output function using homogeneous domination approach. *Int. J. Robust. Nonlinear Control International Journal of Robust and Nonlinear Control*, 22(14): 1543–1561.

Yang, J. & Vyatkin, V. 2008. Design and Validation of Distributed Control with Decentralized Intelligence in Process Industries: A Survey**.** *6th IEEE Conference on Industrial Informatics,* (INDIN'08), Seoul, Korea, July 2008.

Yang, C.-H. & Vyatkin, V. 2012. Transformation of Simulink models to IEC 61499 Function Blocks for verification of distributed control systems. *Control Engineering Practice*: 1259–1269.

Zhang, L., Sui, S., Li, Y. & Tong, S. 2015. Adaptive fuzzy output feedback tracking control with prescribed performance for chemical reactor of MIMO nonlinear systems. *Nonlinear Dynamics Nonlinear Dyn*, 80(1-2): 945–957.

Zhang, T. & Guay, M. 2005. Adaptive control of uncertain continuously stirred tank reactors with unknown actuator nonlinearities. *ISA Transactions*, 44: 55–68.

Zhao, D., Zhu, Q. & Dubbeldam, J. 2015. Terminal sliding mode control for continuous stirred tank reactor. *Chemical Engineering Research and Design*, 9(4): 266–274.

APPENDICES

APPENDIX A1: Function files `openloop_cstr`

Present the function file for the MIMO CSTR process with the parameter values that are used for the development of different models in Simulink.

```
function [dydt] = openloop_cstr(t,y)%function file for the CSTR process
global u1 u2
%=========================================================================
% inputs (2)
% feed flowrate (1)
% coolant flowrate (2)
q=u1;
qc=u2;
%=========================================================================
% states (2)
CA = y(1);     % the concentration of A in the tank, [mol/L]
T  = y(2);     % the reactor temperature(K)
%=========================================================================
% parameters
CAo = 1.0;     % feed concentration (mol/L)
V = 100;       % cstr volume (L)
ko = 7.2e10;   % reaction rate constant (min^?1);
EoverR =1*10^4;   % activation energy term (kelvin)
hA = 7e5;    % heat transfer term (cal/min.K)
Tco = 350.0;    % inlet coolant temperature (T)
To = 350.0;     % feed temperature(K)
dH = 2e5;    % heat of reaction (cal/mol)
rho = 1000;   % liguid density (g/L)
rhoc= 1000; % liguid coolant density (g/L)
Cp = 1.0;       % specific heats of liquid (cal/g.K)
Cpc = 1.0;    % specific heats of coolant (cal/g.K)
%=========================================================================
% Dynamic balance equations for the open loop multi input-multi output CSTR
%  dCA/dt
dydt(1,1) = q*(CAo - CA)/V - ko*CA*exp(-EoverR/T);
%  dT/dt
dydt(2,1) = q*(To - T)/V+(dH*ko/rho/Cp)*CA*exp(-EoverR/T)+...
    rhoc*Cpc/rho/Cp/V*qc*(1-exp(-hA/qc/rhoc/Cpc))*(Tco-T);
end
%=========================================================================
```

APPENDIX A2: Script files openloop_cstrsim

The main file for the CSTR process model for simulating the function openloop_cstr for various magnitudes of perturbations over the initial steady state conditions by a plus or minus 10% from the nominal values The file name is `openloop_cstrsim`

```
%=========================================================================
clear all
clc
global u1 u2
%steady state initial condition for control
u1_ss=102;%steady state initial condition for feed flow rate
u2_ss=97;%steady state initial condition for coolant flow rate
% Integrate the ODE
% =========================================================================
%Set the initial condition(s):
CA_ss = 0.0762;
T_ss = 444.770;
x_ss=[CA_ss;T_ss];
% Set the time range:
tf = 5;%time of simulation
%=========================================================================
% Open loop step change (Case:1)
 u1=u1_ss*1.1; %Perturbation of +10% in feed flow rate from initial
condition
 u2=u2_ss*1.0; %Perturbation of initial condition in coolant flow rate
% Integrate the ODE(s):
[t1, y1] = ode15s('openloop_cstr', [0 tf], x_ss);% solver

% Plot the results:
CA_1=y1(:,1);%reactor concentration
T_1=y1(:,2);%reactor concentration
figure (1)
plot(t1,CA_1);
xlabel('Time [minutes]')
ylabel('Concentration CA of A [mol/L]')
grid('on')
title('open loop step response curves for concentration')
gtext('10% step change in q with qc at steady state')
hold on
figure (2)
plot(t1,T_1);
xlabel('Time [minutes]')
ylabel('Temperature in tank [K]')
grid('on')
title('open loop step response curves')
gtext('10% step change in q with qc at steady state')
hold on
%=========================================================================
%open loop step change (Case:2)
u1=u1_ss/1.1;%Perturbation of -10% in feed flow rate from initial condition
u2=u2_ss*1.0;%Perturbation of initial condition in coolant flow rate
%Open loop step changes
[t2, y2] = ode15s('openloop_cstr', [0 tf], x_ss);
CA_2=y2(:,1);
T_2=y2(:,2);
figure (3)
plot(t1,CA_2);
xlabel('Time [minutes]')
ylabel('Concentration CA of A [mol/L]')
grid('on')
title('open loop step response curves for concentration')
gtext('-10% step change in q with qc at steady state')
hold on
```

```
figure (4)
plot(t1,T_2);
xlabel('Time [minutes]')
ylabel('Temperature in tank [K]')
grid('on')
title('open loop step response curves')
gtext('-10% step change in q with qc at steady state')
hold on
%=========================================================================
% Open loop step changes(case:3)
u1=u1_ss*1.0;%Perturbation of -10% in feed flow rate from initial condition
u2=u2_ss*1.1;%Perturbation of initial condition in coolant flow rate
[t3, y3] = ode15s('openloop_cstr', [0 tf], x_ss);
CA_3=y3(:,1);
T_3=y3(:,2);
figure (5)
plot(t1,CA_3);
xlabel('Time [minutes]')
ylabel('Concentration CA of A [mol/L]')
grid('on')
title('open loop step response curves for concentration')
gtext('10% step change in qc with q at steady state')
hold on
figure (6)
plot(t1,T_3);
xlabel('Time [minutes]')
ylabel('Temperature in tank [K]')
grid('on')
title('open loop step response curves')
gtext('10% step change in qc with q at steady state')
hold on
%=========================================================================
% Open loop step changes(case:4)
u1=u1_ss; %Perturbation of initial condition in feed flow rate
u2=u2_ss; %Perturbation of initial condition in coolant flow rate
[t4, y4] = ode15s('openloop_cstr', [0 tf], x_ss);
CA_4=y4(:,1);
T_4=y4(:,2);
figure (7)
plot(t1,CA_4);
xlabel('Time [minutes]')
ylabel('Concentration CA of A [mol/L]')
grid('on')
title('open loop step response curves for concentration')
gtext('step change in qc and q at steady state')
hold on
figure (8)
plot(t1,T_4);
xlabel('Time [minutes]')
ylabel('Temperature in tank [K]')
grid('on')
title('open loop step response curves')
gtext('step change in qc and q at steady state')
hold on
%=========================================================================
%open loop step changes (Case:5)
u1=u1_ss*1.0;%Perturbation feed flow rate at steady state
u2=u2_ss/1.1;%Perturbation of -10% in coolant flow rate from steady state
[t5, y5] = ode15s('openloop_cstr', [0 tf], x_ss);
CA_5=y5(:,1);
T_5=y5(:,2);
% Plot the results:
figure (9)
plot(t1,CA_5);
```

```
xlabel('Time [minutes]')
ylabel('Concentration CA of A [mol/L]')
grid('on')
title('open loop step response curves for concentration')
gtext('-10% step change in qc with q at steady state')
hold on
figure (10)
plot(t1,T_5);
xlabel('Time [minutes]')
ylabel('Temperature in tank [K]')
grid('on')
title('open loop step response curves')
gtext('-10% step change in qc with q at steady state')
hold on
%=========================================================================
```

APPENDIX B: Script file linearize_mod.m

Script file for the linearization of the CSTR process model by finding the Jacobian matrices, the state space matrices and the transfer functions of the state space model.

```
%=========================================================================
%Script file for the linearization of the CSTR process model for simulating
%the cstr process by finding the Jacobian matrices and
%transfer functions of the state space model.
%Julius Ngonga Muga
%=========================================================================
Clear all;
Close all;
Clc;
syms x1 x2 a1 a2 a3 a4 ko V CAo Tco To u1 u2 real
x = [x1 x2]';
u=[u1 u2]';
fx = [-ko*x(1)*exp(-a1/x(2))+(1/V)*(CAo-x(1))*u(1); a2*x(1)*exp(-
a1/x(2))+(1/V)*(To-x(2))*u(1)+a3*(Tco-x(2))*u(2)*(1-exp(-a4/u(2)))]
gx =x;
Avar = jacobian(fx,x)
Bvar = jacobian(fx,u)
Cvar = jacobian(gx,x)
Dvar = jacobian(gx,u)
A =
subs(Avar,{a1,a2,a3,a4,ko,V,CAo,Tco,To,x1,x2,u1,u2},{9.98e3,1.44e13,0.01,70
0,7.2e10,100,1.0,350,350,0.0762,444.7,102,97})
p=eig(A)
B =
subs(Bvar,{a1,a2,a3,a4,ko,V,CAo,Tco,To,x1,x2,u1,u2},{9.98e3,1.44e13,0.01,70
0,7.2e10,100,1.0,350,350,0.0762,444.7,102,97})
E =
subs(Evar,{a1,a2,a3,a4,ko,V,CAo,Tco,To,x1,x2,u1,u2},{9.98e3,1.44e13,0.01,70
0,7.2e10,100,1.0,350,350,0.0762,444.7,102,97})
C =
subs(Cvar,{a1,a2,a3,a4,ko,V,CAo,Tco,To,x1,x2,u1,u2},{9.98e3,1.44e13,0.01,70
0,7.2e10,100,1.0,350,350,0.0762,444.7,102,97})
p=eig(A)
D =
subs(Dvar,{a1,a2,a3,a4,ko,V,CAo,Tco,To,x1,x2,u1,u2},{9.98e3,1.44e13,0.01,70
0,7.2e10,100,1.0,350,350,0.0762,444.7,102,97})
Bmat=[B];
Dmat=[D];
[num1,den1]=ss2tf(A,Bmat,C,Dmat,1);
[num2,den2]=ss2tf(A,Bmat,C,Dmat,2);
g1=num1(1,1:3);
g11=tf(g1,den1)
g3=num1(2,1:3);
g21=tf(g3,den1)
g5=num2(1,1:3);
g12=tf(g5,den2)
g7=num2(2,1:3);
g22=tf(g7,den2)
g=[g11 g12;g21 g22];
[gr,infor]=reduce(g,'Algorithm','balance','order',2)
figure(1)
bode(g,'b-',gr,'r--')
title('Additive Error method');
legend('Original','Reduced');
%=========================================================================
```

APPENDIX C: Script file conc_code_3.m

This algorithm simulates the nonlinear linearizing feedback control response of the closed loop MIMO CSTR model for various magnitudes of set-point step changes, as well as disturbances at the outputs (y1) and (y2). The Simulink closed loop model to be simulated is *li_2015*.

```
%==========================================================================
%This algorithm simulates the nonlinear linearizing feedback control
%response characteristics of the closed loop MIMO CSTR model for various
%magnitudes of step changes as well as disturbances at the outputs (y1) and
(y2). The Simulink closed loop model to be simulated is li_2015.
%Julius Ngonga Muga
%==========================================================================
clear all,
close all,
clc
li_2015% Call the Simulink model for the I/O linearization of the MIMO Cstr
process sim('li_2015')
%Simulate the model
%kp1=8;kp2=29;ki1=11.1;ki2=52;%PI controller tuning parameter values for
%the model
%ysp1=0.0762mol/L;ysp2=0.13mol/L;ysp3=0.06mol/L.%setpoint values
%noise on y1=+/-1e-3;+/-4e-3;+/-0.01;+/-0.04;
%noise on y2=+/-04;+/-1;+/-2;+/-4;
figure(1)
plot(t,y1)%plot the concentration response for various set point conditions
grid on
xlabel('Time [min]','FontSize',12);
ylabel('Concentration[mol/L]', 'FontSize',12);
title('Closed loop concentration response with noise under the feedback
linearization control','FontSize',12');
gtext({'ysp1=0.0762mol/L','ysp2=0.13mol/L','ysp3=0.06mol/L'},'FontSize',12'
);
legend('Set point','Concentration loop tracking response')
%legend('Setpoint','Concentration loop tracking response with noise')
%gtext({'ysp1=0.0762mol/L','ysp2=0.13mol/L','noise on y1=+/-
0.04mol/l'},'FontSize',12')
%gtext({'ysp1=0.0762mol/L','ysp2=0.13mol/L','ysp3=0.06mol/L','noise on
y2=+/-4K'})
%==========================================================================
hold on
figure(2)
plot(t,y2)
grid on
xlabel('Time [min]','FontSize',12);
ylabel('Temperature[K]', 'FontSize',12);
title('Closed loop response of the nonlinear CSTR process under the
feedback linearization control','FontSize',12');
legend('Setpoint','Temperature loop tracking response')
gtext({'ysp1=444.7','ysp2=455'},'FontSize',12')
% gtext({'ysp1=444.7','ysp2=455','noise=+/-0.4K'},'FontSize',12')
%gtext({'ysp1=444.7','ysp2=455','noise on y1=+/-0.04mol/l'},'FontSize',12')
hold on
%==========================================================================
```

APPENDIX D: Script file dyn_conc_code.m

This file simulates the dynamic decoupling control response of the closed loop MIMO CSTR model for various magnitudes of the set-point step changes, as well as disturbances at the outputs (y1),y(2) and the interaction junctions (u1) and (u2). The Simulink closed loop model to be simulated is *dyn_dec_2015.*

```
%=========================================================================
%This algorithm simulates the dynamic decoupling control response
%characteristics of the closed loop MIMO CSTR model for various magnitudes
%of step changes as well as disturbances at the outputs (y1),y(2) and the
%interaction junctions (u1) and (u2). The Simulink closed loop model to be
%simulated is dyn_dec_2015.
%Julius Ngonga Muga
%=========================================================================
dyn_dec_2015
sim('dyn_dec_2015')
figure(1)
plot(TIME,CONC)
xlabel('Time [min]','FontSize',12);
ylabel('Concentration[mol/L]', 'FontSize',12);
title('Closed loop response of the nonlinear CSTR process under the dynamic
decoupling control','FontSize',12');
grid on
gtext({'ysp1=0.0762','ysp2=0.13','ysp3=0.1'})
%gtext({'ysp1=0.0762','ysp2=0.13','ysp3=0.10','noise of +/-0.04 mol/L'})
%gtext({'ysp1=0.0762','ysp2=0.13','ysp3=0.10','noise on y2 of +/-4K'})
%gtext({'ysp1=0.0762','ysp2=0.13','ysp3=0.10','noise on u2 of +/-80L/min'})
%legend('Setpoint', 'Tracking concentration response with noise on y2',12)
%legend('Setpoint', 'Tracking concentration response with noise on y1',12)
%legend('Setpoint', 'Tracking concentration response with noise on u2',12)
legend('Setpoint', 'decoupling tracking concentration response',12)
hold on
%=========================================================================
figure(2)
plot(TIME,TEMP)
xlabel('Time [min]','FontSize',12);
ylabel('Temperature[K]', 'FontSize',12);
grid on
title('Closed loop response of the nonlinear CSTR process under the dynamic
decoupling control','FontSize',12');
%gtext({'ysp1=445','ysp2=455','ysp3=445','noise of +/-0.04 mol/L on y1'})
%gtext({'ysp1=445','ysp2=455','noise on u2 of +/-100l/min'})
%gtext({'ysp1=0.0762','ysp2=0.14','ysp3=0.10','noise of +/-1e-3 mol/L on
y1'})
legend('Setpoint', 'decouling tracking temperature response',12)
%legend('Setpoint', 'Tracking temperature response with noise on y1',12)
legend('Setpoint', 'Tracking temperature response with noise on u2',12)
%=========================================================================
```

APPENDIX E1: Script file diag_decentsim.m

This file simulates the diagonal decentralized closed loop system response for various magnitudes of the set-point step changes, as well as disturbances at the output (y1) and the interaction junction (u1). The Simulink closed loop models to be simulated are *diag_decent_temp'* and *'decentconc_2015'.*

```
%=========================================================================
%This algorithm simulates the diagonal decentralized control response
characteristics of the closed loop MIMO CSTR model for various magnitudes
of step changes as well as disturbances at the output (y1) and the
interaction junction (u1). The Simulink closed loop models to be simulated
are ‘diag_decent_temp’ and 'decentconc_2015'.
%Julius Ngonga Muga
%=========================================================================
close all;
clc
kp2=1.606;
taui2=0.3407;
tauD2=0.1556
diag_decent_temp
sim('diag_decent_temp')
figure(1)
plot(t, y2)
grid on
xlabel('Time [min]','FontSize',12);
ylabel('Temperature[K]', 'FontSize',12);
title('Decentralized digaonal control temperature response for the CSTR
process','FontSize',12')
gtext({'ysp1=444.7','ysp2=460'})
%gtext({'ysp1=444.7','ysp2=455','ysp3=440'})
%gtext({'ysp1=444.7','ysp2=455','noise +/-40l/min'})
legend('Tracking temperature response','Setpoint',12)
%legend('Setpoint', 'Tracking temperature response with noise',12)
%=========================================================================
kp1=426.98;
taui1=0.3407;
tauD1=0.167;
hold on
decentconc_2015
sim('decentconc_2015')
figure(2)
plot(T,CONC)
grid on
xlabel('Time [min]','FontSize',12);
ylabel('Concentration[mol/L]', 'FontSize',12);
title('Decentralized concentration response for the CSTR
process','FontSize',12'');
gtext({'ysp1=0.0762','ysp2=0.13','ysp3=0.06'})
%gtext({'ysp1=0.14mol/L'})
%gtext({'ysp1=0.0762','ysp2=0.14','ysp3=0.08','noise of+/-0.04mol/L'})
%gtext({'ysp1=0.0762','ysp2=0.14','ysp3=0.08','noise on u1 of +/-80L/min'})
%legend('Setpoint', 'Nonlinear linearized concentration response',12)
legend('Tracking concentration response','Setpoint',12)
%=========================================================================
```

APPENDIX E2: Script file conc_code_4.m

This file simulates the decentralized control response of the closed loop MIMO CSTR with and without detuning, for various magnitudes of set-point step changes as well as disturbances. The Simulink closed loop model to be simulated is *decent1_2015*

```
%==========================================================================
%This algorithm simulates the decentralized control response
%characteristics of the closed loop MIMO CSTR with and without detuning.
%The model for various magnitudes of step changes as well as disturbances.
%The Simulink closed loop model to be simulated is decent1_2015.
%Julius Ngonga Muga
%==========================================================================
decent1_2015_detuning
sim('decent1_2015_detuning')
figure(1)
plot(t_o,y1)
grid on
xlabel('Time [min]','FontSize',12);
ylabel('Concentration[mol/L]', 'FontSize',12);
title('Closed loop response of the nonlinear CSTR process under the
decentralized control under detuning and without','FontSize',12');
legend({'Setpoint','Concentration response','Concentration response under
detuning'})
gtext({'ysp1=0.0762','ysp2=0.13','ysp3=0.06'})
%gtext({'ysp1=0.14mol/L'})
%gtext({'ysp1=0.0762','ysp2=0.14','ysp3=0.08','noise of +/-0.04 mol/L'})
%gtext({'ysp1=0.0762','ysp2=0.14','ysp3=0.08','noise on u1 of +/-80L/min'})
hold on
%==========================================================================
figure(2)
plot(t_o,y)
grid on
xlabel('Time [min]','FontSize',12);
ylabel('Temperature[K]', 'FontSize',12);
title(' Closed loop response of the nonlinear CSTR process under the
decentralized control under detuning and without','FontSize',12')
gtext({'ysp1=444.7','ysp2=455','ysp3=440'})
%legend('Setpoint', 'Decentralized temperature response','Decentralized
temperature response with detuning','FontSize',12')
%gtext({'ysp1=445','ysp2=455','ysp3=445','noise of +/-0.04 mol/L on y1'})
%gtext({'ysp1=445','ysp2=455','noise on u2 of +/-100l/min'})
%gtext({'ysp1=0.0762','ysp2=0.14','ysp3=0.10','noise of +/-1e-3 mol/L on
y1'})
%gtext({'ysp1=444.7','ysp2=455','noise +/-40l/min'})
legend('Tracking temperature response','Setpoint',12)
%legend('Setpoint', 'Tracking temperature response with noise',12)
%==========================================================================
```

APPENDIX F: Simulink models developed for the thesis

These are the Simulink models developed for the thesis

decent_2015.	Model of MIMO closed loop decentralized control	Model of the MIMO closed loop system under decentralized control
dyn_dec_2015	Model of MIMO closed loop dynamic decoupling control	The MIMO closed loop under dynamic decoupling control
decen1_2015	Model of MIMO closed loop decentralized control incorporating the detuning	The closed loop MIMO system under decentralized control incorporating the detuning
li_2015	Model of MIMO closed loop I/O feedback linearization control	The closed loop MIMO system under I/O feedback linearization control
openloop_cstr_mod	Model of MIMO open loop CSTR system	The open loop CSTR process
diag_decent_temp	Model of diagonal temperature closed loop control	The temperature diagonal closed loop control system
decenconc_2015	Model of diagonal concentration closed loop control	The concentration diagonal closed loop control system

APPENDIX G: TwinCAT models developed for the thesis

APPENDIX G1: TwinCAT model under dynamic control

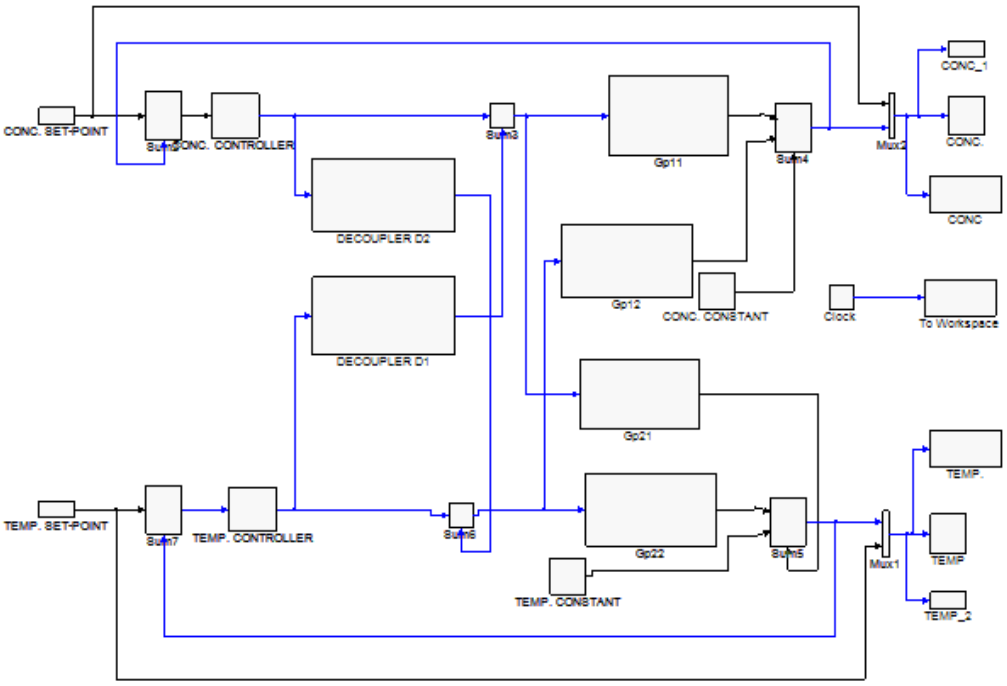

APPENDIX G2: TwinCAT model under dynamic control with disturbances

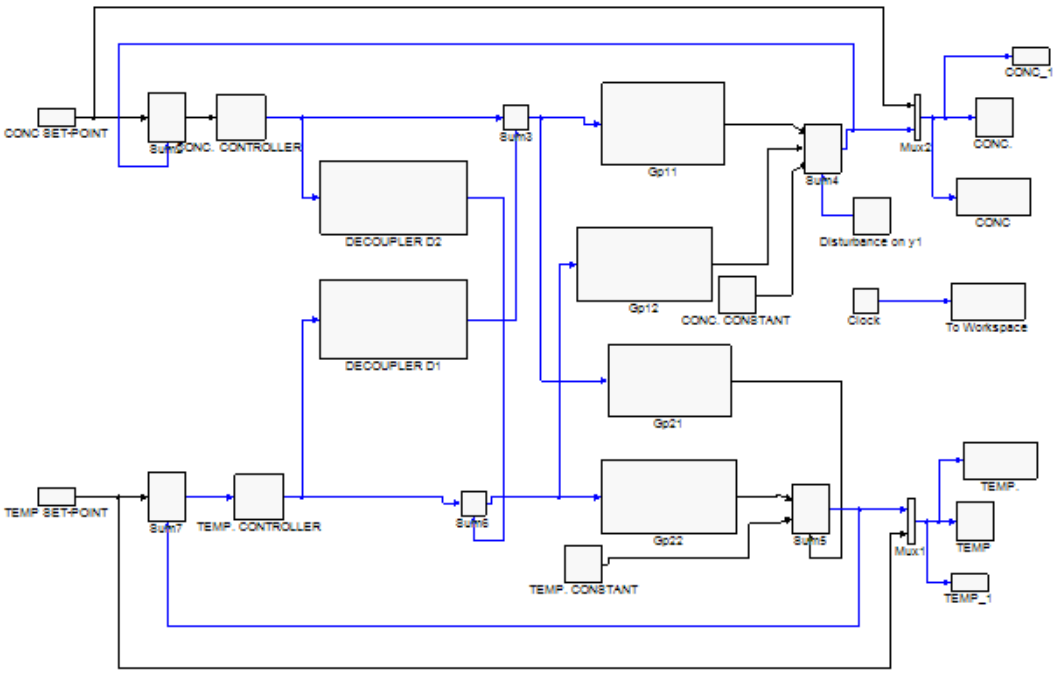

APPENDIX G3: TwinCAT model under decentralized control

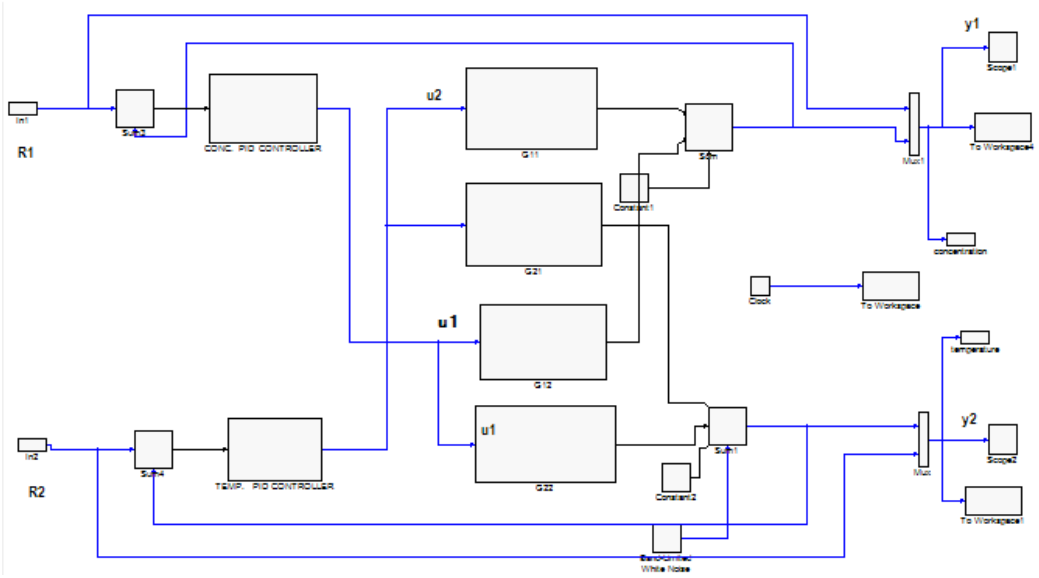

APPENDIX G4: TwinCAT model under I/O feedback linearization control

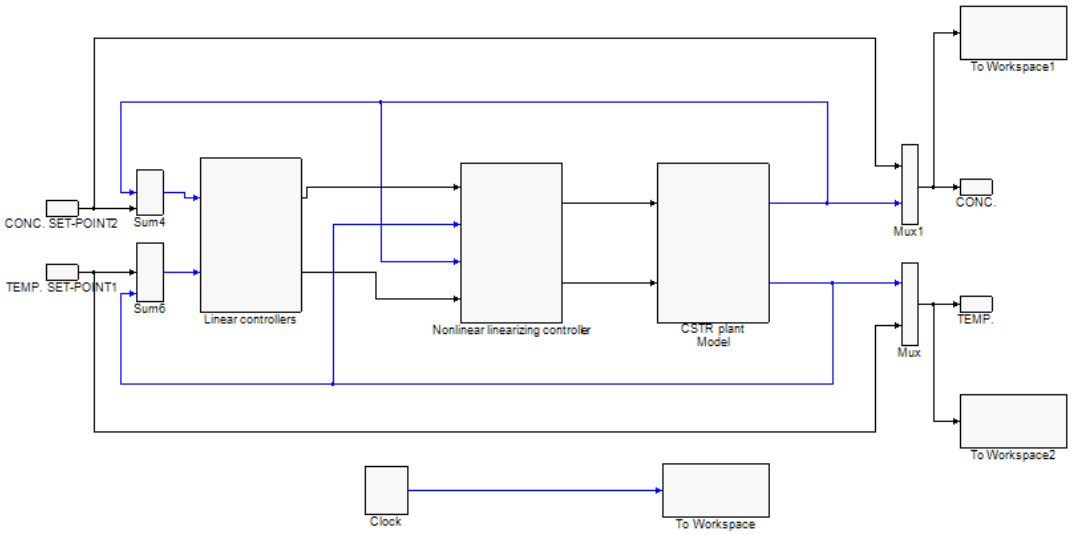

APPENDIX H1: Beckhoff PLC CX-5020

CX5010, CX5020

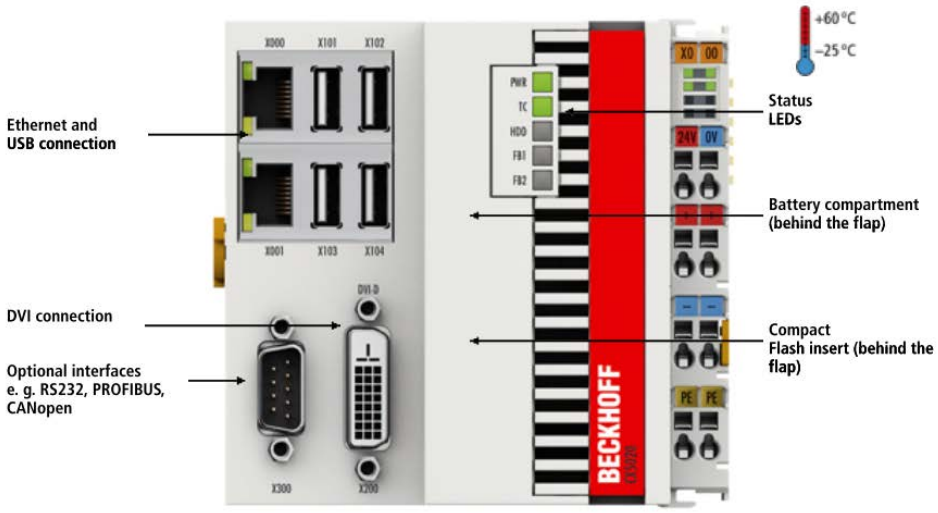

APPENDIX H2: Beckhoff PLC CX-5020 technical data

Technical data	CX5010-x1xx	CX5020-x1xx
Processor	processor Intel® Atom™ Z510, 1.1 GHz clock frequency	processor Intel® Atom™ Z530, 1.6 GHz clock frequency
Flash memory	64 MB Compact Flash card (optionally extendable)	
Internal main memory	512 MB RAM (internal, not expandable)	512 MB RAM (optionally 1 GB installed ex factory)
Persistent memory	integrated 1-second UPS (1 MB on Compact Flash card)	
Interfaces	2 x RJ 45, 10/100/1000 Mbit/s, DVI-D, 4 x USB 2.0, optional 1 x RS232/RS422/RS485	
Diagnostics LED	1 x power, 1 x TC status, 1 x flash access, 2 x bus status	
Clock	internal battery-backed clock for time and date (battery exchangeable)	
Operating system	Microsoft Windows CE or Microsoft Windows Embedded Standard	
Control software	TwinCAT 2 PLC runtime or TwinCAT 2 NC PTP runtime	
Power supply	24 V DC (-15 %/+20 %)	
Dielectric strength	500 V (supply/internal electronics)	
Current supply I/O terminals	2 A	
Max. power loss	12 W (including the system interfaces)	12.5 W (including the system interfaces)
Dimensions (W x H x D)	100 mm x 100 mm x 91 mm	
Operating/storage temperature	-25…+60 °C/-40…+85 °C	
Relative humidity	95 %, no condensation	
Vibration/shock resistance	conforms to EN 60068-2-6/EN 60068-2-27/29	

APPENDIX I: PID CONTROLLER SETTINGS BASED ON IMC

Table 6.2. Summary of PID controller settings based on IMC or direct synthesis

Process model	Controller	K_c	τ_I	τ_D
$\frac{K_p}{\tau_p s+1}$	PI	$\frac{\tau_p}{K_p \tau_c}$	τ_p	—
$\frac{K_p}{(\tau_1 s+1)(\tau_2 s+1)}$	PID	$\frac{\tau_1+\tau_2}{K_p \tau_c}$	$\tau_1+\tau_2$	$\frac{\tau_1 \tau_2}{\tau_1+\tau_2}$
	PID with $\tau_1 > \tau_2$	$\frac{\tau_1}{K_p \tau_c}$	τ_1	τ_2
	PI (underdamped)	$\frac{\tau_1}{4K_p \zeta^2 \tau_2}$	τ_1	—
$\frac{K_p}{\tau^2 s^2+2\zeta\tau s+1}$	PID	$\frac{2\zeta\tau}{K_p \tau_c}$	$2\zeta\tau$	$\frac{\tau}{2\zeta}$
$\frac{K_p}{s(\tau_p s+1)}$	PD	$\frac{1}{K_p \tau_c}$	—	τ_p
$\frac{K_p e^{-t_d s}}{\tau_p s+1}$	PI	$\frac{\tau_p}{K_p(\tau_c+t_d)}$	τ_p	—
	PID	$\frac{1}{K_p}\frac{2\tau_p/t_d+1}{2\tau_c/t_d+1}$	$\tau_p+t_d/2$	$\frac{\tau_p}{2\tau_p/t_d+1}$
$\frac{K_p}{s}$	P	$\frac{1}{K_p \tau_c}$	—	—

Dec 2015